Electric Vehicle (EV)-Assisted Demand-Side Management In Smart Grid

Nanduni Nimalsiri

A thesis submitted for the degree of
Doctor of Philosophy at
The Australian National University

November 2021

Except where otherwise indicated, this thesis is my own original work.

Nanduni

Nanduni Nimalsiri
12 November 2021

To my husband Pubudu and my parents

Acknowledgments

First and foremost, I would like to offer my sincere gratitude and thanks to my primary supervisor, Dr. David Smith, for his guidance, encouragement, patience and dedicated involvement throughout my PhD studies. I would also like to thank my co-supervisors, Dr. Elizabeth Ratnam, Dr. Chathurika Mediwaththe, Prof. Saman Halgamuge, and the chair of committee, Dr. Marnie Shaw, for their immense support and guidance offered throughout all these years, which made this thesis possible.

I would like to acknowledge the Australian National University for awarding me the HDR Fee Remission Merit Scholarship and the Australian Government Research Training Program Fee-Offset Scholarship, and CSIRO Data61 for awarding me the Data61 PhD Scholarship and Data61 Top-up Scholarship, which provided me financial support throughout these years.

My research was conducted initially in Canberra at the Australian National University and then in Sydney at the CSIRO's Data61. I would like to thank the academic and professional staff at both institutes who assisted me in many ways. Thanks also to my colleagues and friends in the Battery Storage and Grid Integration Program (BSGIP) at the Australian National University, the Information Security and Privacy Group (ISPG) at the Data61 and the Optimization, and Pattern Recognition Research Group at the University of Melbourne.

I am also grateful to my many friends who have encouraged and supported me along this PhD journey. Last but not least I would like to thank my husband Pubudu and our respective families for their love, guidance, patience and all-round support in all of my career choices including this PhD.

Abstract

While relieving the dependency on diminishing fossil fuels, Electric Vehicles (EVs) provide a promising opportunity to realise an eco-friendly and cost-effective means of transportation. However, the enormous electricity demand imposed by the wide-scale deployment of EVs can put power infrastructure under critical strain, potentially impacting the efficiency, resilience, and safety of the electric power supply. Interestingly, EVs are deferrable loads with flexible charging requirements, making them an ideal prospect for the optimisation of consumer demand for energy, referred to as demand-side management (DSM). Furthermore, with the recent introduction of Vehicle-to-Grid (V2G) technology, EVs are now able to act as residential battery systems, enabling EV customers to store energy and use them as backup power for homes or deliver back to the grid when required.

Hence, this thesis studies Electric Vehicle (EV)-assisted demand-side management strategies to manage peak electricity demand, with the long-term objective of transforming to a fully EV-based transportation system without requiring major upgrades in existing grid infrastructure. Specifically, we look at ways to optimise residential EV charging and discharging for smart grid, while addressing numerous requirements from EV customer's perspective and power system's perspective.

First, we develop an EV charge scheduling algorithm with the objective of tracking an arbitrary power profile. The design of the algorithm is inspired by water-filling theory in communication systems design, and the algorithm is applied to schedule EV charging following a day-ahead renewable power generation profile. Then we extend that algorithm by incorporating V2G operation to shape the load curve in residential communities via valley-filling and peak-shaving services. In the proposed EV charging and discharging algorithm, EVs are distributedly coordinated by implementing a non-cooperative game. Our numerical simulation results demonstrate that the proposed algorithm is effective in flattening the load curve while satisfying all heterogeneous charge requirements across EVs.

Next, we propose an algorithm for network-aware EV charging and discharging, with an emphasis on both EV customer economics and distribution network aspects. The core of the algorithm is a Quadratic Program (QP) that is formulated to minimise the operational costs accrued to EV customers while maintaining distribution feeder nodal voltage magnitudes within prescribed thresholds. By means of a receding horizon control approach, the algorithm implements the respective QP-based EV charge-discharge control sequences in near-real-time. Our simulation results demonstrate that the proposed algorithm offers significant reductions in operational costs associated with EV charging and discharging, while also mitigating under-voltage and over-voltage conditions arising from peak power flows and reverse power flows in the distribution network. Moreover, the proposed algorithm is shown to be robust

to non-deterministic EV arrivals and departures.

While the previous algorithm ensures a stable voltage profile across the entire distribution feeder, it is limited to balanced power distribution networks. Therefore, we next extend that algorithm to facilitate EV charging and discharging in unbalanced distribution networks. The proposed algorithm also supports distributed EV charging and discharging control, where EVs determine their individual charge-discharge profiles in parallel, using an Alternating Direction Method of Multipliers (ADMM)-based approach driven by peer-to-peer EV communication. Our simulation results confirm that the proposed algorithm is computationally efficient when compared to its centralised counterpart, where a central entity determines the charge-discharge profiles for all EVs. Moreover, the proposed algorithm is shown to be successful in terms of correcting any voltage violations stemming from non-EV load, as well as, satisfying all EV charge requirements without causing any voltage violations.

Contents

List of Abbreviations

AC	Alternating Current
ADMM	Alternating Direction Method of Multipliers
AIMD	Additive Increase Multiplicative Decrease
AMI	Advanced Metering Infrastructure
BEV	Battery Electric Vehicle
C-VF	Coordinated Valley Filling
C-VF-PS	Coordinated Valley Filling and Peak Shaving
DC	Direct Current
DC-ADMM	Dual Consensus - Alternating Direction Method of Multipliers
DECSaT	Decentralised EV Charge Scheduling and Tracking
Dis-Net-EVCD	Distributed and Network-aware EV Charging and Discharging
DSM	Demand-Side Management
ESR	Equivalent Series Resistance
EV	Electric Vehicle
EVs	Electric Vehicles
EVSE	Electric Vehicle Supply Equipment
G2V	Grid-to-Vehicle
ICT	Information and Communication Technology
KKT	Karush–Kuhn–Tucker
MAS	Multi-Agent Systems
N-EVCD	Network-aware Electric Vehicle Charging and Discharging
OPF	Optimal Power Flow
PCC	Point of Common Coupling

PEV	Plug-in Electric Vehicle
PHEV	Plug-in Hybrid Electric Vehicle
POP	Preferred Operating Point
PV	Photovoltaics
QP	Quadratic Program
RES	Renewable Energy Source
RHO	Receding Horizon Optimisation
SoC	State of Charge
SPDS	Shrunken Primal Dual Sub-gradient
ToU	Time-of-Use
V2B	Vehicle-to-Building
V2G	Vehicle-to-Grid
V2H	Vehicle-to-Home

Statement of Contribution

Chapters 2 - 6 consist of five co-authored papers that are published or have been submitted for publication in scholarly journals and conferences. Specifically, three papers have been published in refereed journals, one paper has been published in conference proceedings, and one paper has been submitted to a journal for publication at the time of submission of this thesis. For each of these co-authored papers, a statement of contribution detailing the extent of contribution and endorsement for inclusion in this thesis is included in the following pages.

Australian National University

Statement of Contribution

This thesis is submitted as a Thesis by Compilation in accordance with https://policies.anu.edu.au/ppl/document/ANUP_003405

I declare that the research presented in this Thesis represents original work that I carried out during my candidature at the Australian National University, except for contributions to multi-author papers incorporated in the Thesis where my contributions are specified in this Statement of Contribution.

Title: A Survey of Algorithms for Distributed Charging Control of Electric Vehicles in Smart Grid

Authors: **Nanduni I. Nimalsiri**, Chathurika P. Mediwaththe, Elizabeth L. Ratnam, Marnie Shaw, David B. Smith, Saman K. Halgamuge

Publication outlet: IEEE Transactions on Intelligent Transportation Systems

Current status of paper: Published

Contribution to paper: Did the majority of work in reviewing the literature; organising and categorising the existing work in literature based on different criteria; summarising research findings from the literature; identifying trends, pros and cons, and gaps in existing work; identifying potential future research directions; taking primary responsibility (as the lead author) for conceptualising, preparing, drafting, editing and revising the journal publication.

Senior author or collaborating authors endorsement: (Dr. David Smith)

Nanduni Indeewaree Nimalsiri		02.11.2021
Candidate – Print Name	Signature	Date

Endorsed

David Smith		03.11.2021
Primary Supervisor – Print Name	Signature	Date
Ian Petersen		04/11/21
Delegated Authority – Print Name	Signature	Date

Australian National University

Statement of Contribution

This thesis is submitted as a Thesis by Compilation in accordance with https://policies.anu.edu.au/ppl/document/ANUP_003405

I declare that the research presented in this Thesis represents original work that I carried out during my candidature at the Australian National University, except for contributions to multi-author papers incorporated in the Thesis where my contributions are specified in this Statement of Contribution.

Title: A Decentralized Electric Vehicle Charge Scheduling Scheme for Tracking Power Profiles

Authors: **Nanduni I. Nimalsiri**, David B. Smith, Elizabeth L. Ratnam, Chathurika P. Mediwaththe, Saman K. Halgamuge

Publication outlet: Proceedings of the IEEE Power & Energy Society Innovative Smart Grid Technologies (ISGT)

Current status of paper: Published

Contribution to paper: Did the majority of work in conceptualising the research problem and proposed solutions; developing the high-level framework and algorithmic solutions; developing the software codes for implementing the algorithms and testing; conducting the numerical simulations; analysing and optimising the numerical simulation results; taking primary responsibility (as the lead author) for preparing, drafting and editing the conference publication; preparing the poster for presentation at the conference; presenting at the conference.

Senior author or collaborating authors endorsement: David Smith (Dr. David Smith)

Nanduni Indeewaree Nimalsiri	Nanduni	02.11.2021
Candidate – Print Name	Signature	Date

Endorsed

David Smith	David Smith	03.11.2021
Primary Supervisor – Print Name	Signature	Date
Ian Petersen	Ian Petersen	04/11/21
Delegated Authority – Print Name	Signature	Date

Australian National University

Statement of Contribution

This thesis is submitted as a Thesis by Compilation in accordance with https://policies.anu.edu.au/ppl/document/ANUP_003405

I declare that the research presented in this Thesis represents original work that I carried out during my candidature at the Australian National University, except for contributions to multi-author papers incorporated in the Thesis where my contributions are specified in this Statement of Contribution.

Title: Coordinated Charge and Discharge Scheduling of Electric Vehicles for Load Curve Shaping

Authors: **Nanduni I. Nimalsiri**, Elizabeth L. Ratnam, David B. Smith, Chathurika P. Mediwaththe, Saman K. Halgamuge

Publication outlet: IEEE Transactions on Intelligent Transportation Systems

Current status of paper: Published

Contribution to paper: Did the majority of work in conceptualising the research problem and proposed solutions; developing the high-level framework and algorithmic solutions; developing the software codes for implementing the algorithms and testing; conducting the numerical simulations; analysing and optimising the numerical simulation results; taking primary responsibility (as the lead author) for preparing, drafting, editing and revising the journal publication.

Senior author or collaborating authors endorsement: David Smith (Dr. David Smith)

Nanduni Indeewaree Nimalsiri	Nanduni	02.11.2021
Candidate – Print Name	Signature	Date

Endorsed

David Smith	David Smith	03.11.2021
Primary Supervisor – Print Name	Signature	Date
Ian Petersen	Ian Petersen	04/11/21
Delegated Authority – Print Name	Signature	Date

Australian National University

Statement of Contribution

This thesis is submitted as a Thesis by Compilation in accordance with https://policies.anu.edu.au/ppl/document/ANUP_003405

I declare that the research presented in this Thesis represents original work that I carried out during my candidature at the Australian National University, except for contributions to multi-author papers incorporated in the Thesis where my contributions are specified in this Statement of Contribution.

Title: Coordinated Charging and Discharging Control of Electric Vehicles to Manage Supply Voltages in Distribution Networks: Assessing the Customer Benefit

Authors: **Nanduni I. Nimalsiri**, Elizabeth L. Ratnam, Chathurika P. Mediwaththe, David B. Smith, Saman K. Halgamuge

Publication outlet: Applied Energy

Current status of paper: Published

Contribution to paper: Did the majority of work in conceptualising the research problem and proposed solutions; developing the high-level framework and algorithmic solutions; developing the software codes for implementing the algorithms and testing; conducting the numerical simulations; analysing and optimising the numerical simulation results; taking primary responsibility (as the lead author) for preparing, drafting, editing and revising the journal publication.

Senior author or collaborating authors endorsement: David Smith (Dr. David Smith)

Nanduni Indeewaree Nimalsiri	Nanduni	02.11.2021
Candidate – Print Name	Signature	Date

Endorsed

David Smith	David Smith	03.11.2021
Primary Supervisor – Print Name	Signature	Date
Ian Petersen	Ian Petersen	04/11/21
Delegated Authority – Print Name	Signature	Date

Australian National University

Statement of Contribution

This thesis is submitted as a Thesis by Compilation in accordance with https://policies.anu.edu.au/ppl/document/ANUP_003405

I declare that the research presented in this Thesis represents original work that I carried out during my candidature at the Australian National University, except for contributions to multi-author papers incorporated in the Thesis where my contributions are specified in this Statement of Contribution.

Title: Distributed Optimization-based Electric Vehicle Charging and Discharging in Unbalanced Distribution Grids

Authors: **Nanduni I. Nimalsiri**, Elizabeth L. Ratnam, David B. Smith, Chathurika P. Mediwaththe, Saman K. Halgamuge

Publication outlet: IEEE Transactions on Smart Grid

Current status of paper: Submitted

Contribution to paper: Did the majority of work in conceptualising the research problem and proposed solutions; developing the high-level framework and algorithmic solutions; developing the software codes for implementing the algorithms and testing; conducting the numerical simulations; analysing and optimising the numerical simulation results; taking primary responsibility (as the lead author) for preparing, drafting and editing the journal submission.

Senior author or collaborating authors endorsement: David Smith (Dr. David Smith)

Nanduni Indeewaree Nimalsiri	Nanduni	02.11.2021
Candidate – Print Name	Signature	Date

Endorsed

David Smith	David Smith	03.11.2021
Primary Supervisor – Print Name	Signature	Date
Ian Petersen		04/11/21
Delegated Authority – Print Name	Signature	Date

Chapter 1

Introduction

1.1 Background and Motivation

The advent of Electric Vehicles (EVs) is a game-changer in driving both transportation and power industries towards a sustainable future. Recently, there has been an escalating demand for EVs, with global electric car sales rising by around 140% in the first-quarter of 2021 compared to the same period in 2020 [IEA, 2021]. It is expected that this trend in accelerated EV uptake will continue into the next decade, expanding the global EV stock across all transport modes to almost 145 million vehicles by 2030 [IEA, 2021].

Some of the key drivers behind this mass adoption of EVs include, fossil fuel depletion; current global trends towards reductions in green house gas emissions; reduced noise levels; better quality of air; energy security; cheaper electricity prices over fuel prices; lower operating costs compared to vehicles with internal combustion engines; decreasing cost of batteries that power EVs; and ability to be charged with locally produced renewable energy sources [Sanguesa et al., 2021; Graham and Brungard, 2021; Haddadian et al., 2015; Carley et al., 2013]. These drivers, in conjunction with developments of the modern smart grid, have led to the world's biggest automotive manufacturers to introducing various types of new EV models with improved user convenience [Earl and Fell, 2019; energysage, 2021].

On the downside, the transition to support a rapid uptake in EVs requires significant additional electricity generation and distribution, which may put excessive stress on existing electricity infrastructure [Putrus et al., 2009; Dharmakeerthi et al., 2011; Su et al., 2011; Gong et al., 2011; Monteiro et al., 2011; Shafiee et al., 2013; Xiao et al., 2014; Schuller and Stuart, 2018; Shaukat et al., 2018; Rizvi et al., 2018; Kasprzyk et al., 2018; Kapustin and Grushevenko, 2020]. For instance, if every one switches over to an electric passenger vehicle and charges their batteries spontaneously, the electric grid will likely end up facing disastrous load congestion problems, potentially leading to a need for extensive grid expansion. From a practical viewpoint, such network reinforcements are time-consuming and require large capital investments [Celli et al., 2013]. An alternative, yet a highly effective way of managing the ever-increasing power demands of EVs, in the absence of extensive network upgrades in the power grid, is to control EV charging in a way that their charging operations are distributed across a longer period of time, which is known as *demand-side man-*

agement (DSM) [Finn et al., 2012; Pang et al., 2012; Mesarić and Krajcar, 2015; López et al., 2015; Earl and Fell, 2019]. Since EVs are deferrable loads with charging flexibility and they remain parked for most of the time of the day, they are well-suited for assisting DSM in the electric grid. For instance, if a driver typically comes home from work, plugs in the EV, and doesn't need to drive it again until the next morning, it may be beneficial to have the EV not commence charging until the middle of the night (when demand for electricity is low) rather than right away in the early evening hours (peak hours). That is, instead of adapting power generation to meet the EV power demand, EV-assisted DSM aims to adapt EV power demand to make the best use of the electric power available in the grid.

Importantly, EV-assisted demand-side management potentially defers (or avoids) significant costs associated with distribution network reinforcement, which otherwise would require to enable EV proliferation.

The next-generation electricity grid referred to as the *smart grid* (or intelligent grid) has revolutionised the structure and capabilities of the traditional electric grid [Farhangi, 2009; Fang et al., 2011; Jenkins et al., 2012; Momoh, 2012]. The future smart grid, typified by advanced power, communication, control and data processing capabilities, offers an ideal platform for DSM of EVs via smart EV charging [Igbinovia et al., 2016; Hildermeier et al., 2019]. *Smart EV charging* schemes, in particular, refers to intelligent algorithms that run within smart devices using data connections between the EV and the charger [Wallbox, 2021]. With smart charging, EVs remain plugged-in (grid-connected), but they do not have to be actively charging the whole time. Instead, charging rates corresponding to different time points are determined by executing a smart charging algorithm that is designed to meet the EV charging requirement with minimal impact on the electric grid. Specifically, a customised charging plan (schedule) is made for each EV considering multiple criteria such as the EV owner's requirements and preferences, and technical limitations associated with EV battery technologies and EV charging infrastructures [Rajakaruna et al., 2015].

One of the goals of EV-assisted DSM is to mitigate grid congestion, and thereby allow EVs to meet their charging demands with minimal to zero adverse impact on the existing grid operation. Apart from reducing grid congestion, EV-assisted DSM can also serve multiple other goals of EV customers and grid operators, for example, minimisation of the charging costs, minimisation of the power generation costs, maximisation of the utilization of local renewable energy generation, maximisation of user convenience, maximisation of the grid revenue, maximisation of the operational efficiency, load regulation, voltage regulation and provisioning of various ancillary services [Luo et al., 2012; Gelazanskas and Gamage, 2014; García-Villalobos et al., 2014; Hiskens and Callaway, 2009; Callaway and Hiskens, 2010; Wang et al., 2016; Kong and Karagiannidis, 2016; Shuai et al., 2016; Nimalsiri et al., 2019; Fachrizal et al., 2020].

With the recent introduction of bidirectional (two-way) EV chargers, electricity can flow both ways, in and out of the EV battery, enabling further opportunities for EV-assisted DSM in smart grid [Pang et al., 2012; Kisacikoglu et al., 2012; Pinto et al., 2013; Kwon et al., 2015; Gago et al., 2016; Restrepo et al., 2016; Kwon and Choi, 2016; Tushar et al., 2017; Sahinler and Poyrazoglu, 2020; Semsar et al., 2020; Seth and Singh, 2020; He et al., 2021]. Fig. 1.1 depicts different forms of smart charging techniques that are based on unidirectional charging and bidirectional charging. As the name implies, *unidirectional charging* or *V1G* allows electricity to flow only one way, that is from the electric grid into the EV battery [Yilmaz and Krein, 2012a]. *Vehicle-to-Grid* or *V2G* is when a bidirectional EV charger is used to return electricity from an EV's battery to the grid via a Direct Current (DC) to Alternating Current (AC) converter system usually embedded in the EV charger [Cvetkovic et al., 2009; Hosseini et al., 2012; Liu et al., 2013; Tan et al., 2014; Lazzeroni et al., 2019]. Another concept known as *Vehicle-to-Home* (*V2H*) or *Vehicle-to-Building* (*V2B*) is when a bidirectional EV charger is used to supply electricity from an EV's battery to a home [Haines et al., 2009; Alirezaei et al., 2016; Li et al., 2017; Colmenar-Santos et al., 2017; Luo et al., 2018; Lazzeroni et al., 2019] or, possibly, another kind of building [Nguyen and Song, 2012; Barone et al., 2019; Buonomano, 2020; Heredia et al., 2020; Borge-Diez et al., 2021]. V2H (or V2B) is achieved via a DC to AC converter system usually embedded within the EV charger. Importantly, with V2H (or V2B), EVs can act as supplement power suppliers to the home (or building). As such, owning a bidirectional charger over a unidirectional charger offers many benefits, particularly to make money by selling excess energy back to the grid; save money in the context of time varying electricity tariffs; become energy self-sufficient by connecting with onsite renewable energy sources; support various types of grid services and thereby receive compensation [Wallbox, 2021; Singh and Tiwari, 2020].

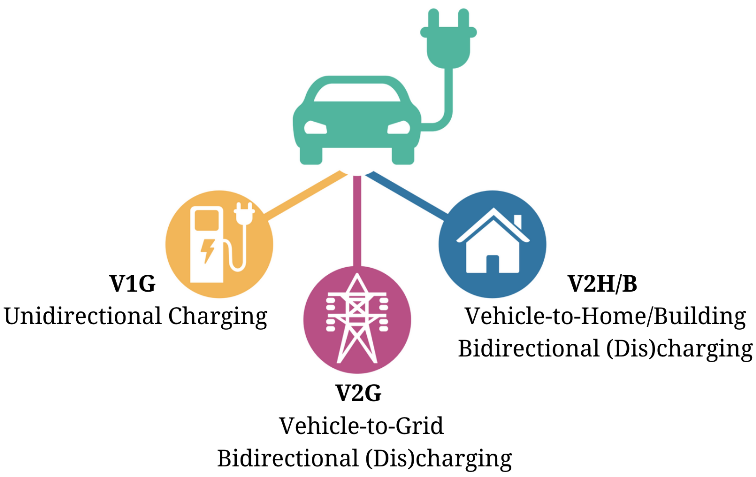

Figure 1.1: Different forms of smart charging

Bidirectional power flows and bidirectional communication channels constitute the foundation of the interactive smart grid [Wang et al., 2011; Gungor et al., 2011; Ma et al., 2013]. Specifically, the power networks and communication networks together compose a complex network, which requires specially designed EV charging control systems to manage the interactions between EVs and the smart grid [Kong and Karagiannidis, 2016]. Fig. 1.2 depicts the layout of an exemplary EV charging control system that consists of three levels: device level, communication network level, and application level [Ahmed and Kim, 2017]. The device level consists of EVs, EV Supply Equipment (EVSE), metering devices and electric power connections. The Information and Communication Technology (ICT)-enabled, two-way, secure communication network is responsible for data transfer between different smart entities via both wired and wireless technologies. The application level is supported by intelligent algorithms, whereby the grid operator at the control center monitors and directly or indirectly controls the charging of EVSEs to ensure grid stability.

The existing EV charging control approaches primarily fall under two types of coordination architectures, known as *centralised* and *distributed* coordination architectures [Nimalsiri et al., 2019]. Centralised approaches require a central operator as the controller, who is usually the grid operator or utility operator, to whom EVs submit their charging requests. The central operator is then responsible for performing all the computational tasks, in order to obtain the charge profiles that satisfy each EV's charging demand within the specified time duration. In this way, centralised approaches directly control EV charging operations. Distributed approaches, on the other hand, distribute the computational load required for computing EV charge profiles across individual EVs, such that each EV (equipped with computing capabilities) determines their own charge profile locally in collaboration with other entities. Importantly, EV coordination in distributed approaches is supported by the transmission of communication signals across the communication network.

Common to most of the existing distributed EV coordination approaches is the existence of a central coordinating body, who is in charge of indirectly coordinating the EV charging operations. However, mechanisms for fully distributed EV coordination without employing a central coordinator are also conceivable [Galus et al., 2013]. Distributed charging control of EVs via *hierarchical* coordination is regarded as another promising option, which assumes the existence of a so-called *aggregator* operating as the intermediary between EVs and other entities such as the grid operator, distribution system operator or energy service providers. Specifically, hierarchical coordination systems divide EVs/EVSEs into a number of groups, each of which is assigned to an aggregator at a local control center who communicates with the grid operator at main control center.

To realise centralised and distributed EV charging (and discharging) coordination, researchers have explored numerous algorithms that are based on various mathematical optimisation tools [Rahman et al., 2016; Hu et al., 2016a; Amjad et al., 2018; Shen et al., 2019]. In particular, these algorithmic approaches can be categorized into (1) conventional *mathematical optimisation-based algorithm*s, which include linear programming, quadratic programming, dynamic programming, Lagrange relaxation, binary linear programming, mixed-integer linear programming, mixed-integer nonlinear programming, stochastic programming, mixed-integer linear stochastic programming, game theory, queuing theory etc., and (2) *meta-heuristic algorithms* which include population-based methods (e.g., ant colony optimisation, biogeography-based

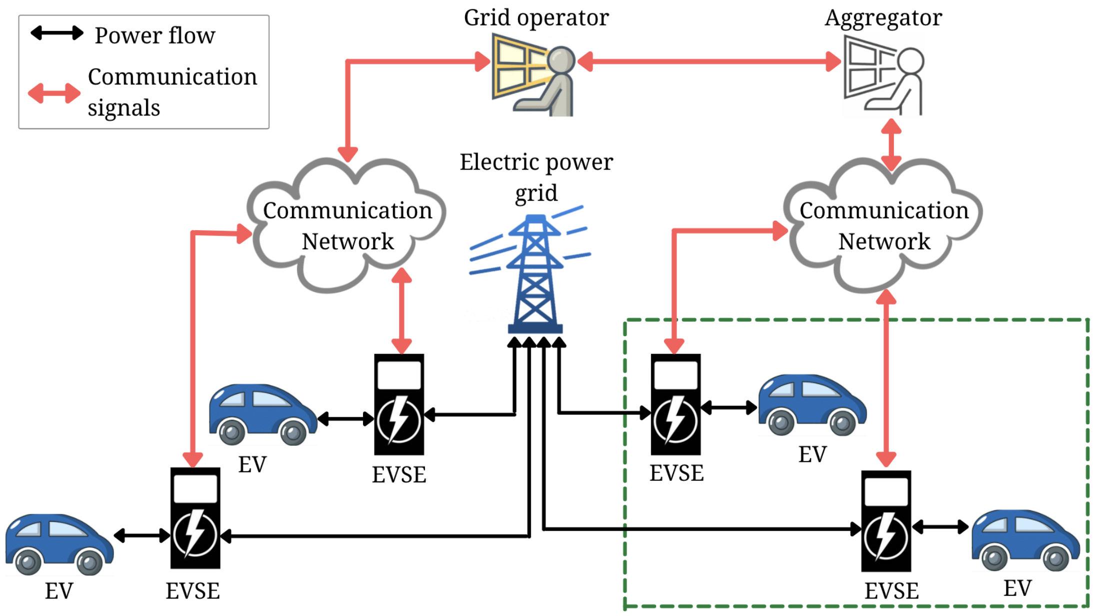

Figure 1.2: Interactions between EVs and the smart grid

optimisation, evolutionary algorithms, genetic algorithms, particle swarm optimisation etc.) and trajectory-based methods (e.g, hill climbing and simulated annealing) [El-Bayeh et al., 2021]. Depending on the nature of the optimisation problem considered for EV charging coordination, these different algorithmic tools may become more or less applicable.

This background and motivation, leads to this thesis investigating how mathematical optimisation-based tools can be leveraged to promote EV-assisted DSM in the smart grid, and thereby address numerous objectives of EV customers and grid operators concerning their financial and operational performance.

1.2 Thesis Objectives

Following from the previous section, in order to fully harness the benefits of expected massive EV rollout, the electric grid must stay prepared to handle the tremendous electric load arising from EV charging at a large scale. As more and more EVs add into the grid, DSM becomes crucial for effective and safe grid operation.

Hence, the primary objective of this thesis is to develop demand-side approaches to coordinate EV charging and discharging operations in the smart grid. We expect that by incorporating these approaches, the existing electric grid will be able to sustain the anticipated surge in EV numbers without requiring major upgrades in existing grid infrastructure., thus enabling a smoother EV-grid integration accompanied by a successful transformation into a fully electrified transportation system.

Specifically, this thesis aims to mitigate adverse impacts of large-scale EV charging (and discharging) in residential distribution networks. By means of coordinated EV charging (and discharging), we manage to overcome undesirable overload conditions and unstable voltage conditions in distribution networks, which otherwise would result in severe power outages and blackouts. To summarise, this thesis presents a set of algorithmic solutions that broadly seek to address the following questions:

> Q1: How can EVs be utilised in demand-side management to provide grid services such as congestion management and voltage regulation?
>
> Q2: How can both EV customers and electrical distributors be benefited via EV-assisted demand-side management?
>
> Q3: How can EV-assisted demand-side management be made highly scalable via distributed computational algorithms?

Here is an example to further elaborate each of the above research questions in a smart grid context. Consider a case where the majority of houses in a residential distribution network have EVs, which take part in home charging by plugging into an electrical outlet at home. As a result of the enormous charging load imposed by residential EVs, the distribution network will likely get impacted by transformer overloads and voltage instabilities. Under Q1, we investigate how EV charging and discharging operations can be coordinated through demand-side management to address such problems and thereby assist electrical distributors to maintain safe power operations. In order to motivate EV users to participate in such demand-side approaches, it is important that they are economically benefited. Hence, the second research question investigates demand-side approaches to balance the interests of EV users and electrical distributors. When the EV numbers increase, it is also important that these demand-side approaches be highly scalable. Hence, the third research question addresses the requirement to develop distributed computational algorithms to coordinate EVs more efficiently.

1.3 Thesis Outline

The remainder of this thesis is organised into three thematic parts to address the thesis objectives described, followed by the concluding chapter that provides a summary of key findings of the research and possible future research directions.

Part 1 (Chapter 2) includes the background and literature review, providing context to the EV charging coordination problem.

Part 2 (Chapter 3 and 4) addresses the question of how to involve EVs for grid congestion management. More specifically, Chapters 3 and 4 investigate approaches to shape the grid load curve, such that the electric load arising from EV charging does not lead to undesirable overload conditions exceeding the network capacity, and Chapter 4 additionally looks at assisting peak load curtailment via EV discharging.

Part 3 (Chapter 5 and 6) addresses the question of how to involve EVs in voltage regulation, where each of the Chapters 5 and 6 proposes a coordinated EV charge (and discharge) approach for under- and over-voltage prevention. Specifically, we look at approaches that combine EV customer economics and voltage regulatory requirements.

At the beginning of each contribution chapter in Parts 2 and 3 of the thesis, descriptions of the motivation for the research study and introductions to the proposed solution are provided. Then, at the end of each contribution chapter in Parts 2 and 3 of the thesis, summaries and explanations of key contributions of the respective chapters are provided. Finally, Chapter 7 draws the conclusions from each of the contribution chapters together and summarises the further work.

References at the end of the thesis correspond to Chapter 1 (introductory chapter), Chapter 2 (background and literature review) and Chapter 7 (concluding chapter) of the thesis, and each paper included in Chapters 2 - 6 contains a separate list of references.

1.4 List of Publications

A complete list of our publications included in subsequent chapters of this thesis is as follows.

[Nimalsiri et al., 2019] N. I. Nimalsiri, C. P. Mediwaththe, E. L. Ratnam, M. Shaw, D. B. Smith, S. K. Halgamuge, "A Survey of Algorithms for Distributed Charging Control of Electric Vehicles in Smart Grid," *IEEE Transactions on Intelligent Transportation Systems*, vol. 21, no. 11, pp. 4497 – 4515, Nov. 2020.

[Nimalsiri et al., 2020] N. I. Nimalsiri, D. B. Smith, E. L. Ratnam, C. P. Mediwaththe, S. K. Halgamuge, "A Decentralized Electric Vehicle Charge Scheduling Scheme for Tracking Power Profiles," in *Proceedings IEEE Power & Energy Society Innovative Smart Grid Technologies (ISGT)*, Washington, DC, USA, Feb. 2020.

[Nimalsiri et al., 2021b] N. I. Nimalsiri, E. L. Ratnam, D. B. Smith, C. P. Mediwaththe, S. K. Halgamuge, "Coordinated Charge and Discharge Scheduling of Electric Vehicles for Load Curve Shaping," *IEEE Transactions on Intelligent Transportation Systems*, May. 2021.

[Nimalsiri et al., 2021a] N. I. Nimalsiri, E. L. Ratnam, C. P. Mediwaththe, D. B. Smith, S. K. Halgamuge, "Coordinated Charging and Discharging Control of Electric Vehicles to Manage Supply Voltages in Distribution Networks: Assessing the Customer Benefit," *Applied Energy*, vol. 291, pp. 116857, June. 2021.

[Nimalsiri et al., 2021c] N. I. Nimalsiri, E. L. Ratnam, D. B. Smith, C. P. Mediwaththe, S. K. Halgamuge, "A Distributed Coordination Approach for Electric Vehicle Charging and Discharging in Unbalanced Distribution Grids," in preparation for submission.

1.5 Overview of Thesis Content and Contributions

1.5.1 Part 1 Background and Literature Review

- **Chapter 2**

  Related publications: [Nimalsiri et al., 2019]

  Overview: Chapter 2 introduces important background concepts on EV charging, providing a more thorough motivation for our interest in EV-assisted DSM. A review is also given of the algorithmic approaches available in the literature for optimising EV charging and discharging in smart grid. Finally, a more focused literature review is provided on the operational objectives which have been selected for study in the subsequent contribution chapters.

  Contributions:

  – An explicit review of existing EV charging control algorithms is provided, with an emphasis on distributed EV charging coordination based on our publication in [Nimalsiri et al., 2019].
  – Different permutations of EV charging control architectures are identified, and their characteristics, benefits and limitations are analysed.
  – A comprehensive classification of existing optimisation problems for EV charging control is presented.
  – A detailed discussion of optimisation tools that can be applied to solve those optimisation problems is provided.
  – A summary of the main features (e.g., control architecture, objective, V2G operation, continuous/discrete rate charging, pricing scheme, mobility awareness, network awareness etc.) of existing distributed EV charging control algorithms is presented.
  – Uncertainties pertaining to EV charging are investigated, and potential algorithmic approaches for managing those uncertainties are analysed.
  – A meticulous literature review on research problems specifically addressed in Parts 2 and 3 of the thesis is presented.

1.5.2 Part 2 Coordinated EV charging and discharging for grid congestion management

- **Chapter 3.** *Coordinated EV charging for tracking arbitrary power profiles*

Related publications: [Nimalsiri et al., 2020]

Overview:

EVs, being deferrable loads, can assist DSM by shifting their charging demands to periods with less congestion or sufficient power generation. For example, EV charging can be coordinated such that the aggregate load profile composed of cumulative residential (non-EV) load and EV charging load follows a given power profile, which, for example, could be the grid's power generation profile (or renewable generation profile). Such coordinated EV charging approaches are expected to improve energy efficiency of the electric grid by yielding a proper energy balance between energy production and consumption. Consequently, electricity suppliers get the maximal benefit from the available power generation, eliminating the requirement to build new electric generators to meet the excessive power demands from EVs.

Contributions:

– An optimisation-based algorithm is proposed for EV charge scheduling with the objective of tracking an arbitrary power profile, while accounting for heterogeneity in EV charging specifications and uncertainty in EV arrival times.

– While shaping the load profile to follow the trend of the given power profile, all EV charging demands are satisfied within each EV user-specified time duration.

– EV charging at both variable rates and discrete rates is facilitated, and charging beyond an EV-specific charge rate is restricted, making the proposed algorithm compatible with different types of EV chargers and battery technologies available in the market.

– The performance of the proposed algorithm is demonstrated using a case study, where EV charging is scheduled following the day-ahead PV generation profile of a microgrid.

• **Chapter 4.** *Coordinated EV charging and discharging for load curve flattening (valley-filling and peak-shaving)*

Related publications: [Nimalsiri et al., 2021b]

Overview:

A load curve with large demand peaks could create a disproportionate effect on power distribution systems by overloading the transformers and other electrical appliances. A flattened load curve, on the other hand, makes grid operation much easier by eliminating the requirement to ramp up and down the power generators to serve the end-user power demands. To achieve a flat load curve, EVs can be coordinated such that they contribute to releasing power to the grid when the non-EV load is at its peak, which is called peak-shaving, and drawing of power from the grid when the non-EV load is at its lowest, which is called valley-filling. It is also of importance to coordinate EVs in a way that they determine their charge-discharge profiles in a distributed manner so that the system scales to handle a large population of EVs.

Contributions:

– A distributedly coordinated, distributed optimisation-based algorithm is proposed for EV charge and discharge scheduling, with the objective of flattening the grid load curve, which is a special case of the more general problem of tracking power profiles considered in Chapter 3.

– The algorithm is designed to incorporate EVs with charge-only capabilities and EVs with both charge and discharge capabilities referred to as gridable EVs. Accordingly, the load curve is flattened by shifting the charging operations of both charge-only EVs and gridable EVs to the valley-period (valley-filling) and discharging operations of gridable EVs to the peak-period (peak-shaving).

– The algorithm is designed to support underlying load curves of arbitrary shapes, and not limited to load curves of particular shapes.

– While flattening the load curve as much as possible, all EV charging demands are satisfied within each EV user-specified time duration.

– Charging and discharging operation of each EV is restricted to be within a given range of rates to accommodate limitations in EV charger and battery technologies. Further, the SoC of each EV battery is restricted to be within a given range of values to prolong the battery health.

– A battery model with separate charging and discharging efficiencies is integrated into the optimisation to ensure operational effects on battery degradation are taken into account.

– EVs are distributedly coordinated by implementing a non-cooperative game, wherein EVs determine their charge (and discharge) profiles locally using a specifically designed algorithm that involves simple computations.

– The uncertainty of EV arrivals and departures is taken into account, allowing the EVs to join and leave the system at random times.

– The performance of the proposed algorithm is evaluated using latest EV specifications and real historical data of the residential power consumption of customers in an Australian distribution network.

1.5.3 Part 3 Coordinated EV charging and discharging taking distribution network considerations and economic considerations into account

• **Chapter 5.** *Coordinated EV charging and discharging for EV operational cost minimisation and voltage regulation in balanced distribution networks.*

Related publications: [Nimalsiri et al., 2021a]

Overview:

The enormous electricity demand imposed by a large population of grid-connected EVs may cause several problems to the electric grid, including excessive voltage deviations, which are detrimental to the reliability and security of grid operations. With the integration of V2G enabled EVs into power grids, electrical distributors are particularly concerned with both peak power flows and reverse power flows inducing significant voltage deviations that lead to regulatory voltage limit violations. Therefore, it is of great importance to develop EV charge-discharge control approaches that specifically consider the distribution grid topology and the associated voltage limitations. Equally important is to benefit the EV customers with minimal charging (and discharging) costs, so that they are motivated to partake in such demand-side approaches.

Contributions:

– An optimisation-based, network-aware EV charging and discharging control algorithm is proposed to balance operational costs accrued to EV customers against improvements in supply voltages across a balanced distribution grid, thus providing benefits to both EV customers and electrical distributors.

– The underlying optimisation problem is formulated as a quadratic program with an objective function to minimise the operational costs accrued to EV customers, which combines the monetary costs of EV charging and discharging and costs of battery degradation, subject to each EV-specific local constraints and coupled voltage constraints. A time-of-use (ToU) financial policy is considered for electricity billing, where V2G operation is compensated by the electricity retailer via net metering.

– In addition to minimizing the financial costs associated with EV charging and discharging, the costs of battery degradation are also minimised to prolong battery lifespan.

– A receding-horizon optimisation approach is combined to accommodate non-deterministic arrivals and departures of EVs, making the algorithm suitable for practical implementation.

– The effectiveness of the proposed algorithm is evaluated by means of extensive numerical simulations carried out on a modified version of the IEEE 13 node test feeder using empirical real-life data of residential EV customers in an Australian distribution network.

• **Chapter 6.** *Coordinated EV charging and discharging for EV operational cost minimisation and voltage regulation in unbalanced distribution networks.*

Related publications: [Nimalsiri et al., 2021c]

Overview: While distribution networks are typically unbalanced, most of the existing network-aware coordinated EV charging approaches are designed for single-phase balanced distribution networks or single-phase equivalents of three-phase distribution networks. Therefore, it is of great importance to design coordinated EV charging approaches focused on regulating voltages in unbalanced distribution networks. The ability to facilitate distributed coordination of EVs without having an aggregator or a centralised coordinator brings an added value to such demand-side approaches.

Contributions:

– A distributedly coordinated, network-aware EV charging and discharging control algorithm is proposed to balance the EV customers' operational costs against improvements in managing bi-directional distribution power flows and supply voltages across an unbalanced distribution grid, thus benefitting both EV customers and electrical distributors.

– The underlying optimisation problem is formulated to minimise the operational costs accrued to EV customers, which combines the monetary costs of EV charging and discharging and costs of battery degradation, while maintaining voltages across an unbalanced distribution feeder within the operational thresholds. A time-of-use (ToU) financial policy is considered for electricity billing, where V2G operation is compensated by the electricity retailer via net metering.

– A distributed coordination algorithm is proposed, whereby the proposed optimisation problem is solved via peer-to-peer communication of EVs in a (arbitrary) connected network.

– A receding-horizon optimisation approach is combined to support near-real-time charging and discharging control operations, while incorporate various scenarios of uncertainties, including non-deterministic EV arrivals and departures, non-EV load forecasts, and changes to EV charging demands.

– The effectiveness of the proposed algorithm is evaluated by means of extensive numerical simulations carried out on the IEEE 13 node test feeder populated with a real-world dataset of residential load collected from households within an Australian distribution network.

Part 1: Background and Literature Review

Chapter 2

Background and Literature Review

Part 1 of this thesis is comprised of Chapter 2, which provides context to the problem of EV charging coordination and reviews the literature on smart EV charging from an algorithmic perspective.

Section 2.1 provides the background of different types of EVs, EV charging options, impacts of EV charging, technological advancements in the EV charging domain (includes V2G), impacts of V2G etc. Section 2.1 also explains how smart EV charging is performed in a smart grid. Then, starting from a discussion on how EVs could assist DSM, existing smart EV charging algorithms are subsequently investigated within two categories: centralised EV charging and distributed EV charging.

Section 2.2 presents our published journal paper that reviews algorithmic approaches on distributed EV charging, which is one of the objectives of this thesis.

Finally, Section 2.3 and Section 2.4 present an up-to-date and focused literature review on EV charging coordination problems that are studied in Parts 2 and 3 of this thesis, respectively.

2.1 Background

The term "*Electric Vehicles* (EVs)" can refer to a broad range of vehicles that are capable of being powered (or charged) by electricity rather than liquid fuels, including road and rail vehicles, surface and underwater vessels, electric air crafts etc. In this thesis, we narrow the use of "Electric Vehicle (EV)" to refer to a passenger car with a battery that requires electrical energy for propulsion.

Plug-in Electric Vehicles (PEVs) refer to a superset of different types of EVs with plug-in feature, including *Battery Electric Vehicles* (BEVs) and *Plug-in Hybrid Electric Vehicles* (PHEVs). BEVs are fully-electric, meaning they are solely powered by electricity and do not have petrol, diesel, or liquefied petroleum gas engine, fuel tank, or exhaust pipe. PHEVs are powered by a combination of liquid fuel and electricity, meaning they have a gasoline or diesel engine coexisting with an electric motor to extend their driving range [ARENA, 2021]. In this thesis, we use "EV" to refer to both types of vehicle, PHEV and BEV. The current EV market has various models of these different types of EVs built by the world's biggest car manufacturers including Tesla, Volkswagen, Nissan, Mitsubishi Motors, Hyundai, General Motors, Toyota and Ford [statista, 2021].

The carriers of electricity in EVs are rechargeable batteries. EV batteries can be recharged by plugging into an electric outlet at homes, workplaces, parking facilities or dedicated charging stations. The time required to fully restore a battery's charge depends on the battery's capacity, the outlet's output power, and battery's current *State of Charge* (SoC), where SoC is a measure of the amount of energy remaining in the battery, expressed either as an energy value (in KWh) or as a fraction/percentage of the battery capacity.

EVs are typically plugged into a charging station (EVSE) to charge their batteries through charger outlets (usually at home garages). Charging facilities for EVs also include parking lots with many charging stations in physical proximity and belonging to the same entity; on-road stations which are relays for EVs on long journeys; and battery-swapping stations. Additionally, wireless power transfer techniques (e.g., inductive power transmission [Khaligh and Dusmez, 2012; Wu et al., 2011b; Lukic and Pantic, 2013]) have been commercially introduced as a convenient alternative to charging conductively. However, the scope of this thesis is narrowed to residential EV charging via EV chargers available at homes and small business places.

In recent years, lithium-ion batteries are increasingly used in EVs due to their superior characteristics such as high energy density, slow self-discharge, long life and less environmental influence [Hannan et al., 2018]. The Constant Current-Constant Voltage (CC-CV) charging method is utilized for the high efficiency charge. The behaviour of CC-CV charging process in lithium-ion batteries is shown in Fig. 2.1 (extracted from [Xing et al., 2015]). In Stage 1, the battery is charged with a constant current. When the battery voltage reaches its limit and becomes a constant, Stage 2 begins. The best functional range of SOC for lithium-ion batteries is from 20% to 85%. When Stage 1 terminates, the battery SoC generally reaches 85%, and therefore it is often recommended to ignore Stage 2 [Wu et al., 2010].

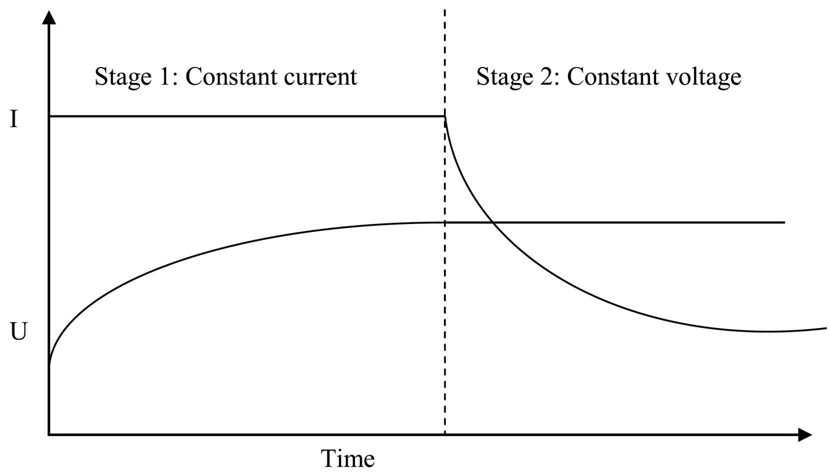

Figure 2.1: CC-CV charging process of lithium-ion batteries (I, current; U, voltage) [Xing et al., 2015]

Charging options for EV batteries can be classified into *slow charging* and *fast charging* with different power ratings [Kong and Karagiannidis, 2016]. Slow charging includes Level 1 AC charging (expected power varies from 1.3 kW to 2.3 kW) and Level 2 AC charging (expected power up to 19.2 kW) using an on-board charger [Yilmaz and Krein, 2012e,b]. Level 1 charging uses a cord in which one end is a standard connector that can be plugged directly to a wall outlet, and the other end is a SAE J1772 standard connector that can be plugged into the EV's charge port [Tuttle and Baldick, 2012]. Level 2 AC charging uses the same SAE J1772-compliant charging cord as in Level 1, however, requires additional charging equipment installation for charging at home, as well as at public charging facilities. Level 2 charging is preferred over Level 1 charging due to its shorter charging time. Fast charging includes Level 3 AC charging (expected power up to 130 kW) for very rapid restoration of battery SOC and is usually available at commercial and industrial locations. Another emerging option for EV charging is DC fast charging, which offers faster and more efficient charging compared to AC fast charging, but requires significant investment in the infrastructure. A comprehensive review of battery charger topologies, charging power levels, and infrastructure for EVs has been presented in [Yilmaz and Krein, 2012c], and a comprehensive discussion of EVs and fundamental industrial informatics infrastructures has been provided in [Su et al., 2011].

Each grid-connected EV is a variable load added to the electric grid, and the impact of EV charging on the distribution networks, especially residential distribution networks, can be substantial with high penetration levels of EVs. According to [Ipakchi and Albuyeh, 2009], a single EV is estimated to double the average household load during charging. Consequently, when a large number of EVs are charged simultaneously, the additional electric load may cause a number of grid problems, including excessive voltage deviations, thermal overloads, elevated power losses, increased aging of transformers and lines, degraded power quality, leading to malfunctioning of home appliances, power outages and blackouts. More reviews on the potential impacts of EV integration to power distribution networks are presented in [Schneider et al., 2008; Putrus et al., 2009; Pillai and Bak-Jensen, 2010; Gong et al., 2011; Green II et al., 2011; Shafiee et al., 2013; Foley et al., 2013; Richardson, 2013; Rizvi et al., 2018; Shaukat et al., 2018].

Interestingly, EVs are deferrable loads with flexible charging requirements as they are often parked for periods of time that are longer than the time required to charge their batteries (e.g., overnight charging). A statistical analysis in [Bhattarai et al., 2017] reports that more than 94% of EVs are available for charging throughout the day, while another study in [Khan et al., 2018] reports that the probability that an EV is parked anywhere during the midday period is over 90%, and that the probability that it is parked at home for most of the day is over 50%. Hence, by exploiting this flexibility of EVs to coordinate their charging demands (i.e., by shifting EV charging demands to time periods with lower residential load), the previously described negative impacts of EV charging on the power distribution networks can be eliminated. Such approaches to control and coordinate the charging of EVs to reduce peak load, are part of a broader context called *Demand-Side Management* (DSM) [Mets et al., 2012]. From the grid operator's perspective, coordinated EV charging ensures power quality, network stability, and operation efficiency of the electric grid, and thereby prevents or delays investments in reinforcing the grid [Kong and Karagiannidis, 2016].

An emerging technology in the EV charging domain is *bidirectional charging* (two-way charging), which allows energy to flow to and from the EV battery. Unlike typical EV chargers that only send energy into the EV (to charge the battery), bidirectional chargers additionally draw power from the EV (discharge the battery when technically supported) to power homes or deliver back to the grid. When an EV is charged, AC electricity from the grid is converted to DC electricity by either the EV's own converter or a converter located in the EV charger. By contrast, when the energy stored in the EV battery is used to power home electrical appliances (V2H) or is sent back to the grid (V2G), the DC electricity used in the EV is converted back to AC electricity [Yilmaz and Krein, 2012f]. A detailed discussion of the technical, economic and commercial viability of V2G operation is provided in [Mullan et al., 2012].

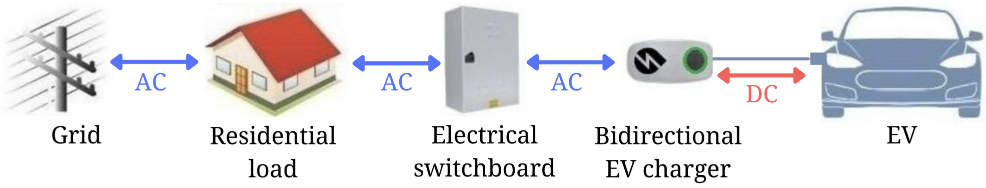

Figure 2.2: Bidirectional charging

EVs with V2G capabilities referred to as *gridable EVs* can also inject electricity back into the grid, serving as distributed energy sources or mobile energy sources [He et al., 2012]. Importantly, V2G may also be used to buffer renewable energy sources, such as rooftop solar or wind turbine generators, by storing excess energy and feeding it back into the grid during high-load periods, thus effectively counteracting the influence of intermittent renewable energy generation [Stüdli et al., 2015]. With bidirectional EV charging, EV owners have the added benefit of earning compensation or incentives by discharging energy at peak hours to reduce the mismatch between power supply and demand. Moreover, bidirectional EV charging has the ability to provide more flexibility in charging and discharging over unidirectional charging, which can also be leveraged to provide ancillary services such as frequency regulation and spinning reserves [Kempton and Tomić, 2005b,a; Han et al., 2010; Sortomme and El-Sharkawi, 2010; Saber and Venayagamoorthy, 2010; Sortomme and El-Sharkawi, 2011b; Saber and Venayagamoorthy, 2011; Wu et al., 2011a; Ota et al., 2011; Luo et al., 2012; Jin et al., 2013]. In these ways, EVs can be active contributors in the smart grid instead of passive consumers.

As described above, V2G comes with many prospects. However, it also comes with several issues for both EV customers as well as power distribution system operators. Distribution grids are typically designed for one-way power from high voltage substations to low voltage customers. Therefore, a significant penetration of EVs when executing V2G operations, potentially degrades the effectiveness of existing voltage control and protection schemes, creating the need for substantial network investment. More specifically, V2G may create undesirable power flows in the distribution network inducing significant voltage fluctuations, power losses, and overloading of transformers (leading to loss of transformer life), cables, and feeders etc, calling for additional investments in larger underground cables and overhead lines, and more transformer capacity.

Another major challenge to V2G transition is the faster battery degradation due to excessive cycling. Battery degradation depends on the amount and rate of energy withdrawn and is a function of discharge depth and cycling frequency. Hence, V2G is likely to reduce battery life drastically. For many battery types, a deeper discharge increases the cell deterioration rate and results in a faster equivalent series resistance (ESR) increase [Dogger et al., 2010], reducing the battery life. However, the ESR tends to increase at low temperatures and at higher levels of SOC. Therefore, the cost of battery degradation can be reduced by using the battery in the middle SOC range (by imposing SoC limits) and restricting the charge-discharge battery cycling. A comprehensive evaluation of the impact of V2G on degradation of EV batteries is presented by the authors in [Bishop et al., 2013].

Other significant issues associated with V2G includes the need for intensive communication between the vehicles and the grid, effects on grid distribution equipment, infrastructure changes, and social, political, cultural and technical obstacles [Yilmaz and Krein, 2012d]. A more comprehensive examination of the benefits and barriers with respect to V2G transition is presented in [Sovacool and Hirsh, 2009]. A review on the V2G technologies and the impact of V2G operation on the distribution grid and utility interfaces is provided in [Yilmaz and Krein, 2012f; Clement-Nyns et al., 2011; Yilmaz and Krein, 2012g]. Then, a review on V2G and renewable energy sources integration is presented in [Mwasilu et al., 2014]. Finally, a review of controlled charging–discharging issues with respect to system performance such as overloading, deteriorating power quality, and power loss is presented in [Solanke et al., 2020].

The importance of information and communication technologies (ICT) for the implementation of coordinated EV charging control approaches can never be overemphasized. Interestingly, the transformation of the traditional electric grid to the smart grid facilitates fast and secure communication and data transmission via ICT, enabling EVs to coordinate with other smart entities. An overview of different communication technologies that facilitate communication in smart grid, such as Wi-Fi, power line communications, IEEE 802.15.4 (Zigbee), ZWave, and cellular networks is provided in [Markel et al., 2009; Gungor et al., 2011].

Designing an algorithm for EV charging control and coordination generally requires an optimisation approach, which determines a set of charge profiles specifying when EVs are to be charged and at what rates (if the rate of charging can be tuned) in order to meet their anticipated energy requirements. Specifically, a *charge profile* for an EV is characterised by a tuple of values, each of which represents the EV charge rate assigned to some time interval. Much of the literature formulates EV charging coordination as a constrained optimisation problem, which optimises a certain operational or financial/cost performance objective of the grid-operator, EV user, or aggregator, subject to constraints specifying various limitations in terms of charging infrastructure and grid infrastructure, and various requirements of entities involved (e.g., the primary requirement of EV users is to have their batteries charged to the expected SoC by the time they need their vehicle). The types of objective functions and constraints for EV charging control span a very wide range, giving rise to different forms of optimisation problems [Callaway and Hiskens, 2010], and no single mathematical formulation exists for the problem in general. For instance, there have been EV charging studies aimed to optimise *grid-side objectives* such as minimising cost of power supply [Hutterer et al., 2012], minimising grid operation cost [Khodayar et al., 2012], minimising system load variance [Li et al., 2011], minimising distribution system losses [Sortomme et al., 2010], maximising the profits of thermal and wind plants [Al-Awami and Sortomme, 2011]; *EV user objectives* such as minimising charging cost [He et al., 2012; Saber and Venayagamoorthy, 2011; Erol-Kantarci and Hussein, 2010; Cao et al., 2011], maximising the average SOC of EVs [Su and Chow, 2011], maximising user convenience [Wen et al., 2012]; and *aggregator objectives* such as maximising aggregator profits [Jin et al., 2013] and reducing the imbalances arising out of the energy purchased by the aggregator from the day-ahead market and the actual energy consumed by EVs [Vandael et al., 2010].

In the literature, there have been several surveys and reviews of coordinated EV charging approaches. In [García-Villalobos et al., 2014], a detailed review of smart charging approaches is presented, and in [Rahman et al., 2016], the literature on the use of optimisation methods for EV charging control is reviewed. A comprehensive review on the optimisation objectives of various charging strategies and challenges facing V2G implementation is presented by the authors in [El-Bayeh et al., 2021]. A survey of economy-driven approaches for charging EVs in a smart city is presented in [Shuai et al., 2016], with game theory as a special tool to model and analyse the interactions among self-interested actors. In Xiang et al. [2019], a survey on charging load modelling methods (e.g., Monte–Carlo methods, Markov chain theory, fuzzy logic etc.) is presented. Then in [Islam et al., 2019a], a systematic review and a comparison of the performance of techniques available to mitigate the network unbalance of a distribution grid integrated with or without distributed generation and EVs, is presented.

In [Mukherjee and Gupta, 2014], EV charge scheduling algorithms are classified into two broad classes of unidirectional versus bidirectional charging, and then each class into centralised or distributed and whether any mobility aspects are considered or not. Then in [Wang et al., 2016], the interactions between the smart grid and EVs are studied and coordinated EV charging is analysed from three different perspectives, in terms of smart grid-oriented, aggregator-oriented and customer-oriented smart charging. By contrast, in [Kong and Karagiannidis, 2016], the state-of-the-art of existing EV battery charging schemes is reviewed by classifying them into four classes, namely uncontrolled, indirectly controlled, smart, and bidirectional charging, the last three of which are collectively called controlled charging. In [El-Bayeh et al., 2021], EV charging and discharging strategies are categorised based on: complexity; economics and power losses on the grid side; ability to provide ancillary services; operation aspects; and detrimental impact on the EV, the power grid, or the environment.

An important aspect to be considered when developing an EV charging control algorithm is the design of the control scheme. There exists in the literature, a plethora of algorithmic approaches proposed for coordinated control of EV charging in smart grid, which can be primarily categorised into (1) *centralised* and (2) *distributed control* schemes [Nimalsiri et al., 2019].

In centralised EV charging coordination schemes, a central operator directly controls EV charging operations [Jian et al., 2017; Sundstrom and Binding, 2011; Clement-Nyns et al., 2009; Sortomme et al., 2010; Yi et al., 2020; Sortomme and El-Sharkawi, 2010; Han et al., 2010; Sortomme and El-Sharkawi, 2011b; Saber and Venayagamoorthy, 2011; Khodayar et al., 2012; Erol-Kantarci and Hussein, 2010; Sortomme et al., 2010; Sortomme and El-Sharkawi, 2011a; Al-Awami and Sortomme, 2011; Deilami et al., 2011; Richardson et al., 2012; Su and Chow, 2011; Lee et al., 2012; Kim et al., 2012; Xu and Pan, 2012; Jin et al., 2013]. In particular, the central operator collects from each EV, information about their power requirement, expected departure time and charging specifications (parameters such as initial SoC, maximum battery capacity, maximum charge rate etc.) and then solves a centralised optimisation problem to determine the charge profile for each EV. However, centralised control algorithms raise concerns on EV user privacy as they require the acquiring of accurate and complete EV information from each EV. On the other hand, centralised approaches become computationally intractable when a large number of EVs is involved in the optimisation problem.

2.2 Distributed EV Charging Coordination

As EV uptake continues to increase worldwide, the centralised control paradigm becomes less practical and will potentially be augmented with distributed control schemes that are highly scalable. Hence, the development of algorithms for distributed charging control of EVs has lately been a subject of significant research interest. Compared to centralised EV coordination approaches, distributed EV charging coordination approaches offer several potential advantages: shared computing leading to lower computational burden; parallel computing allowing faster computational time; limited amounts of information sharing leading to lower communication burden and lower expense for the necessary communication infrastructure; enhanced robustness with respect to failure of individual entities; improved cybersecurity; and enhanced EV user privacy preservation [Nimalsiri et al., 2019]. Importantly, distributed EV charging control schemes allow the collaboration of multiple entities to make EV charging decisions via distributed computation and communication, and hence unlock the full benefits of technological advancements of the smart grid.

Much of the existing distributed EV charging approaches employ an *aggregator*, which acts as the intermediary between the demand side (EV users) and the supply side (e.g., grid operator or distribution system operator) to coordinate EV charging operations. In the real-world, an aggregator could be an EV charging facility such as a charging station, a parking lot, a power network substation, or an electric retailer [Gkatzikis et al., 2013; Bessa and Matos, 2012]. In the literature, distributed EV charging approaches are more commonly implemented using *decentralised* coordination structures, wherein EV users determine their charge profiles locally by communicating with a central coordinator (e.g., grid operator or an aggregator) or with other EVs participating in the coordination scheme. Researchers have also explored distributed EV charging approaches using *hierarchical* coordination structures, where EVs are clubbed into groups assigned to multiple aggregators and the charging decisions for each group of EVs is either directly controlled by the aggregator in a centralised manner, or coordinated (indirectly controlled) by the aggregator in a decentralised manner.

2.2.1 Published Manuscript

This paper reviews state-of-the-art distributed EV charging control algorithms for smart grid. It serves as a comprehensive one-stop reference that summarises the key features and implementation details of distributed EV charging schemes proposed in the literature.

N. I. Nimalsiri, C. P. Mediwaththe, E. L. Ratnam, M. Shaw, D. B. Smith, S. K. Halgamuge, "A Survey of Algorithms for Distributed Charging Control of Electric Vehicles in Smart Grid," IEEE Transactions on Intelligent Transportation Systems, vol. 21, no. 11, pp. 4497 – 4515, Nov. 2020.
https://doi.org/10.1109/TITS.2019.2943620

A Survey of Algorithms for Distributed Charging Control of Electric Vehicles in Smart Grid

Nanduni I. Nimalsiri, Chathurika P. Mediwaththe, *Member, IEEE*, Elizabeth L. Ratnam, *Member, IEEE*, Marnie Shaw, David B. Smith, *Member, IEEE*, and Saman K. Halgamuge, *Fellow, IEEE*

***Abstract*— Electric vehicles (EVs) are an eco-friendly alternative to vehicles with internal combustion engines. Despite their environmental benefits, the massive electricity demand imposed by the anticipated proliferation of EVs could jeopardize the secure and economic operation of the power grid. Hence, proper strategies for charging coordination will be indispensable to the future power grid. Coordinated EV charging schemes can be implemented as centralized, decentralized, and hierarchical systems, with the last two, referred to as distributed charging control systems. This paper reviews the recent literature of distributed charging control schemes, where the computations are distributed across multiple EVs and/or aggregators. First, we categorize optimization problems for EV charging in terms of operational aspects and cost aspects. Then under each category, we provide a comprehensive discussion on algorithms for distributed EV charge scheduling, considering the perspectives of the grid operator, the aggregator, and the EV user. We also discuss how certain algorithms proposed in the literature cope with various uncertainties inherent to distributed EV charging control problems. Finally, we outline several research directions that require further attention.**

***Index Terms*— Decentralized control, distributed optimization, electric vehicles, hierarchical control.**

I. Introduction

INCREASED societal awareness of environmental issues associated with vehicular emissions has spurred the development of cleaner solutions for transportation. In this respect, electrified vehicles are emerging as the defining trend of transportation [1]. Recently, a dramatic increase in the adoption of EVs has additionally been attributed to decreasing battery costs and cheaper electricity prices compared to escalating fuel prices [2]. Despite the numerous benefits of EVs, large populations of grid-connected vehicles will potentially create grid congestion problems leading to costly network expansion. For example, charging a single EV will potentially double the energy consumption of an average household [3]. In cases where millions of EVs simultaneously charging across the grid, new peak load events will arise and/or existing peak load events will be compounded.

By contrast, coordinated EV charging using intelligent control strategies supported by Information and Communication Technology (otherwise known as *smart charging*) potentially offers opportunities to improve grid utilization and limit network expansion. Researchers have been developing numerous smart charging algorithms, many of which require the acquisition and processing of large amounts of information at a central point. In cases where the large computational overhead, or requirements for supporting communication infrastructure are considered impractical, alternatives to centralized approaches, such as distributed algorithms have been considered. In particular, distributed algorithms are highly scalable both from computation and communication points of view.

As opposed to centralized control schemes where all the relevant parameters are collected and a central calculation is performed by a single entity, distributed control schemes are performed by several entities that obtain certain relevant parameters via communication. Specifically, a distributed charge control scheme assigns the processing load over several agents, so that each agent only needs to solve its own small-scale problem, and as such, each agent bears the control of the charge schedules to a certain extent. Distributed charging schemes, in particular, can be realized as *decentralized* and *hierarchical* schemes, where decentralized schemes share the computational load across EVs and hierarchical schemes share the computational load across both EVs and aggregators (intermediaries between the power grid and the EV users).

In this paper, we review a specific class of EV charging schemes, namely *distributed EV charging schemes*. The key contributions of this paper are summarized as follows: distributed EV charging has not seen a focused survey, and to the best of our knowledge, this paper is the first (1) to present an explicit review of distributed charging control algorithms; (2) to elucidate the distinction between different permutations of distributed charging control architectures, based on the method of sharing computation and the structure of communication; (3) to provide a comprehensive classification of EV charging optimization problems (OPs) to better understand the existing distributed EV charging schemes studied under operational and cost aspects of grid operators, EV users, and aggregators; and (4) to assess several distributed EV charging schemes with respect to managing uncertainties related to the power grid, the electricity market, and the behaviour of EV users.

Manuscript received December 12, 2018; revised June 3, 2019 and August 2, 2019; accepted September 6, 2019. Date of publication October 2, 2019; date of current version October 30, 2020. The Associate Editor for this article was A. Malikopoulos. *(Corresponding author: Nanduni I. Nimalsiri.)*

N. I. Nimalsiri and D. B. Smith are with the Research School of Electrical, Energy and Materials Engineering, The Australian National University, Canberra, ACT 2601, Australia, and also with Data61, CSIRO, Eveleigh, NSW 2015, Australia (e-mail: nanduni.nimalsiri@anu.edu.au; david.smith@data61.csiro.au).

C. P. Mediwaththe, E. L. Ratnam, and M. Shaw are with the Research School of Electrical, Energy and Materials Engineering, The Australian National University, Canberra, ACT 2601, Australia (e-mail: chathurika.mediwaththe@anu.edu.au; elizabeth.ratnam@anu.edu.au; marnie.shaw@anu.edu.au).

S. K. Halgamuge is with the Department of Mechanical Engineering, The University of Melbourne, Melbourne, VIC 3010, Australia, and also with the Research School of Electrical, Energy and Materials Engineering, The Australian National University, Canberra, ACT 2601, Australia (e-mail: saman.halgamuge@anu.edu.au).

Digital Object Identifier 10.1109/TITS.2019.2943620

There have been several surveys related to EVs and their influences [4]–[6]. A number of surveys related to EV charging schemes are presented in [7]–[10]. By contrast, we review a specific category of EV charging schemes referred to as distributed EV charging schemes. Specifically, the authors in [7] describe centralized and decentralized schemes, without mention of hierarchical schemes that have been widely explored in the recent literature. The authors in [8] propose a more general classification of charging schemes as uncontrolled, indirectly controlled, smart, and bidirectional. In [9], charging schemes are first classified as unidirectional or bidirectional and then as centralized or decentralized, and whether mobility aspects are considered or not. Complementary to [8] and [9], we review distributed charging schemes based on two significant classifications that consider: (1) the distributed control architecture model; and (2) the objective function of the OP, and thus we present a concise and comprehensive overview of distributed charging schemes. Further, we consider several other uncertain aspects of EV charging other than EV mobility. The authors in [10] present a classification based on grid, aggregator, and customer oriented charging. By contrast, we first classify charging schemes based on the operational and cost aspects of the OP, and then further classify with regard to the objectives of grid-operator, aggregator, and EV user.

This paper is organized as follows. In Section II, we provide background to EV charging. In Section III, we identify several properties of EV charge control schemes. In Section IV, control architectures for coordinated EV charging are introduced. Section V reviews a number of distributed EV charging control schemes and related uncertainties. In Section VI, we highlight several future research directions, followed by the conclusion in Section VII.

II. Background

An EV uses electrical energy as the principle means of propulsion. Fig. 1 illustrates the bidirectional power flow between EVs and the smart grid, where electrical energy generated by power plants and renewable energy sources (RESs) recharges the EV battery (grid-to-vehicle: G2V) and the electrical energy delivered back to the grid discharges the EV battery (vehicle-to-grid: V2G). An aggregator often acts as a proxy between EVs and the power grid as well as the electricity market in managing smart interactions, so that the grid-operator need not directly deal with a large number of EVs. In reality, an aggregator could be a utility company, an EV charging facility, a fleet operator of a parking lot or a communication device at a transformer [11]. The information exchange between smart entities is through two way digital communication enabled by ubiquitous wireless networks and broadband power lines. The power networks and communication networks together build up a complex network. Therefore, proper control strategies supported by well established communication, measurement, and control infrastructures are crucial for the successful rollout of EVs.

In an EV battery, the state of charge (SoC) is the percentage of remaining energy capacity. The relationship between the external charging power and the rate of change of SoC of the battery can be approximated using a battery model [12].

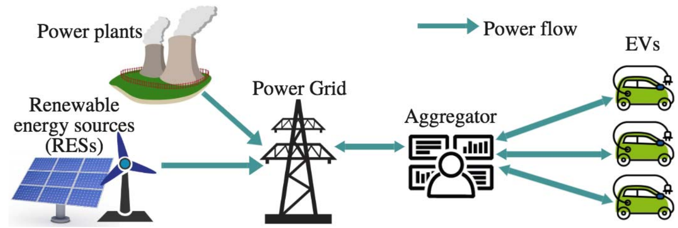

Fig. 1. Interactions between EVs and the smart grid.

Due to the conversion losses during charging, only a part of the total amount of energy drawn from the grid is effectively dispatched for charging an EV [13].

Demand-side management (DSM) of EVs refers to reducing the peak load by shifting EV charging to time periods with less congestion [14]. Given the duration that EVs are typically idle (e.g., overnight at a residence and during work hours at an office), EVs are considered an ideal prospect for DSM. As such, the three key dimensions that need to be considered for DSM of EVs are: (1) space (where to charge); (2) time (when to charge); and (3) speed (at what rate to charge). An EV owner might charge the battery overnight, e.g., start when arriving home and finish the next morning when departing for work. During the day time, an EV owner might charge the battery at the kerbside or in a parking lot. EVs can also be charged in EV charging stations (EVCSs) at times when immediate charging becomes inevitable during a trip. Compared to charging at home, EVCS operators may offer lower prices because they generally purchase large volumes of power from the wholesale power market at cheap rates. In addition, the deployment of fast charging stations, especially in densely populated areas where the majority of users have no access to over-night charging is also becoming increasingly popular. Importantly, fast charging solutions reduce long charging times and potential range anxiety of drivers. Furthermore, wireless power transfer for EVs using magnetic resonance is also gaining widespread interest [15].

EVs outfitted with bidirectional power converters (chargers and inverters) can act as electrical loads (during charging) as well as electrical sources (during discharging). Because EVs remain mostly stationary over the course of a day, opportunities to partake in ancillary services through V2G operations are possible. Nonetheless, V2G operation exhibits several drawbacks, including premature degradation of batteries and increased operational energy losses.

III. Properties of EV Charging Control Schemes

Here we introduce some important properties relating to EV charging control schemes.

A. One-Time, Open-Loop Versus Recursive Closed-Loop Control

One-time, open-loop control strategies (*offline strategies*) are calculated once, based on the predicted operation of the system, and thus assume perfect knowledge in advance of EV scheduling. For instance, EV charging schemes such

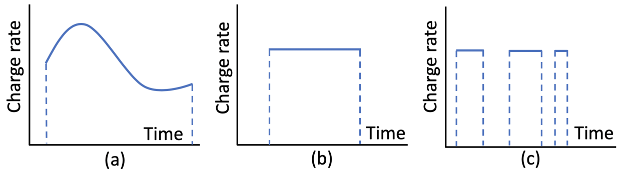

Fig. 2. Charging at (a) variable rates and (b-c) discrete rates.

as [13], [16], [17] are formulated such that all the EVs are available for negotiating their charge schedules at the beginning of the time horizon. However, in a more realistic setting, neither the EV arrival times nor the status of the distribution power network is known a priori. By contrast, recursive closed-loop control strategies (*online strategies*) are calculated multiple times, based on feedback measurements, hence capable of handling numerous uncertainties, including the mobility of EVs. For instance, EV charging schemes such as [18]–[20] solve the control problem progressively in the order that information becomes available (See Section V-C for more details).

B. Charging at Variable Versus Discrete Rates

In the literature, EV charge rate is often considered a variable that can take an infinite number of values between zero and the maximum charge rate, as depicted in Fig. 2(a) [21]–[24]. In practice, residential charging is mostly done at discrete rates (Fig. 2(b-c)), because discrete rate chargers with simple on-off controllers are much cheaper than variable rate chargers that require sophisticated equipment to modulate the power. Further, the efficiency of a charger potentially decreases if charging is not conducted at its full capacity [25]. Nevertheless, *variable rate charging (VRC)* can be better exploited for DSM, compared to charging at a fixed rate.

For an OP with VRC, it is required to find the charge rates for each time instant at which the EVs are grid-connected. In the cases of *discrete rate charging (DRC)*, the maximum output power of the charging equipment or the maximum charging power of the battery restricts the charge rate. In particular, DRC can be implemented in an uninterrupted (constant) [26] or interrupted (binary) [27] manner as shown in Figs. 2(b-c). The decision variables for the former DRC are the times at which each EV starts charging. The additional decision variables for the later DRC, where EVs are charged at discrete time slots that are separated by idle slots, are to charge at a predefined rate or to not charge at all. With such a charging approach, the battery gets to cool down during the idle slots, which in turn improves the battery life [28]. For effective operation, the number of on-off switchings should not be too high, as frequent switching will also deteriorate some batteries [29], and in cases of wide-spread implementation, frequent switching reduces the quality of power delivered to grid-connected customers [30], [31]. To balance the flexibility of VRC against the practicality of DRC, researchers have recently considered charging schemes with a finite set of charge rates between zero and a maximum value [32].

C. Homogeneous Versus Heterogeneous EV Specifications

Certain EV charge scheduling algorithms such as the one presented in [16] perform well for a homogeneous or identical EV population. However, a practical algorithm should perform with heterogeneous charging specifications from the EV population. In particular, heterogeneity in the charge duration, charge rate, along with heterogeneity in user preferences such as charging location are needed for practical demonstrations.

D. Pricing Strategies

A *flat* rate refers to a pricing scheme with a fixed fee for each energy unit regardless of the time at which energy is consumed. In contrast, a time-varying pricing regime provides an incentive to coordinate EV charging. For example, a *time-of-use* (TOU) rate, where electricity is billed at a different rate during peak, shoulder and off-peak periods, provides an incentive to shift EV charging from the peak pricing period. In this way, grid congestion co-incident with the peak pricing period is alleviated. However, new charging peaks (or rebound peaks) potentially form when many EVs charge simultaneously during the off-peak pricing period. To mitigate the rebound peaks, a resurgence of interest in *real-time pricing* (RTP) strategies that reflect contemporaneous power system conditions has occurred. RTP represents either the actual energy cost for a utility generating electricity or purchasing electricity at a wholesale level, or the cost imposed by a utility for load control. RTP rates are generally increasing functions of the instantaneous demand, hence users can influence the real-time electricity rate by adjusting their energy consumption [33]. In addition, *customized* pricing strategies are also proposed in certain EV charging control schemes [34], [35].

IV. EV Charging Control Architectures

In this section, we describe EV charging control architectures illustrated in Fig. 3. We consider charging decisions for a group of EVs that are made by a central entity or by individual EVs, with the former called *centralized* control, and the later called *decentralized* control. *Hierarchical* control features aggregators and EVs arranged like a tree structure. An aggregator may either directly or indirectly control a group of EVs. A *direct aggregator* decides the charge schedule for each EV in the group. By contrast, an *indirect aggregator* broadcasts information signals to the EVs to coordinate their charge profiles. As such, an indirect aggregator is not required to be computationally powerful since the computation load is shared by the other entities.

A. Centralized Control Architecture

Fig. 3(a) depicts a centralized architecture, where the charge schedule of each EV is decided by a direct aggregator, who collects the charge requirements of all the EVs, then solves an OP to determine the rate at which each EV will charge, and communicates the optimization-based charge schedule back to the EV owners. Consequently, each EV owner relinquishes some autonomy over their charge schedule. Nevertheless, centralized schemes have the advantage that they often produce

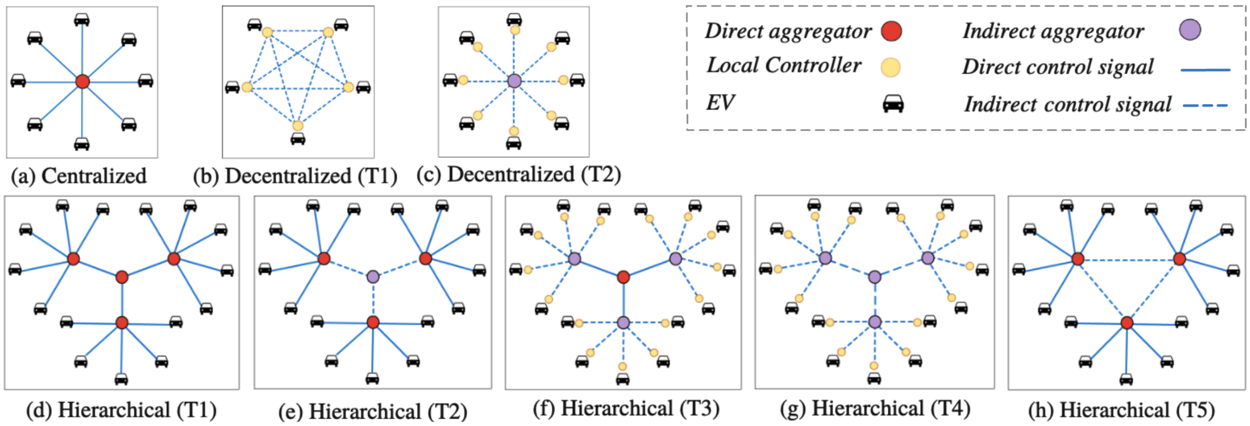

Fig. 3. Centralized EV charging control architecture and variations of distributed (decentralized, hierarchical) EV charging control architectures.

optimal solutions as complete information of the entire system is available to the aggregator. Further, centralized schemes can readily consider various global system states and coupling constraints. However, such benefits must be weighed against the EV owner concerns with the privacy of information relayed to the communication network. Moreover, a single point of failure at the aggregator (e.g., failure to solve the OP) could potentially collapse the entire system, creating the need for a backup system.

A key challenge for centralized approaches is scalability, especially when the size of the OP increases in the length of the planning time horizon and the number of connected EVs. Therefore, a centralized approach is potentially computationally intractable with respect to the implementation time. Additional complexities arise when the number of control variables and constraints of each EV increases. Furthermore, centralized approaches require EV users to communicate to the central controller complete information of charging requirements and technical specifications of EVs. This may potentially lead to practical obstacles such as communication bottlenecks, bandwidth limitations, and costly expansion of the supporting infrastructure to handle the explosive increase of data from rapid EV uptake. Consequently, centralized approaches may lose their efficiency and become impractical when large numbers of EVs grid-connect.

B. Decentralized Control Architecture

Decentralized systems are different from the centralized systems in that each EV acts as an independent decision-maker who solves its own problem that is small in size. As such, decentralized solutions do not always correlate with optimal charging regimes, especially in cases where there is a lack of complete information at the individual EV tier. Nevertheless, there is considerable interest in decentralized solutions, since they are highly scalable (in terms of computational complexity) and practical with respect to field implementation.

Depending on the structure of the communication network, Figs. 3(b-c) depict two decentralized control architectures. The *decentralized Type 1 (T1)* is a center free design where EVs locally compute and adjust their schedules by communicating with the other EVs, until a global equilibrium is achieved. Such an architecture enforces EVs to continuously communicate their scheduling information with the other EVs, resulting in a large communication overhead, especially when the number of EVs is very high. The *decentralized* (*T2*) architecture reduces the communication overhead by introducing an indirect aggregator who gathers certain information and broadcasts control (coordination) signals to all the EVs. As such, the requirement for large scale communication infrastructure is reduced. Importantly, decentralized charging schemes are more resilient to network failures, especially when controllers are designed to operate in the event of a centralized communication failure.

C. Hierarchical Control Architecture

In the recent literature, we observe a particular interest in hierarchical control system design that is not fully centralized, nor fully decentralized. Unlike centralized systems, hierarchical systems delegate control and computational load to multiple direct or indirect aggregators via a tree-like communication topology. By doing so, the need for network-wide communication is also reduced. Each aggregator coordinates a group of EVs while influencing the decisions of the other aggregators. A group may include EVs in a single location, e.g., situated in a parking lot or located in an apartment block. Each hierarchical architecture, depicted in Figs. 3(d-h), balances the benefits of centralized and decentralized architectures in a distinctive manner. First four structures (depicted in Figs. 3(d-g)) feature three tiers: a central aggregator on the top tier, sub-aggregators in the middle tier, and EVs at the lower tier. A *hierarchical* (*T1*) architecture features a central aggregator that calculates a collective charging plan for all the sub-aggregators, where sub-aggregators decide each EV-specific schedule. In the *hierarchical* (*T2*) architecture, the central aggregator issues control signals to each sub-aggregator, transferring the computational overhead to multiple sub-aggregators that determine the charge schedules of EVs in their groups. In the *hierarchical (T3)* architecture, a central aggregator calculates a collective charging plan for all sub-aggregators, whereby each sub-aggregator indirectly controls a group of EVs by broadcasting signals, transferring the computational overhead of calculating charge schedules to the EVs. The *hierarchical* (*T4*) is a communication structure where all the aggregators (central aggregator and sub-aggregators) and EVs coordinate via indirect control signals. It is worth mentioning that the hierarchical (T3) and (T4) control architectures preserve decentralized behavior of EVs.

The hierarchical structures depicted in Figs. 3(d-g) are still vulnerable to single points of failure. For example, if the central aggregator collapses, all the sub-aggregators and EVs will be left uncontrolled. To mitigate against such an occurrence, the *hierarchical* (*T5*) architecture that is composed of a communication network across the aggregators (as depicted in Fig. 3(h)) is proposed. In cases where a link between two aggregators collapses, an alternative communication path connecting the aggregators would improve system resilience. However, if one of the aggregators collapses, EVs connected to that particular aggregator will remain uncontrolled.

V. Distributed EV Charging Control Algorithms

A distributed algorithmic approach divides a centralized OP into a set of subproblems of a much smaller scale, that is solved by several EVs and/or aggregators. As such, decentralized and hierarchical control architectures naturally align with distributed computational systems. In this section, we review numerous decentralized and hierarchical charging control schemes that have been proposed in the literature.

Much of the early literature formulates the EV charging control problem as a *constrained OP*, with charge rates and charge durations defined as the decision variables, and with various constraints introduced to incorporate requirements of the grid operator, aggregators, and EV users. The realization of a distributed algorithm for a centralized OP is notably challenging, especially in certain non-convex OPs where the objective function and constraints are coupled to the individual charge rates of EVs, to network capacity or to electricity prices. Despite non convexity and NP-hardness, certain OPs have been solved to attain optimality or near optimality using a variety of techniques, e.g., relaxation [36], cuts [37], preprocessing [38], heuristics [19], randomization [39].

In Fig. 4, and in what follows, we organize EV charging control OPs into two categories based on (A) *Operation aspects* and (B) *Cost aspects*, and discuss numerous distributed algorithmic approaches that have been proposed to solve them.

A. Operation Aspects

1) Grid Operator's Perspective:

a) Load regulation: Among all possible ways of regulating the EV load, numerous studies are focused on flattening the aggregate load (EV and non-EV load) curve. By flattening load curve peaks, the risk of overloading transformers and other electrical infrastructure is reduced. Further, a flattened load curve eliminates the requirement to ramp up and down the generators, enabling a steady-state operation with maximum efficiency. Scheduling EVs to fill the overnight load valley, where the non-EV load is at its lowest, is widely addressed in the literature. Although the influence of a single EV is minor, the aggregate influence of a fleet of EVs can be substantial in terms of load flattening.

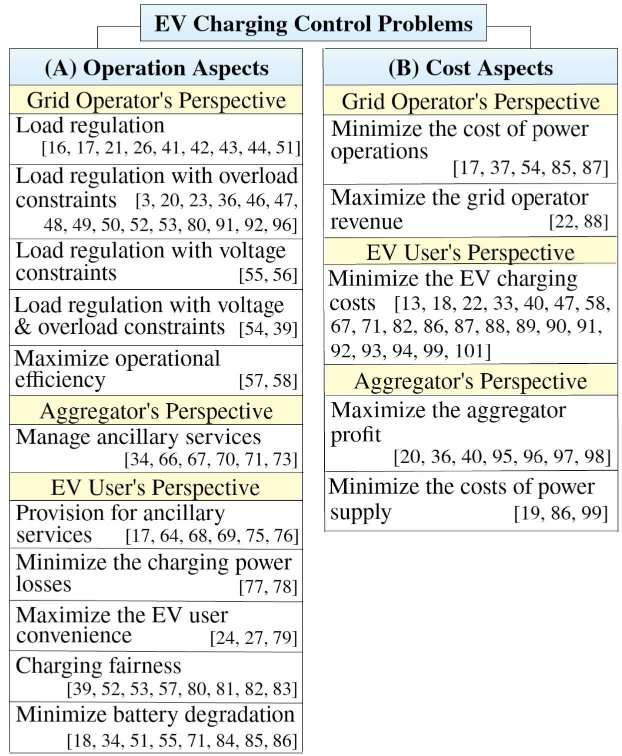

Fig. 4. The classification of EV charging control problems and the respective distributed EV charging control schemes from the literature.

Consider a power system where N number of EVs schedule their charge profiles over T time slots, each of length Δ_t. Let s_i^{arr}, s_i^{dep}, b_i, p_i^{min}, p_i^{max} and η_i be the SoC at arrival, the expected SoC at departure, the battery capacity, the minimum charging power, the maximum charging power, and the charging efficiency of the ith EV. Let $D(t)$ be the non-EV load profile, which is known a priori. The charge rates denoted by $p_i(t)$ are the decision variables. The most intuitive approach for load flattening (or valley filling) is minimizing variance of the aggregate load profile [41] and the corresponding OP is

$$\min_{p_i(t)} \sum_{t=1}^{T}(D(t) + \sum_{i=1}^{N} p_i(t))^2 \tag{1a}$$

$$\text{subject to, } \sum_{t=1}^{T} \eta_i p_i(t)\Delta_t = (s_i^{dep} - s_i^{arr})b_i, \tag{1b}$$

$$p_i^{min} \leq p_i(t) \leq p_i^{max}, \tag{1c}$$

where the energy demand and the range of acceptable charge rates of the EV are defined by constraints (1b) and (1c) respectively. One potential approach to fill the load valley is to influence EV users through electricity prices [21]. As such, an aggregator may broadcast control signals, for example, price-like signals that vary in proportion to the aggregate demand. Accordingly, each EV user will selfishly seek to minimize charging costs by scheduling the EV to charge at a time that fills the load valley.

Game theory is a promising tool that can be used to coordinate EV charging by way of optimizing individual EV charge preferences. In [16], a non-cooperative game is established to coordinate a large population of EVs who are weakly coupled via a common electricity price. The proposed game is based on a decentralized (T2) architecture, where the utility (indirect aggregator) broadcasts the aggregate EV demand after collecting the charge strategies of all the EVs. In response, EVs update their charge strategies and report them to the utility. The process iterates until the penalty imposed for the deviations of individual charge strategies from the average charge strategy vanishes. Specifically, the load curve valley is filled at the Nash Equilibrium (NE) of the game – a state where none of the EVs benefit by unilaterally deviating from their chosen charge strategies [21]. More formally,

$$f_i(p_i^*;\, p_{-i}^*) \geq f_i(p_i;\, p_{-i}^*);\quad \forall\ p_i \in P_i,\ \forall\ i \in \{1, .., N\} \tag{2}$$

where f is the payoff function, p_i is the charge schedule vector of EV i, p_{-i} is the vector containing the charge schedules of all the EVs other than EV i ($p_{-i} = [p_1, .., p_{i-1}, p_{i+1}, .., p_N]$), P_i is the set of all feasible charge schedule vectors of EV i, and p^* are the EV charge schedule vectors at the NE [21]. Due to nature of the specific penalization strategy in [16], the proposed algorithm is proved to be optimal only for an infinite, homogeneous EV population.

In contrast, Gan *et al.* [21] present an optimal decentralized (T2) charging (ODC) algorithm that converges to optimality for both homogeneous and heterogeneous EV fleets. In the proposed algorithm, the utility (indirect aggregator) progressively guides EVs by altering a control signal (e.g., electricity price) in response to the last received EV charge profiles. At each iteration, upon receiving the control signal from the utility, EVs individually update their charge profiles in order to minimize the sum of the electricity cost and the penalty for deviating from the charge schedule calculated in the previous iteration. Importantly, the ODC algorithm performs well even with asynchronous consumption, e.g., where EVs do not necessarily update their charge profiles in each iteration or update their charge profiles using outdated control signals. Therefore, the proposed charging scheme is quite robust to communication delays and failures. In [42], a variant of the ODC algorithm is developed to solve a discrete OP that is focused on charging EVs at discrete charge rates. In each iteration, a communication device at the transformer (indirect aggregator) broadcasts the normalized demand using the EV charge profiles from the previous iteration. Accordingly, each EV computes a probability distribution over its potential charge profiles and samples from the distribution to update its charge profile.

Based on the decentralized (T2) architecture, Li *et al.* [41] presents an online algorithm to regulate EV loads through an indirect aggregator who publishes a charging reference using the real-time aggregate EV load, after which EVs make binary decisions to charge or not, by comparing their SoC with the reference signal. It is shown that such an algorithm solves a generalized maximum weight OP. Importantly, the proposed algorithm is an on-line algorithm, which does not rely on forecasts, and as such, it is not affected by forecast errors. Using dynamic programming (DP) and game theory, an algorithm for valley filling and peak load shaving is developed in [43]. The problem of scheduling a single EV is solved using a forward induction DP algorithm. Since including multiple EVs in the DP algorithm increases the quantity of states at each time step, a non-cooperative game is formulated to coordinate multiple EVs in a decentralized (T2) manner.

A possible drawback of the mentioned charging schemes in [16], [21], [41]–[43] is the iterative nature of the respective routines, and the subsequent time they potentially take to reach the global equilibrium. Alternatively, the authors in [26] propose a non-iterative approach of scheduling a single EV at a time in a sequential manner in accordance with a decentralized (T2) model. The algorithm aims to minimize both the variance and the maximum peak of the aggregate load. A weight factor is carefully chosen to adjust the priorities between the two objectives. Once connected to the grid, an EV receives from the grid operator (indirect aggregator), the aggregate load profile for the scheduling horizon, i.e., non-EV load plus the power required to charge EVs already scheduled. Based on that information, EV solves a local OP to find its charge schedule and reports the updated load profile to the grid operator, who then submits it to the next EV. Such a scheduling approach is greedy in the sense that it determines the charge schedule of an EV only once, which occurs at the time when the EV grid-connects. Although the extensive bidirectional communication at each time step is eliminated, a possible disadvantage is the waiting period encountered by EVs that connect simultaneously. To overcome that issue, the authors modify the algorithm to update the total load profile by combining the charge schedules of all the EVs that connect simultaneously. Still, there exists the risk of forming adverse second peaks if a large number of EVs grid-connect at the exact same time. The study in [44] also utilizes a sequential scheduling approach to design a decentralized (T2) charging scheme that aims to minimize the mean square error between the real-time aggregate load and a reference operating point estimated offline using data related to non-EV load and EV mobility.

Network-aware charging refers to the consideration of distribution network constraints (e.g., overload control constraints, nodal voltage constraints) in EV charge scheduling. With network-aware charging, the operational envelopes of existing power systems are considered to limit costly network expansion. In what follows, we discuss load regulation schemes focused on network-aware EV charging.

b) Load regulation with overload control: Sustained overloading of a transformer can overheat the transformer windings, which results in its premature failure. Incorporating a distribution overload constraint as follows

$$\sum_{i=1}^{N} p_i(t) + D(t) \leq C;\quad \forall\ t \in \{1, .., T\}, \tag{3}$$

where C is the rated capacity of the transformer/feeder, is a way to minimize congestion by limiting the maximum power that a transformer can carry at any time. By considering the optimal valley filling theory of ODC [21] and the distribution network topology across EVs, Ghavami *et al.* [3] develop two decentralized (T2) algorithms based on the gradient projection method (GPM), to minimize the load variance subject to the overload constraint (3). In the first algorithm, the primal problem of (1) is augmented with a cost function that associates to the overload constraint of the feeder and the GPM is applied. A limitation that exists in that algorithm is requiring the step size of the GPM to be smaller than a certain system dependent threshold. The second algorithm is an application of the primal-dual method to circumvent the nonseparability of the problem and interestingly, the second approach does not require a specific upper bound on the step size. While both overload control methods are observed to be quite effective in controlling feeder overload, the first algorithm seems to attain faster convergence whereas the second algorithm seems to perform better in terms of overload control.

By extending the algorithms in [21] and [45], the reference [23] proposes three decentralized (T2) algorithms to minimize the total load variance subject to network capacity constraint (3). Since the charge rates of EVs are coupled by both the electricity cost and the transformer capacity, two control signals are introduced to flatten the load profile and to manage the overload constraint. The first two algorithms minimize load variance using the ODC algorithm and enforce capacity constraint using the alternating direction method of multipliers (ADMM) – a powerful tool for solving large scale OPs by breaking the problem into smaller and manageable subproblems which are easier to solve. Those two algorithms differ in the time scale at which the two subroutines execute. The third algorithm employs ADMM for both subroutines. These different algorithms result in different message passing structures and exhibit different trade-offs between the feasibility and the optimality of the solutions. A sparsity promoting EV charging scheme in [46] also employs the ADMM method to generate a set of sub-problems with decoupled feeder overload constraints, which are solved by EVs independently using the dual-gradient method. However, none of the algorithms in [23], [46] are online, hence they do not capture real-time dynamics of the system.

In the decentralized (T2) charging scheme proposed in [47], the transformer overload constraints are handled by incorporating the transformer load levels in the price-signals published by the aggregator. In [48], a decentralized (T2) ant-based swarm algorithm is proposed, where EVs are treated as ants of a dynamic reunion. Each ant (EV) decides a valley filling charge schedule according to the pheromones released by the other ants, which are updated whenever the total load surpasses the maximum power capacity of the transformer. Although the convergence of the proposed algorithm is guaranteed, the time to converge is uncertain, and as such, the approach is potentially impractical for real-time implementations. Inspired by the water filling principle in information theory, the authors in [49] propose a decentralized (T2) algorithm for flattening the load profile. For each single EV, a constant water level is defined and it is adjusted through an iterative bisection method until the charge rates obtained by subtracting the non-EV load profile from the water level satisfy the energy demand of the EV. The water filling process is performed by EVs, one at a time, in coordination with the indirect-aggregator. The overload constraints of transformers are handled by reducing the energy demands of EVs according to a specific ratio, and as such, the congestion is prevented at the expense of not totally satisfying the EV demands. In order to ensure a fair dispatch of power, EVs are served in a circular order, and consequently certain EVs may encounter a considerably long waiting period. In [50], the algorithm in [49] is extended to a decentralized (T2) charging control scheme with discrete rates, using the idea of pulse width modulation. Later in [51], the algorithm in [49] is utilized to approximately solve the problem of valley filling and peak load shaving, by defining a time point before and after which EVs discharge and charge respectively.

The study in [52] presents a decentralized (T2) algorithm to avoid persistent bus congestion while ensuring a proportionally fair share of the distribution network capacity among the EVs. It is assumed that the congestion level of every branch can be measured and communicated to the downstream EVs in real-time with a reasonably low delay. To avoid bus congestion, EVs are charged at the maximum rate when the network is lightly loaded, and at a relatively low rate when the network is highly loaded. Hence, the intuition of the algorithm is to quickly control the charge rates in real-time such that the bottleneck lines and transformers are appropriately utilized. At times when the grid is overly congested, some EVs may not be fully charged by their deadlines, in favor of protecting the power system assets, thus the algorithm provides a best effort service. Since charge rates of EVs that belong to the same transformer are coupled, the dual decomposition method is used to obtain a set of distributively solvable subproblems, each of which is solved by an individual EV. Further, charge rates of EVs are adjusted based on the congestion price signals issued by the measurement nodes installed on the way to the substation. In a later work [53], the authors extend the algorithm to a dynamic setting where household loads and the number of EVs being charged change over time. The main limitation of charging schemes in [52], [53] is the heavy communication overhead, where each EV receives a message every 20ms. Moreover, the algorithms rely heavily on fast scale measurements and low latency broadband communications, hence a robust communication and measurement infrastructure is crucial.

c) Load regulation with voltage control: Another important consideration of a network-aware charging control scheme is the maintenance of a proper voltage level at every node of the grid. It can be enforced using an approximated power flow model [54], [55]. The authors in [55], [56] introduce an algorithm called shrunken-primal-dual subgradient, to minimize load variance while regulating nodal voltage magnitudes. The algorithm features a two-tier projection where primal and dual variables are shrunken and expanded. The system operator (indirect aggregator) guides EVs through several iterations by broadcasting the dual variable associated with the nodal voltages and the Lagrangian gradient calculated from the recent charge profiles of EVs. Unlike an ordinary primal-dual subgradient method which suffers from regularization errors, the proposed algorithm converges to optimality without regularizing the Lagrangian. However, such an algorithm requires an accurate network model and knowledge of injections and extractions of real and reactive power at every point in the network, which in practice will always be imprecise, and therefore real-time control methods to make up for these errors will be necessary.

d) Load regulation with voltage and overload control: By utilizing a linearized power flow model, the authors in [54] formulate an OP to regulate the charging load of EVs while minimizing the operational cost. Specifically, a network-aware charging scheme that respects both voltage and feeder transformer limits is developed. Since the transformer capacity and nodal voltages couple power flow across buses, a decoupled and decentralized (T2) algorithm is formulated using the ADMM and Frank-Wolfe methods. Besides provable convergence, the algorithm protects the privacy of users by only sharing the sum of EV charge profiles with the control center (indirect aggregator) through a communication protocol arranged over a tree graph rooted at the control center. As such, EVs which constitute the tree nodes add their charge profiles to the aggregate charge profiles from the downstream nodes and forward to the parent nodes. Upon receiving the sum of charge schedules, the control center broadcasts the cost gradient vector, based on which the EVs reschedule.

The authors in [39] present a random access charging algorithm to protect the distribution grid from bus congestion and voltage drop. The OP is formulated to maximize the number of EVs that can be charged under the given system capacity. The underlying system architecture is a decentralized (T2) model, where EVs take charging decisions based on the information of load capacities and voltage drops of system buses published by the control center (indirect aggregator). At every time slot, a set of EVs suspend charging process to provide opportunities to the waiting EVs, thereby ensures fairness within the implementation. It is worth mentioning that the respective algorithm involves no forecasts, and no convex optimizations – and as such, implementation appears to be simpler than other considered approaches.

e) Maximize operational efficiency: Another important operational aspect from the grid operator's standpoint is balancing the electricity generation and the demand for enhanced operational efficiency. To this end, the authors in [57] present a decentralized (T2) and token based IT infrastructure, which provides energy as a service via generation and consumption of tokens of energy. It is comprised of a heuristic algorithm to maximize the average utilization of generation, while ensuring that the total amount of power consumed by EVs is less than the amount of power allocated for charging the EVs. The practical implementation of such a system requires a perfect and seamless communication infrastructure for the negotiation of token exchange between the producers and the consumers of energy. In [58], a game theoretic approach following a decentralized (T2) architecture is proposed to balance the planned electricity generation in real-time. It is a two-stage algorithm where EVs and energy storage systems aim to flatten the load profile by adjusting the residential load to follow a day ahead energy plan. In the first stage, EV users play a non-cooperative game with mixed strategies to determine the day ahead anticipated demands that minimize the electricity costs, based on which the aggregator determines a plan to generate or purchase electricity for the next day. In the second stage, EV owners play a real-time game to adjust their consumption patterns so as to stay close to the predicted demands. The implementation of such a scheme requires specific equipment to be installed at the houses, and hence incurs a high capital investment for the EV customers.

2) Aggregator's Perspective:

Manage ancillary services: If proper incentives are offered, EV users are likely to actively participate in a multitude of ancillary services: frequency regulation [59]–[62], voltage control [63], spinning reserve [64], [65], active and reactive power compensation [66], [67] etc. To manage the variability of renewable power generation, contribution from a large number of EVs is required. In a market environment, EVs seeking to contribute to ancillary services could be managed by a third party aggregator.

Frequency regulation is a short time scale ancillary service which aims to establish an instantaneous balance between the generation and the demand. As such, energy stored in EV batteries can be used to fine-tune the frequency and voltage of the grid by charging them when generation exceeds demand and discharging them when demand exceeds generation. A number of charging schemes are proposed to suppress the primary frequency fluctuations of the power grid [68]–[70].

Liu *et al.* [70] present a decentralized (T2), V2G control scheme, where the aggregator estimates the regulation capability of the EV fleet. Whenever the frequency deviation is out of the predefined dead band, EVs with sufficient SoC discharge power using an adaptive frequency droop control method. A potential drawback of such a method is that it requires a priori analysis of the specification of droop parameters. On the contrary, the authors in [71] propose a decentralized (T2) regulation algorithm that follows a plug-and-play concept, without requiring such parameterization. It has an indirect aggregator generating a set of virtual price signals to reflect the deviation of the aggregate EV charge/discharge profiles from the day ahead energy schedule derived from [72]. Based on these signals, EVs compute their schedules to optimize the virtual cost/income from charging and discharging.

The authors in [73] propose a backup battery bank deployed by an aggregator to maintain a stable regulation capacity. The interactions between aggregator and EVs in a V2G market are modelled as a decentralized (T2) game, where the payoff of an EV is interpreted as the payment that an EV receives for participating in the frequency regulation service. Based on the command signal issued by the grid, specifying a power level for regulation, the aggregator computes all possible Nash equilibria, selects one randomly, and then EVs simply follow it. However, the authors have not incorporated the EVs' own charging requirements into the game model.

The authors in [34] develop a V2G scheme for providing distributed spinning reserve to customers with different reliability levels. When a shortage of generation capacity or a power outage happens, customers with lower subscription of reliability are cut off, and distributed spinning reserve from EVs is used to provide power to those customers with higher subscription of reliability. The proposed decentralized (T2) scheme consists of two levels of games that are coordinated by the electricity retail market (indirect aggregator). At the lower level is a non-cooperative game that coordinates the charge schedules based on a specific V2G strategy. At the upper level, an evolutionary game is implemented to evolve the EVs' V2G strategies. For each evolving step of the evolutionary game, the lower level non-cooperative game finds a new NE. Hence, both levels reach equilibrium when the evolutionary equilibrium is reached. Although a reliability-differentiated pricing scheme appears very beneficial for realizing DSM, in practice, it is hard to differentiate the delivery of electricity in terms of reliability due to the intrinsic limitations of current power systems [74]. As a result, the research direction outlined in [34] has not received sufficient attention in the recent literature.

Active and reactive power compensation contributes to voltage regulation, power loss reduction and power factor correction [67]. The authors in [66] present a hierarchical (T1) V2G scheme for the active power compensation of EVCSs that intend to provide active power with minimum incremental costs of EVs. The aggregators (EVCS controllers) coordinate using a task-swap mechanism, such that, for each active current, a single aggregator receives the current measurement information of sudden active load change, according to which a command signal specifying the appropriate active power to be compensated is distributed to their EVs. In contrast, the authors in [67] present an algorithm for reactive power compensation of EVs. The objective function of the aggregator is interpreted as the total insufficiency of reactive power reservoir, which is to be minimized. The objective function of an EV is defined as the sum of parking cost, charging cost, and penalty cost (for unscheduled EVs), which is also to be minimized. The resultant multi objective OP is solved using the normalized normal constraint method to obtain a set of well-distributed pareto optimal solutions. Then a decentralized (T2) algorithm based on Lagrangian decomposition is proposed to make the optimization scalable as the number of EVs grows.

3) EV User's Perspective:

a) Provision of ancillary services: There is considerable literature on approaches to involve EVs in ancillary services without an intermediary, e.g., a third party aggregator. For example, the authors in [75] present a decentralized (T1) algorithm where consensus filtering is utilized to acquire consistent and accurate frequency signals by all the EVs. However, consensus mechanisms often require a large number of iterations before reaching the stopping criterion, and hence take a significantly longer computing time. In contrast, the decentralized (T2) algorithms proposed in [64], [68], [69] facilitate EVs to contribute to frequency regulation and spinning reserve according to the frequency deviation at the plug-in terminal, which is a signal of supply and demand imbalance in the power grid. The decentralized (T2) scheme proposed in [17] is comprised of two algorithms for load shifting and frequency regulation, with the later based on a frequency droop control method. Since the two control algorithms are functionally separated by time scale (load shifting on a long time scale and frequency regulation on a short time scale), they are combined to balance both objectives. The study in [76] proposes an iterative, decentralized (T2) algorithm for voltage control, where an indirect aggregator broadcasts the voltage on all pilot nodes based on the charge profiles of EVs in the previous iteration. Accordingly, EVs updates their charge profiles to limit their impact on the voltage plan.

b) Minimize the charging power losses: From the EV user's standpoint, another objective to consider is the minimization of power losses caused by the internal resistance of a battery during charging. The authors in [77] propose a decentralized (T1) scheme to minimize the power losses during charging, while satisfying the system constraints. The OP is characterized by a Lagrangian variable called incremental cost, and the charge rates are determined by exchanging the information of incremental cost and available global power capacity, using a consensus algorithm. A limitation of [77] is the required initialization procedure during each EV charge cycle. Later, the authors in [78] extended the work to an initialization-free charge control scheme where EVs start from any charge power allocation.

c) Maximize the EV user convenience: EV users often wish to attain a high level of user convenience in their charging operations. A form of an objective function for maximizing user convenience is

$$\max_{p_i(t)} \sum_{i=1}^{N} \sum_{t=1}^{T} w_i(t)\ p_i(t), \tag{4}$$

where w_i is a weight factor. The authors in [27] devise a DRC scheme to select the optimal EV subset that maximizes the weighted sum (4), with a weight factor chosen to characterize the charging duration and the final SoC of EVs. The resultant combinatorial, non-convex OP is solved using the ADMM method. In the proposed hierarchical (T4) system, the sub-aggregators report the average EV energy demand of their respective groups to the central aggregator, who then completes the update of the dual variable and broadcasts to the EVs to decide whether they should charge or not based on a threshold discriminator. In contrast, Malhotra *et al.* [24] present a DRC scheme with a hierarchical (T5) control architecture to maximize the cumulative user convenience characterized by the remaining SoC, remaining time to charge, and charge rate, while also sharing the limited amount of power available from the grid (global power constraint). Here, sub-aggregators at the substations exchange EV user convenience values through a consensus algorithm and locally evaluate the specific threshold control signals to define the set of EVs allowed to charge within the global power constraint. Additionally, the local power constraints of substations are ensured by truncating the ordered set of EV user convenience values of each substation. Although the algorithm is shown optimal for the homogeneous case, it exhibits a very small optimality gap for the heterogeneous case.

In contrast to maximizing the weighted sum as in (4), another form of an objective function focused on enhancing the EV user convenience is maximizing the charge rates of EVs, such that the desired final SoC is achieved within the shortest time. The authors in [79] propose a local control method where EVs are able to act independently without relying on external control signals to operate. Specifically, each individual EV maximizes the charge rate while maintaining the service cable loading and the voltage of the customer point of connection within acceptable limits. An additional charge rate constraint is imposed to avoid large variations of the charge rate over consecutive time steps, for the purpose of prolonging the battery service time. However, when compared to the corresponding centralized control method, the proposed local control method is not as capable of maintaining network parameters within the specified limits, and thus requires larger safety margins.

d) Charging fairness: Classical heuristic charge scheduling algorithms ensure various types of fairness criteria, such as the first come first serve, earliest deadline first, shortest job first, lottery policy [26]. Except for the first come first serve, the other policies require centralized data collection of EVs to decide their ordering, hence can undermine the efficiency of the algorithm. Depending on the objective function chosen, the solution may provide different notions of fairness: equal access fairness, proportional fairness, max-min fairness, etc.

Inspired by the bandwidth sharing approach that is used in communication networks, the authors in [80] develop a packetized, decentralized (T2) charge control approach, where sharing power among EVs is considered analogous to the problem of sharing a constrained channel in communication systems. All the EVs are assigned with a similar automaton in order to ensure fair and equal access to the feeder capacity. EVs are then charged over multiple short time intervals using charge packets that are approved after checking whether their load could be accommodated into the distribution system. The algorithm does not require EVs to report their charge schedules back, and thus provides benefits over many other schemes by reducing communication overhead significantly.

Several charging schemes have been proposed to ensure proportional fairness based on certain priority criteria (e.g., current SoC, remaining time to charge). The authors in [81] formulate a decentralized (T1) charge control scheme to maximize the weighted sum of SoC of EVs for the next time step, using Karush-Kuhn-Tucker (KKT) conditions of optimality and consensus algorithms. Interestingly, by ensuring fairness in the SoC distribution, EVs attain a reasonable SoC even in the event of an early departure. Inspired by the concept of congestion pricing in Internet traffic control, the authors in [82] propose a charging scheme, where fairness is ensured based on the amount that the EVs wish to pay, defined in terms of a parameter called willingness-to-pay (WTP). The objective function of an EV user is chosen to maximize the difference of its utility (a non-decreasing logarithmic function of the EV demand and the WTP value) and the energy cost. An interesting observation made is that as EVs with large WTP values finish charging, the price turns cheaper for EVs with smaller WTP value.

Additive increase multiplicative decrease (AIMD) is an algorithm that is suitable for large scale systems where users join and leave frequently. AIMD also exhibits the notion of fairness by sharing the available resources fairly among all the system entities. Using the AIMD algorithm, the authors in [83] develop a set of decentralized (T2) charge control schemes to maximize the limited amount of power that can be obtained from the grid. During the additive phase of the algorithm, EVs increase their charge rates by additive factors until the aggregate power demand of EVs reaches the available power capacity, which is known as a capacity event. Upon detecting a capacity event, the multiplicative decrease phase activates and EVs reduce their charge rates by multiplicative factors determined in a probabilistic manner. Specifically, three scenarios of interest are considered, namely a domestic, a workplace, and an EVCS, with utility functions of equal power sharing, fair power sharing, and minimum time power-sharing respectively. Parameters of the domestic charging scenario are fine-tuned to assign the same priority to each EV (equal fairness), whereas the parameters of the workplace charging scenario are fine-tuned to allocate higher charge rates for EVs who are in need of more energy (proportional fairness). Compared to the algorithms which require extensive communication among system entities, AIMD is proven to be highly efficient as it can be implemented by EVs without any communication at all, except that of the notification of the capacity event.

e) Minimize battery degradation: In certain distributed charge-discharge schemes, as in [34], [51], [84], the minimum and maximum SoC are specified to protect the battery from early degradation. In several other schemes such as [18], [34], [55], [71], [85], [86], the cost of battery degradation is included in the objective function of the OP.

B. Cost Aspects

Here we review cost aspects and associated objective functions for distributed algorithmic approaches from the perspective of the (1) grid operator, (2) EV user, and (3) aggregator.

1) Grid Operator's Perspective:

a) Minimize the cost of power operations: Cost of power generation is an important concern of the grid operator. Shao *et al.* [37] present a bidirectional power control framework to minimize fuel costs and startup-shutdown costs of generators. A hierarchical (T3) framework is developed to model the cooperative power dispatch among the system operator (SO) on the top level, aggregators in the middle level and EVs at the bottom level. Since the grid side formulation (upstream) and the EVs side formulation (downstream) can be connected via the aggregator net power, the system architecture fits Benders decomposition – a technique that is useful when the number of constraints of an OP is considerably high. The SO solves the master problem for determining the net power of each aggregator that contributes to a minimal overall generation cost, while also considering a series of constraints such as grid reserve, power balance, transmission capacity, and minimum/maximum aggregator net power. The resultant power shares of the aggregators and the charge/discharge powers determined by the EVs are then fine-tuned for several iterations using approximate benders cuts.

In addition to minimizing the generation cost, the algorithm in [17] aims to charge EVs with minimal carbon dioxide emissions, while reducing the dependency of conventional regulation plants. Here, the grid controller (indirect aggregator) publishes a cheap power trajectory, upon which EVs execute a decentralized (T2) algorithm that consists of two parts: gain and SoC deficiency. The former becomes significant when the due time is short and the power is cheap. The latter ensures that

EVs with lower SoC receive higher charge rates. In contrast, the OP in [87] is formulated as a multi-objective OP aimed to minimize both the generator costs and the EV charging costs. In the proposed hierarchical (T2) system, the SO (central aggregator) optimizes the system dispatch using the most recent charge schedules of EVs and alters the price signal, so that the sub-aggregators reschedule. The negotiation process happens until neither SO nor sub-aggregators change decisions between two successive iterations. At this point, the system achieves a socially optimal equilibrium. In the hierarchical (T1) charge-discharge control scheme in [85], the upper-level aims to minimize the total cost of system operation by jointly dispatching generators and aggregators, and accordingly the lower-level computes the charge-discharge strategies for each EV following the dispatch instructions from the upper-level.

b) Maximize the grid operator revenue: Stackelberg game (SG) is a type of a non-cooperative game that deals with multi-level decision making processes of a group of followers in response to the decision of a leader [22]. For an energy trading game between the grid operator and EV groups (EVGs), Tushar *et al.* [22] model a hierarchical (T2) SG to decide the strategic electricity price that optimizes both the EV charging cost and the revenue of the grid operator from selling energy. Given the amount of energy requested by EVGs, the grid operator (leader) chooses an electricity price to maximize the revenue. Accordingly, EVGs (followers) choose the amount of energy that they wish to purchase in order to optimize a utility that captures a trade-off between the benefit from charging and the associated cost. Since the total amount of energy offered to the set of EVGs is constrained in the study, EVGs seek a variational equilibrium, which is a type of a generalized-NE (GNE) that is more socially stable. For a given GNE demands of EVGs, the grid chooses an energy price that maximizes the revenue of the grid. The game eventually converges to a socially optimal Stackelberg equilibrium, where EVGs achieve their equilibrium strategies for the optimal energy price determined by the grid operator. In [88], a decentralized (T2) charge/discharge control framework is proposed to optimize the revenue of a set of microgrids and the charging cost of EVs. Specifically, a dynamic pricing policy is proposed to decide the electricity price based on the real-time supply-demand curve of each microgrid. In response, the charging decisions are made by EVs using a multi-attribute decision process.

2) EV User's Perspective:

Minimize the EV charging costs: EV users are often considered as price anticipators who are willing to adjust their charge profiles according to their impact on the electricity price. A form of an objective function for minimizing the charging cost of a group of EVs is

$$\min_{p_i(t)} \sum_{t=1}^{T}\sum_{i=1}^{N} c(t)\ p_i(t), \tag{5}$$

where $c(t)$ represents the electricity price, which with respect to RTP is a function of the instantaneous total demand. The intuition from equation (5) is that the action taken by a user affects the performance of the other users through $c(t)$. In a decentralized charging setup, each EV user wishes to selfishly choose an action which minimizes its individual charging cost. As such, EV charging can be interpreted as a non-cooperative game among the EV users. If every EV user of the game picks their cost-minimizing strategy, there will be a stable state, known as the NE, where no user can decrease the cost unilaterally (2). Given the vector of charge schedules of all the other EVs other than EV i (p_{-i}), and assuming that p_{-i} is fixed, the *best response strategy* of EV i can be defined by

$$\min_{p_i}\ f_i(p_i;\ p_{-i}), \tag{6}$$

where f_i is the payoff function and $p_i = \sum_{t=1}^{T} p_i(t)$. In the decentralized (T1) energy scheduling game described in [33], each user computes the best response strategy by solving (6) and announces that to the other users to update their best responses accordingly. The update process takes place until no new schedule is announced by any user. When users simply follow what is best for them, the total energy cost monotonically decreases in each iteration until the game converges to the NE. Besides provable convergence, such an algorithm is strategy proof, which means no user benefits from being untruthful when broadcasting the charge schedule. Similarly, in [47], a decentralized (T2), non-cooperative and dynamic game is proposed to coordinate EVs through price-signals that are broadcasted by an indirect aggregator.

For the problem of minimizing the overall energy cost of a set of EVs controlled by a set of aggregators, the authors in [13] devise a non-cooperative game that follows a hierarchical (T5) control architecture. For each potential subgame among the aggregators, the optimal charge profiles that result in the NE are calculated using the best response strategies (6). The significance of their study is incorporating two user behavioral models called expected utility theory and prospect theory to evaluate the ideal and non-ideal actions of the aggregators respectively. In contrast, the authors in [86] propose a non-cooperative game implemented as a decentralized (T2) system, in which the NE is calculated by considering the distribution of driving patterns and the relationship between the EV demand and its influence on the electricity spot prices. In [89], a strictly convex N-person game in the form of a decentralized (T2) system is developed using a probabilistic model of the EV charging patterns. In more detail, a data center notifies to the EVs, the mean and variance of the historical EV loads, based on which the EV users calculate the most cost-effective time to start charging their EVs for that particular day. The game continues for the next day with updated information from the previous day, and as such, each day is an iteration of the game seeking the NE state. Most importantly, smart chargers tend to learn a better strategy in a progressive manner. However, all the above-mentioned game theoretic approaches require a lot of computational overhead due to the iterative routine. In contrast, Cao *et al.* [90] propose a heuristic algorithm to minimize the charging costs in a regulated market operated under TOU pricing. Specifically, the authors consider a much realistic scenario, where the maximum EV charging power is different at various SoC levels. In addition to minimizing the charging costs (day-ahead), the authors in [91] consider minimizing the thermal overloading of transformers. The combined OP is transferred to a partial Lagrangian problem which is separable between fleet operators who coordinate with the Distribution System Operator (DSO) in a decentralized (T2) manner. The authors in [92] propose a hierarchical (T2) control scheme to minimize the EV charging costs while abiding by substation supply constraints. To avoid peak load at the substation transformer, a capacity based tariff scheme is proposed to surcharge load excursions exceeding a penalty load threshold.

None of the charging schemes mentioned above consider discharging of EVs. Interestingly, Nguyen and Song propose a decentralized (T2) algorithm to coordinate charge and discharge of multiple EVs in a building's garage. Here, EVs intend to charge and discharge in a way that the total payment to the building is minimized. Since each EV wants to schedule its energy profile in order to pay less, a non-cooperative game is played to select their best strategies (6) independently. In contrast, the authors in [93] propose a decentralized (T1) charge control system that constitutes a retail market layer of EVs and a set of aggregators who are requested to provide certain amounts of energy from EVs. In response to the prices announced by the aggregators, EVs play a multi-stage game to minimize the charge-discharge costs. The NE of the game is sought using a consensus-based algorithm, where EVs estimate the average charge available in their immediate neighborhoods and decide the amount of energy to trade.

3) Aggregator's Perspective:

a) Maximize the aggregator profit: In the real world, an aggregator is a profit-seeking entity with a large customer base. Oftentimes, aggregators purchase energy at wholesale prices through long term bilateral contracts or by participating in the day ahead electricity market based on forecasted electricity prices [94]. The OP for maximizing profits earned from selling the purchased electricity is

$$\max_{p_i(t)} \sum_{j=1}^{J}\sum_{i=1}^{N_j}\sum_{t=1}^{T}(\ c_{ret}(t) - c_{pur}(t)\ )\ p_i(t), \tag{7}$$

where i, N_j, c_{ret}, and c_{pur} denote EV i, number of EVs of aggregator j, electricity retail price, and purchase price respectively. For charging EVs in multiple local communities with multifamily dwellings, Qi *et al.* [36] propose a hierarchical (T2) scheme where a primary distribution transformer (central aggregator) serves multiple parking decks (sub-aggregators) that purchase electricity from the utility at TOU rates and sell it to the customers at retail prices. In addition to maximizing the revenue of the sub-aggregators, the unfulfilled charging demands are penalized to minimize the loss of customer goodwill. The transformer capacity constraints are enforced by applying Lagrangian relaxation and including them as penalty terms in the original objective function. The resultant OP is solved using the distributed subgradient method with respect to each parking deck. In detail, the sub-aggregators constantly report their projected power consumption profiles to the central aggregator, who then updates the Lagrangian multipliers and broadcasts to the charging decks back. Interestingly, only the aggregate charging demand of each parking deck is required to be publicized, hence the algorithm does not disclose individual EV charging information to the central aggregator.

Xu *et al.* [20] present a hierarchical (T1) charging control framework to maximize the profit of the aggregator by minimizing the energy purchase costs under TOU tariffs. A three-step procedure is carried out wherein the first step each aggregator reports to the DSO the aggregate power boundaries based on customer charging requirements and local transformer capacity limit. In the second step, the DSO decides the optimal power share of each aggregator. Then in the final step, each aggregator allocates charge rates to the EVs in their groups, using a heuristic method which chooses to dispatch power in the order of the desired SOC and the remaining parking duration of EVs. Most importantly, heuristic power allocation algorithms are often fast to compute, lending themselves to real-time operation solutions for large populations of EVs. In [95], a decentralized (T2) charging scheme is proposed, where EVs respond to the distribution locational marginal prices that are published by the aggregators, who aim to receive incentives for preventing congestion induced by the EV loads.

Setting an appropriate electricity price quote, especially at EVCSs has several trade-offs. A very high rate may turn away the customers and reduce the revenue of EVCS, whereas a very low rate may overwhelm the EVCS without earning a proper revenue. Consequently, this leads to a price competition among EVCSs under different ownership. The authors in [96] propose a decentralized (T2) framework that consists of a hierarchical game. At the upper level, a non-cooperative game models the competition between EVCSs who aim to maximize the profits by buying power at a lower price and selling them at a higher price. Based on those prices obtained from the non-cooperative game, multiple evolutionary games take place at the lower level to evolve EVs' strategies in choosing EVCSs.

EVCSs are also capable of producing their own electricity by installing renewable power generators (RPGs) and thereby earn revenue from selling electricity to both the grid and the EVs. The authors in [97] propose a decentralized (T2), supermodular, non-cooperative game to coordinate multiple EVCSs that carefully select electricity prices to maximize their revenues. If the amount of electricity generated by the RPGs is insufficient to satisfy the demand of customers, then the EVCS buys electricity from the grid at retail price. If the EVCS has excess electricity, it is sold to the grid at wholesale price. In the proposed game, a unique NE among EVCSs is achieved by playing the best response strategies. Given that the infrastructure cost incurred is not extremely high, adopting RPGs at EVCSs is considered very beneficial.

b) Minimize the costs of power supply: In certain schemes proposed in the literature, minimizing the costs of supplying power is considered as an objective from the aggregator perspective. For example, the authors in [86] develop a decentralized (T2) algorithm to minimize the operational cost of a utility (aggregator) and the charging cost plus battery degradation cost of the EVs, using the ADMM method. The problem is initially formulated as a joint OP with a trade-off parameter between the dual objective functions. It is then converted to a standard exchange OP with EVs and the aggregator considered as agents with coupled objective functions. At each time step, the aggregator solves its local OP and propagates incentive signals, upon which EVs schedule their charging jobs. In [98], a decentralized charging scheme is proposed to minimize the utility's cost related to active power. Specifically, a reduction of the EV charging cost is offered by the utility as an added incentive for the EV owners. By leveraging a time-dependent extension of the well known optimal power flow (OPF) problem, the authors first formulate a joint OPF-EV charging control problem, which is then solved using a valley filling bisection algorithm that is performed by EVs in a decentralized (T2) manner. However, the proposed algorithm employs time-invariant prices, therefore it is not applicable for a time-varying electricity market. In [19], a hierarchical (T3) scheme is proposed to minimize the costs for electricity supply. It comprises a set of fleet agents (FAs), each of whom manages a number of contracted EVs through three main steps. In the first step, the local EV constraints are aggregated towards the FA, and in the second step, a collective charging plan for the EV fleet is determined using dynamic programming. In the final step, the FA propagates a control signal, based on which EVs locally determine their charge schedules using a heuristic function. It is interesting to note that the proposed scheme ensures a constant execution time in terms of vertical scalability (independent of the EV fleet size).

C. Uncertain Aspects of EV Charging Control Optimization

Deterministic OPs assume that the data for a problem is known accurately in advance. However, for many practical problems like EV charging, certain information (e.g., power demand, power generation, plug-in and plug-out times of EVs, electricity prices) cannot be known with certainty. Although there is a rich literature on distributed EV charging control, not all of them have considered such uncertain aspects. In a real-world implementation, algorithms that do not adapt to these uncertain aspects are unlikely to be successful. In this section, we review how certain distributed charging schemes have managed uncertainties that are depicted in Fig. 5.

Many of the charge scheduling algorithms proposed in the literature do not consider the mobility aspects of EVs, instead, they treat EVs as static loads with fixed spatio-temporal parameters (e.g., [27], [73], [82], [94]). In contrast, a *mobility-aware* EV charge scheduling scheme adapts to various temporal variations, such as random arrivals; unplanned departures; and spatial variations that include charging locations, availability of charging slots at EVCSs, EVs' locations at different points in time along with their varying power requirements across different locations, etc. In more detail, an EV may plug-in at any random time of the day, and may plug-out before the designated deadline. Having these uncertainties present, it is not possible to follow the original charge schedule until the end of the scheduled time horizon. In order to deal with the random behaviors of EVs, many of the proposed distributed charge scheduling schemes repeat their static algorithm at the beginning of every time slot with updated information [19], [21]. For instance, in the hierarchical (T3) charging scheme [19], the adaptability to a dynamic environment is achieved through continuous repetition of the three steps of the algorithm at each time step. In contrast, the authors in [56] propose an event driven approach, which triggers the system to recompute charge sequences when one or more EVs plug-in or one or more of connected EVs plug-out before their designated deadlines. The authors in [99] model a stochastic game that embeds a Markov decision process, defined in terms of a state transition matrix that takes into consideration the randomness of EV arrivals, departures, and charging demand. Another type of an optimization method that is often used to tackle EV mobility issue is moving (receding) horizon optimization [18], [20]. This approach first finds charge schedules of EVs for a finite time horizon which begins at the current time and ends at some future time (e.g., latest departure time among all the EVs). The charge rates that are found for the current time step are executed in real, while the rest are discarded. When the next time step arrives, the control time horizon is shifted forward by one time step, and the optimization is repeated with updated information. Other than the aforementioned techniques, probability distributions can also be employed to tackle the uncertainties of EV charging with respect to the EV arrival and departure times.

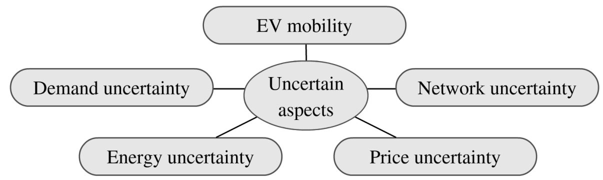

Fig. 5. Uncertain aspects of EV charging control problems.

An EV user may need to charge the battery at any location during its journey. Given the EV's route information, average speed, charging specification and location of the charging stations, the authors in [100] model a mobility-aware framework where a set of aggregators (charging service providers), each of which controls a set of charging stations, collaborate among themselves to schedule EVs that are subscribed to each aggregator in any of the charging stations of its own or others. It is interesting to note that the proposed framework is a dynamic version of the hierarchical (T5) architecture since EVs are allowed to move between aggregators.

The non-EV demand of a community often follows a trend, hence most papers consider non-EV load as deterministic and predictable ahead of time using methods like regression, time-series methods, machine learning, etc. The algorithms in [18], [92] use a similar day approach, where the loads from recent days with identical EV user behaviors and weather conditions are averaged out. Using forecasted non-EV load approximations eliminates the requirement of real-time communication and synchronization among system entities. Nevertheless, forecasted information is vulnerable to errors. Thus, it is likely that there is a discrepancy between the forecasted load and the actual power consumption. A technique that can possibly be applied to cope with demand uncertainty is recomputing the charge schedules at each new time step, with real-time non-EV load data. Alternatively, the decentralized

(T2) charging scheme in [48] performs a charging adjustment mechanism to shift the charging time periods of EVs with respect to the deviation of the real-time non-EV load profile from the forecasted one.

An online charge control scheme proposed in [101] controls EV charging in each time slot entirely based on the current information, without relying on any prediction of future information. Therefore, the algorithm is robust under any EV and non-EV demand profile. It employs an event-driven discrete time model, where an event is defined by an EV arrival, an EV departure, or a change in the non-EV load profile. At any time, the scheduler computes charge sequences using the information that is available so far (charge profiles of EVs already scheduled and the past and current non-EV load) and keeps the schedules unchanged until the occurrence of the next event. As opposed to the traditional time slotted models where lengths of time slots are fixed, the time intervals of the proposed algorithm are defined by the occurrence of events, such that neither the non-EV load nor the number of EVs changes in the middle of a time interval. By doing so, the algorithm is more capable of capturing the system dynamics, which is not achievable through traditional time slotted models unless the time slots are set infinitely small.

The daily and seasonal variability of renewable energy generation contribute to energy uncertainty. The impact of energy uncertainty is particularly high if the system has a large number of small scale distributed generators, such as wind and solar. In the decentralized (T2) algorithm proposed in [17], EV charge rates are regulated to mitigate the uncertainties of electric power generation from a wind farm. The decentralized (T2) algorithm presented in [45] schedules deferrable (EV) loads to compensate for the random fluctuations in renewable generation and uncertain predictions about future power demands, which are modeled as causal filters with random deviations around their expectation. The real-time version of the particular algorithm shifts EV loads to periods with high renewable generation using information that is currently available and the updated predictions. The hierarchical (T2) SG formulated in [22] is later extended to a discrete time feedback SG in order to accommodate the time-varying nature of the amount of energy available from the grid. Further, in [83], the AIMD algorithm is exploited to assign charge rates to the EVs in almost real-time while accommodating the time varying nature of both the available power capacity and the number of EVs being charged. Another technique that is possible – although not commonly applied in the distributed EV charging context – is the Monte Carlo simulation method where the energy uncertainties can be modeled as different probability distributions.

Network uncertainty is generally related to the time-varying thermal loading sensitivities of grid components. For example, transformers and distribution feeders are sensitive to temperature and their capacities may be lower than continuous rated values on a hot day [3]. Grid components (e.g., transmission and distribution assets) may sometimes malfunction beyond a certain temperature threshold, hence their thermal capacities are required to be considered when modeling network-aware charging schemes. The thermal constraints of distribution feeders are captured in [3]. For charging control of EVs served by a single temperature-constrained substation transformer, the authors in [102] present a decentralized (T2), incentive-based and price-coordinated demand scheduling scheme that determines EV charge schedules using a dual-ascent algorithm, embedded in a predictive control scheme to introduce robustness against disturbances.

In an electricity market, price fluctuations are often a consequence of power demand fluctuations, thus price uncertainty correlates to the demand uncertainty. For example, with RTP rates, users are charged less during the valley periods and more during the peak periods. However, if users cooperate to achieve a flat load curve, then everyone will be charged by a nearly equal, and fair electricity rate, which in turn will mitigate the price uncertainty. As such, coordination of EV charging creates an opportunity for the community to save money together.

Table I summarizes several important features of distributed EV charging schemes reviewed in this paper. *Online* algorithms compute the EV charge schedules progressively, without perfect knowledge of inputs available from the start (Section III-A). The *VRC* characteristic allows for charging at variable rates (Section III-B). *Pricing scheme* indicates the type of pricing (flat rates, day-ahead, RTP, TOU or customized) used in the charging scheme, if any (Section III-D). *Mobility aware* charging considers the uncertainty of EV behaviour (e.g., arrival/departure times) (Section V-C), while *network aware* charging considers the distribution network constraints (Section V-A1). *Iterative* algorithms involve repeated computation of the charge profiles, until meeting a specific stopping criterion. Further, it is indicated whether any forecast data is used for the computation and whether V2G operations are supported by the charging scheme.

VI. Research Directions

In our survey of distributed charging schemes, we have presented Table I, which provides a number of useful insights. With respect to the algorithmic techniques involved, many of the distributed charging schemes require iterative calculation of the charge schedules. The computation time of such algorithms is highly affected by the time taken by an EV/aggregator to find the charge schedule/s in a single iteration, and the number of iterations is dependent on the number of participating EVs/aggregators. As such, algorithms employing less complex optimization methods to recompute the charge schedules are more practical for a large EV population. Further, many of the distributed charging schemes are driven by control signals that rely on a perfect communication medium. Preferable algorithms for real-world applications are resilient to network latency and other potential network failures, and do not require large investments for extensive bidirectional communications. Moreover, most of the reviewed distributed algorithms commonly utilize forecast data, with precise forecasting techniques deemed critical for real-world implementation.

It is evident that the problem of load regulation (load flattening) is well investigated in many distributed charging schemes related to operation aspects, however very few of them incorporate both network-awareness and

TABLE I

CHARACTERISTICS OF EV CHARGING CONTROL SCHEMES

Objective	**Paper**	**Control architecture[i]**	**Perspective[ii]**	**Online**	**VRC**	**Pricing scheme [iii]**	**Mobility aware**	**Network aware**	**Forecasts**	**Iterative**	**Supports V2G**	**Technique**
Operation aspects												
Load regulation	[16]	D(T2)	G	✗	✓	-	✗	✗	✓	✓	✗	Game theory
	[21]	D(T2)	G	✓	✓	-	✓	✗	✓	✓	✓	GPM
	[41]	D(T2)	G	✓	✓	-	✓	✗	✗	✓	✗	Max-weight algorithm
	[42]	D(T2)	G	✓	✗	-	✓	✗	✓	✓	✗	Stochastic programming
	[43]	D(T2)	G	✗	✓	-	✗	✗	✓	✓	✓	DP+ Game theory
	[44]	D(T2)	G	✓	✓	-	✓	✗	✓	✗	✗	Arithmetic operations
	[45]	D(T2)	G	✓	✓	-	✓	✗	✓	✓	✗	GPM
	[51]	D(T2)	G	✗	✓	-	✗	✗	✓	✓	✓	Water filling
Load regulation with overload control constraints	[3]	D(T2)	G	✗	✓	-	✗	✓	✓	✓	✗	GPM
	[23]	D(T2)	G	✗	✓	-	✗	✓	✓	✓	✗	GPM + ADMM
	[46]	D(T2)	G	✗	✓	-	✗	✓	✓	✓	✗	ADMM
	[48]	D(T2)	G	✓	✓	-	✓	✓	✓	✓	✗	Ant-based swarm algorithm
	[49]	D(T2)	G	✓	✓	-	✓	✓	✓	✗	✗	Water filling
Load regulation with voltage and overload control constraints	[39]	D(T2)	G	✓	✗	-	✓	✓	✗	✗	✗	Random access algorithm
Load regulation with voltage constraints + Minimize battery degradation cost	[55]	D(T2)	G/E	✗	✓	-	✗	✓	✓	✓	✗	Primal-dual subgradient
Provision of ancillary services (voltage control)	[76]	D(T2)	E	✓	✓	-	✓	✓	✗	✓	✗	Game theory
Frequency regulation	[70]	D(T2)	A	✓	✓	-	✗	✗	✗	✗	✓	Adaptive droop control
	[75]	D(T1)	E	✓	✓	-	✗	✗	✗	✗	✓	Consensus filtering
	[73]	D(T2)	A	✓	✓	CP	✗	✗	✗	✓	✓	Game theory
Manage ancillary services (providing spinning reserve)	[34]	D(T2)	A	✗	✓	CP	✗	✓	✓	✓	✓	Game theory
Manage ancillary services (active power compensation)	[66]	H(T1)	A	✓	✓	-	✗	✗	✗	✗	✓	Task swap mechanism
Maximize user convenience	[27]	H(T4)	E	✗	✗	-	✗	✓	✓	✓	✗	ADMM
	[24]	H(T5)	E	✓	✗	-	✓	✓	✓	✓	✗	Convex optimization
Minimize charging power losses	[77]	D(T1)	E	✓	✓	-	✓	✓	✗	✓	✗	Consensus coordination
	[78]	D(T1)	E	✓	✓	-	✓	✓	✗	✓	✗	Consensus coordination
Charging fairness (Proportional fairness)	[83]	D(T2)	E	✓	✓	-	✓	✓	✗	✗	✗	AIMD
Charging fairness (Equal access) + Overload control	[80]	D(T2)	E/G	✓	✓	-	✓	✓	✗	✗	✗	Packetized approach
Charging fairness + Minimize charging cost	[82]	D(T1)	E	✓	✓	RTP	✓	✗	✗	✓	✗	Congestion pricing technique
Minimize bus congestion + Charging fairness	[52]	D(T2)	G/E	✓	✓	-	✗	✓	✓	✗	✗	Lagrangian decomposition
Maximize operational efficiency + Charging fairness	[57]	D(T2)	G/E	✓	✓	-	✓	✓	✗	✗	✗	Heuristic algorithm
Cost aspects												
Minimize the cost of power operations	[37]	H(T3)	G	✗	✓	-	✗	✓	✓	✓	✓	Benders decomposition
	[85]	H(T1)	G	✗	✓	-	✗	✓	✗	✓	✓	Convex optimization
Minimize EV charging costs	[13]	H(T5)	E	✗	✓	RTP	✗	✗	✓	✓	✗	Game theory
	[33]	D(T1)	E	✗	✓	RTP	✗	✗	✓	✓	✗	Game theory
	[103]	D(T2)	E	✗	✓	-	✗	✗	✓	✓	✗	Game theory
	[104]	D(T2)	E	✗	✓	DAP	✗	✗	✓	✗	✗	Game theory
Minimize the power supply cost	[19]	H(T3)	A	✓	✓	-	✓	✗	✗	✗	✗	DP + Heuristic algorithm
Minimize the electricity purchase cost	[20]	H(T1)	A	✓	✓	TOU	✓	✓	✓	✗	✗	Linear Programming + heuristic
Maximize aggregator revenue	[36]	H(T2)	A	✓	✓	TOU	✓	✓	✓	✓	✗	Lagrangian relaxation
	[97]	D(T2)	A	✗	✓	CP	✗	✓	✓	✗	✗	Game theory
Minimize power supply cost + Minimize EV charging costs	[98]	D(T2)	A/E	✓	✓	Flat	✓	✓	✓	✓	✗	Nonsmooth separable programming
Maximize grid operator revenue + Minimize EV charging costs	[22]	H(T2)	G/E	✓	✓	CP	✓	✓	✗	✓	✗	Game theory
Maximize aggregator revenue + Minimize EV charging costs	[105]	D(T1)	A/E	✗	✓	CP	✗	✓	✗	✓	✓	Consensus coordination
Operation aspects and Cost aspects												
Maximize operation efficiency + Minimize EV charging costs	[58]	D(T2)	G/E	✓	✓	RTP	✓	✗	✓	✓	✓	Game theory
Minimize EV charging costs + Overload control	[91]	H(T2)	E/G	✓	✓	-	✗	✓	✓	✓	✗	Lagrangian decomposition
	[92]	H(T2)	E/G	✓	✓	CP	✓	✓	✓	✓	✗	DP + Convex optimization
Frequency regulation + Minimize EV charging costs	[71]	D(T2)	A/E	✗	✓	-	✗	✓	✓	✓	✓	Convex optimization
Load regulation + Frequency regulation + Minimize the electricity generation cost and carbon dioxide emissions	[17]	D(T2)	G/E	✗	✓	-	✗	✗	✓	✗	✗	Linear programming
Load regulation with voltage and overload control constraints + Minimize cost of power operation	[54]	D(T2)	G	✓	✓	RTP	✓	✓	✓	✓	✗	ADMM
Minimize power supply cost + Minimize EV charging costs + Minimize battery degradation cost	[86]	D(T2)	A/E	✗	✓	CP	✗	✗	✗	✓	✗	ADMM

[i] C: Centralized, D: Decentralized, H: Hierarchical [ii] G: Grid operator, E: EV user, A: Aggregator [iii] CP: Customized Pricing, DAP: Day Ahead Pricing

mobility-awareness. In the literature for distributed EV charging, algorithms for minimizing network energy losses are not investigated satisfactorily. It is also noticeable that many papers on distributed V2G frameworks consider only one operational objective, either regulating load or regulating frequency, but not both. Hence, extensions to existing distributed V2G frameworks to achieve more than one operational objective will potentially have significant impact. Moreover, distributed EV charging schemes that consider OPs with multiple operational objectives are limited to the perspective of a single entity (e.g., they do not consider overload control and voltage control while maximizing EV user convenience). With respect to the cost aspects of EV charging control, it can be realized that distributed charging control schemes focused on enhancing the system-wide social welfare through cost optimization of multiple parties (EV users, grid operators, aggregators) are very limited.

Distributed charging schemes that consider combinations of multiple objectives with respect to both the operational and cost aspects (e.g., maximizing user convenience and minimizing charging costs) are yet to be explored further. Another potential topic of interest is to study OPs where different individuals of the same entity have distinct objective functions, e.g., distributed coordination of several aggregators where certain aggregators aim to minimize the charging costs on behalf of their EV customers and the other aggregators aim to maximize their profit from selling energy to the EV customers. In addition, future research can focus on developing distributed EV charging algorithms to accommodate various uncertain aspects discussed in Section V-C.

Many of the existing distributed EV charge control schemes exploit simpler and linear battery models. However, those battery models are not accurate in practice, since the real internal power of the battery is a nonlinear function of the external power, due to internal power losses. Hence, distributed EV charge control schemes involving realistic and accurate battery models [12] are required. Moreover, the consideration of transient process of the batteries and variations in charging efficiencies is needed to improve future practical applications.

The traditional electric grid transports electricity over long distances and through complex electricity transportation routes. Alternatively, EVs can obtain electricity from other EVs through vehicle-to-vehicle (V2V) power exchange. For example, in parking lots or EVCSs, EVs with V2G capability can exchange or trade electricity in a localized peer-to-peer (P2P) manner [106]. Formulation of decentralized algorithmic approaches for supporting demand response through P2P transaction systems is another research direction of growing interest. In addition, blockchain-based, decentralized charge-discharge schemes (e.g., [107]) are preferable for managing secured and distributed energy transactions in a V2G and V2V market without reliance on a third party aggregator.

VII. Conclusion

A distributed control paradigm, in contrast to a centralized approach, addresses numerous challenges (e.g., computational and communication challenges) in coordinating a large population of EVs. In this paper, we have presented a comprehensive survey of distributed EV charge control algorithms that are compatible with decentralized and hierarchical control architectures. First, we have classified OPs for EV charging control with respect to operational aspects and cost aspects. Under each category, we have reviewed the state-of-the-art distributed charge control schemes from the perspectives of the grid operator, the EV user, and the aggregator.

From the perspective of the grid operator, we have reviewed numerous distributed algorithms for load regulation, congestion management, improved efficiency, maximized revenue and minimized power generation and supply costs. With respect to the EV user, we have reviewed distributed algorithms for improved user convenience, provision of ancillary services, minimized charging losses, lower EV charging costs, and the relative fairness of different charging approaches. In considering the aggregator perspective, distributed charge control schemes with respect to managing ancillary services, maximizing the revenue, and minimizing the power supply costs are also reviewed. A crucial aspect of any EV charge control system is uncertainty. Thus, we have reviewed numerous algorithms that have been proposed to tackle various uncertain aspects of EV charging. Finally we have identified several research directions with respect to distributed EV charging control.

References

[1] C. MacHaris, J. Van Mierlo, and P. Van Den Bossche, "Combining intermodal transport with electric vehicles: Towards more sustainable solutions," *Transp. Planning Technol.*, vol. 30, nos. 2–3, pp. 311–323, Apr. 2007.

[2] N. Zart. (2017). *Batteries Keep on Getting Cheaper*. CleanTechnica. [Online]. Available: http://cleantechnica.com/2017/12/11/batteries-keep-getting-cheaper

[3] A. Ghavami, K. Kar, and A. Gupta, "Decentralized charging of plug-in electric vehicles with distribution feeder overload control," *IEEE Trans. Autom. Control*, vol. 61, no. 11, pp. 3527–3532, Nov. 2016.

[4] W. Su, H. Rahimi-Eichi, W. Zeng, and M.-Y. Chow, "A survey on the electrification of transportation in a smart grid environment," *IEEE Trans. Ind. Informat.*, vol. 8, no. 1, pp. 1–10, Feb. 2012.

[5] H. Xiao, Y. Huimei, W. Chen, and L. Hongjun, "A survey of influence of electrics vehicle charging on power grid," in *Proc. 9th IEEE Conf. Ind. Electron. Appl.*, Hangzhou, China, Jun. 2014, pp. 121–126.

[6] R. C. Green, II, L. Wang, and M. Alam, "The impact of plug-in hybrid electric vehicles on distribution networks: A review and outlook," *Renew. Sustain. Energy Rev.*, vol. 15, no. 1, pp. 544–553, 2011.

[7] J. García-Villalobos, I. Zamora, J. I. S. Martín, F. J. Asensio, and V. Aperribay, "Plug-in electric vehicles in electric distribution networks: A review of smart charging approaches," *Renew. Sustain. Energy Rev.*, vol. 38, pp. 717–731, Oct. 2014.

[8] P. Y. Kong and G. K. Karagiannidis, "Charging schemes for plug-in hybrid electric vehicles in smart grid: A survey," *IEEE Access*, vol. 4, pp. 6846–6875, 2016.

[9] J. C. Mukherjee and A. Gupta, "A review of charge scheduling of electric vehicles in smart grid," *IEEE Syst. J.*, vol. 9, no. 4, pp. 1541–1553, Dec. 2015.

[10] Q. Wang, X. Liu, J. Du, and F. Kong, "Smart charging for electric vehicles: A survey from the algorithmic perspective," *IEEE Commun. Surveys Tuts.*, vol. 18, no. 2, pp. 1500–1517, 2nd Quart., 2016.

[11] D. S. Callaway and I. A. Hiskens, "Achieving controllability of electric loads," *Proc. IEEE*, vol. 99, no. 1, pp. 184–199, Jan. 2011.

[12] W. Su and M.-Y. Chow, "Sensitivity analysis on battery modeling to large-scale PHEV/PEV charging algorithms," in *Proc. 37th Annu. Conf. IEEE Ind. Electron. Soc.*, Melbourne, VIC, Australia, Nov. 2011, pp. 3248–3253.

[13] C. P. Mediwaththe and D. B. Smith, "Game-theoretic electric vehicle charging management resilient to non-ideal user behavior," *IEEE Trans. Intell. Transp. Syst.*, vol. 19, no. 11, pp. 3486–3495, Nov. 2018.

[14] S. Vandael, N. Boucké, T. Holvoet, and G. Deconinck, "Decentralized demand side management of plug-in hybrid vehicles in a smart grid," in *Proc. 1st Int. Workshop Agent Technol. Energy Syst.*, 2010, pp. 67–74.

[15] X. Mou, O. Groling, A. Gallant, and H. Sun, "Energy efficient and adaptive design for wireless power transfer in electric vehicles," in *Proc. 83rd IEEE Conf. Veh. Technol.*, Nanjing, China, May 2016, pp. 1–5.

[16] Z. Ma, D. S. Callaway, and I. A. Hiskens, "Decentralized charging control of large populations of plug-in electric vehicles," *IEEE Trans. Control Syst. Technol.*, vol. 21, no. 1, pp. 67–78, Jan. 2013.

[17] C. Ahn, C.-T. Li, and H. Peng, "Optimal decentralized charging control algorithm for electrified vehicles connected to smart grid," *J. Power Sources*, vol. 196, no. 23, pp. 10369–10379, Dec. 2011.

[18] Y. He, B. Venkatesh, and L. Guan, "Optimal scheduling for charging and discharging of electric vehicles," *IEEE Trans. Smart Grid*, vol. 3, no. 3, pp. 1095–1105, Sep. 2012.

[19] S. Vandael, B. Claessens, M. Hommelberg, T. Holvoet, and G. Deconinck, "A scalable three-step approach for demand side management of plug-in hybrid vehicles," *IEEE Trans. Smart Grid*, vol. 4, no. 2, pp. 720–728, Jun. 2013.

[20] Z. Xu, Z. Hu, Y. Song, W. Zhao, and Y. Zhang, "Coordination of PEVs charging across multiple aggregators," *Appl. Energy*, vol. 136, pp. 582–589, Dec. 2014.

[21] L. Gan, U. Topcu, and S. H. Low, "Optimal decentralized protocol for electric vehicle charging," *IEEE Trans. Power Syst.*, vol. 28, no. 2, pp. 940–951, May 2013.

[22] W. Tushar, W. Saad, H. V. Poor, and D. B. Smith, "Economics of electric vehicle charging: A game theoretic approach," *IEEE Trans. Smart Grid*, vol. 3, no. 4, pp. 1767–1778, Dec. 2012.

[23] W.-J. Ma, V. Gupta, and U. Topcu, "On distributed charging control of electric vehicles with power network capacity constraints," in *Proc. Amer. Control Conf. (ACC)*, Portland, OR, USA, Jun. 2014, pp. 4306–4311.

[24] A. Malhotra, G. Binetti, A. Davoudi, and I. D. Schizas, "Distributed power profile tracking for heterogeneous charging of electric vehicles," *IEEE Trans. Smart Grid*, vol. 8, no. 5, pp. 2090–2099, Sep. 2017.

[25] Y. Lu, K. W. E. Cheng, and S. W. Zhao, "Power battery charger for electric vehicles," *IET Power Electron.*, vol. 4, no. 5, pp. 580–586, May 2011.

[26] G. Binetti, A. Davoudi, D. Naso, B. Turchiano, and F. L. Lewis, "Scalable real-time electric vehicles charging with discrete charging rates," *IEEE Trans. Smart Grid*, vol. 6, no. 5, pp. 2211–2220, Sep. 2015.

[27] C.-K. Wen, J.-C. Chen, J.-H. Teng, and P. Ting, "Decentralized plug-in electric vehicle charging selection algorithm in power systems," *IEEE Trans. Smart Grid*, vol. 3, no. 4, pp. 1779–1789, Dec. 2012.

[28] L.-R. Chen, S.-L. Wu, D.-T. Shieh, and T.-R. Chen, "Sinusoidal-ripple-current charging strategy and optimal charging frequency study for li-ion batteries," *IEEE Trans. Ind. Electron.*, vol. 60, no. 1, pp. 88–97, Jan. 2013.

[29] A. Malhotra, N. Erdogan, G. Binetti, I. D. Schizas, and A. Davoudi, "Impact of charging interruptions in coordinated electric vehicle charging," in *Proc. IEEE Global Conf. Signal Inf. Process.*, Washington, DC, USA, Dec. 2016, pp. 901–905.

[30] N. R. Watson, J. D. Watson, R. M. Watson, K. Sharma, and A. Miller, "Impact of electric vehicle chargers on a low voltage distribution system," in *Proc. Conf., Electr. Eng. Assoc.*, Wellington, New Zealand, 2015.

[31] C. Harris, I. Dusparic, E. Galván-López, A. Marinescu, V. Cahill, and S. Clarke, "Set point control for charging of electric vehicles on the distribution network," in *Proc. IEEE Conf. Innov. Smart Grid Technol.*, Washington, DC, USA, Feb. 2014, pp. 1–5.

[32] K. Jhala, B. Natarajan, A. Pahwa, and L. Erickson, "Coordinated electric vehicle charging solutions using renewable energy sources," in *Proc. IEEE Symp. Comput. Intell. Appl. Smart Grid*, Orlando, FL, USA, Dec. 2014, pp. 1–6.

[33] A.-H. Mohsenian-Rad, V. W. S. Wong, J. Jatskevich, R. Schober, and A. Leon-Garcia, "Autonomous demand-side management based on game-theoretic energy consumption scheduling for the future smart grid," *IEEE Trans. Smart Grid*, vol. 1, no. 3, pp. 320–331, Dec. 2010.

[34] J. Tan and L. Wang, "Enabling reliability-differentiated service in residential distribution networks with PHEVs: A hierarchical game approach," *IEEE Trans. Smart Grid*, vol. 7, no. 2, pp. 684–694, Mar. 2016.

[35] S. Chen, Y. Ji, and L. Tong, "Large scale charging of electric vehicles," in *Proc. IEEE Power Energy Soc. Gen. Meeting*, San Diego, CA, USA, Jul. 2012, pp. 1–9.

[36] W. Qi, Z. Xu, Z.-J. M. Shen, Z. Hu, and Y. Song, "Hierarchical coordinated control of plug-in electric vehicles charging in multifamily dwellings," *IEEE Trans. Smart Grid*, vol. 5, no. 3, pp. 1465–1474, May 2014.

[37] C. Shao, X. Wang, X. Wang, C. Du, and B. Wang, "Hierarchical charge control of large populations of EVs," *IEEE Trans. Smart Grid*, vol. 7, no. 2, pp. 1147–1155, Mar. 2016.

[38] A. Aabrandt *et al.*, "Prediction and optimization methods for electric vehicle charging schedules in the EDISON project," in *Proc. IEEE PES Conf. Innov. Smart Grid Technol.*, Washington, DC, USA, Jan. 2012, pp. 1–7.

[39] K. Zhou and L. Cai, "Randomized PHEV charging under distribution grid constraints," *IEEE Trans. Smart Grid*, vol. 5, no. 2, pp. 879–887, Mar. 2014.

[40] R. Wang, G. Xiao, and P. Wang, "Hybrid centralized-decentralized (HCD) charging control of electric vehicles," *IEEE Trans. Veh. Technol.*, vol. 66, no. 8, pp. 6728–6741, Aug. 2017.

[41] Q. Li, T. Cui, R. Negi, F. Franchetti, and M. D. Ilic, "On-line decentralized charging of plug-in electric vehicles in power systems," Jun. 2011, *arXiv:1106.5063*. [Online]. Available: https://arxiv.org/abs/1106.5063

[42] L. Gan, U. Topcu, and S. H. Low, "Stochastic distributed protocol for electric vehicle charging with discrete charging rate," in *Proc. IEEE Power Energy Soc. General Meeting*, San Diego, CA, USA, Jul. 2012, pp. 1–8.

[43] A. Ovalle, A. Hably, and S. Bacha, "Optimal management and integration of electric vehicles to the grid: Dynamic programming and game theory approach," in *Proc. IEEE Int. Conf. Ind. Technol.*, Seville, Spain, Mar. 2015, pp. 2673–2679.

[44] M. C. Kisacikoglu, F. Erden, and N. Erdogan, "Distributed control of PEV charging based on energy demand forecast," *IEEE Trans. Ind. Informat.*, vol. 14, no. 1, pp. 332–341, Jan. 2018.

[45] L. Gan, A. Wierman, U. Topcu, N. Chen, and S. H. Low, "Real-time deferrable load control: Handling the uncertainties of renewable generation," in *Proc. 4th ACM Int. Conf. Future Energy Syst.*, Jan. 2013, pp. 113–124.

[46] J. Li, C. Li, Z. Wu, X. Wang, K. L. Teo, and C. Wu, "Sparsity-promoting distributed charging control for plug-in electric vehicles over distribution networks," *Appl. Math. Modell.*, vol. 58, pp. 111–127, Jun. 2018.

[47] E. L. Karfopoulos and N. D. Hatziargyriou, "A multi-agent system for controlled charging of a large population of electric vehicles," *IEEE Trans. Power Syst.*, vol. 28, no. 2, pp. 1196–1204, May 2013.

[48] S. Xu *et al.*, "Ant-based swarm algorithm for charging coordination of electric vehicles," *Int. J. Distrib. Sensor Netw.*, vol. 9, no. 5, May 2013, Art. no. 268942.

[49] Y. Mou, H. Xing, Z. Lin, and M. Fu, "Decentralized optimal demand-side management for PHEV charging in a smart grid," *IEEE Trans. Smart Grid*, vol. 6, no. 2, pp. 726–736, Mar. 2015.

[50] Y. Mou, H. Xing, M. Fu, and Z. Lin, "Decentralized PWM-based charging control for plug-in electric vehicles," in *Proc. IEEE Eur. Control Conf.*, Linz, Austria, Jul. 2015, pp. 1070–1075.

[51] H. Xing, M. Fu, Z. Lin, and Y. Mou, "Decentralized optimal scheduling for charging and discharging of plug-in electric vehicles in smart grids," *IEEE Trans. Power Syst.*, vol. 31, no. 5, pp. 4118–4127, Sep. 2016.

[52] O. Ardakanian, C. Rosenberg, and S. Keshav, "Distributed control of electric vehicle charging," in *Proc. 4th ACM Int. Conf. Future Energy Syst.*, 2013, pp. 101–112.

[53] O. Ardakanian, S. Keshav, and C. Rosenberg, "Real-time distributed control for smart electric vehicle chargers: From a static to a dynamic study," *IEEE Trans. Smart Grid*, vol. 5, no. 5, pp. 2295–2305, Sep. 2014.

[54] L. Zhang, V. Kekatos, and G. B. Giannakis, "Scalable electric vehicle charging protocols," *IEEE Trans. Power Syst.*, vol. 32, no. 2, pp. 1451–1462, Mar. 2017.

[55] M. Liu, P. K. Phanivong, Y. Shi, and D. S. Callaway, "Decentralized charging control of electric vehicles in residential distribution networks," Oct. 2017, *arXiv:1710.05533*. [Online]. Available: https://arxiv.org/abs/1710.05533

[56] M. Liu, P. K. Phanivong, and D. S. Callaway, "Electric vehicle charging control in residential distribution network: A decentralized event-driven realization," in *Proc. 56th IEEE Annu. Conf. Decis. Control*, Melbourne, VIC, Australia, Dec. 2017, pp. 214–219.

[57] R. Smruti Sarangi, P. Dutta, and K. Jalan, "IT infrastructure for providing energy-as-a-service to electric vehicles," *IEEE Trans. Smart Grid*, vol. 3, no. 2, pp. 594–604, Jun. 2012.

[58] M. H. K. Tushar, A. W. Zeineddine, and C. Assi, "Demand-side management by regulating charging and discharging of the EV, ESS, and utilizing renewable energy," *IEEE Trans. Ind. Informat.*, vol. 14, no. 1, pp. 117–126, Jan. 2018.

[59] S.-L. Andersson *et al.*, "Plug-in hybrid electric vehicles as regulating power providers: Case studies of Sweden and Germany," *Energy Policy*, vol. 38, no. 6, pp. 2751–2762, Jun. 2010.

[60] S. Han, S. Han, and K. Sezaki, "Development of an optimal vehicle-to-grid aggregator for frequency regulation," *IEEE Trans. Smart Grid*, vol. 1, no. 1, pp. 65–72, Jun. 2010.

[61] N. Rotering and M. Ilic, "Optimal charge control of plug-in hybrid electric vehicles in deregulated electricity markets," *IEEE Trans. Power Syst.*, vol. 26, no. 3, pp. 1021–1029, Aug. 2011.

[62] C. Jin, J. Tang, and P. Ghosh, "Optimizing electric vehicle charging: A customer's perspective," *IEEE Trans. Veh. Technol.*, vol. 62, no. 7, pp. 2919–2927, Sep. 2013.

[63] A. S. Masoum, S. Deilami, P. S. Moses, M. A. S. Masoum, and A. Abu-Siada, "Smart load management of plug-in electric vehicles in distribution and residential networks with charging stations for peak shaving and loss minimisation considering voltage regulation," *IET Generat., Transmiss. Distrib.*, vol. 5, no. 8, pp. 877–888, Aug. 2011.

[64] Y. Ota *et al.*, "Autonomous distributed vehicle-to-grid for ubiquitous power grid and its effect as a spinning reserve," *J. Int. Council Elect. Eng.*, vol. 1, no. 2, pp. 214–221, 2011.

[65] D. Dallinger, D. Krampe, and M. Wietschel, "Vehicle-to-grid regulation reserves based on a dynamic simulation of mobility behavior," *IEEE Trans. Smart Grid*, vol. 2, no. 2, pp. 302–313, Jun. 2011.

[66] Z. Peng and L. Hao, "Decentralized coordination of electric vehicle charging stations for active power compensation," in *Proc. 86th IEEE Conf. Veh. Technol.*, Toronto, ON, Canada, Sep. 2017, pp. 1–5.

[67] B. Jiang and Y. Fei, "Decentralized scheduling of PEV on-street parking and charging for smart grid reactive power compensation," in *Proc. IEEE Conf. Innov. Smart Grid Technol. (ISGT)*, Washington, DC, USA, Feb. 2013, pp. 1–6.

[68] Y. Ota, H. Taniguchi, T. Nakajima, K. M. Liyanage, J. Baba, and A. Yokoyama, "Autonomous distributed V2G (vehicle-to-grid) considering charging request and battery condition," in *Proc. IEEE PES Innov. Smart Grid Technol. Conf. Eur.*, Gothenberg, Sweden, Oct. 2010, pp. 1–6.

[69] Y. Ota, H. Taniguchi, T. Nakajima, K. M. Liyanage, J. Baba, and A. Yokoyama, "Autonomous distributed V2G (vehicle-to-grid) satisfying scheduled charging," *IEEE Trans. Smart Grid*, vol. 3, no. 1, pp. 559–564, Mar. 2012.

[70] H. Liu, Z. Hu, Y. Song, and J. Lin, "Decentralized vehicle-to-grid control for primary frequency regulation considering charging demands," *IEEE Trans. Power Syst.*, vol. 28, no. 3, pp. 3480–3489, Aug. 2013.

[71] E. L. Karfopoulos, K. A. Panourgias, and N. D. Hatziargyriou, "Distributed coordination of electric vehicles providing V2G regulation services," *IEEE Trans. Power Syst.*, vol. 31, no. 4, pp. 2834–2846, Jul. 2016.

[72] E. Sortomme and M. A. El-Sharkawi, "Optimal combined bidding of vehicle-to-grid ancillary services," *IEEE Trans. Smart Grid*, vol. 3, no. 1, pp. 70–79, Mar. 2012.

[73] C. Wu, H. Mohsenian-Rad, and J. Huang, "Vehicle-to-aggregator interaction game," *IEEE Trans. Smart Grid*, vol. 3, no. 1, pp. 434–442, Mar. 2012.

[74] J.-M. Glachant. (2009). *Electricity Reform in Europe: Towards a Single Energy Market*. Edward Elgar Publishing. [Online]. Available: http://hdl.handle.net/1814/11771

[75] H. Yang, C. Y. Chung, and J. Zhao, "Application of plug-in electric vehicles to frequency regulation based on distributed signal acquisition via limited communication," *IEEE Trans. Power Syst.*, vol. 28, no. 2, pp. 1017–1026, May 2013.

[76] O. Beaude, Y. He, and M. Hennebel, "Introducing decentralized EV charging coordination for the voltage regulation," in *Proc. IEEE PES Int. Conf. Innov. Smart Grid Technol. Eur.*, Lyngby, Denmark, Oct. 2013, pp. 1–5.

[77] Y. Xu, "Optimal distributed charging rate control of plug-in electric vehicles for demand management," *IEEE Trans. Power Syst.*, vol. 30, no. 3, pp. 1536–1545, May 2015.

[78] T. Zhao and Z. Ding, "Distributed initialization-free cost-optimal charging control of plug-in electric vehicles for demand management," *IEEE Trans. Ind. Informat.*, vol. 13, no. 6, pp. 2791–2801, Dec. 2017.

[79] P. Richardson, D. Flynn, and A. Keane, "Local versus centralized charging strategies for electric vehicles in low voltage distribution systems," *IEEE Trans. Smart Grid*, vol. 3, no. 2, pp. 1020–1028, Jun. 2011.

[80] P. Rezaei, J. Frolik, and P. D. H. Hines, "Packetized plug-in electric vehicle charge management," *IEEE Trans. Smart Grid*, vol. 5, no. 2, pp. 642–650, Mar. 2014.

[81] N. Rahbari-Asr and M.-Y. Chow, "Cooperative distributed demand management for community charging of PHEV/PEVs based on KKT conditions and consensus networks," *IEEE Trans. Ind. Informat.*, vol. 10, no. 3, pp. 1907–1916, Aug. 2014.

[82] Z. Fan, "A distributed demand response algorithm and its application to PHEV charging in smart grids," *IEEE Trans. Smart Grid*, vol. 3, no. 3, pp. 1280–1290, Sep. 2012.

[83] S. Studli, E. Crisostomi, R. Middleton, and R. Shorten, "A flexible distributed framework for realising electric and plug-in hybrid vehicle charging policies," *Int. J. Control*, vol. 85, no. 8, pp. 1130–1145, 2012.

[84] B. Škugor and J. Deur, "Dynamic programming-based optimization of electric vehicle fleet charging," in *Proc. IEEE Int. Electr. Veh. Conf.*, Florence, Italy, Dec. 2014, pp. 1–8.

[85] W. Yao, J. Zhao, F. Wen, Y. Xue, and G. Ledwich, "A hierarchical decomposition approach for coordinated dispatch of plug-in electric vehicles," *IEEE Trans. Power Syst.*, vol. 28, no. 3, pp. 2768–2778, Aug. 2013.

[86] J. Rivera, P. Wolfrum, S. Hirche, C. Goebel, and H.-A. Jacobsen, "Alternating direction method of multipliers for decentralized electric vehicle charging control," in *Proc. 52nd IEEE Annu. Conf. Decis. Control*, Florence, Italy, Dec. 2013, pp. 6960–6965.

[87] X. Xi and R. Sioshansi, "Using price-based signals to control plug-in electric vehicle fleet charging," *IEEE Trans. Smart Grid*, vol. 5, no. 3, pp. 1451–1464, May 2014.

[88] S. Misra, S. Bera, and T. Ojha, "D2P: Distributed dynamic pricing policy in smart grid for PHEVs management," *IEEE Trans. Parallel Distrib. Syst.*, vol. 26, no. 3, pp. 702–712, Mar. 2015.

[89] S. Bahrami and M. Parniani, "Game theoretic based charging strategy for plug-in hybrid electric vehicles," *IEEE Trans. Smart Grid*, vol. 5, no. 5, pp. 2368–2375, Sep. 2014.

[90] Y. Cao *et al.*, "An optimized EV charging model considering TOU price and SoC curve," *IEEE Trans. Smart Grid*, vol. 3, no. 1, pp. 388–393, Mar. 2012.

[91] J. Hu, S. You, M. Lind, and J. Ostergaard, "Coordinated charging of electric vehicles for congestion prevention in the distribution grid," *IEEE Trans. Smart Grid*, vol. 5, no. 2, pp. 703–711, Mar. 2014.

[92] D. M. Anand, R. T. de Salis, Y. Cheng, J. Moyne, and D. M. Tilbury, "A hierarchical incentive arbitration scheme for coordinated PEV charging stations," *IEEE Trans. Smart Grid*, vol. 6, no. 4, pp. 1775–1784, Jul. 2015.

[93] B. Gharesifard, T. Basar, and A. D. Domínguez-García, "Price-based distributed control for networked plug-in electric vehicles," in *Proc. IEEE Amer. Control Conf.*, Washington, DC, USA, Jun. 2013, pp. 5086–5091.

[94] D. Wu, C. D. Aliprantis, and L. Ying, "Load scheduling and dispatch for aggregators of plug-in electric vehicles," *IEEE Trans. Smart Grid*, vol. 3, no. 1, pp. 368–376, Mar. 2012.

[95] R. Li, Q. Wu, and S. S. Oren, "Distribution locational marginal pricing for optimal electric vehicle charging management," *IEEE Trans. Power Syst.*, vol. 29, no. 1, pp. 203–211, Jan. 2014.

[96] J. Tan and L. Wang, "Real-time charging navigation of electric vehicles to fast charging stations: A hierarchical game approach," *IEEE Trans. Smart Grid*, vol. 8, no. 2, pp. 846–856, Mar. 2017.

[97] W. Lee, L. Xiang, R. Schober, and V. W. S. Wong, "Electric vehicle charging stations with renewable power generators: A game theoretical analysis," *IEEE Trans. Smart Grid*, vol. 6, no. 2, pp. 608–617, Mar. 2015.

[98] N. Chen, C. W. Tan, and T. Q. S. Quek, "Electric vehicle charging in smart grid: Optimality and valley-filling algorithms," *IEEE J. Sel. Top. Signal Process.*, vol. 8, no. 6, pp. 1073–1083, Dec. 2014.

[99] Y. Liu, R. Deng, and H. Liang, "A stochastic game approach for PEV charging station operation in smart grid," *IEEE Trans. Ind. Informat.*, vol. 14, no. 3, pp. 969–979, Mar. 2018.

[100] J. C. Mukherjee and A. Gupta, "Distributed charge scheduling of plug-in electric vehicles using inter-aggregator collaboration," *IEEE Trans. Smart Grid*, vol. 8, no. 1, pp. 331–341, Jan. 2017.

[101] W. Tang, S. Bi, and Y. J. A. Zhang, "Online coordinated charging decision algorithm for electric vehicles without future information," *IEEE Trans. Smart Grid*, vol. 5, no. 6, pp. 2810–2824, Nov. 2014.

[102] R. Hermans, M. Almassalkhi, and I. Hiskens, "Incentive-based coordinated charging control of plug-in electric vehicles at the distribution-transformer level," in *Proc. Amer. Control Conf. (ACC)*, Montreal, QC, Canada, Jun. 2012, pp. 264–269.

[103] H. K. Nguyen and J. B. Song, "Optimal charging and discharging for multiple PHEVs with demand side management in vehicle-to-building," *J. Commun. Netw.*, vol. 14, no. 6, pp. 662–671, Dec. 2012.
[104] Z. Liu, Q. Wu, S. Huang, L. Wang, M. Shahidehpour, and Y. Xue, "Optimal day-ahead charging scheduling of electric vehicles through an aggregative game model," *IEEE Trans. Smart Grid*, vol. 9, no. 5, pp. 5173–5184, Sep. 2018.
[105] N. Rahbari-Asr, M.-Y. Chow, Z. Yang, and J. Chen, "Network cooperative distributed pricing control system for large-scale optimal charging of PHEVs/PEVs," in *Proc. 39th IEEE Conf. Ind. Electron. Soc. (IECON)*, Vienna, Austria, Nov. 2013, pp. 6148–6153.
[106] J. Kang, R. Yu, X. Huang, S. Maharjan, Y. Zhang, and E. Hossain, "Enabling localized peer-to-peer electricity trading among plug-in hybrid electric vehicles using consortium blockchains," *IEEE Trans. Ind. Informat.*, vol. 13, no. 6, pp. 3154–3164, Dec. 2017.
[107] C. Liu, K. K. Chai, E. T. Lau, and Y. Chen, "Blockchain based energy trading model for electric vehicle charging schemes," in *Proc. Int. Conf. Smart Grid Inspired Future Technol.*, Jul. 2018, pp. 64–72.

Nanduni I. Nimalsiri received the B.Sc.Eng. degree (Hons.) in computer science and engineering from the University of Moratuwa, Moratuwa, Sri Lanka. She is currently pursuing the Ph.D. degree in engineering and computer science, majoring in engineering, with the Research School of Engineering, The Australian National University (ANU), Canberra, ACT, Australia. She is also a Research Student with Data61, CSIRO. Her current research interests include distributed control and optimization of EV charging in smart grid.

Chathurika P. Mediwaththe (Member, IEEE) received the B.Sc. degree (Hons.) in electrical and electronic engineering from the University of Peradeniya, Sri Lanka, and the Ph.D. degree in electrical engineering from the University of New South Wales, Sydney, NSW, Australia, in 2017. She is currently a Research Fellow with the Research School of Electrical, Energy and Materials Engineering (RSEEME) and the Battery Storage and Grid Integration Program, The Australian National University, Australia. Her research interests include electricity demand-side management, renewable energy integration into distribution power networks, game theory and optimization for resource allocation in distributed networks, and machine learning.

Elizabeth L. Ratnam (Member, IEEE) received the B.Eng. degree (Hons.) and the Ph.D. degree from The University of Newcastle, Australia, all in electrical engineering, in 2006 and 2016, respectively. She subsequently held post-doctoral research positions with the Center for Energy Research, University of California at San Diego, and with the California Institute for Energy and Environment, University of California at Berkeley. From 2001 to 2012, she held various positions at Ausgrid, a utility that operates one of the largest electricity distribution networks in Australia. She currently holds a Future Engineering Research Leader (FERL) Fellowship from The Australian National University (ANU). She joined the Research School of Engineering, ANU, as a Research Fellow and a Lecturer in 2018. Her research interests include applications of optimization and control theory to power distribution networks.

Marnie Shaw received the B.Sc. (Hons.) and Ph.D. degrees from the School of Physics, The University of Melbourne, Melbourne, VIC, Australia, in 1999 and 2003, respectively. She was the Head of Data Analysis at Descartes Therapeutics Inc., Boston, an Instructor at Harvard University, and a Scientist at the University of Heidelberg, Germany. She is currently a Research Leader of the Battery Storage and Grid Integration Program with the Australian National University and the Convenor of the Energy Efficiency Research Cluster at the ANU Energy Change Institute. Her research interests lie in applying data analytics and machine learning to a range of data-rich problems, including the integration of renewable energy into the electricity grid.

David B. Smith (Member, IEEE) received the B.E. degree in electrical engineering from the University of New South Wales, Sydney, NSW, Australia, in 1997, and the M.E. (research) and Ph.D. degrees in telecommunications engineering from the University of Technology, Sydney, in 2001 and 2004, respectively. Since 2004, he has been with National Information and Communications Technology Australia (NICTA; incorporated into Data61 of CSIRO in 2016) and The Australian National University (ANU), Canberra, ACT, Australia. He is currently a Principal Research Scientist with Data61, CSIRO, and an Adjunct Fellow with ANU. He has a variety of industry experience in electrical and telecommunications engineering. He has published over 150 technical refereed articles. His current research interests include wireless body area networks, game theory for distributed signal processing, disaster tolerant networks, 5G networks, the IoT, distributed optimization for smart grid, electric vehicles, and privacy for networks. He has made various contributions to the IEEE standardization activity in personal area networks. He was a recipient of four conference Best Paper Awards. He is an Area Editor of *IET Smart Grid* and has served on the technical program committees for several leading international conferences in the fields of communications and networks.

Saman K. Halgamuge (Fellow, IEEE) received the B.Sc.Eng. degree in electronic and telecommunication engineering from the University of Moratuwa, Moratuwa, Sri Lanka, and the Dr. Ing. and Dipl.Ing. degrees in electrical engineering (data engineering) from TU Darmstadt, Darmstadt, Germany, in 1990 and 1995, respectively. He has held appointments as the Director/Head of the Research School of Engineering, The Australian National University (ANU), Canberra, ACT, Australia, and the Associate Dean International of the Melbourne School of Engineering, The University of Melbourne, Melbourne, VIC, Australia, where he is currently a Professor with the Department of Mechanical Engineering. He is an honorary Professor of ANU and the ANU's Energy Change Institute. His research interests are in AI and applications in energy, mechatronics, and biomedical engineering. He has published over 250 articles and graduated 42 Ph.D. students in the above areas and obtained substantial research grants from the ARC, NHMRC, and industry. He is a Distinguished Lecturer of the IEEE Computational Intelligence Society.

2.3 Coordinated EV Charging for Load Curve Shaping

A large number of EVs added to the electric grid will create new demand peaks or exacerbate existing demand peaks in the grid load curve, overloading power distribution infrastructure and possibly endangering the safe operation of power systems [Fernandez et al., 2010; Mu et al., 2014; Salah et al., 2015]. Therefore, EV-based DSM strategies to reduce load congestion in the electric grid are becoming increasingly important [Hiskens and Callaway, 2009; Callaway and Hiskens, 2010].

A growing body of literature has proposed numerous EV-assisted load curve shaping strategies to tackle the problem of load congestion. These strategies have aimed to mitigate the power imbalance between supply and demand by using the available power generation and distribution capacity, thus eliminating the requirement to build new power generation plants or implement massive upgrades in existing distribution infrastructure.

Researchers have primarily considered load curve shaping by means of flattening the load curve composed of aggregated EV and non-EV load (base load) attributed to end-customers. A flattened load curve reduces the peak-to-average power ratio, enhancing the quality of power and enabling steady-state grid operation. *Valley-filling*, as depicted in Fig. 2.3, is a technique of flattening the load curve by shifting power demands to valley regions of the load curve (off-peak periods), where the demand for electricity is at its lowest [Ma et al., 2012]. In EV-assisted valley-filling strategies, EV charging is scheduled such that EVs utilise surplus power in the lower-demand hours, thereby alleviating the demand pressure during peak hours [Hu et al., 2016b; Jian et al., 2017; Yi et al., 2020; Wang et al., 2019; Ma et al., 2012; Chen et al., 2014]. For example, Jian et al. [2017] propose a centrally coordinated valley-filling strategy consisting of two key indices called capacity margin index and charging priority index, where the former selects the target time slots in which the power grid has abundant surplus power for EV charging, and the latter determines the charging priority of EVs on each time slot.

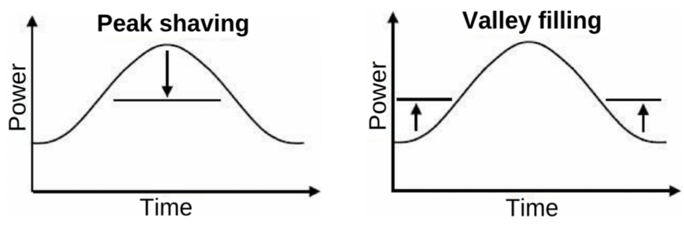

Figure 2.3: Peak-shaving and valley-filling

The commonly used optimisation objectives for load curve flattening include minimising the aggregated load, minimising the load variance, minimising the energy costs for charging EVs, and minimising power fluctuations [Nimalsiri et al., 2019]. These objective functions exhibit the common characteristic that they are coupled by the EV charge rates and are not separable across individual EVs, making it challenging to solve the optimisation problem in a distributed manner. In order to tackle this challenge, various distributed optimisation algorithms have been proposed in the literature.

In [Vandael et al., 2010], EV charging is treated as a DSM problem and two solutions are proposed: a centralised Quadratic Programming (QP)-based solution and a decentralised Multi-Agent Systems (MAS) solution. While the QP scheduler is able to optimally flatten peak loads, it is not scalable. In contrast, the MAS solution is proven to be scalable and adaptable to incomplete and unpredictable information.

Li et al. [2011] propose a decentralised EV charging algorithm to obtain a flat load curve by minimising the distribution system load variance. In the proposed algorithm, binary charging decisions (charge or not charge) are made locally by each EV after comparing its SoC to a charging reference signal that is carefully chosen by an aggregator, based entirely on the current states of the power system, such as the SoC of plugged-in EVs, the output of distributed generation, the household non-EV load, and the external regulation signals. Importantly, the EV charging decisions are determined in a real-time manner, without requiring predictions of any quantity such as EV driving patterns and non-EV load.

Ma et al. [2011a] exploit a game-theoretic approach to develop a decentralised EV charging scheme for valley-filling, with optimality proved for the homogeneous case where EVs are identical, i.e., all EVs plug in for charging at the same time, have the same deadline, needing to charge the same amount of electricity, and have the same maximum charge rate. Assuming that EVs are cost-minimising and weakly coupled via a common electricity price, the authors design a non-cooperative game, which converges to a unique Nash equilibrium in the infinite system limit (for the case of a very large EV population). The proposed algorithm is proven globally optimal for the homogeneous case and nearly globally optimal for the heterogeneous case, where EVs are non-identical, i.e., EVs plug in at different times, have different deadlines, charge a different amount of electricity, and have different maximum charge rates. However, the decentralized charging algorithm in [Ma et al., 2011a] is effective only if available generation, non-EV demand and electricity price over the charging interval are known with perfect accuracy. Therefore, the authors in [Ma et al., 2011b] later present a decentralized, model predictive control-based approach to manage forecast uncertainty by allowing decentralized agents to continually update their optimal control trajectories subject to revised forecasts of system states.

Ghavami et al. [2013] also propose non-cooperative game framework for a much more general setting that does not assume an infinite EV population. Karfopoulos and Hatziargyriou [2012] also apply game theory to develop a distributed and multi-agent EV charging control method for valley-filling. The proposed multi-agent framework consists of EV supplier aggregator agents, regional aggregation unit agents, microgrid aggregation unit agents and vehicle controller agents, and is implemented as a non-cooperative and dynamic game, which converges to a ε-Nash equilibrium under the Nash Certainty Equivalence Principle [Huang et al., 2007].

In [Gan et al., 2012a], the authors exploit a gradient projection method to develop a decentralised EV charging algorithm for valley-filling. The proposed algorithm consists of an iterative routine, which is driven by price signals issued by a central operator that plays the role of an aggregator. At each iteration, after receiving the price signal from the central operator, each EV autonomously determines their charging profile and informs that to the central operator. Upon receiving the charging profiles from all EVs, the central operator alters the price signal to guide EV charge profile updates for the subsequent iteration and the same process repeats. Unlike [Ma et al., 2011a], the algorithm in [Gan et al., 2012a] converges to optimal charging profiles in both homogeneous and heterogeneous cases. Furthermore, it is proven that the algorithm in [Gan et al., 2012a] is guaranteed to converge as the number of iterations approaches infinity and that the flatness of the load profile is optimal at the convergence. The authors in [Ma et al., 2016] also propose a similar decentralised framework that seeks to fill the overnight load valley by facilitating the trade-off between total generation cost and local costs associated with overloading and battery degradation. Similar to [Gan et al., 2012a], the approach in [Ma et al., 2016] involves each EV iteratively minimising their charging cost with respect to a forecast price signal. While the approach in [Gan et al., 2012a] is guaranteed to converge to optimal charge profiles as the number of iterations approaches infinity, the approach in [Ma et al., 2016] is guaranteed to converge to an ϵ-optimal strategy in no more than $K(\epsilon)$ iterations. The reference [Zou et al., 2017] considers a completely distributed protocol where the central entity in [Ma et al., 2016] is eliminated and a consensus algorithm is used to fully distribute the price update mechanism. In [Ma et al., 2015], an auction-based game is formulated for coordinating EV charging over a finite horizon, and in [Zou et al., 2016], a distributed approach to coordinating EV charging based on the progressive second price auction mechanism is proposed.

In [Ma et al., 2014], the authors extend the algorithm in Gan et al. [2012a] to minimise the total load variance while also satisfying the capacity constraints in the power distribution network. As opposed to [Gan et al., 2012a], the algorithm in [Ma et al., 2014] utilises two different price-like control signals to govern the iterative routine. One signal is used, as in [Gan et al., 2012a], to coordinate the EV charge profiles to obtain a valley-filling load profile, while the other signal is introduced to satisfy the capacity constraints via an Alternating Direction Method of Multipliers (ADMM)-based routine.

Gan et al. [2012b] propose a stochastic distributed EV charging algorithm, with charging limited to discrete rates. Similar to the algorithmic approaches in [Ma et al., 2011a; Gan et al., 2012a; Ma et al., 2016], the algorithm in Gan et al. [2012b] also comprises an iterative procedure, where at each iteration, an aggregator at the transformer receives charge profiles computed by EVs in the previous iteration and broadcasts the corresponding normalised total demand to EVs. Afterward, each EV generates a probability distribution over their potential charge profiles and samples from the distribution to obtain a new charge profile. It is proven that this algorithm almost surely converges to one of its equilibrium charge profiles and each of its equilibrium charge profiles has a negligible sub-optimality ratio. By contrast, Zhan et al. [2015] develop a decentralised EV charging algorithm to fill the overnight load valley, which is implemented by calculating a probability transition matrix at the aggregator side, which acts as the control signal to guide the EV charging process through an iterative routine.

Kundu and Hiskens [2012] propose a hysteresis-based EV charging control strategy that is capable of regulating charging load to satisfy system-wide services, including valley filling and balancing fluctuations in renewable generation. Chen et al. [2012] formulate a joint Optimal Power Flow (OPF) and EV charging control problem, which is solved using a nested optimisation approach that decomposes the original problem using dual theory. The authors characterise the optimal offline EV charging schedule as a valley-filling profile, which leads to the design of an optimal offline algorithm with computational complexity that is significantly lower than centralised interior point solvers. The authors also propose a decentralised online algorithm that dynamically tracks the valley-filling profile.

Rivera et al. [2013] propose a decentralised EV charging algorithm based on an ADMM approach, which decomposes the original problem into smaller subproblems that are assigned to each EV and an aggregator and solved consistently by passing incentive signals between them. Interestingly, the proposed algorithm is designed in a way such that it can be parameterised to trade-off the importance of various aggregator goals (e,g, valley-filling) versus individual EV goals (e.g., minimal-cost charging). Pajic et al. [2018] also propose a distributed EV charging algorithm based on the ADMM method in combination with a blockchain method to solve the valley-filling problem by efficiently distributing the electricity demands of EVs over time periods in which the electric grid is underutilised.

Zhan et al. [2016] propose a hierarchical EV charging control method for valley-filling, with an architecture that consists of a main-control center and sub-control centers, each assigned with a group of EVs. The objective of the main-control center is to flatten the load curve by coordinating sub-control centers. To do that, the main-control center calculates the optimal load plan for each sub-control center using a two-stage optimisation method. The sub-control centers then coordinate charging of EVs assigned to each of them, such that the load profile follow the load plan received from the main-control center.

Zhang et al. [2016] propose a decentralised EV charging algorithm based on the Frank–Wolf algorithm that consists of an iterative routine, where at each iteration, a charging control center (aggregator) evaluates and broadcasts time slot pricing ordering (from cheapest to most expensive) to EVs, and in response, EVs update their charge profiles and communicate back to the charging control center. In an effort to preserve the privacy of EV users, the authors also include a simple communication protocol arranged over a tree graph rooted at the charging control center, and EVs constitute the remaining tree nodes. Each node receives aggregated charging profiles from its downstream nodes, adds them up to its own profile, and forwards the updated aggregated charging profile to its parent node. In this way, only the summation of EV charging profiles is transmitted to the charging control center and the charging control center does not require knowing the individual EV charging profiles.

Liu et al. [2017] develop a decentralised EV charging algorithm based on the shrunken-primal-dual sub-gradient method, to achieve valley-filling while satisfying distribution network constraints. As with many other distributed algorithms, the algorithm in [Liu et al., 2017] is also iterative and consists of an operator (aggregator), who, at each iteration, broadcasts a Lagrangian gradient, upon which EVs fine-tune their charging profiles.

A common feature that exists in the prior distributed EV charging algorithms is that they use an iterative approach that requires several round trips of bi-directional communication between the aggregator and each EV. The number of iterations generally increases as the number of EVs becomes very large, resulting in a large communication overhead. Alternatively, Binetti et al. [2015] propose a non-iterative load curve shaping algorithm to schedule a large population of EVs in a decentralised fashion. The proposed algorithm schedules one EV at a time, only once (i.e., at the time the EV connects to the grid), and therefore does not require heavy computations, broadcast messages, or extensive bi-directional communication, making it suitable for real-time implementation. The key limitation that exists in such a sequential scheduling approach is the scalability, especially for scenarios when a large number of EVs grid-connect at the same time. Zhang et al. [2014b] also develop a non-iterative approach for distributed EV charging that minimises the amount of communication needed between the grid operator (aggregator) and EVs. It uses a cost schedule that reflects the valleys for EVs to charge (by assigning low costs to such periods), which is then shared with EVs, each solving a simple linear program to identify the periods for charging. The charging profiles of EVs are then sent back to the grid operator for necessary updates. Importantly, the data is transmitted each way only once. Ahn et al. [2011] propose a command-based decentralised EV charging algorithm, wherein EVs receive a simple command from a centralised grid controller (aggregator) and then determine their individual charge profiles. The proposed algorithm requires no complex bi-directional communication network, however, it only achieves a near-optimal valley-filling effect, which is also affected by the willingness of EV owners to relinquish their charging autonomy. Zhang et al. [2014a] propose another decentralised charging algorithm for valley-filling that eliminates the requirement for bidirectional communication between the grid and EV owners. In the proposed algorithm, individual EV charging behaviors are indirectly coordinated by broadcasting to EV owners, a day-ahead pricing scheme, which is derived by solving a minimum-cost optimisation problem that yields a valley-filling effect at the system level.

We also note that most existing distributed EV charging schemes (e.g., [Ma et al., 2011a; Gan et al., 2012a; Liu et al., 2017]), have the limitation that the aggregator needs to collect in each iteration, all individual EV charging profiles to update the coordination signal that is broadcast back to the EVs in the subsequent iteration. Such approaches require a highly reliable bi-directional communication network between the aggregator and EVs. Moreover, those approaches result in a high communication overhead since all communication signals traverse through the aggregator. On the other hand, those approaches raise concerns with respect to EV user privacy as EV charge profiles have to be shared with the aggregator. To solve these issues, Rahbari-Asr and Chow [2014] propose a fully distributed and multi-agent

EV charging control algorithm based on the Karush–Kuhn–Tucker (KKT) conditions and consensus networks, where the power allocation to EVs under all local and global constraints is reached through peer-to-peer EV coordination, thus eliminating the need for an aggregator (central coordinator) and improving robustness against single-link/node failures. Mohammadi et al. [2016] also propose a consensus and innovation-based multi-agent EV charging algorithm that enables a fully distributed implementation without the need for an aggregator. The proposed multi-agent algorithm encompasses an iterative procedure, which finds a distributed solution for the first order optimality conditions of the underlying optimisation problem through local computations and limited information exchange with neighboring agents (EVs). In particular, the information exchange between neighboring agents over the course of the iterative routine is restricted to communicating a Lagrange multiplier, which defines the value of power consumption from each EV point of view. The proposed algorithm is shown successful in scheduling most charging demand during the low-demand hours of the night, thereby contributing to valley-filling.

In addition to valley-filling of the load curve by charging during periods of lower electricity demand, V2G-enabled EVs can facilitate supply-demand balance by also discharging during peak periods, and thereby contribute to *peak-shaving* of the load curve, as depicted in Fig. 2.3. In [Tse et al., 2016], the authors analyse the feasibility of using EV batteries for peak-shaving in the V2G domain. The major findings of their study reveal that the financial savings from peak-shaving could be used as incentives to offset the extra cost of EV batteries.

Stüdli et al. [2014, 2015] explore the potential of EVs for peak shaving, load tracking and reactive power support purposes, and propose a distributed algorithm using the Additive Increase Multiplicative Decrease (AIMD) algorithm to regulate the energy exchange between the grid and the EV fleet in an optimal and fair fashion. Specifically, the proposed approach in [Stüdli et al., 2012b,a] supports only G2V operations, and the work in [Stüdli et al., 2014] extends that approach to both implement the Vehicle-to-Grid (V2G) concept and to provide reactive power compensation. In [Stüdli et al., 2013], the authors propose a AIMD-based game between multiple fixed structure automata for peak shaving tasks, as well as for slow varying load tracking. Interestingly, the proposed algorithm allows binary (on/off) charging and does not rely on any day-ahead forecasts.

By considering the potential role of EVs as distributed energy storage resources to support peak-shaving, Erdogan et al. [2018] develop a discharging control scheme that consists of two stages. In the first stage, a desired level for peak-shaving and duration for V2G service are determined off-line based on forecast load profile and EV mobility model, and in the second stage, EV discharge rates are dynamically adjusted in real time by considering the actual grid load and the characteristics of grid-connected EVs.

Several centralised EV charging and discharging schemes to support both peak-shaving and valley-filling of the grid load curve are proposed in [Jian et al., 2012; Wang and Wang, 2013; Ortega-Vazquez, 2014; Ioakimidis et al., 2018; Zhou et al., 2020a]. Wang and Wang [2013] propose a V2G control algorithm for peak shaving and valley filling, where a smart-grid control center determines the EV charge and discharge targets according to the load demand and data on available V2G capacity. Ortega-Vazquez [2014] propose an EV charging and discharging algorithm under a real time pricing scheme with battery degradation costs and price uncertainty also taken into account. Ioakimidis et al. [2018] propose an EV charging and discharging algorithm to peak-shave and valley-fill the load curves of non-residential buildings using EVs in a parking lot. In [Jian et al., 2012] and [Zhou et al., 2020a], the authors investigate the possibility of utilising V2G operation for peak-shaving and valley-filling in a microgrid.

Luo et al. [2013a] investigate EV coordination strategies for peak shaving and valley filling at a macro level, thus supporting grid-related policy making. Specifically, the authors develop a suite of methods to obtain an optimal EV coordination strategy for peak-load shaving and also provide a method to quantitatively analyse the benefits and costs of the EV coordination strategy from a social welfare approach. The study in [Luo et al., 2013b] applies the techniques in [Luo et al., 2013a] in a case study on cost-benefit analysis.

In [Karfopoulos and Hatziargyriou, 2015], the authors extend their game-theoretic EV charging algorithm proposed in [Karfopoulos and Hatziargyriou, 2012] to develop a distributed EV coordination algorithm that utilises both the flexibility of EV demand and the V2G capability to minimise system load variance. The authors in [Kaur et al., 2015] also exploit game theory to develop a distributed and hierarchical EV charging and discharging scheme that aims to flatten a microgrid's load curve. It involves scheduling EVs one by one based on a list arranged in the order of players' (EVs) payoff values, and as such, the proposed approach is not scalable for a large EV population.

In [Le Floch et al., 2015] and [Le Floch et al., 2016], the authors propose three distributed algorithms to flatten the total load curve based on dual splitting optimisation methods, namely a gradient ascent method, and two incremental stochastic gradient methods. The proposed algorithms include an iterative framework where each iteration consists of two primary steps. In the first step, each EV solves a local optimal program based on a broadcast price signal (the dual variables) and communicates their response to the aggregator, and then in the second step, the aggregator updates the price signal to achieve minimal load variance. Importantly, the proposed algorithms allow EVs to operate in either Grid-to-Vehicle (G2V) or V2G mode, facilitating both valley-filling and peak-shaving.

Water-filling theory in communication systems [Gallager, 1968] is leveraged by various researchers to design EV charging schemes, specifically for valley-filling and peak-shaving purposes. Mou et al. [2014] first implement a water-filling based decentralised EV charging algorithm for valley-filling. In [Xing et al., 2015] and [Li et al., 2019], the authors extend the algorithm in [Mou et al., 2014] to additionally support peak load shaving via EV discharging coordination. However, the algorithms presented in [Xing et al., 2015; Li et al., 2019] are limited to load curves of specific shapes only. Interestingly, Xing et al. [2017] propose an ADMM-based algorithmic extension of [Mou et al., 2014], which is compatible with load curves of all general shapes.

In [Meikandasivam et al., 2018], the authors first identify time zones that need load flattening and then accomplish optimal energy distribution among the time intervals in each zone using a water-filling based algorithm. The authors in [Rajendhar and Jeyaraj, 2020] implement a water-filling based energy distribution algorithm involving appliances such as PEVs, thermal comforts of heat pumps, combined heat and power units, washing machines, cloth dryers and dish washes.

2.3.1 Coordinated EV charging for tracking arbitrary power profiles

Another class of studies in the EV charging literature have considered the more general objective of following a target load curve, in which the classical valley filling behavior is just a sub-case. The objective of following or tracking a target load profile becomes important in several scenarios, for example, to schedule EV charging following an arbitrary power profile (e.g., renewable power generation profile) or to schedule EV charging to track the electricity profile that an aggregator has bought in the day-ahead market.

Kisacikoglu et al. [2018] propose a distributed EV charging algorithm to smoothen the grid load profile by tracking a preferred operating point (POP). The proposed algorithm consists of an offline stage to estimate a reference operating power level based on the forecast EV mobility, energy demand and base load profile, and a real-time stage to determine EV charge rates such that the aggregated load tracks the reference loading level. However, the proposed approach restricts to tracking a single POP value, which is constant over the time horizon, and hence is unable to track a load profile where the POP varies over time. By contrast, Gan et al. [2012a] present an extension of their decentralised valley-filling algorithm that is capable of tracking a given load profile.

In [Zhang et al., 2014b], the authors show that a slightly modified version of their algorithm proposed for valley-filling can be utilised to approach a predefined target load, which the grid operator favors by using the gap between current load and the target load as the cost. Di Giorgio et al. [2014] propose a model predictive control framework that minimises the cost of energy consumption while tracking a reference load profile defined by the grid operator.

In [Malhotra et al., 2017], the problem of tracking an arbitrary power profile by coordinated charging of EVs is formulated as a discrete scheduling process, which restricts charging to only the maximum rated power for the EV. The proposed algorithm is implemented in a distributed fashion, allowing a set of sub-aggregators, each assigned with a set of EVs, to coordinate via a consensus process, thus eliminating the need for a central aggregator and making the algorithm scalable and tolerant to network faults. The proposed algorithm also maximises the user convenience and guarantees to track, and not exceed, the power profile imposed by the power utility.

2.4 Coordinated EV Charging for Voltage Regulation

Voltage stability is defined as the ability of a power system to maintain steady voltages at all nodes in the distribution feeder after being subjected to a disturbance from a given initial operating condition [Kundur et al., 2004]. The enormous electricity demand imposed by a large population of grid-connected EVs put the power distribution networks under a critical strain, leading to issues on voltage stability. In particular, voltage deviations beyond a nominal voltage range lead to lower power quality, which may affect proper operation of electrical equipment. For example, when voltage thresholds are exceeded, electrical appliances may malfunction or shorten their lifetimes, resulting in heavy fines for distribution companies [de Hoog et al., 2015].

With the rapid uptake of grid-connected solar photovoltaics (PV) together with the introduction of V2G operation, electrical distributors are now concerned with bi-directional power flows inducing both under-voltage conditions as well as over-voltage conditions. Therefore, it is of great importance to devise coordination strategies that regulate EV charging and discharging to maintain system voltages within acceptable limits. Doing so will also reduce load peaks and power losses in the distribution systems.

2.4.1 Centralised EV charging coordination for voltage regulation

Centralised approaches for voltage-aware EV charging in balanced distribution networks are studied in [Zhan et al., 2012; Singh et al., 2013; Chen et al., 2014; Benetti et al., 2014; Alonso et al., 2014]. The work in [Singh et al., 2013] focuses on using EV batteries as distributed energy storage systems to flatten the load profile while maintaining the nodal voltages of a balanced three-phase distribution network within an acceptable limit. For this purpose, the authors develop a fuzzy logic controller to control the aggregated power flow at the connection bus.

Presuming at most one EV per bus, EV charging coordination under balanced network constraints is tackled using a water-filling algorithm in [Chen et al., 2014]. In particular, the authors first formulate a joint OPF-EV charging problem that optimises the operation of a power grid subject to the voltage constraints, line constraints and power balance constraints arising from charging EVs at different locations, and then propose a centralised algorithm to solve the joint OPF-EV charging problem with a computational complexity significantly lower than the centralised interior point solvers.

In [Benetti et al., 2014], the authors propose a real-time EV charging algorithm with a centralised control architecture that aims to limit the peak load and increase the number of rechargeable EVs with respect to the scenario in which no coordination action is performed. In addition, voltage constraints in a balanced distribution network are also incorporated, where a power-flow procedure based on the Newton–Raphson method is applied to assess voltages on all network buses.

Alonso et al. [2014] propose an EV charging coordination algorithm to flatten the load profile at a transformer, while taking into consideration the thermal line limits, load on transformers, voltage limits and parking availability patterns. The objective function of the proposed optimisation problem is given as a measure of transformer load profile deviation between consecutive hours. To obtain the optimal solution to the proposed optimisation problem, the authors adopt a meta-heuristic approach based on a genetic algorithm, in which each gen in a chromosome defines the charging power at a specific charging outlet.

Deilami et al. [2011] propose a real-time EV charging coordination strategy with the objective of minimising power losses while keeping system voltages within an acceptable limit and ensuring total power demand can be adequately supported by the existing infrastructure. The proposed approach reduces power generation cost by incorporating time-varying market energy prices. Moreover, it complies with network operation criteria such as limits on power losses, generation, and voltages and it enables EVs to begin charging as soon as possible by considering the EV owner preferred charging time zones based on priority selection. In [Zhan et al., 2012], the authors aim to maximise profits of distribution companies while addressing network voltage constraints. The proposed algorithm employs an approach that iteratively solves a linear program until all voltages fall within the required levels.

Approaches to coordinate EV charging in unbalanced distribution systems are much less prevalent compared to those ones considering balanced (or single-phase) distribution systems. Perhaps, only a very few studies are found to have considered coordinated EV charging in unbalanced distribution networks [Clement-Nyns et al., 2009; Clement et al., 2009; Sortomme et al., 2010; Sojoudi and Low, 2011; Richardson et al., 2011; De Hoog et al., 2014; Franco et al., 2015]. In [Clement-Nyns et al., 2009] and [Clement et al., 2009], EV charging control algorithms are proposed to minimise power losses, while maintaining the voltage deviation at each bus within an acceptable limit and keeping the output powers at all chargers below their maximum ratings. The backward-forward sweep method [Kersting, 2006] is used to compute the voltage at each node and the optimisation problem is solved using a QP-based technique. Same as in [Clement-Nyns et al., 2009] and [Clement et al., 2009], the authors in [Sortomme et al., 2010] also aim to improve voltage profile by minimising power losses. The authors explore relationships between power losses, load factor, and load variance and discover that power loss minimisation can be achieved by maximising load factor or minimising load variance. Sojoudi and Low [2011] propose a way of centralised EV charging using an OPF optimisation problem formulation, which aims to minimise generation and charging costs while satisfying all constraints imposed by the distribution network. Clement-Nyns et al. [2011] investigate coordinated charging and discharging to minimise charging costs while supporting the grid for voltage control and congestion management.

Richardson et al. [2011] propose an EV charging algorithm that maximises the total power delivered to EVs while operating within tolerable voltage deviations. Specifically, the authors discover that both voltage and thermal loading sensitivities are approximately linear, which leads to the formulation of a simple linear programming problem that determines the optimal charging rate for each EV. The proposed algorithm also includes a limit in variation in charging power between two consecutive time steps, which is practically important because rapid and large variation in charging power is harmful to the EV battery.

De Hoog et al. [2014] formulate EV charging as a linear optimisation problem, with voltage drop modelled as a linear constraint, on a phase-by-phase basis, in every lateral of an unbalanced network. It is shown that such a linear approximation of the voltage constraint is quick to compute, and still ensures that network constraints are not violated. Moreover, two objectives are considered: the first to maximise total charging of all EVs, and the second to minimise the cost of charging. It is concluded that the linear approximation of key network constraints such as transformer capacity, line current ratings, and voltage drop is an effective way to simplify the problem and allow faster and more repeated computation of the solution in a receding horizon manner. Franco et al. [2015] propose a mixed-integer linear programming model to minimise the charging cost of EVs in unbalanced distribution networks, with operational constraints such as voltage and current limits taken into account. In both [De Hoog et al., 2014] and [Franco et al., 2015], the optimal solution is found using generic commercial solvers.

Luo and Chan [2014] propose a scalable real-time scheduling scheme for EV charging in low-voltage, unbalanced distribution systems. The proposed algorithm schedules EV charging either to minimise system losses or to avoid voltage dropping below the lower limit, depending on whether the EV penetration level is sufficiently high to make the voltage drop become the binding constraint. The proposed scheme also levels the system voltage profiles by considering the effect of charging location on the network voltage drop, and then derive a power/voltage levelling factor to allow adaptive switching of the EV charging plan from voltage-safety-oriented scheduling (to level voltage profiles) to loss-minimisation-oriented scheduling (to level system load profile), or vice versa.

Islam et al. [2019b, 2020a] propose a multi-objective optimisation technique for mitigating network imbalance and improving voltages considering both EVs and distributed generation. The proposed approach also ensures the distribution system operators use the available network capacity efficiently and increases the level of comfort to EV users. Islam et al. [2020b] propose a hierarchical control method that allows the participation of distribution network operators, PVs and EVs to improve power quality by minimising both voltage unbalance and neutral current.

2.4.2 Distributed EV charging coordination for voltage regulation

Distributed approaches to coordinating EV charging with the aim of improving supply voltages in distribution networks are recently been considered in [Zhang et al., 2016; Liu et al., 2017]. By leveraging a linearised model for unbalanced distribution grids proposed in [Gan and Low, 2014], the authors in Zhang et al. [2016] aim to minimise the power supply cost while respecting voltage regulation and substation capacity limitations. The resultant optimisation problem has a non-separable objective function and strongly coupled inequality constraints specifying network limitations. The authors then propose a decentralised EV charging algorithm, in which optimising variables across grid nodes is accomplished by exchanging information only between neighboring buses via an ADMM method.

To achieve valley-filling while complying with network voltage limitations, Liu et al. [2017] propose a decentralised EV charging control algorithm, which is formulated into an optimisation problem with a non-separable objective function and strongly coupled voltage constraints and solved using the shrunken-primal-dual subgradient (SPDS) algorithm. The proposed algorithm includes an iterative routine, which is driven by an operator (aggregator) that computes and broadcasts a Lagrangian gradient based on the charging profiles computed by EVs and transmitted to the operator in the previous iteration. The algorithm in [Liu et al., 2017], unlike [Zhang et al., 2016], does not pose computing burdens to buses of the network, and ensures convergence of primal and dual variables without regularizing the Lagrangian. However, the proposed algorithm applies to balanced distribution networks, only. In [Liu et al., 2018], the authors exploit the SPDS algorithm in [Liu et al., 2017] to develop a decentralised EV charging control scheme for valley-filling under both nodal voltage constraints and transformer thermal constraints. By contrast, the authors in [Liu and Sahraei-Ardakani, 2019] extend the work in [Liu et al., 2017] to develop a chance-constrained SPDS approach to handle decentralised EV charging control problems that have chance constraints on nodal voltages. In [Huo and Liu, 2020], the work in [Liu et al., 2017] is extended to include a novel dimension reduction methodology that groups EVs and establishes voltage updating subsets for each EV group in the distribution network. To solve the reduced-dimension problem, the authors then develop a shrunken primal-multi-dual subgradient optimisation algorithm.

Zhou et al. [2020b] propose a distributed EV charging method based on a hierarchical ADMM approach to minimise the total cost of charging and power losses, while preventing nodal voltages dropping below nominal ranges in distribution networks. Then et al. [2021] propose a decentralised EV charging control strategy using droop-based control to mitigate local voltage rise caused by rooftop PV systems and phase unbalance caused by unbalance loads in a low-voltage distribution network. The proposed algorithm also smooths out the voltage profiles. Interestingly, the authors also include a price-based incentive scheme to compensate for the inconvenience caused to EV owners. Zhang and Leung [2018] propose a hierarchical framework for joint OPF routing and decentralised EV scheduling with V2G regulation services. First, the OPF problem is formulated and solved through the semidefinite programming relaxation. Then, the scheduling problem with V2G regulation service is proposed as a convex optimisation problem and a decentralised algorithm is designed to find the EV charging profiles.

Assuming that the grid is balanced and the node loads are all connected to the same phase on the feeder branch, Cao et al. [2020] propose a a distributed EV charging approach with a voltage compensation algorithm to recover voltage violations. In particular, the voltage compensation is achieved through a negotiation between the grid-level agent and microgrid agents using the ADMM method, where in each negotiation round, individual agents pursue their own objectives.

The studies in [Richardson et al., 2012; Xia et al., 2014; Al-Awami et al., 2015] investigate distributed EV charging methods to control EV charging using local voltage measurements at the customer Point of Common Coupling (PCC) without requiring no real-time communication between the EV and the utility. In more detail, Richardson et al. [2012] propose a local control technique, whereby EVs attempt to maximise their own charging rate while maintaining the voltage at customer point of connection and service cable loading within acceptable operating limits. It allows the optimal charge rates of EVs to be determined individually based solely on local network conditions and their battery SoC. The proposed local control charging method is compared with a centralised control charging method wherein a central controller manages the charging rates of all the EVs in the network, and the results indicate that the local control charging method can deliver a similar amount of energy to the EVs as with the centralised control method, however, it is not as capable at maintaining network parameters within specified limits and may require larger safety margins.

Xia et al. [2014] also propose a distributed EV charging method in which charging decisions are made individually at each household, based totally on local information without having any access to the full network state. The objective of the proposed algorithm is to maximally use grid capacity at all times, while still ensuring fairness among all EVs across the network. In particular, the algorithm uses varying charging power and passive back-off strategy to ensure grid safety and to maintain power supply quality. Al-Awami et al. [2015] propose an adaptive voltage-feedback controller for an on-board EV charger, which compares the system voltage at the point of charging with a preset reference voltage and reduces EV charging as the system voltage approaches this reference.

2.4.3 Coordinated EV charging taking both distribution network considerations and economic considerations into account

Several researchers have proposed EV charging algorithms that incorporate both distribution network considerations and economic/cost considerations. For instance, Dong et al. [2018] propose an EV charging pricing scheme for EV fast charging stations to determine the prices that support voltage control, which consists of a simulation model of EV mobility and a double-layer optimisation model. By taking into account the total income of fast charging stations and the EV users' response to the pricing scheme, the double-layer optimisation model is developed to minimise the total voltage deviation of the distribution network. Sun et al. [2020] propose a method for cost-minimising, day-ahead scheduling of overnight charging of EVs in low voltage networks, which also incorporates constraints on voltage, current and apparent power computed via a linear power flow approximation.

In order to benefit EV customers by reduced cost of EV charging, and distribution grid operators by reduced power losses, the work in [Bharati and Paudyal, 2016] presents a bi-level hierarchical optimisation framework, in which the distribution grid and its control/operation form one level, and the operation of EVs form the another level. At the distribution grid level, distribution operational constraints such as voltage limits, feeder current limits, and transformer capacity are taken into account.

By considering EV fleets as a massive support for active and reactive power demands in microgrids, Shekari et al. [2016] propose a multi-objective framework for optimal day-ahead operation scheduling of microgrids with minimal operational cost. The corresponding optimisation problem, which takes into account the power quality concerns including voltage limitations, is formulated as a mixed-integer linear programming problem, and is tackled using an ϵ-constraint method.

2.5 Summary

In this chapter, first we have provided the background on EVs, including different models of EVs, different charging facilities, charging infrastructures, uni-directional and bi-directional charging, and adverse impacts of EV charging and discharging. We have also introduced the basic terminology describing EV charging coordination problems.

Then we have described solutions to mitigate negative impacts of EVs on the electric grid via DSM, where we have also explained the capabilities of the smart grid and the role of EVs in the smart grid. Then we have explained the generic design process of an EV charging algorithm, followed by descriptions of various types of EV charging algorithms that are developed based on various optimisation problems and EV coordination architectures.

We have provided an up-to-date literature review on both centralised and distributed demand-side approaches for coordinated EV charging and discharging, followed by our journal paper on algorithms for distributed charging control of EVs in smart grid.

Finally, we have presented a more focused literature review on EV charging algorithms for load curve shaping and voltage regulation, which provide the motivation to develop the EV charging control algorithms proposed in subsequent chapters, in Parts 2 and 3 of the thesis.

Part 2 of this thesis, which follows, is comprised of Chapter 3 and Chapter 4, each of which presents a novel algorithmic approach of coordinating EV charging (and discharging) for load curve shaping.

Part 2: Coordinated EV Charging and Discharging for Grid Congestion Management

Chapter 3

Coordinated EV charging for tracking arbitrary power profiles

While the deployment of EVs introduces an additional electric load on the power grid, the temporal flexibility of EV loads provides promising opportunities to implement demand-side approaches to reduce load congestion arising from EV charging. By coordinating EVs to shape the grid load curve, the grid congestion caused by excessive EV charging loads can be reduced.

In this work, EV charging is coordinated to track an arbitrary power profile (or a target power profile), which means to shape the final grid load profile — composed of aggregate EV and non-EV load profiles of end customers — such that it follows the trend/behaviour of a (arbitrary) target power profile. Such an objective is useful in various scenarios. For example, utility operators may have planning objectives with respect to aligning the power consumption of customers to follow certain trends. Another scenario characterizing the importance of tracking a target load curve is when an aggregator intends to schedule EV charging in such a way that follows the electricity profile that they bought in the day-ahead market. Valley-filling and peak-shaving of the load curve is also a special scenario of tracking a target load profile, where the target load profile is a flat load profile.

The increased penetration of non-dispatchable Renewable Energy Sources (RESs) such as wind power and solar photovoltaic (PV), and the intermittency (i.e., the uncontrollable variation in output level) in such renewable energy generation are significant challenges faced by the grid operators, which lead to the requirement to track variable generation to support the grid or to achieve a load curve that closely matches the available electricity generation [Stüdli et al., 2013]. Demand-side approaches to shape the load curve by allowing EVs to charge during periods having surplus energy generation and refraining EVs from charging during periods having deficient energy generation can relieve stress on the electric grid.

Water-filling theory [Gallager, 1968] has been initially proposed for power allocation in communication systems to maximise system throughput [Palomar and Fonollosa, 2005; He et al., 2013]. It has later been employed in numerous studies for computing the optimal solutions to load balancing problems of smart grid systems, with lower degree polynomial computational complexity [Mou et al., 2014;

Xing et al., 2015; He et al., 2016; Meikandasivam et al., 2018; Li et al., 2019; Rajendhar and Jeyaraj, 2020].

Hence, given the effectiveness of the water-filling concept for load regulation problems, this chapter is dedicated to the study of how EV charge scheduling can be coordinated using a water-filling based approach to shape the final load profile following a (arbitrary) target power profile. The contributions in this chapter are presented in our published manuscript.

3.1 Published Manuscript

In the paper presented below, an EV charging coordination algorithm is proposed to schedule EV charging to track an arbitrary power profile. Outcomes from this paper address research objective Q1 of the thesis (see Chapter 1 - Section 1.2) by scheduling EV charging for shaping the grid load curve (hence reducing grid congestion) and research objective Q3 by proposing a decentralized approach for EV charge scheduling (hence yielding a scalable coordination approach).

N. I. Nimalsiri, D. B. Smith, E. L. Ratnam, C. P. Mediwaththe, S. K. Halgamuge, "A decentralized electric vehicle charge scheduling scheme for tracking power profiles," in *Proceedings of the IEEE Power & Energy Society Innovative Smart Grid Technologies (ISGT)*, Washington, DC, USA, Feb. 2020.
https://doi.org/10.1109/ISGT45199.2020.9087797

A Decentralized Electric Vehicle Charge Scheduling Scheme for Tracking Power Profiles

Nanduni Nimalsiri, David Smith
Australian National University & CSIRO Data61.
Sydney, Australia
nanduni.nimalsiri@anu.edu.au

Elizabeth Ratnam,
Chathurika Mediwaththe
Australian National University.
Canberra, Australia

Saman Halgamuge
Australian National University
& University of Melbourne.
Melbourne, Australia

***Abstract*—Electric vehicles (EVs) are flexible electric loads whose consumption can be shifted over time, and thus controlled charging of EVs is possible. This paper proposes a decentralized control scheme called 'DECSaT' for charge scheduling of EVs with the objective of tracking an arbitrary power profile while accounting for heterogeneity in EV charging specifications and also uncertainty in EV arrival times. More specifically, we aim to align the charge profiles of EVs to follow a microgrid's forecast energy generation profile, while guaranteeing that the EV charging requirements are satisfied by the intended departure times. DECSaT is decentralized because each EV computes its charge schedule locally, using the information received from the microgrid operator. Interestingly, DECSaT is applicable for charging EVs at both variable rates and discrete rates, making it suitable for practical operation. Numerical simulations considering EV charging in a microgrid confirm the effectiveness of DECSaT in terms of power profile tracking.**

***Index Terms*—Coordinated charging, decentralized control, electric vehicle, microgrid, power profile tracking.**

I. Introduction

A massive uptake of electric vehicles (EVs) has occurred in recent years, due to their numerous economical and environmental benefits [1]. With large scale integration of EVs into the power distribution network, the implementation of controlled charging strategies is of vital importance. The charge control schemes in previous work are basically divided into centralized and decentralized approaches, with the former involving a centralized entity to directly control EV charging, and the latter allowing EVs to control charging on their own. In particular, decentralized approaches are highly scalable and practical over centralized approaches, due to low computation and communication complexities.

The large scale adoption of renewable energy sources in the electrical power grid, especially in microgrids, leads to a high volume of electricity generation, which should be either consumed immediately or stored for later use. However, existing electrical grid systems are not equipped with sufficient storage capacity, and as such, a cost-effective solution is to balance the power supply and demand by shifting EV charging to periods with abundant power generation. For example, a self-sufficient microgrid can be formed by scheduling EV charging to track the microgrid's local power generation profile.

There have been numerous studies of EV demand-side management (e.g., [2]–[9] to name a few), many of which have been focused on minimizing the charging cost or flattening the demand curve. A few studies on EV charge scheduling for tracking a given point/profile are found in [10]–[12]. The authors in [10] propose a charging scheme to align EV charging with renewable energy generation. However, the proposed algorithm is not decentralized, and as such, the EV owners must voluntarily provide all the information to a central aggregator. The study in [11] present a decentralized charge strategy to smooth the load profile. Yet their study is restricted to tracking a preferred operating point, which is constant throughout the time horizon. In [12], a set of aggregators aim to track a power profile by coordinating EVs through a consensus algorithm. The main drawback of their algorithm is the long computational time associated with the iterative routine, where EVs have to compute the schedules repeatedly to reach consensus. Further, the proposed scheme is restricted to charging EVs only at the maximum rated power. The majority of charging schemes proposed in the literature consider variable rate charging (VRC) (e.g., [7], [9], [11]), where it is considered that the EV can withdraw power at any rate using power electronic chargers that support variable rates. Due to the limitations of charger technologies [12] and the costs of variable rate chargers, EVs are more commonly charged using chargers that support binary rates (on/off) [6] or a set of discrete rates [13], known as discrete rate charging (DRC). In particular, DRC streamlines the process of modulating power over a limited set of rates. Thus, the capability of an EV charging scheme to be compatible with both VRC and DRC is important for practical operating scenarios.

This paper proposes a control scheme called DECSaT, for Decentralized EV Charge Scheduling and Tracking an arbitrary power profile. Our objective is to adjust the EV charge profiles to follow the forecast energy generation profile of a microgrid, while ensuring that each EV has the expected state of charge (SoC) at the time of departure. The key contributions of this paper are listed below.

1) The problem of EV charge scheduling for tracking an arbitrary power profile is formalized as a convex optimization problem (OP), where the charging is carried out at variable charge rates, and later modified to a discrete OP, where the charging is carried out at a set of predefined discrete charge rates.
2) Inspired by the water-filling algorithm proposed in communication systems design [14], an algorithm is proposed

978-1-7281-3103-0/20/$31.00 ©2020 IEEE

to solve the aforementioned OPs with less computation overhead, resulting in a short execution time. Although the water-filling approach has been applied to several load scheduling problems (e.g., [7], [15]), to the best of our knowledge, this paper is the first to exploit the notion of water-filling to track a power profile.

3) The uncertainty of EV arrival times is incorporated in designing the decentralized coordination framework.

It is worth mentioning that DECSaT can be applied to other EV charge scheduling scenarios focused on tracking a power profile, e.g., tracking the electricity profile that an aggregator has bought in the day-ahead electricity market. Moreover, valley-filling is a specific case of the more general problem considered in this paper. The remainder of this paper is organized as follows. In Section II, we present the algorithm of DECSaT. Section III presents the simulation results for a case study, followed by the conclusion in Section IV.

II. Problem Formulation

Here we consider charge scheduling of EVs in a microgrid. First, we formulate a centralized OP to track an arbitrary power profile by means of VRC. Then we propose DECSaT to solve that centralized OP in a decentralized manner. Later, we extend DECSaT to conduct EV charging at discrete charge rates.

A. Centralized Power Profile Tracking

Consider a scenario where a Microgrid Operator (MO) negotiates with $\mathcal{N} = \{1, ..., N\}$ EVs to schedule their charge profiles over a discrete time horizon divided into T time slots, each of length Δ. That is $\mathcal{T} = \{0\Delta, ..., t\Delta, ..., (T-1)\Delta\}$ where t denotes the time index. The goal of each EV user is to get their battery charged to the target SoC by their intended departure time. For example, a user may plug-in the EV for charging at 9:00 am in the morning, specifying that the battery must be fully charged by 4:00 pm in the evening.

The *charging specification* of EV i is characterized by the initial SoC s_i^{in}, the target SoC s_i^{out}, the plug-in time index t_i^{in}, the intended plug-out time index t_i^{out}, the battery capacity b_i, the charging efficiency η_i and the maximum charging power p_i^{max}. Denoted by H_i is the set of time indices during which EV i is available for charging, i.e., $H_i = \{t_i^{in}, .., t_i^{out} - 1\}$.

Let $\mathcal{D}$ be the *non-EV demand profile* that is composed of the total power demand of the houses served by the microgrid excluding the EV charging demand. Let $\mathcal{V}$ be the *target power profile* that is intended to be tracked, e.g., preplanned non-renewable power generation plus the short term forecast of renewable power generation. We assume that both $\mathcal{D}$ and $\mathcal{V}$ are precisely forecast ahead of charge scheduling. The *charge profile* of EV i is defined as $p_i = [p_i(0), .., p_i(t), .., p_i(T-1)]$, where $p_i(t)$ is the charge rate of EV i during the timestep t (from time $t\Delta$ to $(t+1)\Delta$). The values of $p_i(t)$, $\mathcal{D}(t)$ and $\mathcal{V}(t)$ are assumed to be kept constant during each sampled timestep. The centralized OP to track the profile $\mathcal{V}$ can be formalized as,

$$\min_{p_i(t)} \sum_{t=0}^{T-1} \left(\mathcal{D}(t) + \sum_{i=1}^{N} p_i(t) - \mathcal{V}(t)\right)^2 \qquad (1a)$$

$$\text{subject to,} \quad \sum_{t=0}^{T-1} p_i(t) = \frac{(s_i^{out} - s_i^{in})b_i}{\eta_i \Delta} \quad ; \forall i \in \mathcal{N}, \qquad (1b)$$

$$p_i(t) = 0 \quad ; \forall i \in \mathcal{N}, \forall t \notin H_i, \qquad (1c)$$

$$0 \leq p_i(t) \leq p_i^{max} \quad ; \forall i \in \mathcal{N}, t \in H_i. \qquad (1d)$$

The objective function (1a) captures the intent of minimizing the variance of net load, which is the difference of total demand (EV and non-EV demand) and generation. The constraint that has to be satisfied to meet the EV user's charging demand is given by the equation (1b). An EV i can perform charging only after it is plugged in at $t_i^{in}\Delta$ and before it is plugged-out at $t_i^{out}\Delta$, as indicated in the constraint (1c). In constraint (1d), the charge rate is restricted by the maximum charge rate supported by the charger or the battery.

To solve the OP (1) centrally, all the EVs have to provide their charging specifications to the MO in advance of scheduling, which requires extensive communication networks. Such an approach may also raise concerns from the privacy point of view. Moreover, the computation and communication overhead that is required to solve the centralized OP increases as the number of control variables scales with the number of EVs and the timesteps. In addition, a centralized approach may become infeasible due to the uncertainty of EV arrival times. Alternatively, a decentralized controller will be more scalable and practical for real-world implementations.

B. Case 1: Decentralized Power Profile Tracking with VRC

In practice, the charging requirements of EV users are revealed only after they are arrived at the charging point. However, the arrival times of EVs are variable and uncertain, and therefore it is not possible to determine all the EV charge profiles simultaneously as in the centralized approach. Without loss of generality, we determine the charge profile of each EV, one at a time, at their plug-in time. Upon arrival of EV i, the following step-by-step process is performed.

1) EV i receives a control signal from the MO, specifying the profiles $\mathcal{V}$ and $\mathcal{S}$, where $\mathcal{S}$ is the microgrid's expected aggregate demand profile. In more detail, $\mathcal{S}$ refers to the non-EV demand profile $\mathcal{D}$ plus the EV charge profiles already scheduled by time $t_i^{in}\Delta$, if any. (see Fig 1.)
2) Based on $\mathcal{V}$ and $\mathcal{S}$, EV i determines its charge profile p_i using the proposed algorithm and sends it to the MO.
3) Upon receiving the charge profile p_i from the EV, the MO updates $\mathcal{S}$ by adding p_i to the current $\mathcal{S}$ profile.
4) When a new EV connects, the updated control signal is issued by the MO and Steps 2) and 3) repeat.

Remark 1: In case several EVs connect at the exact same time (which might happen occasionally), those EVs are picked by the MO in a random order. We assume that the waiting times encountered by the EVs are not critical since the algorithm that we propose below takes only a milliseconds of time to compute a single EV charge profile.

Consider a single EV to be scheduled, say EV i. In Step 2) above, EV i has to solve the following localized control problem to determine its charge profile:

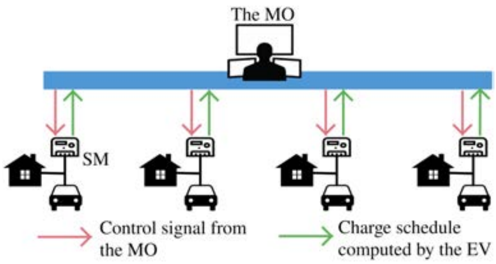

Fig. 1. In DECSaT, EVs determine their charge profiles by communicating with the MO via Smart Meters (SMs). DECSaT does not transmit information of EV SoC into the communication network, hence complies with existing communication standards such as ISO/IEC 15118 [16] and SAE J 2847 [17].

$$\min_{p_i(t), \forall t \in H_i} \sum_{t \in H_i} \big(\mathcal{S}(t) + p_i(t) - \mathcal{V}(t)\big)^2 \tag{2a}$$

$$\text{subject to, } \sum_{t \in H_i} p_i(t) = \frac{(s_i^{out} - s_i^{in}) b_i}{\eta_i \Delta}, \tag{2b}$$

$$0 \leq p_i(t) \leq p_i^{max} \quad ; \forall t \in H_i, \tag{2c}$$

where $\mathcal{S} + p_i = \mathcal{D} + \sum_{k=1}^{N} p_k$. The objective function and the constraints in (2) have the same meanings as those in (1). Since we only consider the charge rates of a single EV i and only over the time indices H_i, the constraint (1c) is ignored. Next, we propose a novel algorithm to solve the OP (2) with less computational time compared to the traditional optimization methods such as the interior point method. Interestingly, our algorithm does not require any sophisticated optimization technique. It is comprised of a set of simple arithmetic operations, which can be executed by a simple microcontroller. Moreover, the algorithm can be easily extended to DRC of the EV.

The classical water-filling algorithm proposed in communication theory [14] solves the problem of maximizing the total communication rate of a channel that is composed of several sub-channels with different noise levels. Interestingly, an analogy exists between the water-filling problem and the EV scheduling problem. In detail, $\mathcal{S}$ and p_i are analogous to the noise inherent in the sub-channels and the power transmitted through the sub-channels respectively. Hence, the scenario of finding the EV charge profile p_i that tracks $\mathcal{V}$ can be interpreted as pouring water over $\mathcal{S}$, following $\mathcal{V}$, such that the EV charging demand is satisfied.

Consider the Lagrangian function of the objective function (2a) with respect to the constraint (2b), which yields

$$\mathcal{L}\big(p_i(t), \lambda\big) = \sum_{t \in H_i} \big(\mathcal{S}(t) + p_i(t) - \mathcal{V}(t)\big)^2 + \lambda\Big(\sum_{t \in H_i} p_i(t) - e_i\Big)$$

where λ is a constant and $e_i = \big((s_i^{out} - s_i^{in}) b_i\big)/(\eta_i \Delta)$. Differentiating $\mathcal{L}\big(p_i(t), \lambda\big)$ with respect to $p_i(t)$ and setting the result to zero gives

$$\partial \mathcal{L}\big(p_i(t), \lambda\big) / \partial p_i(t) = 2\big(\mathcal{S}(t) + p_i(t) - \mathcal{V}(t)\big) + \lambda = 0.$$

By denoting $\lambda/2 = \mu$ (which is independent of t), we obtain

$$p_i(t) = \mathcal{V}(t) - \mathcal{S}(t) - \mu \quad ; \forall t \in H_i. \tag{3}$$

Let $\mathcal{W}(t) = \mathcal{S}(t) + p_i(t) = \mathcal{V}(t) - \mu$, which simplifies (3) to

$$p_i(t) = \mathcal{W}(t) - \mathcal{S}(t) \quad ; \forall t \in H_i. \tag{4}$$

$\mathcal{W}(t)$, which is referred to as the *water-level* at timestep t, represents the height to which the total demand is expected to be filled at time $t\Delta$. That is, the EV is expected to be charged until the total load is equal to $\mathcal{W}(t)$. The classical water-filling solution chooses a constant water-level to allocate power across sub-channels. By contrast, the objective of our problem is to track the profile $\mathcal{V}$, and as such, the water-level varies across the timesteps as implied by the equation (4). Let $\mathcal{W}$ be the *water-profile* that indicates the variation of water-level over time. Specifically, $\mathcal{W}$ is a profile that is parallel to $\mathcal{V}$. Note that μ denotes the gap between $\mathcal{V}$ and $\mathcal{W}$. The equation (4) is the optimality condition without considering the constraint (2c). After incorporating both the constraints, the optimal solution to the OP (2) becomes

$$p_i(t) = \mathcal{P}[\mathcal{W}(t) - \mathcal{S}(t)] \quad ; \forall t \in H_i, \tag{5}$$

where the projection operator $\mathcal{P}$ is defined as

$$\mathcal{P}[x] = \begin{cases} Case1 : 0 & ; \text{if } x < 0, \\ Case2 : x & ; \text{if } 0 \leq x \leq p_i^{max}, \\ Case3 : p_i^{max} & ; \text{if } x > p_i^{max}. \end{cases} \tag{6}$$

Based on the solution in (5) and the three cases specified in (6), Algorithm 1 determines the optimal water-profile $\mathcal{W}$ and the corresponding EV charge profile through a binary search. First, we define the initial search interval $[\mathcal{W}_{min}, \mathcal{W}_{max}]$, where $\mathcal{W}_{min}$ and $\mathcal{W}_{max}$ are the lowermost and uppermost profiles parallel to $\mathcal{V}$, in-between which the optimal $\mathcal{W}$ lies (lines 1-7). In detail, $\mathcal{W}_{max}$ is $(\mu_{min} - p_i^{max})$ of a distance apart from $\mathcal{V}$ and $\mathcal{W}_{min}$ is μ_{max} of a distance apart from $\mathcal{V}$. The main loop of Algorithm 1 performs the iterative binary search of $\mathcal{W}$ (lines 8-24). At each iteration, we set $\mathcal{W}$ as the average profile of $\mathcal{W}_{max}$ and $\mathcal{W}_{min}$ (lines 9-11). Based on $\mathcal{W}$, we then compute the corresponding charge rates according to (5) and (6) (lines 12-14). Then we check if sum of those charge

Algorithm 1 Power Profile Tracking Considering EV i

Input: $e_i, t_i^{in}, t_i^{out}, p_i^{max}, \mathcal{S}(t)\ \forall t \in H_i, \mathcal{V}(t)\ \forall t \in H_i$
Output: $p_i(t)\ \forall t \in H_i$
1: $\mu_{min} = \min_{t \in H_i}\{\mathcal{V} - \mathcal{S}\}, \mu_{max} = \max_{t \in H_i}\{\mathcal{V} - \mathcal{S}\}$
2: **for** $t = t_i^{in}$ to $(t_i^{out} - 1)$ **do**
3: $\quad \mathcal{W}_{max}(t) = \mathcal{V}(t) - \mu_{min} + p_i^{max}$
4: **end for**
5: **for** $t = t_i^{in}$ to $(t_i^{out} - 1)$ **do**
6: $\quad \mathcal{W}_{min}(t) = \mathcal{V}(t) - \mu_{max}$
7: **end for**
8: **while** $\mathcal{W}_{max} - \mathcal{W}_{min} \geq \epsilon$ **do**
9: $\quad$ **for** $t = t_i^{in}$ to $(t_i^{out} - 1)$ **do**
10: $\quad\quad \mathcal{W}(t) = \big(\mathcal{W}_{max}(t) + \mathcal{W}_{min}(t)\big)/2$
11: $\quad$ **end for**
12: $\quad$ **for** $t = t_i^{in}$ to $(t_i^{out} - 1)$ **do**
13: $\quad\quad p_i(t) = \mathcal{P}[\mathcal{W}(t) - \mathcal{S}(t)]$
14: $\quad$ **end for**
15: $\quad$ **if** $\sum_{t \in H_i} p_i(t) > e_i$ **then**
16: $\quad\quad$ **for** $t = t_i^{in}$ to $(t_i^{out} - 1)$ **do**
17: $\quad\quad\quad \mathcal{W}_{max}(t) = \mathcal{W}(t)$
18: $\quad\quad$ **end for**
19: $\quad$ **else if** $\sum_{t \in H_i} p_i(t) < e_i$ **then**
20: $\quad\quad$ **for** $t = t_i^{in}$ to $(t_i^{out} - 1)$ **do**
21: $\quad\quad\quad \mathcal{W}_{min}(t) = \mathcal{W}(t)$
22: $\quad\quad$ **end for**
23: $\quad$ **end if**
24: **end while**
25: **return** $p_i(t)\ \forall t \in H_i$

rates over H_i is more than or less than e_i. Accordingly, the search interval is halved by updating either $\mathcal{W}_{max}$ or $\mathcal{W}_{min}$ (lines 15-23), and the search continues in the updated interval. The algorithm ends when the distance between $\mathcal{W}_{max}$ and $\mathcal{W}_{min}$ is less than a prespecified threshold value ϵ (line 8). The number of iterations ($\mathcal{K}$) required to converge is given by $\mathcal{K} \leq \log_2(\frac{|\mathcal{W}'_{max} - \mathcal{W}'_{min}|}{\epsilon})$, where $\mathcal{W}'_{max}$ and $\mathcal{W}'_{min}$ are the initial profiles of $\mathcal{W}_{max}$ and $\mathcal{W}_{min}$ respectively.

C. Case 2: Decentralized Power Profile Tracking with DRC

Here we consider that an EV can be charged only at a set of discrete charge rates between 0 and p_i^{max}, denoted by $\mathcal{R}_i$. Hence, we replace the inequality constraint in OP (2) with

$$p_i(t) \in \mathcal{R}_i \quad ; \forall t \in H_i. \tag{7}$$

The modified OP is a discrete nonlinear OP, which is non-convex and computationally hard to solve. Alternatively, Algorithm 1 is modified to compute the charge profiles in a heuristic manner. First, we relax the range of charge rates into previous constraint (2c) and obtain the charge rates according to (5). After that, we enforce the constraint (7) using a new projection operator $\mathcal{P}'$, which rounds each of those charge rates to the nearest value in $\mathcal{R}_i$. In the modified algorithm for DRC, $\mathcal{P}$ is replaced by $\mathcal{P}'$ in line 13, and $\mathcal{P}'$ is computed as

$$\mathcal{P}'[x] = \begin{cases} \alpha & ; \text{if } x - \alpha < \beta - x \\ \beta & ; \text{if } x - \alpha \geq \beta - x \end{cases}$$

where $\alpha < x < \beta$ and $\{\alpha, \beta\} \in \mathcal{R}_i$, i.e., α and β are the two adjacent charge rates, in-between which x lies.

III. Simulation Results

A set of EVs and plugin-hybrid EVs composed of Nissan Leaf (b_i: $24kWh$, p_i^{max}: $7.4kW$), Mitsubishi i-MiEV ($16kWh, 3.7kW$), Toyota Prius ($8.8kWh, 3.7kW$), and Chevrolet Volt ($18.4kWh, 3.7kW$) is considered. All the EV charging specifications are assumed to be heterogeneous and similar to [6]. First, we consider VRC of EVs. In Fig 3, we plot the behaviour of DECSaT with two arbitrarily chosen profiles for power generation $\mathcal{V}$ (target power profile) and non-EV demand $\mathcal{D}$. The *Final Demand Profile (FDP)* is composed of the aggregate EV and non-EV demand profiles. During the first half of the period, $\mathcal{D}$ exceeds $\mathcal{V}$, and hence, charging of EVs is not scheduled to take place during that period in order to prevent the addition of further demand beyond the generation. Instead, EV charging is performed when D is lower than $\mathcal{V}$. As such, DECSaT provides an approximate best-effort service. During the second half of the period, the FDP smoothly tracks the fluctuations of $\mathcal{V}$. In particular, EV charge profiles are appropriately controlled to make the FDP follow the exact behaviour of $\mathcal{V}$. That is, whenever $\mathcal{V}$ climbs up, FDP also climbs up by a similar magnitude. And whenever $\mathcal{V}$ descends, so does the FDP. Overall, DECSaT has scheduled the EV charging operations in a way that the power profile $\mathcal{V}$ is successfully tracked and the overloading is mitigated.

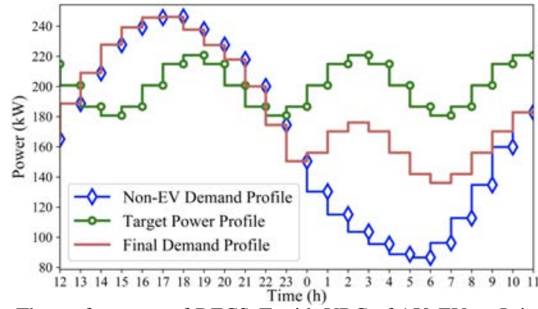

Fig. 3. The performance of DECSaT with VRC of 150 EVs – It is assumed that the plug-in times and the intended plug-out times of EVs follow a Gaussian distribution. EVs are plugged-in at 16h with a standard deviation (SD) of 2h and plugged-out at 8h with a SD of 2h.

Next, we consider a photovoltaic (PV) based microgrid in an office building. For this study, realistic power profiles are taken from [18] and up-scaled to fit the simulations. The target power profile $\mathcal{V}$ is the forecast *PV Generation Profile (PVGP)*. Fig 2 depicts the results obtained from DECSaT for the charge scheduling of three different sets of EVs. Consider the period 8-17h, during which the PV generation is significant. It can be clearly seen that in all the three scenarios, the non-EV demand has been mostly satisfied by the PV generation. Moreover, DECSaT has successfully adjusted the EV charge profiles to follow the trend of PV generation. In Fig 2(a), the FDP very closely follows the PVGP. In Fig 2(b), the FDP does not reach the PVGP due to the absence of sufficient EV availability. By contrast, the EV charging demand surpasses the PV generation in Fig 2(c). Nevertheless, in all the three scenarios, the FDP tracks the PVGP as far as possible. In the first two cases, the microgrid is self sustained. In the second case, the excess PV generation can be sold to the main power grid, whereas in the third case, DECSaT schedules EV charging to minimize the

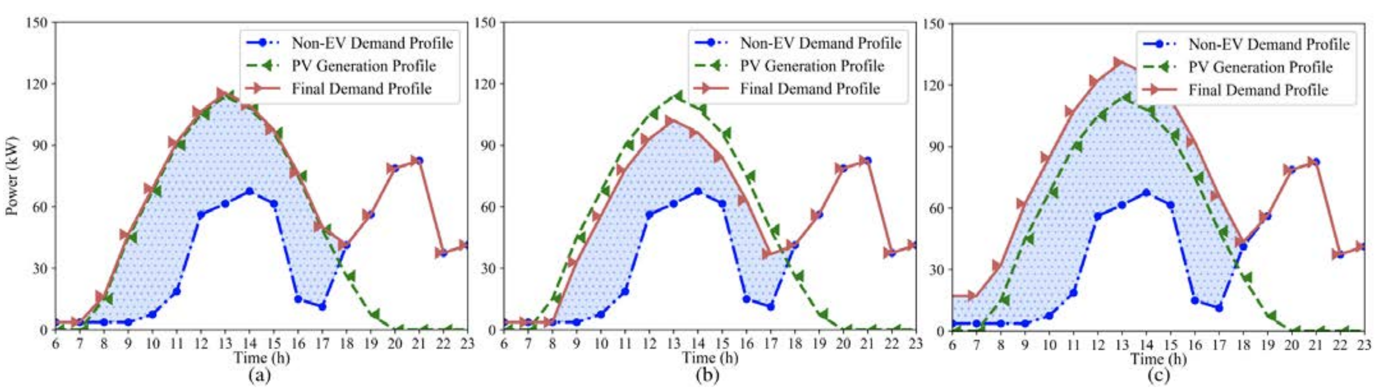

Fig. 2. The results obtained for charge scheduling of (a) 120 EVs, (b) 100 EVs, and (c) 150 EVs in a PV based microgrid. For each of the scenarios, EVs are assumed to be plugged-in at 8h with a SD of 2h, so that the deadlines of EVs lie before 21h. The shaded areas represent the EV charge load.

amount of energy that has to be additionally purchased.

We next compare the decentralized solution given by DECSaT with the centralized solution to the OP in (1). For the latter case, it is assumed that the MO has full knowledge about the EV charging specifications prior to arrival. Accordingly, the OP in (1) is solved by the MO at the beginning of the time horizon. The results shown in Fig 4 confirm that DECSaT is capable to yield the same result that is given by the centralized approach, while also managing the uncertain arrivals of EVs and preserving the benefits of decentralized control.

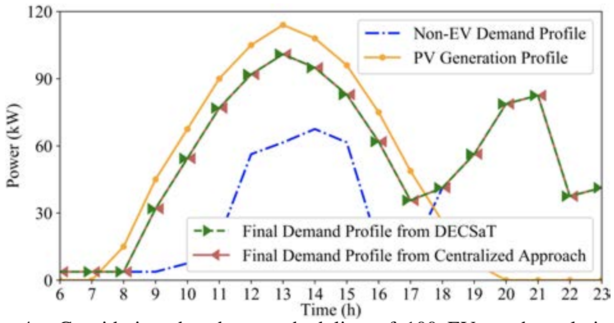

Fig. 4. Considering the charge scheduling of 100 EVs – the solution to centralized OP (1) versus the decentralized solution obtained from DECSaT.

Finally, we evaluate the performance of DECSaT with DRC. For this example, we consider that each EV i can be charged at five equally spaced charge rates between 0 and p_i^{max}. That is $\mathcal{R}_i = \{r_0, r_1, r_2, r_3, r_4\}$, where $r_0 = 0, r_1 = 1\delta, r_2 = 2\delta, r_3 = 3\delta, r_4 = 4\delta$ and $\delta = p_i^{max}/4$. It can be seen from the results in Fig 5 that the FDPs given by VRC and DRC are mostly similar. VRC performs better tracking of the PVGP and yields a smoother FDP. In contrast, the FDP with DRC deviates from the behaviour of $\mathcal{V}$ at certain timesteps (e.g., 11h, 14h). This is because DRC has less flexibility over charge rates compared to VRC. Nevertheless, DRC is preferable in terms of the costs of EV charging infrastructure.

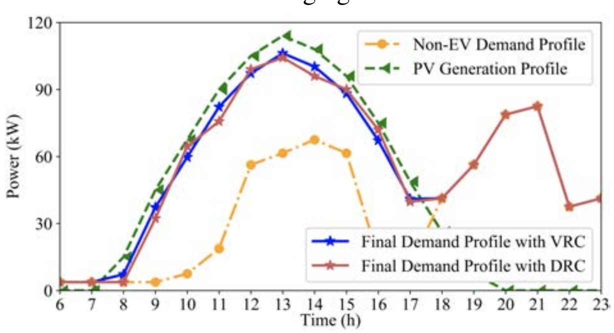

Fig. 5. Charge scheduling of 100 EVs with VRC and DRC.

IV. Conclusion

In this paper, we proposed an EV charge control scheme called DECSaT for tracking an arbitrary power profile. In designing DECSaT, we first formulated a centralized OP for power profile tracking with VRC of EVs. Then we derived a localized OP for finding the charge profile of a single EV. A novel algorithm was proposed to determine an EV charge profile in a way that considerably reduced the computational burden. Later, DECSaT was extended to incorporate DRC of EVs. Finally, the performance of DECSaT was demonstrated for charging a set of EVs, whose objective was to track the PV generation profile of a microgrid.

DECSaT exhibits several important features. It is capable of accommodating EVs with heterogeneous charging specifications. Importantly, DECSaT is resilient to uncertain arrivals of EVs. Unlike the considerable literature on EV scheduling, DECSaT does not require iterative computation of the charge profile, thus limits the need for extensive bi-directional communication. Moreover, the calculation of a charge schedule is performed using a set of simple arithmetic operations, making the algorithm suitable for integrating into the local controller residing within the EV or at the charging point.

References

[1] R. Liu, L. Dow, and E. Liu, “A survey of PEV impacts on electric utilities,” in *Proc. IEEE PES Conf. on Innovative Smart Grid Technologies*, Jan. 2011, pp. 1–8.

[2] W. Tushar, W. Saad, H. V. Poor, and D. B. Smith, “Economics of electric vehicle charging: A game theoretic approach,” *IEEE Trans. Smart Grid*, vol. 3, no. 4, pp. 1767–1778, Dec. 2012.

[3] Z. Ma, D. S. Callaway, and I. A. Hiskens, “Decentralized charging control of large populations of plug-in electric vehicles,” *IEEE Trans. Control Syst. Technol.*, vol. 21, no. 1, pp. 67–78, Jan. 2013.

[4] L. Gan, U. Topcu, and S. H. Low, “Optimal decentralized protocol for electric vehicle charging,” *IEEE Trans. Power Syst.*, vol. 28, no. 2, pp. 940–951, May 2013.

[5] N. Chen, C. W. Tan, and T. Q. Quek, “Electric vehicle charging in smart grid: Optimality and valley-filling algorithms,” *IEEE J. Sel. Topics Signal Process.*, vol. 8, no. 6, pp. 1073–1083, Dec. 2014.

[6] G. Binetti, A. Davoudi, D. Naso, B. Turchiano, and F. L. Lewis, “Scalable real-time electric vehicles charging with discrete charging rates,” *IEEE Trans. Smart Grid*, vol. 6, no. 5, pp. 2211–2220, 2015.

[7] Y. Mou, H. Xing, Z. Lin, and M. Fu, “Decentralized optimal demand-side management for PHEV charging in a smart grid,” *IEEE Trans. Smart Grid*, vol. 6, no. 2, pp. 726–736, Mar. 2015.

[8] A. Ghavami, K. Kar, and A. Gupta, “Decentralized charging of plug-in electric vehicles with distribution feeder overload control,” *IEEE Trans. Autom. Control*, vol. 61, no. 11, pp. 3527–3532, Nov. 2016.

[9] C. P. Mediwaththe and D. B. Smith, “Game-theoretic electric vehicle charging management resilient to non-ideal user behavior,” *IEEE Trans. Intell. Transp. Syst.*, Feb. 2018.

[10] G. Wang, J. Zhao, F. Wen, Y. Xue, and G. Ledwich, “Dispatch strategy of PHEVs to mitigate selected patterns of seasonally varying outputs from renewable generation,” *IEEE Trans. Smart Grid*, vol. 6, no. 2, pp. 627–639, 2014.

[11] M. C. Kisacikoglu, F. Erden, and N. Erdogan, “Distributed control of PEV charging based on energy demand forecast,” *IEEE Trans. Ind. Informat.*, vol. 14, no. 1, pp. 332–341, Jan. 2018.

[12] A. Malhotra, G. Binetti, A. Davoudi, and I. D. Schizas, “Distributed power profile tracking for heterogeneous charging of electric vehicles,” *IEEE Trans. Smart Grid*, vol. 8, no. 5, pp. 2090–2099, Sep. 2017.

[13] K. Jhala, B. Natarajan, A. Pahwa, and L. Erickson, “Coordinated electric vehicle charging solutions using renewable energy sources,” in *Proc. IEEE Symp. Comput. Intell. Appl. in Smart Grid*, 2014, pp. 1–6.

[14] R. G. Gallager, *Information theory and reliable communication*. Springer, 1968, vol. 588.

[15] Z. M. Haider, K. K. Mehmood, M. K. Rafique, S. U. Khan, L. Soon-Jeong, and K. Chul-Hwan, “Water-filling algorithm based approach for management of responsive residential loads,” *Journal of Modern Power Systems and Clean Energy*, vol. 6, no. 1, pp. 118–131, 2018.

[16] International Organization for Standardization, *ISO 15118-1: 2013 Road VehiclesVehicle to Grid Communication InterfacePart 1: General Information and Use-Case Definition*, 2013. [Online]. Available: https://www.iso.org/standard/55365.html

[17] SAE International, *Communication for Smart Charging of Plugin Electric Vehicles Using Smart Energy Profile 2.0.*, 2013. [Online]. Available: https://saemobilus.sae.org/content/j2847/1_201311

[18] R. Rahmani, I. Moser, and M. Seyedmahmoudian, “Multi-agent based operational cost and inconvenience optimization of pv-based microgrid,” *Solar Energy*, vol. 150, pp. 177–191, 2017.

3.2 Summary and Contributions

This chapter proposed an optimisation-based algorithmic approach to schedule EV charging following a target load profile. First, an optimisation problem with a coupled objective function to minimise the mismatch between the target load profile and the final load profile, and separable constraints indicating individual EV battery constraints was formulated. Then, a decentralised algorithm called "DECSaT" was developed to obtain the charge schedule for each EV locally, considering two special cases: variable rate charging and discrete rate charging.

A few important features of the proposed DECSaT algorithm include: it accommodates the heterogeneity in EV attributes (e.g. plug-in time, expected plug-out time, maximum charge rate, battery capacity, initial SoC, power demand or expected SoC, charging efficiency); it facilitates EVs to conduct charging with both variable rates and discrete rates (predefined), making it compatible with different types of EV chargers and battery technologies available in the market; it allows EVs to compute charge schedules locally without sharing any of the EV information with the aggregator; it requires simple computations that can be easily executed by a microcontroller at EV side with less cost; it requires limited bidirectional communication (one round trip) between the aggregator and each EV to determine their charge schedule; it applies to non-EV load (base load) curves and target load curves of arbitrary shapes; and it manages uncertainties with respect to EV mobility.

The performance of the DECSaT algorithm was analysed through numerical simulations. The results of these simulations demonstrated that depending on the number of EVs and their availability, the resultant load at a particular time may come closer to the target load, approach (overlap) the target load, or exceed the target load corresponding to that time. Nevertheless, the algorithm returned a final load profile that closely followed the trend of the target load profile while also satisfying all EV charging requirements before their expected departure times. Moreover, compared to discrete rate EV charging, the flexibility offered by variable rate EV charging yielded better results in terms of tracking the target load curve.

To summarise, the key contributions of this chapter were as follows.

1. The formulation of an optimisation problem to coordinate EV charging operations with the objective of tracking a target power profile while complying with charging limitations of individual EVs (e.g., maximum charging power) and satisfying the anticipated charging requirements of all EVs within the EV user-specified time duration.

2. The introduction of a distributed EV coordination framework consisting of an operator communicating with individual EVs via Advanced Metering Infrastructure (AMI).

3. The proposal of an algorithm called DECSaT, incorporating the proposed coordination framework, for solving the proposed optimisation problem efficiently with less computation overhead. Importantly, DECSaT, for the first time to the

best of our knowledge, applies the notion of water-filling concept to schedule EV charging to track a given power profile.

4. An application of DECSaT for EV charge scheduling in a PV based microgrid in an office building and analysis of numerical simulation results.

Specifically, numerical simulations were conducted considering three scenarios, which differ by the number of EVs participating in the scheme. Results obtained from numerical simulations demonstrated that in all the three scenarios, DECSaT successfully adjusted the EV charge profiles to follow the trend of PV generation. In more detail, the first scenario occupying 120 EVs generated a final demand profile that almost overlapped the PV generation profile. The second scenario that occupied 100 EVs resulted in a surplus of PV generation, and the third scenario that occupied 150 EVs resulted in a deficit of PV generation. However, both second and third scenarios still generated a final demand profile that followed the trend of PV generation profile.

Numerical simulation results further demonstrated that DECSaT yielded the same result that was given by the centralized counter approach, while still managing the uncertain arrivals of EVs and preserving the benefits of decentralized control.

In this chapter, we have not considered the capability of gridable EVs to discharge energy back to the grid. However, inclusion of V2G operation provides more opportunities to attain the desired shape of the load curve. Therefore, the next chapter focuses on designing an algorithm for load curve shaping involving both EV charging and discharging.

Chapter 4

Coordinated EV charging and discharging for load curve flattening (valley-filling and peak-shaving)

Two types of interactions are possible between EVs and the power grid, namely, Grid-to-Vehicle (G2V) and Vehicle-to-Grid (V2G). V2G-enabled EVs or gridable EVs enable the shaping of grid load curve by means of releasing power to the grid when the non-EV (base) load is at its peak (peak-shaving via V2G) and drawing of power from the grid when the non-EV (base) load is at its lowest (valley-filling via G2V). Specifically, the target of peak shaving and valley filling is to the achieve a flat load curve. By flattening the load curve, the power losses in the distribution system are reduced and the distribution transformer aging is reduced, improving the overall grid reliability. Besides, discharging energy during peak periods and recharging energy during off-peak periods (valley periods) saves on the energy bill for EV customers under time-based pricing regimes.

Distributed EV coordination has attracted attention of the research community as it has the key advantage of dividing the computational tasks among multiple entities and providing each of them with a problem of manageable size. Interestingly, recent advancements in smart grid technology imply that mathematical tools supporting distributed decision-making processes such as game theory will naturally become prominent in a wide range of energy-related applications, including distributed co-ordination of EV charging.

Game theory is an analytical and conceptual framework that can be used to study complex and self-interested interactions among independent rational players [Saad et al., 2012; Mediwaththe, 2017]. Non-cooperative game theory, in particular, is a key branch in game theory, which essentially studies the settings where several players who have partially or totally conflicting interests interact with each other. In this work, we employ insights from non-cooperative game theory to model the coordination of a number of EV users, each of whom tries to determine a charge-discharge profile that results in a minimal load variance (flat load profile). Under real-time pricing, such an approach is also expected to yield a lower charging cost to each participating EV.

Given the effectiveness of non-cooperative game theory in coordinating EV charging decisions via distributed communication and computation, and the suitability of water-filling theory for the optimal allocation of constrained EV charge rates over a given timespan, this chapter is dedicated to the application of those tools to develop a distributed optimisation-based EV charging and discharging coordination algorithm to achieve the flattening of load curve via valley-filling and peak-shaving. The contributions in this chapter are presented in our published manuscript.

4.1 Published Manuscript

In the paper presented below, an EV charging and discharging coordination algorithm is proposed to valley-fill and peak-shave the load curve of residential communities connected to low voltage transformers. Outcomes from this paper address research objective Q1 of the thesis (see Chapter 1 - Section 1.2) by scheduling EV charging and discharging for shaping the load curve (hence reducing grid congestion) and research objective Q3 by proposing a decentralized approach for EV charge and discharge scheduling (hence yielding a scalable coordination approach).

N. I. Nimalsiri, E. L. Ratnam, D. B. Smith, C. P. Mediwaththe, S. K. Halgamuge, "Coordinated Charge and Discharge Scheduling of Electric Vehicles for Load Curve Shaping," *IEEE Transactions on Intelligent Transportation Systems*, May. 2021.
https://doi.org/10.1109/TITS.2021.3071686

This article has been accepted for inclusion in a future issue of this journal. Content is final as presented, with the exception of pagination.

Coordinated Charge and Discharge Scheduling of Electric Vehicles for Load Curve Shaping

Nanduni I. Nimalsiri, Elizabeth L. Ratnam, *Senior Member, IEEE*, David B. Smith, *Member, IEEE*, Chathurika P. Mediwaththe, *Member, IEEE*, and Saman K. Halgamuge, *Fellow, IEEE*

***Abstract*— In this paper, we propose two decentralized Electric Vehicle (EV) charge scheduling schemes for shaping the load curve of residential communities connected to the electric grid. The first scheme is designed for Coordinated Valley-Filling (C-VF) of the load curve via only EV charging. The second scheme is designed for Coordinated Valley-Filling and Peak-Shaving (C-VF-PS) of the load curve via both EV charging and discharging. In both schemes, a set of grid-connected EVs referred to as an 'EV Group' (EVG) coordinates their charge (and discharge) schedules by means of an iterative routine. Specifically, at each iteration of the respective routine, each EV in the EVG updates its charge (and discharge) schedule using a water-filling based algorithm that is specifically tailored for load curve shaping. To accommodate heterogeneous EV arrival times, which are often non-deterministic, each of C-VF and C-VF-PS is implemented in two methods, which differ in the way the EVG is formed. The first method requires all the grid-connected EVs to reschedule at designated time intervals, whereas the second method requires each EV to schedule only once, yielding lower computation and communication overheads. Numerical simulation results confirm that, compared to uncoordinated EV charging, C-VF and C-VF-PS reduce the load variance (flattens the load curve) by 47% and 65%, respectively. Furthermore, Method 2 is shown to be more effective than Method 1, in terms of computation and communication overheads.**

***Index Terms*— Electric vehicle, load curve shaping, peak-shaving, valley-filling, vehicle-to-grid, water-filling.**

I. Introduction

THE transition to Electric Vehicles (EVs) is gaining traction in many countries due to their distinct advantages over conventional petroleum-based vehicles [1]. However, the co-incident charging of large populations of EVs may overload transformers and other electrical infrastructure. Interestingly, EVs are deferrable loads with flexibility in their charging time epoch, and as such, they could assist in reducing the load congestion via coordinated charging. Moreover, EVs with Vehicle-to-Grid (V2G) facility, also referred to as *grid-able* EVs, enable the release of power to the grid when the non-EV load is at its peak (*peak-shaving*) and the drawing of power from the grid when the non-EV load is at its lowest (*valley-filling*). Consequently, coordinated EV charging and discharging potentially enables load curve shaping for improved load congestion management.

Coordinated schemes for EV charging can be classified into centralized and distributed schemes. In particular, distributed schemes assign the computational tasks across multiple entities such as EVs (decentralized schemes) and/or aggregators (hierarchical schemes), and as such, they are highly scalable with the proliferation of EVs [2]. Numerous studies have considered coordinated EV charging for valley-filling using centralized approaches [3]–[7], as well as distributed approaches [8]–[22] that are based on game theory [8], Alternating Direction Method of Multipliers (ADMM) [9], [10], duality theory [11], primal-dual subgradient [12], probability transition matrices [13], price signals [14]–[17], water-filling [18], [19], sequential scheduling [20], hierarchical control [21], blockchain [22] etc. The EV charging studies in [8]–[22], however, do not allow discharging the stored energy back into the grid.

Several authors have investigated coordinated approaches for peak-shaving and valley-filling of the grid load curve via both EV charging and discharging [23]–[32]. By considering the power consumption and parking lot occupancy of a university building, Ioakimidis *et al.* [26] propose a centralized approach to peak-shave and valley-fill the building's load curve via V2G operation. In [23], a distributed game-theoretical approach is combined with the knapsack problem to flatten the load curve of a microgrid. The proposed algorithm in [23] requires EVs to be scheduled sequentially, which limits the approach to smaller EV populations. By contrast, Nguyen and Song [29] propose a non-cooperative game to shape the load curve of a building by way of decentralized EV scheduling, where EVs determine their charge and discharge schedules simultaneously. The proposed algorithm in [29], however, is only applicable for systems considering simple EV battery models, where efficiencies of charging and discharging are omitted.

Alternatively, Xing *et al.* [30] propose a valley-filling and peak-shaving algorithm based on the water-filling theory, which includes separate energy conversion efficiencies for EV charging and discharging. However, the algorithm in

Manuscript received January 7, 2020; revised November 30, 2020; accepted March 11, 2021. The Associate Editor for this article was P. Kachroo. *(Corresponding author: Nanduni I. Nimalsiri.)*

Nanduni I. Nimalsiri and David B. Smith are with the School of Engineering, The Australian National University, Canberra, ACT 2601, Australia, and also with the CSIRO Data61, Eveleigh, NSW 2015, Australia (e-mail: nanduni.nimalsiri@anu.edu.au; david.smith@data61.csiro.au).

Elizabeth L. Ratnam and Chathurika P. Mediwaththe are with the School of Engineering, The Australian National University, Canberra, ACT 2601, Australia (e-mail: elizabeth.ratnam@anu.edu.au; chathurika.mediwaththe@anu.edu.au).

Saman K. Halgamuge is with Department of Mechanical Engineering, School of Electrical, Mechanical and Infrastructure Engineering, The University of Melbourne, Parkville, VIC 3010, Australia, and also with the School of Engineering, The Australian National University, Canberra, ACT 2601, Australia (e-mail: saman@unimelb.edu.au).

Digital Object Identifier 10.1109/TITS.2021.3071686

[30] includes several assumptions: 1) non-EV demand curves require a particular shape instead of allowing for all general shapes; 2) the flexibility of charge and discharge operations is limited to a fixed window in time; 3) all gridable EVs are required to discharge up to the same State of Charge (SoC); and 4) the EV arrival times are deterministic (known a *priori*). The EV charge-discharge scheme in [30] is later extended in [32] to accommodate non-deterministic EV arrivals, yet the proposed approach is based on the first three assumptions stated above. The study in [31] propose an ADMM-based algorithmic extension of [30] that accommodates non-EV demand curves of any shape and allows for charging and discharging at any time without any restriction. The algorithm proposed in [31], however, assumes that all EVs are available over a predefined time horizon. Consequently, we are motivated to propose an algorithm that addresses all the above-mentioned assumptions in [30]–[32].

In this paper, we propose two coordinated EV charge (and discharge) scheduling schemes for load curve shaping, namely C-VF and C-VF-PS. Specifically, C-VF coordinates EV charge schedules to fill the load curve valleys, and C-VF-PS extends C-VF by incorporating gridable EVs to additionally shave the load curve peaks via V2G. Both schemes are designed to accommodate heterogeneous EV charge requirements, subject to the limitations in EV availability and charge-discharge rates.

In C-VF and C-VF-PS, EVs coordinate their charge (and discharge) schedules in accordance with the decentralized type II architecture proposed in [2]. In more detail, EVs are coordinated by means of a non-cooperative game that includes an iterative routine driven by coordination signals issued by an aggregator. At each iteration of the respective routine, each EV updates its schedule using an algorithm that we designed by leveraging the water-filling theory [33] in communication systems. The proposed algorithms consist of only a few arithmetic operations, which can be easily executed by a low-cost microcontroller. Moreover, EVs locally compute their schedules in parallel, reducing the execution time to yield near-real-time performance for practical applications. We also consider improving the privacy for EV users (as per the standards ISO/IEC 15118 [34] and SAE 2847 [35]) by ensuring the EV SoC information is not transmitted through the communication network [12].

In a realistic setting, EV arrival times are heterogeneous and often subject to uncertainties. Interestingly, both C-VF and C-VF-PS do not require prior knowledge of EV arrival times. In both approaches, an EV Group (EVG) is formed at designated time intervals, and the charge (and discharge) profiles are coordinated only by the EVs in that EVG. We consider two methods for the way the EVG is formed. The first method forms the EVG by involving all the grid-connected EVs, whereas the second method forms the EVG by involving only the newly arrived EVs. Consequently, the second method provides two key benefits. First, each EV is scheduled only once, yielding a significant reduction of computation and communication overheads. Second, the EVG is comprised of only a subset of grid-connected EVs, allowing for faster convergence of the iterative routine.

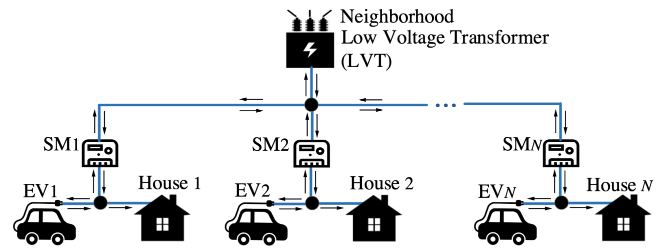

Fig. 1. Power flow between the LVT and multiple residences equipped with Smart Meters (SMs) and EVs outfitted with smart chargers (and inverters).

The key contributions of this paper are summarized below.

1) We propose a coordinated EV charge scheduling scheme, called C-VF, to valley-fill the load curve of a Low Voltage Transformer (LVT).
2) We propose an extension of C-VF, called C-VF-PS, that contributes to both valley-filling and peak-shaving of the load curve via EV charging and discharging. Importantly, C-VF-PS allows for more efficient utilization of the EV idle times (when EVs are parked) to shape the load curve. In C-VF-PS, we incorporate separate energy conversion efficiencies for charging and discharging, which results in a Mixed Discrete Programming (MDP) problem. To solve the respective MDP, we propose a water-filling based algorithm where the original intractable MDP problem is reduced to a tractable form.
3) While coordinating EV schedules to shape the load curve, both schemes satisfy the heterogeneous EV charge requirements within the EV user-specified time duration.
4) Both schemes consider underlying load curves of arbitrary shapes and accommodate EVs with heterogeneous and non-deterministic arrival times.

This paper is organized as follows. Section II introduces the problem of valley-filling. Section III presents the proposed C-VF and C-VF-PS schemes. Section IV presents our simulation results, followed by the conclusion in Section V.

Notation

Let $\mathbb{R}^{\ell}$ denote a ℓ-dimensional vector of real numbers. Let $\mathbf{0}$ denote an all-zero column vector, where the context will make clear the dimension intended. For any vector $\boldsymbol{V} \in \mathbb{R}^{\ell}$, the transpose vector is given by $\boldsymbol{V}^{\top} \in \mathbb{R}^{1\times\ell}$.

II. Preliminaries

A. Centralized Valley-Filling

We consider EV charging in a residential community served by a LVT as shown in Fig. 1. An aggregator (e.g., System Operator) is obliged to schedule charging of EVs after they arrive home, such that EVs reach their target SoC ahead of their designated departure times. When scheduling the EVs, the aggregator also seeks to steer EV charging to time periods that fill the overnight valleys of the demand curve, which is composed of the underlying non-EV demand of customers.

This article has been accepted for inclusion in a future issue of this journal. Content is final as presented, with the exception of pagination.

TABLE I
NOTATION SPECIFIC TO EV n ($n \in \mathcal{N}$)

c_n	Battery capacity (kWh)
$p_n(k)$	Charge (or discharge) rate at time $k\Delta$ (kW)
p_n^{max}	Maximum charge (or discharge) rate (kW)
k_n^a, k_n^d	Arrival time index, Departure time index
$s_n(k)$	SoC at time $k\Delta$ (kWh)
$s_n(k_n^a)$, s_n^*	Initial SoC (kWh), Target SoC (kWh)
s_n^{min}, s_n^{max}	Minimum SoC (kWh), Maximum SoC (kWh)
η_n^c, η_n^d	Charge efficiency (%), Discharge efficiency (%)

Herein, we assume the aggregator has advanced knowledge of each EV's technical specification, the arrival/departure times, the initial SoC and the target SoC. That is, we do not consider EV privacy preservation with centralized valley-filling. Note that we neglect EV discharging in this section, and will be later considered in the Section III-C.

We consider coordinated charging of $\mathcal{N} = \{1, \ldots, n, \ldots, N\}$ EVs over a discrete-time horizon $\mathbb{H} = \{0\Delta, \ldots, k\Delta, \ldots, (K-1)\Delta\}$, where n denotes an EV index and k denotes a time index with sampling time interval Δ (in h). Let $\mathcal{H} := \{0, \ldots, k, \ldots, K-1\}$ denote the set of time indices over $\mathbb{H}$.

The *charge profile* of EV n is defined by $\boldsymbol{p}_n := [p_n(0), \ldots, p_n(k), \ldots, p_n(K-1)]^\top \in \mathbb{R}^K$, where $p_n(k)$ denotes the charge rate (in kW) corresponding to time index $k \in \mathcal{H}$. We consider that $p_n(k)$ remains constant during the time interval $\big(k\Delta, (k+1)\Delta\big)$. Next we denote the aggregate *non-EV demand profile* of the LVT by $\boldsymbol{D} := [D(0), \ldots, D(k), \ldots, D(K-1)]^\top \in \mathbb{R}^K$, where $D(k)$ is the non-EV demand (in kW) of the residential community across the time interval $\big(k\Delta, (k+1)\Delta\big)$. It is assumed that the day ahead forecast of $\boldsymbol{D}$ is precisely known.

We denote by $s_n(k)$ (in kWh) the SoC (energy remaining in the battery) of EV n at time $k\Delta$ ($k \in \mathcal{H}$). Further, we denote by $s_n(k_n^a)$ the initial SoC of EV n at the arrival, and s_n^* the target SoC of EV n. Upon arrival at home, the EV owner must specify a target SoC s_n^* that is feasible to reach before the expected departure time k_n^d.[i] All the notations specific to EV n ($n \in \mathcal{N}$) are summarized in Table I.

An EV can commence charging only at the beginning of a time interval. Suppose an EV arrives at a time that falls into the middle of a time interval. Then, k_n^a is the time index that immediately follows its arrival. Accordingly, we define $H_n = \{k_n^a, \ldots, (k_n^d - 1)\}$ as the set of time indices during which EV n is available for charging. It follows that

$$p_n(k) = 0 \quad \text{if } k \notin H_n; \quad \forall n \in \mathcal{N},\ \forall k \in \mathcal{H}. \tag{1}$$

An EV is allowed to charge at a rate between 0 and p_n^{max}, where $p_n^{max} = \min(p_{n,charger}^{max}, p_{n,battery}^{max})$ is the maximal charging power of the charger or the battery, whichever is smaller. The corresponding inequality constraint [19] that restricts the magnitude of charge rates is

$$0 \leq p_n(k) \leq p_n^{max}; \quad \forall n \in \mathcal{N},\ \forall k \in H_n. \tag{2}$$

[i]The condition $s_n^* \leq s_n(k_n^a) + (k_n^d - k_n^a)\, p_n^{max}\, \eta_n^c \Delta$ must hold.

Then the charge requirement of EV n [19] is expressed by

$$\sum_{k \in \mathcal{H}} p_n(k) = e_n; \quad \forall n \in \mathcal{N} \tag{3}$$

where $e_n = \big(s_n^* - s_n(k_n^a)\big)/(\eta_n^c \Delta)$. Here, the charge efficiency η_n^c depends on the EV charger and the battery type, and it is considered a constant over any charge rate.

The centralized Optimization Problem (OP) for load curve shaping via minimization of the load variance can now be formulated as

$$\min_{p_n(k)} \sum_{k \in \mathcal{H}} \Big(D(k) + \sum_{n \in \mathcal{N}} p_n(k)\Big)^2$$
$$\text{subject to (1), (2) and (3).} \tag{4}$$

The OP in (4) can be solved centrally by the aggregator using numerous convex optimization techniques. However, the computational complexity of the OP increases with the number of control variables (e.g., as N and K become large). Furthermore, communicating EV information with the aggregator may raise privacy concerns for EV owners. Consequently, we are interested in solving the OP in a decentralized manner, such that EVs compute their charge profiles locally and autonomously. That is, we look to solve the OP (4) in a way that the computational load is distributed across the EVs.

We begin by formalizing a localized OP for each EV, with an objective of valley-filling.

B. Localized OP for Valley-Filling

Consider the charge profile of a single EV, say $n \in \mathcal{N}$. By isolating the charge rates of EV n in (4), we obtain

$$\min_{p_i(k)} \sum_{k \in \mathcal{H}} \Big(D(k) + \sum_{i \in \mathcal{N}, i \neq n} p_i(k) + p_n(k)\Big)^2. \tag{5}$$

Let $\boldsymbol{L} \in \mathbb{R}^K$ be the *aggregate demand profile* that is composed of the anticipated total non-EV and EV demand. Formally, $\boldsymbol{L} := [L(0), \ldots, L(k), \ldots, L(K-1)]^\top$ where

$$L(k) = D(k) + \sum_{n \in \mathcal{N}} p_n(k); \quad \forall k \in \mathcal{H}. \tag{6}$$

Next, we define the aggregate demand profile that excludes the charge profile of EV n as $\boldsymbol{d}_{\text{-}n} \in \mathbb{R}^K$. Formally, $\boldsymbol{d}_{\text{-}n} := [d_{\text{-}n}(0), \ldots, d_{\text{-}n}(k), \ldots, d_{\text{-}n}(K-1)]$ where

$$d_{\text{-}n}(k) = L(k) - p_n(k); \quad \forall k \in \mathcal{H}. \tag{7}$$

Hereafter, $\boldsymbol{d}_{\text{-}n}$ is referred to as the *base load profile* available to EV n. Using (5)-(7) and the independent EV constraints (1)-(3), the localized OP for EV n can be written as

$$\min_{p_n(k), k \in H_n} \sum_{k \in H_n} \big(d_{\text{-}n}(k) + p_n(k)\big)^2 \tag{8a}$$

$$\text{subject to} \sum_{k \in H_n} p_n(k) = e_n, \tag{8b}$$

$$0 \leq p_n(k) \leq p_n^{max}; \quad \forall k \in H_n. \tag{8c}$$

Note that the constraint (1) is ignored in (8) as the objective function (8a) is defined to optimize charge rates only across H_n. Since the OP (8) has variables that are only specific to EV

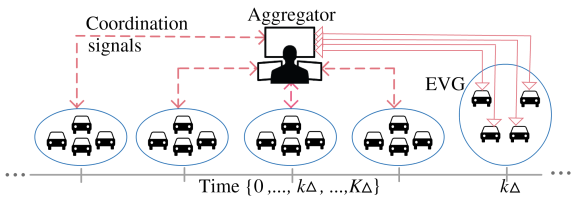

Fig. 2. Coordination of EVGs with the aggregator. Solid lines correspond to time $k\Delta$ and dashed lines correspond to previous time interval(s).

n, it can be solved locally by the EV. However, coordination of EVs is required to ensure that the charge profiles of a large number of EVs won't inadvertently synchronize, as the resultant aggregate demand profile $\boldsymbol{L}$ may destabilize the LVT. To this end, we next design a decentralized method to coordinate EVs, each of whom solves the localized OP (8).

III. Problem Formulation

We first propose a decentralized and *Coordinated Valley-Filling* (C-VF) scheme to shape the load curve of a LVT through EV charging. By 'decentralized', we mean each EV calculates its charge profile locally in coordination with an aggregator. More specifically, the EVs do not communicate their individual parameters (e.g., c_n, $p_n^{max}, k_n^a, k_n^d, s_n(k_n^a), s_n^*, s_n^{min}, s_n^{max}, \eta_n^c$) and variables (e.g., battery SoC $s_n(k)$) to the aggregator. Instead, communication signals representing $\boldsymbol{p}_n$ are transferred from the EV to the aggregator, similar to the approaches in [14]–[19], [29]–[32]. We also propose a decentralized and *Coordinated Valley-Filling and Peak-Shaving* (C-VF-PS) scheme, an extension of C-VF to accommodate EVs capable of both charging and discharging.

A. Coordinated Valley-Filling (C-VF)

EV arrival times are typically unpredictable and non-deterministic — a consequence of uncertain traffic conditions, variable road conditions, and EV user behavior. To coordinate the grid connection of incoming EVs with random arrivals, a sequential scheduling approach is utilized in [20] and [23]. It involves each EV computing the charge profile one-by-one at the EV arrival time and updating the aggregate demand profile $\boldsymbol{L}$ after each computation. The drawback of such an approach is the waiting time encountered by EVs, especially when a large number of EVs grid-connect simultaneously. Hence, we propose an alternative approach whereby the waiting times associated with sequential EV scheduling are reduced.

The C-VF scheme proposed in this paper involves coordination of EVs in groups, as shown in Fig. 2. Specifically, at each time interval, an EV group that is specific to that time interval coordinate with the aggregator to agree upon a set of charge profiles. The set of EVs in the *EVG* corresponding to time interval $\big(k\Delta, (k+1)\Delta\big)$ is denoted by $\mathcal{J}^k$ ($k \in \mathcal{H}$). By defining an EVG for each time interval, C-VF accommodates new EV arrivals.

Consider the EVG $\mathcal{J}^k$. The charge profile of each EV in the EVG is coupled with the preferences of other EVs in that EVG. As such, we model the interactions of EVs in the EVG as a non-cooperative game with the strategic form as follows.

Game $\mathcal{G}^k := \{\mathcal{J}^k, [\mathcal{P}_n]_{n\in\mathcal{J}^k}, [\mathcal{U}_n]_{n\in\mathcal{J}^k}\}$:

- *Players*: EVs in $\mathcal{J}^k$.
- *Strategy*: For each player $n \in \mathcal{J}^k$, a strategy is a charge profile $\boldsymbol{p}_n$ that satisfies constraints of the localized OP (8). $\mathcal{P}_n$ is the set of all feasible strategies for EV n.
- *Utility*: For each player $n \in \mathcal{J}^k$, the utility function is defined as $\mathcal{U}_n(\boldsymbol{p}_n; \boldsymbol{p}_{\text{-}n}) := -C_n$, where $C_n := \sum_{k\in H_n} \big(d_{\text{-}n}(k) + p_n(k)\big)^2$. Here C_n is the cost of variance calculated as per the objective function defined in the localized OP (8). Moreover, $\boldsymbol{d}_{\text{-}n} := \boldsymbol{D} + \boldsymbol{p}_{\text{-}n} \in \mathbb{R}^K$, where $\boldsymbol{p}_{\text{-}n} \in \mathbb{R}^K$ represents the strategies of all EVs except EV n, i.e., $\boldsymbol{p}_{\text{-}n} := \sum_{i\in\mathcal{J}^k, i\neq n} \boldsymbol{p}_i$.

In game theory, the Nash Equilibrium (NE) [36] is defined as a state where no player can improve their utility by changing to another strategy unilaterally. More formally, game $\mathcal{G}^k = \{\mathcal{J}^k, [\mathcal{P}_n]_{n\in\mathcal{J}^k}, [\mathcal{U}_n]_{n\in\mathcal{J}^k}\}$ has a NE if and only if

$$\mathcal{U}_n(\boldsymbol{p}_n^*; \boldsymbol{p}_{\text{-}n}^*) \geq \mathcal{U}_n(\boldsymbol{p}_n; \boldsymbol{p}_{\text{-}n}^*); \quad \forall \boldsymbol{p}_n \in \mathcal{P}_n, \forall n \in \mathcal{J}^k \tag{9}$$

where $(.)^*$ are strategies of EVs at the NE. It is worth mentioning that for each EV $n \in \mathcal{J}^k$, C_n is strictly convex. Therefore, $\mathcal{U}_n$ is strictly concave with respect to $\boldsymbol{p}_n$. Moreover, the constraints in the localized OP (8) are linear, and therefore $\mathcal{P}_n$ is convex, closed, and bounded. Then, by Theorems 1-4 in [37], a NE of game $\mathcal{G}^k$ always exists and the NE is unique.

The NE is also a fixed point of the best responses of all the players. As proposed in [36] and [38], we seek the NE of $\mathcal{G}^k$ using the best responses of EVs, which are fine-tuned in an iterative manner. More specifically, C-VF coordinates the EVs in the EVG $\mathcal{J}^k$ by means of an *iterative routine*, where the iterations are driven by constant updates in $\boldsymbol{L}$. In this way, $\boldsymbol{L}$ acts as a *coordination signal* in C-VF. Throughout, the iteration index j is superscripted within curly brackets.

We propose two potential implementations for C-VF as Method 1 and Method 2 (see Table II), which differ in the way the EVG is formed at each time index. In Method 1, the EVG corresponding to time index $k \in \mathcal{H}$, denoted by $\mathcal{J}^k$, consists of all the EVs that remain grid-connected at time $k\Delta$. By contrast, in Method 2, the EVG $\mathcal{J}^k$ consists of only EVs that arrived between $(k-1)\Delta$ and $k\Delta$. That is, the EVG in Method 2 includes only a subset of grid-connected EVs.

At each iteration of the iterative routine in Methods 1 and 2 (step 7), the EVs in the corresponding EVG first receive the aggregate demand profile $\boldsymbol{L}$ from the aggregator (step 7-a). Using that profile $\boldsymbol{L}$, each EV n then computes their individual base load profile $\boldsymbol{d}_{\text{-}n}$ (step 7-b). Note that for each EV n, $\boldsymbol{d}_{\text{-}n}$ includes the charge profiles of other EVs in the EVG as computed in the previous iteration. Subsequently, each EV n determines their best response strategy $\boldsymbol{p}_n$ that maximizes $\mathcal{U}_n$ (otherwise minimizes C_n) by solving the localized OP in (8) (step 7-c), and sends it to the aggregator (step 7-d). Based on the best responses received from all the EVs in the EVG, the aggregator updates the coordination signal $\boldsymbol{L}$ (step 7-e), in preparation for the next iteration (step 7-f). The stopping criterion of the iterative routine is met when the Euclidean

TABLE II
TWO POTENTIAL IMPLEMENTATIONS FOR C-VF

Method 1

1) Initialize time index $k = 0$.
2) EVs available at time $k\Delta$ form the EVG $\mathcal{J}^k$.
3) Initialize time horizon $s = K - k$.
4) Initialize iteration index $j = 1$ and convergence parameter $\epsilon = 10^{-3}$.
5) Initialize $\boldsymbol{D} = [D(k), .., D(K-1)]^\top \in \mathbb{R}^s$ and $\boldsymbol{L}^{\{j\}} = \boldsymbol{D} \in \mathbb{R}^s$.
6) Each EV $n \in \mathcal{J}^k$ initializes $\boldsymbol{p}_n^{\{j-1\}} = \boldsymbol{0} \in \mathbb{R}^s$.
7) Execute the iterative routine:
   a) The aggregator publishes $\boldsymbol{L}^{\{j\}}$ to EVs in $\mathcal{J}^k$.
   b) Each EV $n \in \mathcal{J}^k$ computes its base load profile $\boldsymbol{d}_{\text{-}n}^{\{j\}} \in \mathbb{R}^s$ as $\boldsymbol{d}_{\text{-}n}^{\{j\}} = \boldsymbol{L}^{\{j\}} - \boldsymbol{p}_n^{\{j-1\}}$ (see Eq. (7)).
   c) Each EV $n \in \mathcal{J}^k$ solves its localized OP to determine $\boldsymbol{p}_n^{\{j\}}$ (see Sections III-B and III-C for algorithms proposed to solve the OP).
   d) Each EV $n \in \mathcal{J}^k$ transmits $\boldsymbol{p}_n^{\{j\}}$ to the aggregator.
   e) The aggregator computes $\boldsymbol{L}$ for the next iteration as $\boldsymbol{L}^{\{j+1\}} = \boldsymbol{D} + \sum_{n \in \mathcal{J}^k} \boldsymbol{p}_n^{\{j\}}$ (see Eq. (6)).
   f) Advance iteration index $j = j + 1$.
   g) Repeat Steps 7(a-f) until $\|\boldsymbol{L}^{\{j\}} - \boldsymbol{L}^{\{j-1\}}\|_2 < \epsilon$.
8) Each EV $n \in \mathcal{J}^k$ charges at the rate $p_n(k)^{\{j-1\}}$ over the time interval $\big(k\Delta, (k+1)\Delta\big)$.
9) Each EV $n \in \mathcal{J}^k$ updates $H_n = \{k+1, .., k_n^d - 1\}$ and $e_n = e_n - p_n(k)^{\{j-1\}}$.
10) Advance time index $k = k + 1$.
11) Repeat Steps (2-10) until $k = K$.

Method 2

1) Initialize time index $k = 0$.
2) EVs available at time $k\Delta$ form the EVG $\mathcal{J}^k$.
3) Initialize time horizon $s = K$.
4) Initialize iteration index $j = 1$ and convergence parameter $\epsilon = 10^{-3}$.
5) Initialize $\boldsymbol{D} = [D(0), .., D(K-1)]^\top \in \mathbb{R}^K$ and $\boldsymbol{L}^{\{j\}} = \boldsymbol{D} \in \mathbb{R}^K$.
6) Each EV $n \in \mathcal{J}^k$ initializes $\boldsymbol{p}_n^{\{j-1\}} = \boldsymbol{0} \in \mathbb{R}^s$.
7) Execute the iterative routine:
   a) The aggregator publishes $\boldsymbol{L}^{\{j\}}$ to EVs in $\mathcal{J}^k$.
   b) Each EV $n \in \mathcal{J}^k$ computes its base load profile $\boldsymbol{d}_{\text{-}n}^{\{j\}} \in \mathbb{R}^s$ as $\boldsymbol{d}_{\text{-}n}^{\{j\}} = \boldsymbol{L}^{\{j\}} - \boldsymbol{p}_n^{\{j-1\}}$ (see Eq. (7)).
   c) Each EV $n \in \mathcal{J}^k$ solves its localized OP to determine $\boldsymbol{p}_n^{\{j\}}$ (see Sections III-B and III-C for algorithms proposed to solve the OP).
   d) Each EV $n \in \mathcal{J}^k$ transmits $\boldsymbol{p}_n^{\{j\}}$ to the aggregator.
   e) The aggregator computes $\boldsymbol{L}$ for the next iteration as $\boldsymbol{L}^{\{j+1\}} = \boldsymbol{L}^{\{j\}} - \sum_{n \in \mathcal{J}^k} \boldsymbol{p}_n^{\{j-1\}} + \sum_{n \in \mathcal{J}^k} \boldsymbol{p}_n^{\{j\}}$.
   f) Advance iteration index $j = j + 1$.
   g) Repeat Steps 7(a-f) until $\|\boldsymbol{L}^{\{j\}} - \boldsymbol{L}^{\{j-1\}}\|_2 < \epsilon$.
8) Each EV $n \in \mathcal{J}^k$ executes the charge schedule $\boldsymbol{p}_n^{\{j-1\}}$ over the remaining time horizon $\big(k\Delta, K\Delta\big)$.
9) Advance time index $k = k + 1$ and update $s = K - k$.
10) The aggregator computes $\boldsymbol{L}^{\{j\}} = [L(k)^{\{j\}}, \ldots, L(K-1)^{\{j\}}]^\top \in \mathbb{R}^s$.
11) EVs that arrived over the time interval $\big((k-1)\Delta, k\Delta\big)$ form EVG $\mathcal{J}^k$.
12) Repeat Steps (6-11) until $k = K$.

distance of the coordination signal $\boldsymbol{L}$ between two consecutive iterations reaches a predefined tolerance value ϵ (step 7-g). At this point, the NE of $\mathcal{G}^k$ is reached, whereby further changes to any charge profile will not increase the utility of any player.

By way of an explanation, when each EV n in $\mathcal{J}^k$ ($k \in \mathcal{H}$) follows its best response strategy, C_n either decreases or remains unchanged at each iteration. Consequently, if all the EVs pick their best response strategies at each iteration, the variance of $\boldsymbol{L}$ monotonically decreases, resulting in a flattened load curve $\boldsymbol{L}$. Since C_n is bounded below (non-negative), the convergence of the iterative routine is also guaranteed.

Lemma 1: *For all $k \in \mathcal{H}$, the NE of $\mathcal{G}^k = \{\mathcal{J}^k, [\mathcal{P}_n]_{n \in \mathcal{J}^k}, [\mathcal{U}_n]_{n \in \mathcal{J}^k}\}$ yields the optimal set of schedules for EVs in the EVG $\mathcal{J}^k$. The proof is given in the Appendix.*

Remark 1: *The individual cost of variance of EV n (C_n) is akin to the charging cost incurred by EV n under the real-time pricing schemes studied in [14], [38], where the price of electricity is modeled as a convex function of the total EV and non-EV demand. Hence, C-VF can be easily extended to incentivize the EV customers for contributing to load curve shaping. However, such economic aspects are not analyzed within the scope of this paper.*

As opposed to a sequential scheduling approach where the execution time is particularly pronounced for large EV populations, C-VF is designed in a way the EVs compute their charge profiles in parallel, allowing for a shorter execution time. When the method of implementation is considered, Method 2 differs from Method 1 in that EVs do not update their scheduled charge profiles as incoming EVs grid-connect. Therefore, Method 2 minimizes the computation and communication overheads significantly, making C-VF suitable for practical implementation with very large EV populations. Nevertheless, Method 1 provides a solution that improves load curve shaping and indeed manages unexpected EV departures.

Remark 2: *Methods 1 and 2 also support an implementation that eliminates the aggregator by establishing a peer-to-peer communication network amongst EVs. Such an implementation requires each EV to broadcast its best response strategy $\boldsymbol{p}_n$ to all other EVs in the EVG (at Step 7-d) so that each EV could compute $\boldsymbol{L}$ independently (at Step 7-e).*

B. Water-Filling Based Load Curve Shaping

EV chargers are not presently designed to run complex algorithms that require a high-level software environment. In fact, computational algorithms for EV charging are required to be simple and fast so that they can support near-real-time performance. The main computational complexity of the C-VF scheme lies in the computation associated with solving the localized OP by each EV in Step 7-c of Methods 1 and 2. In this section, we propose an algorithm based on the water-filling theory [33] to solve the respective localized OP (8) using only a set of simple arithmetic operations, thereby lending the capability to be easily executed by a microcontroller (residing at the EV charging point) with low cost. Importantly, water-filling based algorithms are well-tailored to the problem of valley-filling, and can be extended to also schedule the discharging of EVs, as described in Section III-C.

Consider a single EV n. Let $\mathcal{X}_n = \{\boldsymbol{p}_n \mid 0 \leq p_n(k) \leq p_n^{max}\}$. The objective function (8a) is convex and continuously differentiable in $\mathcal{X}_n$. According to the optimality condition of preposition 3.4.1 in [39], if $\boldsymbol{p}_n^*$ is the optimal solution to (8), then there exists a scalar $\lambda \in \mathbb{R}$ such that $\boldsymbol{p}_n^*$ minimizes the Lagrangian function with respect to constraint (8b). That is,

$p_n^*(k) = \text{argmin}_{p_n \in \mathcal{X}_n} \mathcal{L}\big(p_n(k), \lambda\big)$ where

$$\mathcal{L}\big(p_n(k), \lambda\big) = \sum_{k \in H_n} \big(d_{\text{-}n}(k) + p_n(k)\big)^2 - \lambda\Big(\sum_{k \in H_n} p_n(k) - e_n\Big).$$

Applying the Karush Kuhn Tucker conditions yields

$$\partial \mathcal{L}\big(p_n(k)\lambda\big)/\partial p_n(k) = 2\big(d_{\text{-}n}(k) + p_n(k)\big) - \lambda = 0.$$

Since $p_n(k) \geq 0$, the optimal value of $p_n(k)$ is

$$p_n(k)^* = [\mu - d_{\text{-}n}(k)]^+; \quad \forall k \in H_n \tag{10}$$

where $\mu = \lambda/2$ and $[v]^+$ is equal to v if $v \geq 0$, and 0 otherwise. We note that Eq. (10) resembles the classical water-filling solution proposed in communication theory [33], where a so-called *water-level* is chosen to maximize the information rate of a communication channel that is composed of several sub-channels with different noise levels. Interestingly, an analogy exists between the classical water-filling problem and the EV charging coordination problem (see [19] for more details). As such, the problem of allocating charge rates for EV n over different time steps in H_n can be interpreted as pouring water over the base load profile $\boldsymbol{d}_{\text{-}n}$. When both constraints of the localized OP in (8) are considered, $p_n(k)^*$ simplifies to 3 cases given by **C1**, **C2** and **C3**.

$$p_n(k)^* = \begin{cases} \textbf{C1:}\ 0 & \text{if } \mu < d_{\text{-}n}(k) \\ \textbf{C2:}\ \mu - d_{\text{-}n}(k) & \text{if } d_{\text{-}n}(k) < \mu < d_{\text{-}n}(k) + p_n^{max} \\ \textbf{C3:}\ p_n^{max} & \text{if } d_{\text{-}n}(k) + p_n^{max} < \mu. \end{cases}$$

It follows that the optimal solution to localized OP (8) is

$$p_n(k)^* = [\min(\mu - d_{\text{-}n}(k),\ p_n^{max})\ ]^+; \quad \forall k \in H_n. \tag{11}$$

In what follows, μ is referred to as the *target water-level* and $w(k) = d_{\text{-}n}(k) + p_n(k)$ is referred to as the water-level corresponding to time interval $\big(k\Delta, (k+1)\Delta\big)$. In the classical water-filling problem [33], the water-level is a constant, which is equal to μ. By contrast, in our problem, the constraint (8c) imposes a requirement that the water-level is not constant throughout the time. By way of an explanation, $w(k) > \mu$ in **C1**, $w(k) = \mu$ in **C2**, and $w(k) < \mu$ in **C3**, implying $w(k)$ varies with time.

Algorithm 1 Returns the Charge Profile $\boldsymbol{p}_n$ and the Target Water-Level μ

Input: $d_{\text{-}n}$, e_n, H_n, p_n^{max}, s, $\epsilon = 10^{-3}$, $p_n = \mathbf{0} \in \mathbb{R}^s$
1 $\mu_{min} = \min_{k \in H_n} d_{\text{-}n}(k)$
2 $\mu_{max} = \min\{\max_{k \in H_n} d_{\text{-}n}(k) + p_n^{max}, \Upsilon\}$
3 **while** $\mu_{max} - \mu_{min} > \epsilon$ **do**
4 $\quad \mu = (\mu_{max} + \mu_{min})/2$
5 $\quad$ **foreach** $k \in H_n$ **do**
6 $\quad\quad p_n(k) = \mu - d_{\text{-}n}(k)$
7 $\quad\quad$ **if** $p_n(k) < 0$ **then** $p_n(k) = 0$
8 $\quad\quad$ **else if** $p_n(k) > p_n^{max}$ **then** $p_n(k) = p_n^{max}$
9 $\quad$ **if** $\sum_{k \in H_n} p_n(k) > e_n$ **then** $\mu_{max} = \mu$
10 $\quad$ **else if** $\sum_{k \in H_n} p_n(k) < e_n$ **then** $\mu_{min} = \mu$
11 **return** $p_n \in \mathbb{R}^s$, μ

Recall, s is defined in Step 3 of Method 1 and 2.

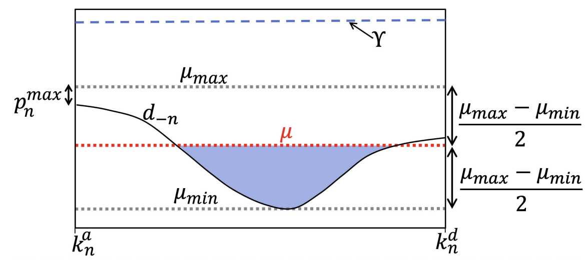

Fig. 3. Here μ_{min} and μ_{max} are as defined in Algorithm 1: lines 1-2. The shaded valley area ($\sum_{k \in H_n} p_n(k)$) is defined in Algorithm 1: lines 9-10.

In Methods 1 and 2 for C-VF, each EV in the EVG solves its localized OP (8) (at Step 7-c) by executing the Algorithm 1. More specifically, Algorithm 1 returns the optimal value of μ using an iterative binary search (lines 3-10), where the initial values of μ_{min} and μ_{max} (defined in lines 1 and 2) are the lowermost and uppermost boundaries of the search interval, as shown in Fig. 3. Here, μ_{max} is additionally constrained by the power rating of the LVT, denoted by Υ. At each iteration of the main loop (lines 3-10), we set the midpoint of the search interval $[\mu_{min}, \mu_{max}]$ as μ, and compute the charge rates $p_n(k)$ for all $k \in H_n$, according to Eq.(11). After that, the upper boundary μ_{max} or the lower boundary μ_{min} is updated (i.e., set to be equal to the current μ value) by comparing the sum of charge rates across all time indices $k \in H_n$, against the EV charge requirement e_n (lines 9-10). In particular, the search interval is halved at each iteration and the same procedure is repeated with an updated μ. Algorithm 1 terminates when the search interval $[\mu_{min}, \mu_{max}]$ is less than a prespecified tolerance value ϵ. At this point, the optimal value of μ is returned along with the optimal charge profile $\boldsymbol{p}_n$ for EV n.

The convergence of Algorithm 1 is guaranteed since $\boldsymbol{d}_{\text{-}n}$ is a continuous function in the initial search interval (defined in lines 1 and 2) and $\int_{k_n^a}^{(k_n^d - 1)} |\mu - d_{\text{-}n}(k)| dk$ is a monotonically increasing function of μ. Further, the number of iterations $\mathcal{K}$ required to converge is given by $\mathcal{K} \leq \log_2(|\mu_{max} - \mu_{min}|/\epsilon)$.

C. Coordinated Valley-Filling and Peak-Shaving (C-VF-PS)

Coordination of gridable EVs to discharge power during peak periods and to recharge during valley periods defers the need for grid expansion that otherwise arises from power flow congestion. We now propose an extension of C-VF called C-VF-PS that incorporates gridable EVs to support both valley-filling and peak-shaving. Similar to C-VF, we implement C-VF-PS as Method 1 or Method 2, with only a slight variation in Step 7-c, where the corresponding localized OP (8) for each EV n is replaced by the localized OP (16), which is formulated below. In the OP (16), the objective function remains as previously defined in OP (8), however the set of constraints changes.

For a gridable EV n, $p_n(k)$ is constrained over $[-p_n^{max}, p_n^{max}]$ for all $k \in H_n$ [19], where discharge rates are negative,

This article has been accepted for inclusion in a future issue of this journal. Content is final as presented, with the exception of pagination.

$p_n(k) < 0$ and charge rates are positive, $p_n(k) > 0$. That is

$$-p_n^{max} \leq p_n(k) \leq p_n^{max}; \quad \forall k \in H_n. \tag{12}$$

We denote by η_n^c and η_n^d the energy conversion efficiencies for EV charging and discharging, respectively. Let $0 \leq \eta_n^c \leq 1$ and $0 \leq \eta_n^d \leq 1$. For each time index $k \in H_n$, we define $\eta_n(k) = \eta_n^c$ if $p_n(k) \geq 0$ (charging), and $\eta_n(k) = 1/\eta_n^d$ if $p_n(k) < 0$ (discharging). In order to prolong the EV battery lifespan during charge-discharge cycles, the SoC $s_n(k)$ is constrained [30] by

$$s_n^{min} \leq s_n(k) \leq s_n^{max}; \quad \forall k \in H_n \tag{13}$$

where, for any $k \in H_n$, $s_n(k+1)$ [30] is

$$s_n(k+1) = s_n(k) + \eta_n(k) p_n(k) \Delta. \tag{14}$$

Finally, the requirement to attain the target SoC by the designated time of departure [30] is captured by

$$s_n(k_n^d) = s_n^*. \tag{15}$$

The localized OP for a gridable EV n can now be stated as

$$\min_{p_n(k), k \in H_n} \sum_{k \in H_n} (d_{\text{-}n}(k) + p_n(k))^2$$
$$\text{subject to, (12), (13), (14) and (15).} \tag{16}$$

The OP (16) is a MDP problem. As described in [30], it is NP-hard due to the complexity of the discrete (and binary) variable set $\left(\eta_n(k)\right)$ and due to the dependence of $\eta_n(k)$ on $p_n(k)$. In this paper, we solve the OP (16) using a heuristic method, which is computationally efficient and lends itself to implementation on existing EV controllers. In solving the OP (16), our strategy is to split the valley-filling and peak-shaving periods, so that $\eta_n(k)$ becomes a constant for each time period. In Methods 1 and 2 for C-VF-PS, each EV in the EVG solves the localized OP (16) at Step 7-c by executing the Algorithm 2.

Algorithm 2 first identifies a set of *Charge-Discharge Sessions (CDSs)* $\mathbb{S} := \{\mathbb{S}_1, \ldots, \mathbb{S}_v, \ldots, \mathbb{S}_V\}$, where V is the number of total CDSs. In particular, a Charge-Discharge Session (CDS) $\mathbb{S}_v \in \mathbb{S}$ is characterized by a set of time indices, $\{k^s, \ldots, k^e\}$, which spans a time window denoted by $(k^s\Delta, k^e\Delta)$. In more detail, the CDS $\mathbb{S}_v \in \mathbb{S}$ ends when the EV halts charging at $k^e\Delta$, whereby another CDS $\mathbb{S}_{v+1} \in \mathbb{S}$ begins. To derive $\mathbb{S}$, we consider the intersection points of $\boldsymbol{d}_{\text{-}n}$ profile and the water-level μ that is returned by Algorithm 1,[ii] and split vertically at the time points where $\boldsymbol{d}_{\text{-}n}$ has a positive gradient. Graphically, $\mathbb{S}$ can be interpreted as a set of sub curves, each of which spans a single CDS, as depicted in Fig. 4. The EV charge-discharge schedule is then determined for each CDS $\mathbb{S}_v \in \mathbb{S}$ separately.

In what follows, we describe the way an EV is scheduled for charging and discharging across a single CDS $\mathbb{S}_v \in \mathbb{S}$ as per Algorithm 2: lines 4-3. For each CDS $\mathbb{S}_v := \{k^s, \ldots, k^e\}$, we seek a *valley-level* (α_{vf}) and a *peak-level* (α_{ps}) that represent the heights up to which the valley is filled and the peak is shaved, respectively. As a higher α_{vf} fills more of the valley, we aim to raise α_{vf} above μ, while preserving the SoC at $k^s\Delta$ and $k^e\Delta$ as per the previous charge profile $\boldsymbol{p}_n$ obtained from Algorithm 1. When α_{vf} is raised, the *surplus charging energy* beyond the EV's initial charge requirement, denoted by $e^\dagger$ (calculated in lines 7-11), must be drawn by the EV. That is, we increase the energy level of EV n by $\eta_n^c e^\dagger$, allowing for a peak demand reduction equivalent to $e' = \eta_n^c \eta_n^d e^\dagger$ (line 12). Herein, the period $[\tau^s\Delta, \tau^e\Delta]$ denotes the EV discharge window, whereby the charge and discharge periods are disjoint (line 13).

[ii]Algorithm 2: line 1 returns a higher water-level μ to EVs with a shorter time-frame for charging so that they are charged at higher rates compared to EVs that have a much longer time-frame for charging. In this way, C-VF-PS prioritizes EV charging up to the target SoC, and in cases where time permits, the EVs then contribute to flattening the load curve.

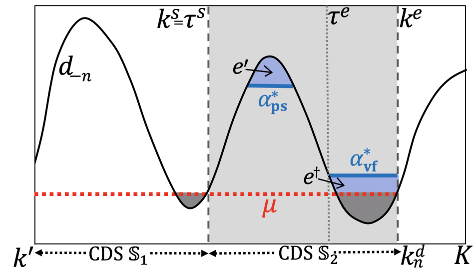

Fig. 4. Here k' is the current time index at which the EV n executes Algorithm 2. For C-VF-PS with Method 2, $k' = k_n^a$. In the example shown in this figure, $\mathbb{S} = \{\mathbb{S}_1, \mathbb{S}_2\}$. For $\mathbb{S}_2 = \{k^s, \ldots, k^e\}$, the optimal valley-level and the optimal peak-level are marked as α^*_{vf} and α^*_{ps}, respectively.

For each CDS $\mathbb{S}_v$ of EV n, we denote the charge profile corresponding to α_{vf} as $\boldsymbol{p}^c_{n,v}$, the discharge profile corresponding to α_{ps} as $\boldsymbol{p}^d_{n,v}$, and the resultant charge-discharge profile as $\overline{\boldsymbol{p}}_{n,v}$. In Algorithm 2, α_{ps} and $\boldsymbol{p}^d_{n,v}$ are obtained by the Function `Inverse-Water-Filling` (`IWF`), where the implementation is similar to Algorithm 1.

In Algorithm 2, the main loop corresponding to each CDS (lines 5-20) seeks the optimal value for α_{vf} using an iterative binary search over the interval $[\alpha_{\text{vf}}^{min}, \alpha_{\text{vf}}^{max}]$, where α_{vf}^{min} denotes the lowest valley-level (and initially equals to μ) and α_{vf}^{max} denotes the highest valley-level bounding the search interval. During each iteration of the binary search, α_{vf}^{max} is updated if any of the following cases occur.

- Case 1: Releasing e' amount of energy is infeasible within the given discharge window $[\tau^s\Delta, \tau^e\Delta]$ (lines 14, 20).
- Case 2: The resultant charge-discharge profile $\overline{\boldsymbol{p}}_{n,v}$ does not comply with the SoC constraint (13), as per the Function `Verify-SoC-Constraint` (`VSC`) (i.e., returns 0 in line 17).

When α_{vf}^{max} is updated accordingly, a lower value for α_{vf} is assigned in the next iteration. Consequently, the EV discharges a lesser amount of energy, and $\overline{\boldsymbol{p}}_{n,v}$ moves towards satisfying the SoC constraint (13). If none of Case 1 or Case 2 occurs, α_{vf}^{min} is updated to generate a higher value for α_{vf} (line 19), enabling further valley-filling and peak-shaving in the next iteration. When this iterative process completes, the optimal values for α_{vf} and α_{ps} are obtained along with the corresponding charge-discharge profile for the CDS $\mathbb{S}_v$, which is given by $\overline{\boldsymbol{p}}_{n,v} = \left[(\boldsymbol{p}^d_{n,v})^\top, (\boldsymbol{p}^c_{n,v})^\top\right]^\top \in \mathbb{R}^{k^e - k^s}$.

Finally, $\overline{\boldsymbol{p}}_{n,v}$ over all the CDSs in $\mathbb{S}$ are concatenated to yield the charge-discharge schedule $\overline{\boldsymbol{p}}_n$ for EV n (line 21).

Algorithm 2 Returns the Charge-disCharge Profile $\overline{\boldsymbol{p}}_n$

Input: $\boldsymbol{d}_{\text{-}n}$, e_n, H_n, p_n^{max}, η_n^c, η_n^d, s_n^{min}, s_n^{max}, k', $s_n(k')$, s, $\epsilon = 10^{-3}$

Function IWF(e', τ^s, τ^e):
- $\alpha_{\text{ps}}^{min} = \min_{k \in \mathbb{S}} d_{\text{-}n}(k) - p_n^{max}$, $\alpha_{\text{ps}}^{max} = \max_{k \in \mathbb{S}} d_{\text{-}n}(k)$
- **while** $\alpha_{\text{ps}}^{max} - \alpha_{\text{ps}}^{min} > \epsilon$ **do**
  - $\alpha_{\text{ps}} = (\alpha_{\text{ps}}^{max} + \alpha_{\text{ps}}^{min})/2$
  - **for** $k \in \{\tau^s, \ldots, \tau^e\}$ **do**
    - $p_{n,\upsilon}^d(k) = \alpha_{\text{ps}} - d_{\text{-}n}(k)$
    - **if** $p_{n,\upsilon}^d(k) < -p_n^{max}$ **then** $p_{n,\upsilon}^d(k) = -p_n^{max}$
    - **else if** $p_{n,\upsilon}(k) > 0$ **then** $p_{n,\upsilon}^d(k) = 0$
  - **if** $-\sum_{t=\tau^s}^{\tau^e} p_{n,\upsilon}^d(k) > e'$ **then** $\alpha_{\text{ps}}^{min} = \alpha_{\text{ps}}$
  - **else if** $-\sum_{t=\tau^s}^{\tau^e} p_{n,\upsilon}^d(k) < e'$ **then** $\alpha_{\text{ps}}^{max} = \alpha_{\text{ps}}$
- **return** $\boldsymbol{p}_{n,\upsilon}^d$

Function VSC($\boldsymbol{p}_n$, $\overline{\boldsymbol{p}}_{n,\upsilon}$, k^s, k^e):
- $s_n(k^s) = s_n(k') + \sum_{j=k'}^{k^s-1} \eta_n^c p_n(j)\Delta$
- **for** $k \in \{k^s + 1, \ldots, k^e\}$ **do**
  - $s_n(k) = s_n(k^s) + \sum_{j=k^s}^{k-1} \eta_n(j)\overline{p}_{n,\upsilon}(j)\Delta$
  - **if** $s_n(k) < s_n^{min}$ **or** $s_n(k) > s_n^{max}$ **then**
    - **return** 0
- **return** 1

1 $\boldsymbol{p}_n, \mu$ = **Algorithm 1**($\boldsymbol{d}_{\text{-}n}$, e_n, H_n, p_n^{max}, s, ϵ)
2 $\mathbb{S} := \{\mathbb{S}_1, \ldots, \mathbb{S}_\upsilon, \ldots, \mathbb{S}_V\}$
3 **foreach** $\mathbb{S}_\upsilon := \{k^s, \ldots, k^e\} \in \mathbb{S}$ **do**
4 $\quad \alpha_{\text{vf}}^{min} = \mu$, $\alpha_{\text{vf}}^{max} = \min\{\max_{k \in \mathbb{S}_\upsilon} d_{\text{-}n}(k) + p_n^{max}, \Upsilon\}$
5 $\quad$ **while** $\alpha_{\text{vf}}^{max} - \alpha_{\text{vf}}^{min} > \epsilon$ **do**
6 $\quad\quad \alpha_{\text{vf}} = (\alpha_{\text{vf}}^{min} + \alpha_{\text{vf}}^{max})/2$
7 $\quad\quad e^\dagger = 0$, $k = k^e$
8 $\quad\quad$ **while** $\alpha_{\text{vf}} - d_{\text{-}n}(k) > 0$ **do**
9 $\quad\quad\quad p_{n,\upsilon}^c(k) = \alpha_{\text{vf}} - d_{\text{-}n}(k)$
10 $\quad\quad\quad e^\dagger = e^\dagger + p_{n,\upsilon}^c(k) - p_n(k)$
11 $\quad\quad\quad k = k - 1$
12 $\quad\quad e' = \eta_n^c \eta_n^d e^\dagger$
13 $\quad\quad \tau^s = k^s$, $\tau^e = k$
14 $\quad\quad$ **if** $p_n^{max} * (\tau^e - \tau^s) \geq e'$ **then**
15 $\quad\quad\quad \boldsymbol{p}_{n,\upsilon}^d = \text{IWF}(e', \tau^s, \tau^e)$
16 $\quad\quad\quad \overline{\boldsymbol{p}}_{n,\upsilon} = \left[(\boldsymbol{p}_{n,\upsilon}^d)^\top, (\boldsymbol{p}_{n,\upsilon}^c)^\top\right]^\top \in \mathbb{R}^{k^e - k^s}$
17 $\quad\quad\quad$ **if** VCS$(\boldsymbol{p}_n, \overline{\boldsymbol{p}}_{n,\upsilon}, k^s, k^e) = 0$ **then**
18 $\quad\quad\quad\quad \alpha_{\text{vf}}^{max} = \alpha_{\text{vf}}$
19 $\quad\quad\quad$ **else** $\alpha_{\text{vf}}^{min} = \alpha_{\text{vf}}$
20 $\quad\quad$ **else** $\alpha_{\text{vf}}^{max} = \alpha_{\text{vf}}$
21 **return** $\overline{\boldsymbol{p}}_n = [\overline{\boldsymbol{p}}_{n,1}, \ldots, \overline{\boldsymbol{p}}_{n,\upsilon}, \ldots, \overline{\boldsymbol{p}}_{n,V}, \boldsymbol{0}]^\top \in \mathbb{R}^s$.

Recall, s is defined in Step 3 of Method 1 and 2. k' is the current time index at which the EV n executes Algorithm 2 and $s_n(k')$ is the SoC of EV n at time $k'\Delta$. For C-VF-PS with Method 2, $k' = k_n^a$ and $s_n(k') = s_n(k_n^a)$. In line 21, $\boldsymbol{0} \in \mathbb{R}^{K - k_n^d}$.

Theorem 1: *For each CDS $\mathbb{S}_\upsilon \in \mathbb{S}$, Algorithm 2 returns the optimal values of the valley-level α_{vf} and the peak-level α_{ps}. Proof is given in the Appendix.*

TABLE III
EV SPECIFICATIONS

EVs	Nissan Leaf	c_n = 24 kWh	p_n^{max} = 7.4 kW
	Mitsubishi i-MiEV	c_n = 16 kWh	p_n^{max} = 3.7 kW
PHEVs	Toyota Prius	c_n = 8.8 kWh	p_n^{max} = 3.7 kW
	Chevrolet Volt	c_n = 18.4 kWh	p_n^{max} = 3.7 kW

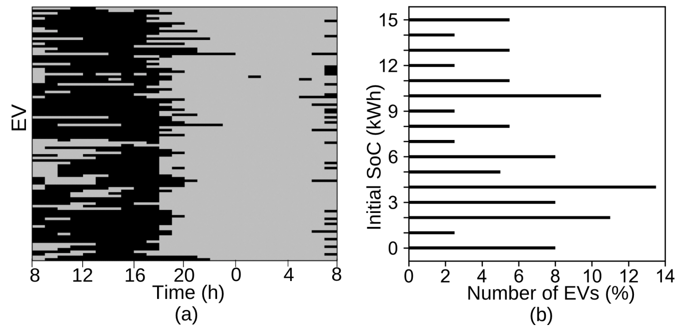

Fig. 5. (a) Charging availability of EVs – Grey areas represent the available time slots (parked at home) and black areas represent the unavailable time slots (away from home), (b) the initial SoC $s_n(k_n^a)$ (in kWh) of EVs.

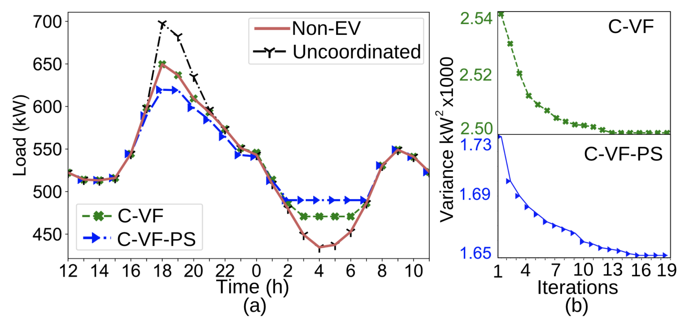

Fig. 6. (a) The aggregate demand profile $\boldsymbol{L}$ obtained from uncoordinated EV charging (load variance of 4,680.16kW^2) versus coordinated EV charging with C-VF (load variance of 2,503.11kW^2) and C-VF-PS (load variance of 1,650.62kW^2). (b) The reduction of load variance along the iterations of $\mathcal{G}^6$.

IV. ASSESSING EV IMPACT ON DEMAND CURVES

Through numerical simulations, we assess load curve shaping at the LVT when EV charge and discharge schedules are coordinated using the proposed C-VF and C-VF-PS schemes. We consider charge-discharge scheduling of 150 EV customers[iii] in a residential community, located in an Australian distribution network in the state of New South Wales, operated by the Australian Energy Market Operator (AEMO). The cumulative non-EV demand profile $\boldsymbol{D}$ of the residential network is reflective of published AEMO data [41].

We assume that each house owns an EV that is equipped with a lithium-ion battery [42]. Table III presents the EV specifications collected from [43].[iv] As proposed in [30], for each EV $n \in \mathcal{N}$, we limit $s_n^{min} = 0.20 * c_n$ and $s_n^{max} = 0.85 * c_n$

[iii] In the Australian context, an average of 100 customers might be connected to a distribution transformer in an urban setting, as reported in [40].

[iv] We include both EVs and Plug-in Hybrid EVs (PHEVs) in our simulations as both of them are widely deployed globally [44]. Note that the C-VF and C-VF-PS schemes apply to both EVs and PHEVs in the same way.

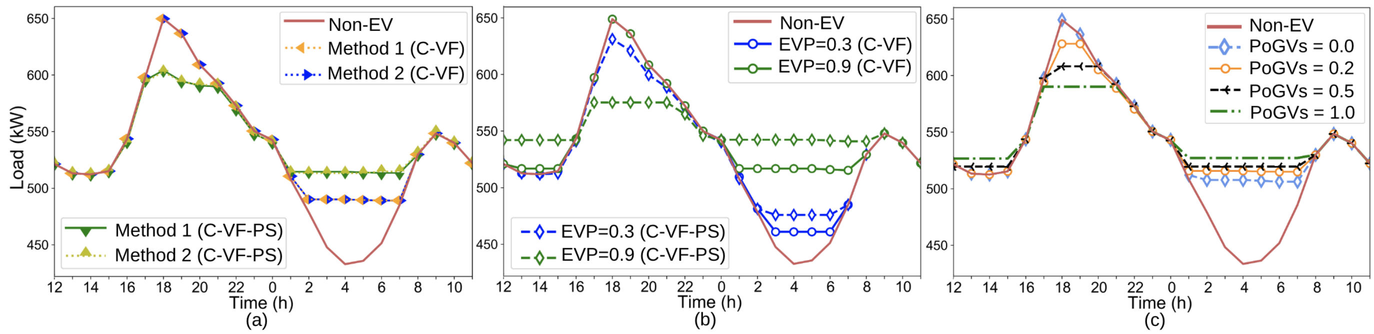

Fig. 7. The aggregate demand profile $\boldsymbol{L}$ at the LVT with C-VF and C-VF-PS: (a) Method 1 and Method 2; (b) EVPs of 0.3 and 0.9; (c) varying PoGEVs.

and we set the target SoC as $s_n^* = s_n^{max}$. Moreover, we set the coefficients of charging and discharging efficiencies as $\eta_n^c = 95\%$ and $\eta_n^d = 90\%$ [30].

Fig. 5(a) depicts the availability of EVs (i.e., arrival and departure times) for charging and discharging, based on the survey data gathered by the Victorian Department of Transport [45], which contains individual vehicle travel records for 24 h periods. Fig. 5(b) depicts the distribution of initial SoC $s_n(k_n^a)$ (in kWh) for all EVs, as provided in [46].[v]

All the simulations below are conducted on a MacBook Pro with 2.3GHz Intel Core i5 and 8GB memory.

A. Uncoordinated Versus Coordinated EV (Dis)charging

Here we consider charging (and discharging) of EVs implemented with and without the coordination of EVs. In the case of *Uncoordinated EV charging*, EVs commence charging immediately upon arrival and continue at their maximum charge rate until they reach the target SoC. In the case of *Coordinated EV charging (and discharging)*, EVs implement the charge (and discharge) schedules that are determined by the proposed C-VF and C-VF-PS schemes.

Fig 6 considers a scenario where charging (and discharging) is scheduled at 18h ($k = 6$), involving an EVG $\mathcal{J}^6$ of 84 EVs (including 16 newly arrived EVs). Fig 6(a) depicts the anticipated non-EV demand profile $\boldsymbol{D}$ and the anticipated aggregate demand profile $\boldsymbol{L}$ (composed of the non-EV demand $\boldsymbol{D}$ and the combined EV schedules) obtained with uncoordinated EV charging and coordinated EV charging via C-VF and C-VF-PS. Unless otherwise specified, C-VF and C-VF-PS are implemented as per Method 1 in the following simulations.

In Fig 6(a), the load variance[vi] of profile $\boldsymbol{D}$ is 3,488.89 kW^2. Uncoordinated EV charging results in a profile $\boldsymbol{L}$ with a load variance of 4,680.16 kW^2, which is reflective of the exacerbated peak demand at 18 h. By contrast, C-VF and C-VF-PS shift EV charging to the valley period (and EV discharging to the peak period), yielding a profile $\boldsymbol{L}$ with a load variance of 2,503 kW^2 for the case of C-VF, and 1,650 kW^2 for the case of C-VF-PS. That is, when compared to uncoordinated charging, C-VF and C-VF-PS reduce the load variance by 47% and 65%, respectively. Further, we observe that C-VF-PS enhances valley-filling compared to C-VF since gridable EVs discharge to lower the peak load, allowing for increased charging during the valley period.

For each of the C-VF and C-VF-PS schemes, Fig 6(b) depicts the reduction of load variance along the iterations of iterative routine corresponding to game $\mathcal{G}^6$. At each iteration, the load variance monotonically decreases until the NE of game $\mathcal{G}^6$ is reached. After the NE point, $\boldsymbol{L}$ cannot be flattened any further. As shown in Fig 6(b), game $\mathcal{G}^6$ reaches the NE after 13 iterations in the case of C-VF, and after 16 iterations in the case of C-VF-PS. The average computation time to execute Algorithm 1 in a single iteration is 0.29 ms[vii] and the approximate execution time for C-VF is $13 \times 0.29 = 3.77$ ms. Moreover, the average computation time to execute Algorithm 2 in a single iteration is 0.66 ms, and the approximate execution time for C-VF-PS is $16 \times 0.66 = 10.56$ ms.[viii] Note that these computation times exclude the time expended for bidirectional communication between the aggregator and EVs.

B. Method 1 Versus Method 2

Fig 7(a) presents the aggregate demand profiles $\boldsymbol{L}$ obtained when C-VF and C-VF-PS are implemented according to Methods 1 and 2. Recall, Method 1 requires each grid-connected EV to reschedule at every time index, whereas Method 2 requires each EV to schedule only at the EV's arrival time index.

In Fig 7(a), we observe that both Methods 1 and 2 produce a similar profile $\boldsymbol{L}$ for both C-VF and C-VF-PS. However, Method 1 incurs a comparatively higher computation and communication overhead, since EVs have to be rescheduled at every time index that they remain grid-connected. Method 2 yields a profile $\boldsymbol{L}$ very close to that of Method 1, but with a lower computation and communication cost, since each EV runs computations only at one time index, thereby limiting communication with the aggregator to a single time index.

[v]We acknowledge that the customer behaviour attributed to EV charging is influenced by seasonal variability, weather conditions, population density of the region along with other location-specific factors. We anticipate the proposed C-VF and C-VF-PS schemes will accommodate the aforementioned variations in EV datasets. In fact, our case-study has been carefully curated to ensure our findings are not geographically-specific.

[vi]The variance of a load profile is the average squared deviation of each element in the corresponding vector from the mean of elements.

[vii]The computation time with the Interior-Point Method (IPM) is 5.7 ms. Hence, Algorithm 1 is 19.6 times computationally faster compared to the IPM.

[viii]An EVG composed of 1500 EVs completes the iterative routine for C-VF-PS in 1.31 s.

TABLE IV
COMPARISON OF C-VF-PS WITH OTHER BENCHMARK SCHEMES

Attribute	BS1 [30]	BS2 [31]	C-VF-PS
Load variance σ^2 (kW^2)	315	174	163
Computational time (sec)	51	285	0.44

Moreover, the iterative routine (which is performed at Step 7) completes in fewer iterations with Method 2, since it involves fewer EVs taking part in the game. For example, the EVG $\mathcal{J}^6$ ($k = 6$) consists of 84 EVs in Method 1 and 16 EVs (newly arrived) in Method 2, and the corresponding iterative routine performed by the EVG $\mathcal{J}^6$ requires 16 iterations for C-VF-PS with Method 1 and 9 iterations for C-VF-PS with Method 2. Nonetheless, Method 1 accommodates unexpected EV departures since the charge-discharge schedules are updated by EVs at every new time step. Overall, in cases where EVs adhere to their specified departure times, Method 2 is advantageous over Method 1 in terms of practical implementation considerations.

C. C-VF and C-VF-PS With Varying EVPs

Previously, we assumed each customer connected to the LVT owned an EV. We now investigate the impact of varying EVPs for load curve shaping, where an EV Penetartion (EVP) is defined as the proportion of customers that own EVs. In Fig 7(b), C-VF and C-VF-PS are implemented for two cases, where EVP = 0.3 and EVP = 0.9. For C-VF, all EVs are considered as charge-only, and for C-VF-PS, all EVs are considered as gridable.

Fig 7(b) shows that a higher EVP (i.e., more customers own EVs) improves valley-filling of the load curve $\boldsymbol{L}$. Furthermore, a higher EVP of gridable EVs also improves the curtailment of load curve peaks. We clearly observe that load curve shaping is more effective with C-VF-PS compared to C-VF since gridable EVs contribute to both valley-filling and peak-shaving.

Next we consider an EVP of 0.9, composed of both charge-only EVs and gridable EVs. In this way, we evaluate the impact of different Proportions of Gridable EVs (PoGEVs) for load curve shaping. When PoGEVs = 0.0, all EVs are charge-only and when PoGEVs = 1.0, all EVs are gridable. In Fig 7(c), all EVs execute Method 1 with a variation in Step (7-c), where charge-only EVs run Algorithm 1 and gridable EVs run Algorithm 2. We observe that as the PoGEVs increases, the aggregate demand peak is gradually lowered and the valleys are gradually filled, yielding a flatter load curve.

D. Comparison With Two Benchmark Schemes (BSs)

We next benchmark C-VF-PS against a water-filling based algorithm proposed in [30] (labeled BS1), and against an ADMM-based algorithm proposed in [31] (labeled BS2). Fig 8 presents numerical simulation for C-VF-PS, BS1, and BS2, where all methods regulate EV charging and discharging to shape the underlying non-EV load curve observed at the LVT.

As we see in Fig 8, C-VF-PS outperforms both BS1 and BS2 in terms of reducing the load variance. According to Table IV, C-VF-PS reduces the load variance by 48.3% compared to BS1, and 6.3% compared to BS2. Furthermore, the computation time for C-VF-PS outperforms both BS1 and BS2. Specifically, the computation time taken by C-VF-PS is 116 times lower than the computation time taken by BS1, and 648 times lower than the computation time taken by BS2.

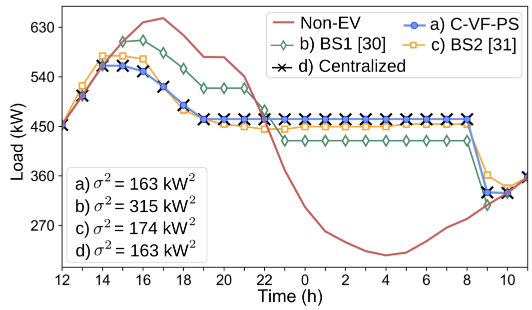

Fig. 8. The aggregate demand profile $\boldsymbol{L}$ returned by the C-VF-PS scheme, the BS1 [30], the BS2 [31] and the centralized OP. The non-EV demand profile $\boldsymbol{D}$ is taken from [30] and up-scaled to fit our simulation.

Performance limitations of BS1 arise from: (1) the imposed restriction on the duration for EV charging and discharging, and (2) the requirement that all EVs share a common value for the SoC at the end of the discharging period. Clearly, C-VF-PS is more personalized in that each EV discharges up to an individually tailored SoC, yielding improved results for load curve shaping. Performance limitations of BS2, especially in terms of the computational time, arise from the computational complexity associated with solving a mixed-integer quadratic programming problem at each iteration of the ADMM routine. It is worth noting that the much lower computational time of C-VF-PS compared to BS2 is a result of the Algorithm 2 that is specifically designed to solve the MDP OP (16) efficiently.

Separately, numerical simulations specific to the corresponding centralized OP (with the objective function in (4) and the constraints in (12)–(15) for all EVs $n \in \mathcal{N}$) are also presented in Fig 8 (labeled Centralized). We observe that the aggregate demand profile $\boldsymbol{L}$ returned by C-VF-PS has converged to the aggregate demand profile resulting from the globally optimal solution of the centralized OP, verifying the accuracy of proposed C-VF-PS scheme.

V. CONCLUSION

We presented two decentralized EV scheduling schemes for shaping the grid load curve, namely C-VF and C-VF-PS. Both schemes coordinated EV charge schedules to fill load curve valleys, and C-VF-PS additionally coordinated EV discharge schedules to shave load curve peaks. In coordinating EV charge (and discharge) schedules, we implemented an iterative routine whereby EVs computed their schedules locally and in parallel, yielding a faster execution time. Importantly, the proposed schemes are resilient to non-deterministic EV arrivals and departures, which lend themselves more readily to practical operating conditions. Simulation results verified that both C-VF and C-VF-PS were effective in shaping the load curve while satisfying all charge requirements across EVs.

APPENDIX

A. Proof of Lemma 1

Consider $\mathcal{G}^k = \{\mathcal{J}^k, [\mathcal{P}_n]_{n\in\mathcal{J}^k}, [\mathcal{U}_n]_{n\in\mathcal{J}^k}\}$. Let V^* be the objective function value of the centralized OP (4) with respect to the optimal solution denoted by $\boldsymbol{p}_n^*$ $(n \in \mathcal{J}^k)$. Formally

$$V^* = \sum_{k\in\mathcal{H}} \left(D(k) + \sum_{i\in\mathcal{N}} p_i^*(k)\right)^2,$$

which with respect to EV $n \in \mathcal{J}^k$ can be expressed as

$$V^* = \sum_{k\in\mathcal{H}} \left(D(k) + p_n^*(k) + p_{\text{-}n}^*(k)\right)^2.$$

By the definition of optimality, for any $\boldsymbol{p}_n \in \mathcal{P}_n$ we have

$$V^* \leq k \in \mathcal{H}\big(D(k) + p_n(k) + p_{\text{-}n}^*(k)\big)^2.$$

Since both sides are non-negative, it follows that

$$-\sum_{k\in\mathcal{H}} \left(D(k) + p_n^*(k) + p_{\text{-}n}^*(k)\right)^2 \geq -\sum_{k\in\mathcal{H}} \left(D(k) + p_n(k) + p_{\text{-}n}^*(k)\right)^2$$

which implies $\mathcal{U}_n(\boldsymbol{p}_n^*; \boldsymbol{p}_{\text{-}n}^*) \geq \mathcal{U}_n(\boldsymbol{p}_n; \boldsymbol{p}_{\text{-}n}^*)$, confirming that the optimal solution to centralized OP (4) yields the NE of game $\mathcal{G}^k$.

B. Proof of Theorem 1

Consider EV n and a CDS $\mathbb{S}_\upsilon \in \mathbb{S}$. We redefine the cost of variance for the time duration of $\mathbb{S}_\upsilon$ as $\mathcal{C}_n(\overline{\boldsymbol{p}}_{n,\upsilon}, \omega) = \sum_{k\in\mathbb{S}_\upsilon}(d_{\text{-}n}(k) + \overline{p}_{n,\upsilon}(k) - \omega)^2$, where ω is the mean of aggregate demand profile. Moreover, we denote the valley-level as α_{vf}^*, the peak-level as α_{ps}^* and the corresponding charge-discharge profile returned by Algorithm 2 as $\overline{\boldsymbol{p}}_{n,\upsilon}^*$. We next prove that α_{vf}^* and α_{ps}^* are optimal for $\mathbb{S}_\upsilon$.

According to Algorithm 2, any value for α_{vf} greater than α_{vf}^* violates the SoC constraint (13). Therefore, we now investigate if there exists any value of α_{vf} lesser than α_{vf}^* that makes the cost $\mathcal{C}_n$ lower than α_{vf}^* does.

Suppose $\alpha_{\text{vf}}^\diamond < \alpha_{\text{vf}}^*$. Let $\alpha_{\text{ps}}^\diamond$ and $\overline{p}_n^\diamond$ be the peak-level and the charge-discharge profile corresponding to $\alpha_{\text{vf}}^\diamond$. With respect to $\overline{\boldsymbol{p}}_{n,\upsilon}^*$ (with valley-level α_{vf}^*), let Γ_c^*, Γ_d^* and Γ_i^* be the mutually exclusive sets of time indices during which the EV charges, discharges and remains idle, respectively, i.e., $\mathbb{S}_\upsilon = \{\Gamma_d^*, \Gamma_i^*, \Gamma_c^*\}$. In what follows, we consider each time set in $\mathbb{S}_\upsilon$ separately.

(a) The charge window Γ_c^*:

Intuitively, for all $k \in \Gamma_c^*$, $\overline{p}_{n,\upsilon}^*(k) > 0$. Since $\alpha_{\text{vf}}^\diamond < \alpha_{\text{vf}}^*$, we obtain that for all $k \in \Gamma_c^*$, $\overline{p}_{n,\upsilon}^\diamond(k) \geq 0$. Moreover, due to the nature of water-filling, it holds that for all $k \in \Gamma_c^*$, $\overline{p}_{n,\upsilon}^\diamond(k) < \overline{p}_{n,\upsilon}^*(k)$ if $\overline{p}_{n,\upsilon}^\diamond(k) < p_n^{max}$ and $\overline{p}_{n,\upsilon}^\diamond(k) = \overline{p}_{n,\upsilon}^*(k)$ if $\overline{p}_{n,\upsilon}^\diamond(k) = p_n^{max}$. It follows that $d_{\text{-}n}(k) + \overline{p}_{n,\upsilon}^*(k) \geq d_{\text{-}n}(k) + \overline{p}_{n,\upsilon}^\diamond(k)$, therefore we have

$$d_{\text{-}n}(k) + \overline{p}_{n,\upsilon}^*(k) - \omega \geq d_{\text{-}n}(k) + \overline{p}_{n,\upsilon}^\diamond(k) - \omega \tag{17}$$

for all $k \in \Gamma_c^*$. According to the valley-filling result in (11), if the EV charges over the time interval $(k\Delta, (k+1)\Delta)$, then $d_{\text{-}n}(k) + \overline{p}_{n,\upsilon}(k) \leq \alpha_{\text{vf}}$. Since $\alpha_{\text{vf}} \leq \omega$, we obtain

$$d_{\text{-}n}(k) + \overline{p}_{n,\upsilon}^*(k) - \omega \leq 0, \quad d_{\text{-}n}(k) + \overline{p}_{n,\upsilon}^\diamond(k) - \omega \leq 0 \tag{18}$$

for all $k \in \Gamma_c^*$. From (17) and (18), it can be derived that

$$\forall k \in \Gamma_c^*, \left(d_{\text{-}n}(k) + \overline{p}_{n,\upsilon}^*(k) - \omega\right)^2 \leq \left(d_{\text{-}n}(k) + \overline{p}_{n,\upsilon}^\diamond(k) - \omega\right)^2. \tag{19}$$

(b) The discharge window Γ_d^*:

Intuitively, for all $k \in \Gamma_d^*$, $\overline{p}_{n,\upsilon}^*(k) < 0$. Since $\alpha_{\text{vf}}^\diamond < \alpha_{\text{vf}}^*$, it can be readily obtained that $\alpha_{\text{ps}}^\diamond > \alpha_{\text{ps}}^*$, which implies that for all $k \in \Gamma_d^*$, $\overline{p}_{n,\upsilon}^\diamond(k) \leq 0$. Moreover, due to the nature of inverse water-filling, it holds that for all $k \in \Gamma_d^*$, $\overline{p}_{n,\upsilon}^\diamond(k) > \overline{p}_{n,\upsilon}^*(k)$ if $\overline{p}_{n,\upsilon}^\diamond(k) > -p_n^{max}$ and $\overline{p}_{n,\upsilon}^\diamond(k) = \overline{p}_{n,\upsilon}^*(k)$ if $\overline{p}_{n,\upsilon}^\diamond(k) = -p_n^{max}$. It follows that $d_{\text{-}n}(k) + \overline{p}_{n,\upsilon}^*(k) \leq d_{\text{-}n}(k) + \overline{p}_{n,\upsilon}^\diamond(k)$, which yields

$$d_{\text{-}n}(k) + \overline{p}_{n,\upsilon}^*(k) - \omega \leq d_{\text{-}n}(k) + \overline{p}_{n,\upsilon}^\diamond(k) - \omega \tag{20}$$

for all $k \in \Gamma_d^*$. Also $d_{\text{-}n}(k) + \overline{p}_{n,\upsilon}(k) \geq \alpha_{\text{ps}}$ and $\alpha_{\text{ps}} \geq \omega$. Therefore we obtain

$$d_{\text{-}n}(k) + \overline{p}_{n,\upsilon}^*(k) - \omega \geq 0, d_{\text{-}n}(k) + \overline{p}_{n,\upsilon}^\diamond(k) - \omega \geq 0 \tag{21}$$

for all $k \in \Gamma_d^*$. From (20) and (21), it can be derived that

$$\forall k \in \Gamma_d^*, \left(d_{\text{-}n}(k) + \overline{p}_{n,\upsilon}^*(k) - \omega\right)^2 \leq \left(d_{\text{-}n}(k) + \overline{p}_{n,\upsilon}^\diamond(k) - \omega\right)^2. \tag{22}$$

(c) The idle window Γ_i^*:

Intuitively, for all $k \in \Gamma_i^*$, $\overline{p}_{n,\upsilon}^*(k) = 0$. According to the nature of water-filling, if $\alpha_{\text{vf}}^\diamond < \alpha_{\text{vf}}^*$ and $\alpha_{\text{ps}}^\diamond > \alpha_{\text{ps}}^*$, then $\overline{p}_{n,\upsilon}^\diamond(k) = 0$ for all $k \in \Gamma_i^*$. Therefore we obtain

$$\forall k \in \Gamma_i^*, \left(d_{\text{-}n}(k) + \overline{p}_{n,\upsilon}^*(k) - \omega\right)^2 = \left(d_{\text{-}n}(k) + \overline{p}_{n,\upsilon}^\diamond(k) - \omega\right)^2. \tag{23}$$

From (19), (22), and (23), it can be concluded that

$$\forall k \in \mathbb{S}_\upsilon, \left(d_{\text{-}n}(k) + \overline{p}_{n,\upsilon}^*(k) - \omega\right)^2 \leq \left(d_{\text{-}n}(k) + \overline{p}_{n,\upsilon}^\diamond(k) - \omega\right)^2,$$

which implies $\mathcal{C}_n(\overline{\boldsymbol{p}}_{n,\upsilon}^*, \omega) \leq \mathcal{C}_n(\overline{\boldsymbol{p}}_{n,\upsilon}^\diamond, \omega)$. Therefore, there is no $\alpha_{\text{vf}} < \alpha_{\text{vf}}^*$ such that the total cost is further lowered. This implies that α_{vf}^* and α_{ps}^* are optimal, thus the theorem holds.

REFERENCES

[1] M. Todorovic and M. Simic, "Current state of the transition to electrical vehicles," in *Proc. Int. Conf. Intell. Interact. Multimedia Syst. Serv.*, Jun. 2018, pp. 130–139.

[2] N. I. Nimalsiri, C. P. Mediwaththe, E. L. Ratnam, M. Shaw, D. B. Smith, and S. K. Halgamuge, "A survey of algorithms for distributed charging control of electric vehicles in smart grid," *IEEE Trans. Intell. Transp. Syst.*, vol. 21, no. 11, pp. 4497–4515, Nov. 2020.

[3] Z. Yi *et al.*, "A highly efficient control framework for centralized residential charging coordination of large electric vehicle populations," *Int. J. Electr. Power Energy Syst.*, vol. 117, May 2020, Art. no. 105661.

[4] L. Jian, Y. Zheng, and Z. Shao, "High efficient valley-filling strategy for centralized coordinated charging of large-scale electric vehicles," *Appl. Energy*, vol. 186, pp. 46–55, Jan. 2017.

[5] G. C. Wang, E. Ratnam, H. V. Haghi, and J. Kleissl, "Corrective receding horizon EV charge scheduling using short-term solar forecasting," *Renew. Energy*, vol. 130, pp. 1146–1158, Jan. 2019.

[6] Z. Ma, D. Callaway, and I. Hiskens, "Optimal charging control for plug-in electric vehicles," in *Control and Optimization Methods for Electric Smart Grids*. New York, NY, USA: Springer, 2012, pp. 259–273.

[7] N. Chen, C. W. Tan, and T. Q. S. Quek, "Electric vehicle charging in smart grid: Optimality and valley-filling algorithms," *IEEE J. Sel. Topics Signal Process.*, vol. 8, no. 6, pp. 1073–1083, Dec. 2014.

[8] Z. Ma, D. S. Callaway, and I. A. Hiskens, "Decentralized charging control of large populations of plug-in electric vehicles," *IEEE Trans. Control Syst. Technol.*, vol. 21, no. 1, pp. 67–78, Jan. 2013.

[9] J. Rivera, P. Wolfrum, S. Hirche, C. Goebel, and H.-A. Jacobsen, "Alternating direction method of multipliers for decentralized electric vehicle charging control," in *Proc. 52nd IEEE Conf. Decis. Control*, Dec. 2013, pp. 6960–6965.

[10] W.-J. Ma, V. Gupta, and U. Topcu, "On distributed charging control of electric vehicles with power network capacity constraints," in *Proc. Amer. Control Conf.*, Jun. 2014, pp. 4306–4311.

[11] C. Le Floch, F. Belletti, and S. Moura, "Optimal charging of electric vehicles for load shaping: A dual-splitting framework with explicit convergence bounds," *IEEE Trans. Transport. Electrific.*, vol. 2, no. 2, pp. 190–199, Jun. 2016.

[12] M. Liu, P. K. Phanivong, Y. Shi, and D. S. Callaway, "Decentralized charging control of EVs in residential distribution networks," *IEEE Trans. Control Syst. Technol.*, vol. 27, no. 1, pp. 266–281, Oct. 2017.

[13] K. Zhan, Z. Hu, Y. Song, N. Lu, Z. Xu, and L. Jia, "A probability transition matrix based decentralized electric vehicle charging method for load valley filling," *Electr. Power Syst. Res.*, vol. 125, pp. 1–7, Aug. 2015.

[14] L. Gan, U. Topcu, and S. H. Low, "Optimal decentralized protocol for electric vehicle charging," *IEEE Trans. Power Syst.*, vol. 28, no. 2, pp. 940–951, May 2013.

[15] L. Zhang, F. Jabbari, T. Brown, and S. Samuelsen, "Coordinating plug-in electric vehicle charging with electric grid: Valley filling and target load following," *J. Power Sources*, vol. 267, pp. 584–597, Dec. 2014.

[16] Z. Ma, S. Zou, L. Ran, X. Shi, and I. A. Hiskens, "Efficient decentralized coordination of large-scale plug-in electric vehicle charging," *Automatica*, vol. 69, pp. 35–47, Jul. 2016.

[17] K. Zhang *et al.*, "Optimal decentralized valley-filling charging strategy for electric vehicles," *Energy Convers. Manage.*, vol. 78, pp. 537–550, Feb. 2014.

[18] N. I. Nimalsiri, D. B. Smith, E. L. Ratnam, C. P. Mediwaththe, and S. K. Halgamuge, "A decentralized electric vehicle charge scheduling scheme for tracking power profiles," in *Proc. IEEE PES Innov. Smart Grid Technol.*, Feb. 2020, pp. 1–5.

[19] Y. Mou, H. Xing, Z. Lin, and M. Fu, "Decentralized optimal demand-side management for PHEV charging in a smart grid," *IEEE Trans. Smart Grid*, vol. 6, no. 2, pp. 726–736, Mar. 2015.

[20] G. Binetti, A. Davoudi, D. Naso, B. Turchiano, and F. L. Lewis, "Scalable real-time EV charging with discrete charging rates," *IEEE Trans. Smart Grid*, vol. 6, no. 5, pp. 2211–2220, Sep. 2015.

[21] K. Zhan, A. Xu, X. Guo, W. Wei, and G. Jian, "A hierarchical control method of massive plug-in electric vehicles for load valley filling," in *Proc. CIRED Workshop*, 2016, pp. 1–4.

[22] J. Pajic, J. Rivera, K. Zhang, and H.-A. Jacobsen, "EVA: Fair and auditable electric vehicle charging service using blockchain," in *Proc. ACM 12th Int. Conf. Distrib. Event-Based Syst.*, Jun. 2018, pp. 262–265.

[23] K. Kaur, A. Dua, A. Jindal, N. Kumar, M. Singh, and A. Vinel, "A novel resource reservation scheme for mobile PHEVs in V2G environment using game theoretical approach," *IEEE Trans. Veh. Technol.*, vol. 64, no. 12, pp. 5653–5666, Dec. 2015.

[24] Z. Wang and S. Wang, "Grid power peak shaving and valley filling using vehicle-to-grid systems," *IEEE Trans. Power Del.*, vol. 28, no. 3, pp. 1822–1829, Jul. 2013.

[25] L. T. Al-Bahrani, B. Horan, M. Seyedmahmoudian, and A. Stojcevski, "Dynamic economic emission dispatch with load dema nd management for the load demand of electric vehicles during crest shaving and valley filling in smart cities environment," *Energy*, vol. 195, Mar. 2020, Art. no. 116946.

[26] C. S. Ioakimidis, D. Thomas, P. Rycerski, and K. N. Genikomsakis, "Peak shaving and valley filling of power consumption profile in non-residential buildings using an electric vehicle parking lot," *Energy*, vol. 148, pp. 148–158, Apr. 2018.

[27] F. Li, H. Guo, Z. Jing, Z. Wang, and X. Wang, "Peak and valley regulation of distribution network with electric vehicles," *J. Eng.*, vol. 2019, no. 16, pp. 2488–2492, Mar. 2019.

[28] W. Li, Z. Y. Lin, and G. F. Yan, "Optimal charging and discharging control of plug-in hybrid electric vehicles in a system-level power distribution network," *J. Phys., Conf. Ser.*, vol. 1304, Aug. 2019, Art. no. 012012.

[29] H. K. Nguyen and J. B. Song, "Optimal charging and discharging for multiple PHEVs with demand side management in vehicle-to-building," *J. Commun. Netw.*, vol. 14, no. 6, pp. 662–671, Dec. 2012.

[30] H. Xing, M. Fu, Z. Lin, and Y. Mou, "Decentralized optimal scheduling for charging and discharging of plug-in electric vehicles in smart grids," *IEEE Trans. Power Syst.*, vol. 31, no. 5, pp. 4118–4127, Sep. 2016.

[31] H. Xing, Z. Lin, and M. Fu, "A new decentralized algorithm for optimal load shifting via electric vehicles," in *Proc. 36th Chin. Control Conf. (CCC)*, Jul. 2017, pp. 10708–10713.

[32] W. Li, Z. Lin, H. Zhou, and G. Yan, "Multi-objective optimization for cyber-physical-social systems: A case study of electric vehicles charging and discharging," *IEEE Access*, vol. 7, pp. 76754–76767, Jun. 2019.

[33] R. G. Gallager, *Information Theory and Reliable Communication*, vol. 2. New York, NY, USA: Wiley, Jan. 1968.

[34] *Road Vehicles Vehicle to Grid Communication Interface Part 1*, Standard ISO 15118-1:2013, ISO, 2013. [Online]. Available: https://www.iso.org/standard/55365.html

[35] SAE Mobilus. *Communication for Smart Charging of Plugin Electric Vehicles Using Smart Energy Profile 2.0*. Accessed: Dec. 20, 2019. [Online]. Available: https://saemobilus.sae.org/content/j2847/1_201311

[36] W. Tushar, W. Saad, H. V. Poor, and D. B. Smith, "Economics of electric vehicle charging: A game theoretic approach," *IEEE Trans. Smart Grid*, vol. 3, no. 4, pp. 1767–1778, Dec. 2012.

[37] J. B. Rosen, "Existence and uniqueness of equilibrium points for concave N-person games," *Econometrica*, vol. 33, no. 3, pp. 347–351, Jul. 1965.

[38] C. P. Mediwaththe and D. B. Smith, "Game-theoretic electric vehicle charging management resilient to non-ideal user behavior," *IEEE Trans. Intell. Transp. Syst.*, vol. 19, no. 11, pp. 3486–3495, Nov. 2018.

[39] D. P. Bertsekas, "Nonlinear programming," *J. Oper. Res. Soc.*, vol. 48, no. 3, p. 334, Mar. 1997.

[40] E. L. Ratnam and S. R. Weller, "Receding horizon optimization-based approaches to managing supply voltages and power flows in a distribution grid with battery storage co-located with solar PV," *Appl. Energy*, vol. 210, pp. 1017–1026, Jan. 2018.

[41] AEMO. *Data (NEM)*. Accessed: Dec. 20, 2019. [Online]. Available: https://aemo.com.au/energy-systems/electricity/national-electricity-market-nem/data-nem

[42] N. I. Nimalsiri, E. L. Ratnam, C. P. Mediwaththe, D. B. Smith, and S. K. Halgamuge, "Coordinated charging and discharging control of electric vehicles to manage supply voltages in distribution networks: Assessing the customer benefit," *Appl. Energy*, vol. 291, Jun. 2021, Art. no. 116857.

[43] EVBOX. *Check Charging Specifications*. Accessed: Dec. 20, 2019. [Online]. Available: https://evbox.com/electric-cars

[44] IEA. (2020). *Global EV Outlook*. [Online]. Available: https://www.iea.org/reports/global-ev-outlook-2020

[45] Victoria State Government. *Victorian Integrated Survey of Travel and Activity*. [Online]. Available: https://transport.vic.gov.au/about/data-and-research/vista

[46] P. Richardson, D. Flynn, and A. Keane, "Local versus centralized charging strategies for electric vehicles in low voltage distribution systems," *Proc. IEEE Power Energy Soc. Gen. Meet.*, Jul. 2013, p. 1.

Nanduni I. Nimalsiri received the B.Sc.Eng. degree (Hons.) in computer science and engineering from the University of Moratuwa, Moratuwa, Sri Lanka. She is currently pursuing the Ph.D. degree in engineering and computer science, majoring in engineering, with the School of Engineering, The Australian National University, Canberra, ACT, Australia. She is also a Research Student with the CSIRO Data61, Australia. Her current research interests include distributed control and optimization of EV charging.

Elizabeth L. Ratnam (Senior Member, IEEE) received the B.Eng. (Hons.) and Ph.D. degrees in electrical engineering from The University of Newcastle, Australia, in 2006 and 2016, respectively. She subsequently held post-doctoral research positions at the Center for Energy Research, University of California at San Diego, and the University of California at Berkeley with the California Institute for Energy and Environment. From 2001 to 2012, she held various positions at Ausgrid, a utility that operates one of the largest electricity distribution networks in Australia. She is currently a Senior Lecturer with the School of Engineering, The Australian National University (ANU), where she holds an ANU Future Engineering Research Leader (FERL) Fellowship. Her research interests include applications of optimization and control theory to power distribution networks.

David B. Smith (Member, IEEE) received the B.E. degree in electrical engineering from the University of New South Wales, Sydney, NSW, Australia, in 1997, and the M.E. (research) and Ph.D. degrees in telecommunications engineering from the University of Technology Sydney, Sydney, in 2001 and 2004, respectively. Since 2004, he has been with National Information and Communications Technology Australia (NICTA), incorporated into Data61 of CSIRO in 2016, and The Australian National University (ANU), Canberra, ACT, Australia. He is currently the Principal Research Scientist of the CSIRO Data61 and also an Adjunct Associate Professor with ANU. He has a variety of industry experience in electrical and telecommunications engineering. He has published more than 150 technical refereed articles. He has made various contributions to IEEE standardization activity in personal area networks. His current research interests include data privacy, privacy for networks, the IoT, game theory for distributed signal processing, disaster tolerant networks, 5G networks, distributed optimization for smart grid, and electric vehicles. He was a recipient of four conference Best Paper Awards. He is also an Area Editor of *IET Smart Grid* and has served on the technical program committees for several leading international conferences in the fields of communications and networks.

Chathurika P. Mediwaththe (Member, IEEE) received the B.Sc. degree (Hons.) in electrical and electronic engineering from the University of Peradeniya, Sri Lanka, and the Ph.D. degree in electrical engineering from the University of New South Wales, Sydney, NSW, Australia, in 2017. From 2013 to 2017, she was a Researcher with the CSIRO Data61, (previously NICTA), Sydney. She is currently a Research Fellow with the School of Engineering and the Battery Storage and Grid Integration Program, The Australian National University, Australia. Her research interests include electricity demand-side management, renewable energy generation and energy storage integration, microgrids and distribution network operation, game theory, and optimization for distributed energy resource allocation. She is the Chair of the Young Professionals Group of the IEEE Australian Capital Territory Chapter.

Saman K. Halgamuge (Fellow, IEEE) received the B.Sc.Eng. degree in electronic and telecommunication engineering from the University of Moratuwa, Moratuwa, Sri Lanka, and the Dr.Ing. and Dipl.Ing. degrees in electrical engineering (data engineering) from TU Darmstadt, Darmstadt, Germany, in 1990 and 1995, respectively. He is currently a Professor with the Department of Mechanical Engineering, The University of Melbourne, Parkville, VIC, Australia, and an honorary Professor with The Australian National University (ANU) and the ANU Energy Change Institute, Canberra, ACT, Australia. His research interests include AI and applications in energy, mechatronics, and biomedical engineering. He is listed as one of the top 2% cited experts for AI and Image Processing in the Stanford University Database published in 2020. He is also a Distinguished Lecturer of the IEEE Computational Intelligence Society.

4.2 Summary and Contributions

This chapter presented a distributed algorithm using both game theory and water-filling theory to coordinate EV charging and discharging to flatten the load curve of a low-voltage transformer. First, a centralised optimisation problem was formulated with the objective of minimizing the system load variance (a coupled objective function), while satisfying each EV's charging requirement before their specified departure time and complying with each individual EV charging and discharging constraints. Then, the centralised optimisation problem was decomposed into a set of subproblems, each of which is specific to a single EV. Next, a distributed algorithm was designed in the form of a non-cooperative game, wherein each EV solved the optimisation problem assigned to each of them and determined a charge-discharge profile locally. To solve the respective optimisation problem efficiently, two separate algorithms based on the water-filling concept were also proposed, one for charge-only EVs and the other for gridable EVs. The implementation of the proposed game was supported by a coordination framework that consists of a two-way communication infrastructure, enabling information exchange between an aggregator (coordinator) and each EV. In particular, the algorithm consisted of an iterative routine, wherein the aggregator drove each iteration by transmitting updated communication signals to EVs sharing the computational load.

A few important features of the proposed algorithm include: it facilitates both EV charging and discharging; it accommodates the heterogeneity in EV attributes (e.g. plug-in time, expected plug-out time, maximum charge/discharge rate, battery capacity, initial SoC, power demand or expected SoC, charge/discharge efficiency); it incorporates separate energy conversion efficiencies for charging and discharging; it allows EVs to compute charge-discharge profiles locally without sharing EV information with the aggregator; it allows parallel computations by EVs and only requires simple computations that can be easily executed by a microcontroller with less cost; it applies to underlying non-EV load (base load) curves of arbitrary shapes, and not limited to non-EV load curves of particular shapes; and it manages the uncertainty arising from EV mobility.

The performance of the proposed algorithm was analysed through numerical simulations. It was found that: (1) as the EV penetration (i.e., proportion of customers that own EVs) increases, valley-filling and peak curtailment of the load curve are gradually improved; (2) load curve flattening becomes more effective when EVs partake in both charging and discharging, compared to only charging, and (3) as the proportion of gridable EVs increases, the aggregated demand peaks are gradually lowered and the valleys are gradually filled, yielding a flatter load curve.

To summarise, the main contributions of this chapter were as follows.

1. The formulation of a (mixed discrete) optimisation problem to coordinate EV charging (and discharging) to achieve valley filling (and peak shaving) of the load curve, while satisfying each EV customer's requirement of getting their EV charged to the required SoC by the specified time and complying with lim-

itations of EV charging (and discharging) infrastructure and EV battery state-of-health thresholds;

2. The proposal of a distributively Coordinated Valley Filling (and Peak Shaving) algorithm, called C-VF (and C-VF-PS) in short, which obtains the EV charge (and discharge) solutions to the formulated optimisation problem using an EV coordination framework based on game theory;

3. The proposal of a water-filling based algorithm (a variant of the DECSaT algorithm proposed in Chapter 3), which solves a localised optimisation problem in the form of a (mixed discrete) quadratic optimisation problem and obtains each EV charge (and discharge) profile locally without running into computational tractability problems;

4. The proposal of two methods (Method 1 and Method 2) based on an EV grouping technique to manage non-deterministic EV arrivals and departures, where the first method results in the computation of each EV charge-discharge profile at every time-step and the second method results in the determination of each EV charge-discharge profile only once;

5. The proofs of optimality of the proposed algorithm(s) and numerical simulations to demonstrate the effectiveness of proposed algorithm(s).

Results obtained from numerical simulations demonstrated that both C-VF and C-VF-PS were effective in shaping the load curve while satisfying all charge requirements across EVs. Furthermore, it was confirmed that, compared to uncoordinated EV charging, C-VF and C-VF-PS reduced the load variance (flattens the load curve) by 47% and 65%, respectively. Moreover, the implementation based on EV grouping technique in Method 2 was shown to be more effective than Method 1, in terms of computation and communication overheads.

In the next part of this thesis, we focus on optimising EV charging and discharging with distribution grid constraints also taken into consideration.

Part 3: Coordinated EV Charging and Discharging taking Distribution Network Considerations and Economic Considerations into account

Chapter 5

A centralised approach to manage supply voltages in distribution networks with EVs

The transition to support an accelerated uptake in EVs has led to greater concerns regarding the management of bi-directional power flows in distribution networks, especially when they lead to violations in regulatory voltage thresholds or voltage instabilities, resulting in costly remediation for distribution operators.

With distribution networks often spanning thousands of metres, customers at the far end of the feeder often experience substantial voltage drops, which are much more pronounced when large numbers of EVs conduct charging simultaneously. Oftentimes, voltage drops become a binding constraint when a distribution feeder is subject to a high EV penetration level [Luo and Chan, 2014; Richardson et al., 2011]. For instance, case studies of uncontrolled EV charging in residential distribution networks in Ireland [Richardson et al., 2011] and Australia [de Hoog et al., 2013] revealed that the first point of network failure was voltage dropping below the operational limits.

With the development of V2G technology, electrical distributors are now particularly concerned about both peak power flows inducing under-voltage conditions, as well as, reverse power flows inducing over-voltage conditions in the distribution grid. To mitigate against such non-compliant voltage deviations arising from EV charging and discharging, this work considers developing coordinated EV charging and discharging approaches incorporating network voltage constraints. Specifically, the main focus of this work is given to maintaining voltage stability in balanced distribution networks under quasi-steady-state operating conditions.

Despite the extensive EV charging literature focused only on either financial performance objectives (e.g., minimal cost charging) or operational performance objectives (e.g., grid congestion management or voltage regulation), only a few studies have considered approaches that combine both financial/economic performance objectives from EV customers' perspective and operational performance objectives from an electrical distributor's perspective. Hence, we identified that approaches enabling EV customers to charge their EVs with minimal charging costs while contributing to voltage regulation in distribution networks are important to balance the interests of both electrical distributors (or grid operators) and EV customers. It is expected that such approaches encourage the participation of EV customers in voltage regulation services.

Given the capability of EVs to assist voltage regulation in distribution grids, this chapter is dedicated to developing a coordinated EV charging and discharging control approach that regulates system voltages to be within the appropriate operational limits while also yielding a lower energy bill for each EV customer. The contributions in this chapter are presented in our published manuscript.

5.1 Published Manuscript

In our paper presented below, a centrally coordinated, network-aware EV charging and discharging approach is proposed to manage supply voltages in residential distribution networks under minimal operational costs accrued to EV customers. Outcomes from this paper address research objective Q1 of the thesis (see Chapter 1 - Section 1.2) by showing how to involve EVs in voltage regulation considering both charging and discharging of EV batteries, and research objective Q2 by taking into account both EV customer economics and electrical distributor concerns on voltage regulatory requirements when scheduling EV charging and discharging.

N. I. Nimalsiri, E. L. Ratnam, C. P. Mediwaththe, D. B. Smith, S. K. Halgamuge, "Coordinated charging and discharging control of electric vehicles to manage supply voltages in distribution networks: Assessing the customer benefit," *Applied Energy*, vol. 291, pp. 116857, June. 2021.
https://doi.org/10.1016/j.apenergy.2021.116857

Applied Energy 291 (2021) 116857

Contents lists available at ScienceDirect

Applied Energy

journal homepage: www.elsevier.com/locate/apenergy

Coordinated charging and discharging control of electric vehicles to manage supply voltages in distribution networks: Assessing the customer benefit

Nanduni I. Nimalsiri [a,b,*], Elizabeth L. Ratnam [a], Chathurika P. Mediwaththe [a], David B. Smith [a,b], Saman K. Halgamuge [a,c]

[a] School of Engineering, Australian National University, Canberra, ACT 2600, Australia
[b] CSIRO Data61, Eveleigh, NSW 2015, Australia
[c] School of Engineering, University of Melbourne, Parkville, VIC 3010, Australia

ARTICLE INFO

Keywords:
Electric vehicles
Quadratic program
Receding horizon
Supply voltages
Time-of-use
Vehicle-to-grid

ABSTRACT

Increased worldwide uptake of Electric Vehicles (EVs) accentuates the need for developing coordinated EV charging and discharging methods that mitigate detrimental and sustained under-voltage and over-voltage conditions in distribution networks. In this paper, a centrally coordinated EV charge-discharge scheduling method is proposed, referred to as Network-aware EV Charging (and Discharging) N-EVC(D), that takes into account both EV customer economics and distribution grid constraints. Specifically, N-EVC(D) is designed to maintain quasi-steady-state feeder voltages within statutory power quality limits, while minimizing EV customer operational costs associated with: (1) purchasing (or otherwise being compensated for delivering) electricity on a time-of-use tariff; and (2) battery degradation due to frequent charging and discharging. The optimization problem for N-EVC(D) is formulated as a quadratic program, with voltage constraints to limit voltage variability across a radial distribution feeder, and individual EV constraints to satisfy heterogeneous EV charge requirements. In N-EVC(D), each grid-connected EV follows an operator-specified battery schedule that is obtained by solving the proposed quadratic program. A receding horizon implementation is also proposed to support near-real-time N-EVC(D) operations while accommodating non-deterministic EV arrivals and departures. The benefits of N-EVC(D) are assessed by means of numerical simulations carried out on an IEEE test feeder populated with a real-world dataset of residential load collected from households within an Australian distribution network. The simulation results confirm that N-EVC(D) mitigates non-compliant voltage deviations that would otherwise occur when voltage constraints are not enforced. Compared to uncoordinated EV charging, N-EVC(D) offers a 92% – 111% reduction in the operational costs incurred by EV customers.

1. Introduction

The recent dramatic increase in Electric Vehicle (EV) uptake around the globe is enabling a significant reduction in carbon emissions from the transportation sector [1]. However, an adverse consequence of EV proliferation is the increased utilization of electric power grids, potentially exacerbating the risk of supply voltage excursions beyond acceptable power quality limits [2].

The studies in [2] and [3] have revealed that uncoordinated EV charging leads to numerous detrimental electrical grid impacts, including thermal over-loading of transformers, increased power system losses, and significant voltage drops. These voltage drops are particularly pronounced when large numbers of EVs conduct charging simultaneously, mostly upon arrival at home after work. In particular, large voltage deviations reduce the quality of power supplied to consumer electrical appliances, potentially causing misoperation or failure. To deliver high-quality power to end-customers without upgrading existing electrical grid infrastructure, numerous coordinated EV charging approaches have been proposed — as reported in the survey paper [4].

Several authors have proposed optimization-based EV charging methods to address under-voltage conditions coincident with peak power demand [5–15]. By applying a linear approximation to voltage drop within the network, De Hoog et al. [5] formulate a linear optimization problem with the objective of providing as much charging power to the EVs as the network will accommodate. A similar approach is followed in [6] to maximize the total power delivered to EVs, while ensuring the network limits are not exceeded. In [7],

* Corresponding author at: Level 5, 13 Garden Street, Eveleigh, NSW 2015, Australia.
E-mail addresses: nanduni.nimalsiri@anu.edu.au (N.I. Nimalsiri), elizabeth.ratnam@anu.edu.au (E.L. Ratnam), chathurika.mediwaththe@anu.edu.au (C.P. Mediwaththe), david.smith@data61.csiro.au (D.B. Smith), saman.halgamuge@anu.edu.au (S.K. Halgamuge).

https://doi.org/10.1016/j.apenergy.2021.116857
Received 23 December 2020; Received in revised form 16 March 2021; Accepted 18 March 2021
Available online 31 March 2021
0306-2619/

a linear program is iteratively solved until voltages fall within the permissible limits. To achieve valley-filling in compliance with the voltage constraints, a shrunken primal–dual subgradient algorithm is proposed in [8], which is later extended in [9] to include a dimension reduction methodology whereby the network topology is partitioned to reduce the complexity. The authors in [10] propose a distributed voltage compensation algorithm to recover voltage violations occurring at distribution nodes. The authors in [11] propose an optimization problem with a variable objective function to improve the voltage profile at the customer Point of Common Coupling (PCC). By contrast, the studies in [12] and [13] investigate methods to control EV charging using local voltage measurements at the PCC. Clement-Nyns et al. [14] minimize distribution system losses under the assumption that mitigating losses will improve the voltage profile. Alternatively, the algorithm in [15] adapts EV charging from voltage-safety-oriented to loss-minimization-oriented, or vice versa, based on EV penetration level. The studies in [16] and [17] propose probabilistic Monte Carlo-based methods to optimize EV charging in a distribution network with renewable power generation, while taking into consideration the minimum voltage allowed for the distribution network.

With the recent introduction of Vehicle-to-Grid (V2G) operation, the management of system voltages within operational limits becomes increasingly challenging, as voltage rise stemming from the reversal of power flow direction must also be addressed. However, with the exceptions of [11] and [14], none of the approaches in [5–17] support V2G operation. Importantly, V2G-based studies that incorporate network constraints together with EV customer economics are less prevalent in the literature [4]. More specifically, the network-aware EV scheduling methods in [5–17] do not consider price-based incentives when charging and discharging EVs. Dong et al. [3] design a pricing scheme for EV fast-charging stations to support voltage control, and Sun et al. [18] propose a cost-minimizing day-ahead charge scheduling approach that regulates network voltages. Bharati and Paudyal [19] propose a hierarchical framework to reduce the cost of EV charging while constraining voltages within the distribution grid. However, all these studies in [3,18,19] assume that EVs do not partake in V2G operation. By contrast, Shekari et al. [20] propose a day-ahead EV scheduling method involving V2G to minimize both network voltage deviations and microgrid operational costs; however, the proposed method does not consider costs associated with the EV customers. Conversely, Crow and others [21] propose an EV scheduling method with V2G to co-optimize customer and system objectives by minimizing both EV charging costs and system load variance; however, the authors do not consider network voltage limitations.

In the literature, many existing approaches, e.g., [7–10,14,19,22], rely on the assumption that EV arrival times are deterministic (known a *priori*), which is not very realistic in general. For example, the algorithm proposed in [22] reduces EV operational costs subject to constraints of EV and power systems; however, day-ahead EV arrival times are required as inputs to the algorithm. Interestingly, the EV charging algorithm in [23] manages EVs with non-deterministic arrivals while minimizing both network voltage deviations and EV charging costs; however, it disregards V2G operation. Numerous receding horizon control approaches are proposed to adapt to various types of uncertainties arising from EV mobility, including stochastic daily trip distances [24], random arrival and departure times [25], and day-ahead forecast errors associated with time-varying load [26] and solar PV estimation [27]. However, these studies in [24–27] do not directly regulate distribution network voltages. Thus, the formulation of an EV charge and discharge scheduling method that minimizes operational costs accrued by EV customers, while circumventing sustained over-voltage and under-voltage conditions, in addition to managing non-deterministic EV arrival and departure times, addresses a significant gap in the existing literature.

In this paper, a Network-aware EV Charging (and Discharging) method called N-EVC(D) is proposed to minimize the operational costs that are accrued to EV customers in the context of time-based financial tariffs, while maintaining feeder nodal voltage magnitudes within prescribed thresholds under quasi-steady-state operating conditions. By supporting both G2V (Grid-to-Vehicle) and V2G operation, N-EVC(D) allows for more efficient utilization of EV idle times (when EVs are parked). To implement N-EVC(D), each EV customer requires to install an energy management system that communicates directly with a Centralized Operator (CO), e.g., an EV aggregator, enabling the CO to coordinate EV battery schedules. The optimization problem for N-EVC(D) is formulated as a Quadratic Program (QP) with the objective of minimizing EV customer related operational costs by: (1) reducing daily payments for electricity received from the grid for EV charging; (2) increasing daily profits from the delivery of electricity to the grid via EV discharging; and (3) reducing excessive EV battery cycling to prolong battery lifespan. In the proposed QP, a network constraint is included to ensure that the voltage delivered to each customer is within the allowable limits at all times. In formulating the respective network constraint, the nodal location of each customer along a radial distribution feeder is specifically taken into account. The proposed QP is also constrained by the requirement to charge all grid-connected EV batteries to their desired State of Charge (SoC) before their specified departure times.

Moreover, this paper combines a receding horizon control approach with N-EVC(D) to manage unexpected connections and disconnections of EVs from the grid. In the proposed Receding Horizon Optimization (RHO)-based N-EVC(D) implementation, the CO repeatedly solves the proposed QP over a moving time horizon and dispatches resultant charge-discharge control sequences to all grid-connected EVs. In summary, the main contributions of this paper are listed as follows.

1. A network-aware EV battery scheduling method called N-EVC(D) is proposed to minimize operational costs associated with EV charging and discharging, while mitigating quasi-steady-state voltage fluctuations falling below a lower voltage limit or exceeding an upper voltage limit.
   - In contrast to the literature focused only on either least-cost EV charging (e.g., [28]) or distribution network congestion management (e.g., [5–15]), N-EVC(D) balances operational costs incurred by EV customers against improvements in supply voltages across the distribution power grid. As such, N-EVC(D) provides benefits to EV customers as well to electrical distributors.
   - N-EVC(D) is formulated as a QP with an objective function that: (1) minimizes EV charging (and discharging) costs in the text of a Time-of-Use (ToU) net metering financial policy as defined in [29], and (2) reduces excessive EV battery degradation caused by frequent charging and discharging.
   - N-EVC(D) leverages a power flow model referred to as the LinDistFlow [30] to capture network power flows and voltages along a radial distribution feeder, wherein each of the EV customers is connected to the wider distribution grid via a PCC, behind which sits a residential power system that consists of an EV and a non-EV load.
   - N-EVC(D) is designed to satisfy all feasible heterogeneous EV charge requirements within the customer-specified time duration.
2. A RHO-based N-EVC(D) algorithm is proposed to accommodate non-deterministic EV arrivals and departures. Specifically, the proposed algorithm supports near-real-time N-EVC(D) control operations as opposed to day-ahead EV charge (and discharge) scheduling, to improve network voltages in the presence of uncertainties including non-deterministic EV arrival times and non-EV load forecast errors.

3. The benefits from N-EVC(D) are assessed via extensive numerical simulations carried out on the IEEE 13 node test feeder using empirical real-life data of residential customers in an Australian distribution network.

The remainder of this paper is organized as follows. In Section 2, the residential power system associated with a single EV customer is introduced. In Section 3, the N-EVC(D) method is proposed to coordinate EV charge and discharge schedules, considering an EV population distributed across a medium voltage distribution network. In Section 4, the numerical simulation results are presented, followed by the Conclusion in Section 5.

Notation

Let $\mathbb{R}^\ell$ denote ℓ-dimensional vectors of real numbers and $\mathbb{R}^\ell_{\geq 0}$ denote ℓ-dimensional vectors with all non-negative components, where, as usual, $\mathbb{R}^1 = \mathbb{R}$. For a vector or matrix $\boldsymbol{A}$, its transpose is denoted by $\boldsymbol{A}^\top$. $\mathbf{0}$ denotes the all-zero column vector of length ℓ and $\mathbf{I}$ denotes the ℓ-by-ℓ identity matrix. $\mathbf{1}$ denotes an all-ones column vector, where the context will make clear the dimension intended. For two matrices $\boldsymbol{A} = [a_{ij}] \in \mathbb{R}^{m\times n}$ and $\boldsymbol{B} = [b_{ij}] \in \mathbb{R}^{p\times q}$, $\boldsymbol{A} \oplus \boldsymbol{B} = [c_{ij}] \in \mathbb{R}^{(m+p)\times(n+q)}$ denotes the matrix satisfying $c_{ij} = a_{ij}$ when $i \leq m$ and $j \leq n$, $c_{ij} = b_{(i-m)(j-n)}$ when $i > m$ and $j > n$, and $c_{ij} = 0$ elsewhere, i.e, $\boldsymbol{A} \oplus \boldsymbol{B} = \mathrm{diag}(\boldsymbol{A}, \boldsymbol{B})$. For two sets $\mathcal{P}$ and $\mathcal{Q}$, $\mathcal{P} \cap \mathcal{Q}$ denotes the set that has only elements common to both $\mathcal{P}$ and $\mathcal{Q}$.

2. Preliminaries

This paper considers EV charge and discharge scheduling in a distribution network serving a set of customers (e.g., residential and small business customers) denoted by $\mathbb{H} := \{1, \dots, n, \dots, h\}$. The set of customers is divided into two subsets $\mathbb{H}_1$ and $\mathbb{H}_2$, i.e., $\mathbb{H} = \mathbb{H}_1 \cup \mathbb{H}_2$, where $\mathbb{H}_1$ consists of customers with *gridable EVs* that can both charge and discharge from or to the electric grid, and $\mathbb{H}_2$ consists of customers with *charge-only EVs*.

A planning time-horizon $[0, T]$ is considered that is discretized into ℓ time intervals of temporal resolution Δ. Let $\mathbb{S} := \{1, \dots, t, \dots, \ell\}$, whereby a time interval is denoted by $((t-1)\Delta, t\Delta)$ for all $t \in \mathbb{S}$. In this paper, T and Δ are set to $T = 24$ h and $\Delta = 0.5$ h, such that $\ell = T/\Delta = 48$. Other choices are certainly possible, subject only to commensurability of T, ℓ and Δ.

Fig. 1 illustrates the assumed topology of a *residential power system* corresponding to customer $n \in \mathbb{H}$, where the EV belonging to customer n is labeled as EV_n. Bi-directional smart meter $\mathbf{M}$ measures and records power flow $y_n(t)$ (in kW), where the measured power flow from (to) the grid to (from) the residential power system of customer n over the period $\big((t-1)\Delta, t\Delta\big)$ is represented by $y_n(t) \in \mathbb{R}_{\geq 0}$ ($y_n(t) \in \mathbb{R}_{<0}$) for all $t \in \mathbb{S}$. Accordingly, the *grid power profile* of customer n over the period $[0, T]$ is defined by $\boldsymbol{y}_n := [y_n(1), \dots, y_n(t), \dots, y_n(\ell)]^\top \in \mathbb{R}^\ell$. Throughout the paper, EV-indices are sub-scripted and time-indices are parenthesized.

Next, the residential power consumption (or excess renewable power generation) of customer n over the period $\big((t-1)\Delta, t\Delta\big)$ is represented by $z_n(t) \in \mathbb{R}_{\geq 0}$ ($z_n(t) \in \mathbb{R}_{<0}$) (in kW) for all $t \in \mathbb{S}$. In more detail, $z_n(t) \geq 0$ when power is delivered to the non-EV load and $z_n(t) < 0$ when the non-EV load generates excess power (e.g., rooftop solar generation is in excess of the non-EV load power consumption). Accordingly, the day-ahead *non-EV load profile* of customer n over the period $[0, T]$ is defined by $\boldsymbol{z}_n := [z_n(1), \dots, z_n(t), \dots, z_n(\ell)]^\top \in \mathbb{R}^\ell$. Likewise, the power flow delivered to (from) EV_n (in kW) over the period $\big((t-1)\Delta, t\Delta\big)$ is represented by $x_n(t) \in \mathbb{R}_{\geq 0}$ ($x_n(t) \in \mathbb{R}_{<0}$) for all $t \in \mathbb{S}$, and the *battery profile* of EV_n over the period $[0, T]$ is defined by $\boldsymbol{x}_n := [x_n(1), \dots, x_n(t), \dots, x_n(\ell)]^\top \in \mathbb{R}^\ell$. By convention, charge rates are positive ($x_n(t) > 0$) and discharge rates are negative ($x_n(t) < 0$).

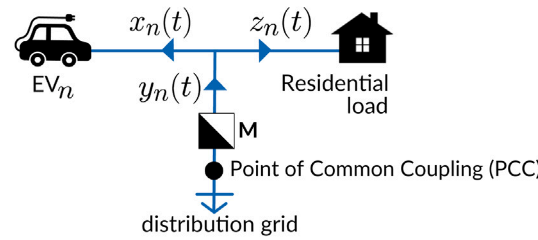

Fig. 1. Residential power system for customer $n \in \mathbb{H}$, illustrating the electrical path from EV_n to the wider distribution grid. The Point of Common Coupling (PCC), which is unique for each customer, represents the point where the customer connects to the distribution grid. Arrows associated with $x_n(t)$, $z_n(t)$ and $y_n(t)$ illustrate the assumed direction of positive power flow, where $t \in \mathbb{S}$. Bidirectional meter $\mathbf{M}$ measures and records power flow $y_n(t)$. For simplicity, reactive power flows (in kVAR) are not shown in the figure.

From the configuration of the residential power system in Fig. 1, the following power balance equation must hold for all $t \in \mathbb{S}$.

$$y_n(t) := z_n(t) + x_n(t) \tag{1}$$

According to Eq. (1), the grid power profile reduces to the non-EV load profile (i.e., $\boldsymbol{y}_n = \boldsymbol{z}_n$) in the absence of an EV in Fig. 1. Each EV_n ($n \in \mathbb{H}$) has a set of arbitrary parameters that include the arrival time index $a_n \in \mathbb{S}$, intended departure time index $d_n \in \mathbb{S}$, battery capacity σ_n (in kWh), initial SoC $\hat{u}_n$ (in kWh), target SoC $\ddot{u}_n$ (in kWh), minimum SoC $\underline{u}_n$ (in kWh), maximum SoC $\overline{u}_n$ (in kWh), maximum charge rate $\overline{x}_n$ (in kW), maximum discharge rate $\underline{x}_n$ (in kW), charge efficiency $\overline{\mu}_n$ ($0 \leq \overline{\mu}_n \leq 1$) and discharge efficiency $\underline{\mu}_n$ ($\underline{\mu}_n \geq 1$). Here, a_n and d_n are within the day-ahead time horizon $[0, T]$, and extensions to adapt the time horizon accommodating later departure times are straightforward.

Let $\Lambda_n := \{a_n \in \mathbb{R}_{\geq 0}, d_n \in \mathbb{R}_{>0}, \sigma_n \in \mathbb{R}_{>0}, \hat{u}_n \in \mathbb{R}_{\geq 0}, \ddot{u}_n \in \mathbb{R}_{\geq 0}, \underline{u}_n \in \mathbb{R}_{\geq 0}, \overline{u}_n \in \mathbb{R}_{>0}, \overline{x}_n \in \mathbb{R}_{\geq 0}, \underline{x}_n \in \mathbb{R}_{\leq 0}, \overline{\mu}_n \in \mathbb{R}_{\geq 0}, \underline{\mu}_n \in \mathbb{R}_{>0}\}$, where Λ_n denotes the *charging specification* for EV_n ($n \in \mathbb{H}$) [31]. For customers in $\mathbb{H}_2$ with charge-only EVs, by definition $\underline{x}_n = 0$. The initial SoC $\hat{u}_n$ is obtained from the EV battery management system. Upon arrival at home, the EV owner must specify an expected departure time index d_n and a target SoC $\ddot{u}_n$ that is feasible to reach before the expected departure time, i.e., the condition $\ddot{u}_n \leq \hat{u}_n + (d_n - a_n)\overline{\mu}_n\, \overline{x}_n \Delta$ must hold for $n \in \mathbb{H}$. For each EV_n ($n \in \mathbb{H}$), the SoC (in kWh) of battery at time $t\Delta$ is denoted by $u_n(t)$, where

$$u_n(t) := \hat{u}_n + \Delta \sum_{j=1}^{t} x_n(j)\mu_n(j) \tag{2}$$

with $\mu_n(j) = \overline{\mu}_n$ if $x_n(j) \geq 0$ and $\mu_n(j) = \underline{\mu}_n$ otherwise. Accordingly, the *SoC profile* of EV_n ($n \in \mathbb{H}$) is defined as $\boldsymbol{u}_n := [u_n(1), \dots, u_n(t), \dots, u_n(\ell)]^\top \in \mathbb{R}^\ell_{\geq 0}$. Eq. (2) employs the battery model in [8], however, more specific battery models as in [32] can be similarly considered.

In minimizing the EV operational cost associated with purchasing and delivering electricity, a ToU pricing scheme is considered, which is fixed by the utility or an energy retailer [33]. The daily variations of electricity price are represented by the *pricing profile* $\boldsymbol{\eta} := [\eta(1), \dots, \eta(t), \dots, \eta(\ell)]^\top \in \mathbb{R}^\ell_{\geq 0}$, where $\eta(t)$ is the price of electricity (in \$/kWh) over the time period $\big((t-1)\Delta, t\Delta\big)$. Along with ToU tariffs, this paper employs a financial policy of *net metering*, the defining characteristic of which is that each customer is billed at the same rate as they are compensated for delivering power to the grid [34]. Accordingly, the energy bill (in \$) for customer $n \in \mathbb{H}$ is defined by $\Delta\boldsymbol{\eta}^\top \boldsymbol{y}_n := \Delta\boldsymbol{\eta}^\top \boldsymbol{z}_n + \Delta\boldsymbol{\eta}^\top \boldsymbol{x}_n$, where $\Delta\boldsymbol{\eta}^\top \boldsymbol{z}_n$ is a nondeferrable cost related to non-EV power consumption (or excess generation) and $\Delta\boldsymbol{\eta}^\top \boldsymbol{x}_n$ is a deferrable cost related to EV charging and discharging.

3. Problem formulation

First, an optimization problem in the form of a QP is formulated to schedule charging and discharging of a single EV that is connected to the electric power grid via the residential power system illustrated in Fig. 1. Next, the N-EVC(D) method is proposed, wherein the former QP is extended to include a voltage constraint, which couples charge-discharge rates of all EVs across a distribution feeder. Lastly, a receding horizon implementation for N-EVC(D) is also proposed.

3.1. EV battery constraints

The problem of scheduling each $\mathrm{EV}_n (n \in \mathbb{H})$ involves a set of constraints as detailed below. To limit the occurrence of over-charging or over-discharging, the safety constraint $\underline{u}_n \le u_n(t) \le \overline{u}_n$ is introduced, such that the SoC profile $\boldsymbol{u}_n$ is constrained by

$$\underline{u}_n \mathbf{1} \le \boldsymbol{u}_n \le \overline{u}_n \mathbf{1}. \tag{3}$$

To simplify the notation, let $\underline{\sigma}_n := (\underline{u}_n - \hat{u}_n)/\Delta$ and $\overline{\sigma}_n := (\overline{u}_n - \hat{u}_n)/\Delta$. Then (2) and (3) can be combined as

$$\underline{\sigma}_n \mathbf{1} \le \mathbf{T}\boldsymbol{x}_n \le \overline{\sigma}_n \mathbf{1}, \tag{4}$$

where $\mathbf{T} = [t_{ij}] \in \mathbb{R}^{\ell \times \ell}$ denotes a matrix satisfying $t_{ij} = \mu_n(j)$ for $i \ge j$ and $t_{ij} = 0$ elsewhere. To accommodate limits on EV battery charge-discharge rates, the constraint $\underline{x}_n \le x_n(t) \le \overline{x}_n$ is introduced for all $t \in \mathbb{S}$, such that the battery profile $\boldsymbol{x}_n$ is constrained by

$$\underline{x}_n \mathbf{1} \le \boldsymbol{x}_n \le \overline{x}_n \mathbf{1}. \tag{5}$$

Considering the initial SoC and the target SoC of the EV battery, the energy requirement for $\mathrm{EV}_n (n \in \mathbb{H})$ can be expressed as $e_n := \ddot{u}_n - \hat{u}_n$ (in kWh). To accommodate the respective charging demand ahead of an expected departure time, the constraint $u_n(\ell) = \ddot{u}_n$ is enforced, which when combined with (2) yields

$$\mathbf{1}^\top \boldsymbol{x}_n = e_n/\Delta. \tag{6}$$

An EV is available for charging (or discharging) only between its arrival and departure times. To constrain the EV charging and discharging time duration, a diagonal matrix $\boldsymbol{\mathcal{L}}_n = [l_{ij}] \in \mathbb{R}^{\ell \times \ell}$ is defined, in which the i^{th} $(1 \le i \le \ell)$ diagonal entry is 1 if the EV is available across time interval $\big((i-1)\Delta, i\Delta\big)$, and 0 if the EV is not available across time interval $\big((i-1)\Delta, i\Delta\big)$. More specifically, if $i = j$ and $a_n < i \le d_n$, then $l_{ij} = 1$, otherwise $l_{ij} = 0$. Clearly, if $i \ne j$ then $l_{ij} = 0$. Consequently, the battery profile $\boldsymbol{x}_n$ is further constrained by

$$(\mathbf{I} - \boldsymbol{\mathcal{L}}_n)\boldsymbol{x}_n = \mathbf{0}. \tag{7}$$

3.2. Minimizing operational costs

The *operational cost* (in \$/day) incurred by EV customer $n \in \mathbb{H}$ is denoted by $\Omega_n(\boldsymbol{x}_n)$, and it is defined as the sum of two cost components: (1) the time-varying cost of purchasing energy for EV charging (and the time-varying profit from delivering energy via EV discharging), and (2) the cost of EV battery degradation. Here, a financial policy of net-metering is assumed in the context of an EV customer purchasing and delivering electricity. The combined operational cost for EV customer $n \in \mathbb{H}$ is then defined by

$$\Omega_n(\boldsymbol{x}_n) := \sum_{t=1}^{\ell} \big(\Delta\eta(t)x_n(t) + \alpha_n x_n(t)^2\big), \tag{8}$$

where α_n is a regularization constant that is introduced to yield a smoother battery profile $\boldsymbol{x}_n$, avoiding unnecessary charging and discharging, or otherwise, reducing the number of charge-discharge cycles. The first term in (8) represents the energy bill attributed to EV charging (and discharging). The second term in (8), previously used in [35], is considered a proxy for the battery degradation cost, which can be alternatively represented by other cost functions as presented in [36].

By combining EV charge and discharge rates with prices for buying and selling electricity, it can be determined if the customer incurs an energy bill, or rather, is compensated. In other words, when $\Omega_n(\boldsymbol{x}_n) > 0$, there exists a *financial cost* from charging and discharging the EV battery, whereas when $\Omega_n(\boldsymbol{x}_n) < 0$, there exists a *financial benefit* from charging and discharging the EV battery. To minimize the operational cost $\Omega_n(\boldsymbol{x}_n)$ for each EV $n \in \mathbb{H}$, the following Lemma is proposed.

Lemma 1 (*QP-1*). *Consider a financial policy of net metering, with* $\boldsymbol{\eta} \in \mathbb{R}^{\ell}_{\ge 0}$ *assumed fixed and known. The minimization of expression (8), subject to EV battery constraints (4)–(7), can be succinctly written as the following QP:*

$$\min_{\boldsymbol{x}_n \in \mathbb{R}^{\ell}} \boldsymbol{c}^\top \boldsymbol{x}_n + \boldsymbol{x}_n^\top \boldsymbol{H}_n \boldsymbol{x}_n \tag{9a}$$

subject to

$$\boldsymbol{A}_n \boldsymbol{x}_n \ge \boldsymbol{b}_n \tag{9b}$$

$$\bar{\boldsymbol{A}}_n \boldsymbol{x}_n = \bar{\boldsymbol{b}}_n, \tag{9c}$$

where

$$\begin{aligned}
\boldsymbol{x}_n &:= \big[\, x_n(1), \dots x_n(t), \dots x_n(\ell) \,\big]^\top && \in \mathbb{R}^{\ell},\\
\boldsymbol{H}_n &:= \alpha_n \mathbf{I} && \in \mathbb{R}^{\ell \times \ell},\\
\boldsymbol{c} &:= \Delta \boldsymbol{\eta} && \in \mathbb{R}^{\ell},\\
\boldsymbol{A}_n &:= \big[\, \mathbf{I} \quad -\mathbf{I} \quad \mathbf{T}^\top \quad -\mathbf{T}^\top \,\big]^\top && \in \mathbb{R}^{4\ell \times \ell},\\
\bar{\boldsymbol{A}}_n &:= \big[\, \mathbf{1} \quad (\mathbf{I} - \boldsymbol{\mathcal{L}}_n) \,\big]^\top && \in \mathbb{R}^{(\ell+1)\times \ell},\\
\boldsymbol{b}_n &:= \big[\, \underline{x}_n \mathbf{1}^\top \quad -\overline{x}_n \mathbf{1}^\top \quad \underline{\sigma}_n \mathbf{1}^\top \quad -\overline{\sigma}_n \mathbf{1}^\top \,\big]^\top && \in \mathbb{R}^{4\ell},\\
\bar{\boldsymbol{b}}_n &:= \big[\, e_n/\Delta \quad \mathbf{0}^\top \,\big]^\top && \in \mathbb{R}^{\ell+1}.
\end{aligned}$$

Proof. The objective function (9a) minimizes the operational cost for EV customer $n \in \mathbb{H}$, which is defined as $\Omega_n(\boldsymbol{x}_n)$ in (8). For EV_n, constraint (9b) combines inequality constraints (4) and (5), and constraint (9c) combines equality constraints (6) and (7). ■

Throughout, the process of a customer $n \in \mathbb{H}_1$ implementing the battery profile returned by QP-1 is referred to as *Price-based EV Charging-Discharging (P-EVCD)*, and the process of a customer $n \in \mathbb{H}_2$ implementing the battery profile returned by QP-1 is referred to as simply *Price-based EV Charging (P-EVC)*. In the assessment of the network and customer benefits, P-EVC(D) serves as a benchmark against the N-EVC(D) method proposed in this paper, which is an extension of QP-1 to alleviate over-voltage and under-voltage conditions arising from P-EVC(D).

3.3. Network-aware EV battery scheduling

A single-phase, radial distribution network is considered that is represented by a graph $\mathcal{G} = \{\mathcal{V}, \mathcal{E}\}$, where $\mathcal{V} = \{0, \dots, g, \dots, k\}$ is the set of vertices representing the nodes along the distribution feeder, and $\mathcal{E} \subseteq \mathcal{V} \times \mathcal{V}$ is the set of edges representing the distribution lines spanning the nodes of the distribution feeder. The edge between two adjacent nodes $i \in \mathcal{V}$ and $j \in \mathcal{V}$ is denoted by $(ij) \in \mathcal{E}$, with node i lying between node 0 and node j. Graph $\mathcal{G}$ is assumed to be simple with no repeated edges or self loops for any vertex $g \in \mathcal{V}$, i.e., $(gg) \notin \mathcal{E}$. Furthermore, graph $\mathcal{G}$ is assumed to be a rooted tree, where root vertex is the feeder head represented by node 0. That means, for every vertex $g \in \mathbb{V}$, where $\mathbb{V} = \mathcal{V} \setminus \{0\} = \{1, \dots, g, \dots, k\}$, there is a unique path from root node 0 to node g, and the set of edges on the unique path from node 0 to node $g \in \mathbb{V}$ is denoted by $\mathcal{E}^g \subseteq \mathcal{E}$. Throughout, node-indices are super-scripted.

Each node $g \in \mathbb{V}$ connects N^g number of residential power systems (shown in Fig. 1), such that $N^g \ge 0$ and $\sum_{g=1}^{k} N^g = h$. For example, in the distribution network depicted in Fig. 2, $k = 12$, and all nodes in

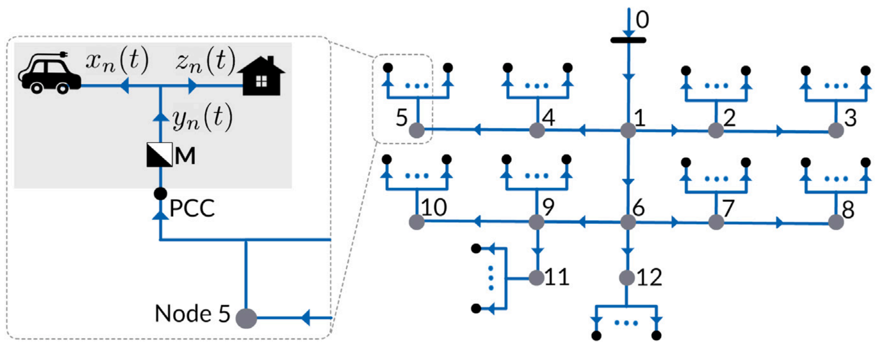

Fig. 2. A radial distribution feeder connecting N^g residential power systems at each node $g \in \mathbb{V}$. Arrows associated with edges in $\mathcal{E}$ illustrate the assumed direction of positive power flow. Left: node 5 is zoomed in for a more detailed representation.

$\mathbb{V}$ except nodes 1 and 6 have one or more residential power systems connected. In Fig. 2, the customer index is initialized as $n = 1$ at node 2, and then n is incremented through all customers connected to node 2, and then through all customers across subsequent nodes $g \in \mathbb{V}$, in ascending order, respectively.

Let $\boldsymbol{\Upsilon} \in \mathbb{R}_{\geq 0}^{k\times h}$ be a matrix specifying the connectivity of customers $n \in \mathbb{H}$ across different nodes $g \in \mathbb{V}$ (i.e, nodal location) along the distribution feeder. For each node $g \in \mathbb{V}$, let $\boldsymbol{\Upsilon}^g = \mathbf{1}^\top \in \mathbb{R}_{\geq 0}^{1\times N^g}$, such that

$$\boldsymbol{\Upsilon} := \oplus_{g=1}^{k} \boldsymbol{\Upsilon}^g \in \mathbb{R}_{\geq 0}^{k\times h}. \tag{10}$$

In what follows, the voltage magnitude at each node $g \in \mathbb{V}$ is approximated using the *LinDistFlow* (linearized Distflow [37]) equations that are proposed in [30]. The LinDistFlow equations are widely exploited and justified in the power systems literature on optimal power flow control of distributed energy resources in radial distribution networks [38].

Let $|v^0|$ denote the voltage magnitude at root node 0, which is set to the nominal voltage, i.e., $|v^0| = 1$ per unit (p.u.). Let $|v^g(t)|$ denote the voltage magnitude at node g at time $t\Delta$. Let $p^g(t) \in \mathbb{R}_{\geq 0}$ ($p^g(t) \in \mathbb{R}_{<0}$) denote the real power (in kW) consumed (injected) at node g over the period $\big((t-1)\Delta, t\Delta\big)$, and $q^g(t) \in \mathbb{R}_{\geq 0}$ ($q^g(t) \in \mathbb{R}_{<0}$) denote the reactive power (in kVAR) consumed (injected) at node g over the period $\big((t-1)\Delta, t\Delta\big)$. Let r^{ij} and x^{ij} ($i, j \in \mathcal{V}$) denote the resistance and reactance of edge $(ij) \in \mathcal{E}$, respectively. Furthermore, let $\boldsymbol{R} \in \mathbb{R}_{\geq 0}^{k\times k}$ and $\boldsymbol{X} \in \mathbb{R}_{\geq 0}^{k\times k}$ denote two positive definite matrices [39] in which the elements corresponding to g^{th} row and $\hat{g}^{\text{th}}$ column are $R^{g\hat{g}}$ and $X^{g\hat{g}}$, respectively. Next, the following are defined:

$$\boldsymbol{V}^0 := \left[\, |v^0|^2, \dots, |v^0|^2, \dots, |v^0|^2 \,\right]^\top \in \mathbb{R}^k, \tag{11a}$$

$$\boldsymbol{V}(t) := \left[\, |v^1(t)|^2, \dots, |v^g(t)|^2, \dots, |v^k(t)|^2 \,\right]^\top \in \mathbb{R}^k, \tag{11b}$$

$$\boldsymbol{P}(t) := \left[\, p^1(t), \dots, p^g(t), \dots, p^k(t) \,\right]^\top \in \mathbb{R}^k, \tag{11c}$$

$$\boldsymbol{Q}(t) := \left[\, q^1(t), \dots, q^g(t)\ , \dots, q^k(t) \,\right]^\top \in \mathbb{R}^k, \tag{11d}$$

$$R^{g\hat{g}} := \textstyle\sum_{(ij)\in(\mathcal{E}^g \cap \mathcal{E}^{\hat{g}})} r^{ij} \in \mathbb{R}, \tag{11e}$$

$$X^{g\hat{g}} := \textstyle\sum_{(ij)\in(\mathcal{E}^g \cap \mathcal{E}^{\hat{g}})} x^{ij} \in \mathbb{R}. \tag{11f}$$

Then the LinDistFlow equation can be written as

$$\boldsymbol{V}(t) := \boldsymbol{V}^0 - 2\boldsymbol{R}\boldsymbol{P}(t) - 2\boldsymbol{X}\boldsymbol{Q}(t). \tag{12}$$

Next, the power flows at a single node $g \in \mathbb{V}$ are described in more detail. Recall, node g is connected to N^g number of customers and therefore the net real and reactive power consumption (or injection) at node g is determined by the total power consumption (and injection) of all EV and non-EV loads associated with those set of customers. The net real power (in kW) consumed (or injected) by all non-EV loads connected to node $g \in \mathbb{V}$ over the period $\big((t-1)\Delta, t\Delta\big)$ is denoted by $\widetilde{p}^g(t) \in \mathbb{R}_{\geq 0}$ ($\widetilde{p}^g(t) \in \mathbb{R}_{<0}$), for all $t \in \mathbb{S}$, and the net reactive power (in kVAR) consumed (or injected) by all non-EV loads connected to node $g \in \mathbb{V}$ over the period $\big((t-1)\Delta, t\Delta\big)$ is denoted by $\widetilde{q}^g(t) \in \mathbb{R}_{\geq 0}$ ($\widetilde{q}^g(t) \in \mathbb{R}_{<0}$), for all $t \in \mathbb{S}$. Similarly, the real power (in kW) consumed (or injected) by all EVs connected to node $g \in \mathbb{V}$ over the period $\big((t-1)\Delta, t\Delta\big)$ is denoted by $\widehat{p}^g(t) \in \mathbb{R}_{\geq 0}$ ($\widehat{p}^g(t) \in \mathbb{R}_{<0}$), for all $t \in \mathbb{S}$, and the reactive power (in kVAR) consumed (or injected) by all EVs connected to node g over the period $\big((t-1)\Delta, t\Delta\big)$ is denoted by $\widehat{q}^g(t) \in \mathbb{R}_{\geq 0}$ ($\widehat{q}^g(t) \in \mathbb{R}_{<0}$), for all $t \in \mathbb{S}$. By ignoring losses over the period $\big((t-1)\Delta, t\Delta\big)$, $p^g(t)$ and $q^g(t)$ can be expressed as

$$p^g(t) := \widetilde{p}^g(t) + \widehat{p}^g(t), \quad q^g(t) := \widetilde{q}^g(t) + \widehat{q}^g(t) \tag{13}$$

for all $t \in \mathbb{S}$ and $g \in \mathbb{V}$. Next, the following vectors are defined:

$$\widetilde{\boldsymbol{P}}(t) := \left[\, \widetilde{p}^1(t), \dots, \widetilde{p}^g(t), \dots, \widetilde{p}^k(t) \,\right]^\top \in \mathbb{R}^k, \tag{14}$$

$$\widetilde{\boldsymbol{Q}}(t) := \left[\, \widetilde{q}^1(t), \dots, \widetilde{q}^g(t), \dots, \widetilde{q}^k(t) \,\right]^\top \in \mathbb{R}^k, \tag{15}$$

$$\widehat{\boldsymbol{P}}(t) := \left[\, \widehat{p}^1(t), \dots, \widehat{p}^g(t), \dots, \widehat{p}^k(t) \,\right]^\top \in \mathbb{R}^k, \tag{16}$$

$$\widehat{\boldsymbol{Q}}(t) := \left[\, \widehat{q}^1(t), \dots, \widehat{q}^g(t), \dots, \widehat{q}^k(t) \,\right]^\top \in \mathbb{R}^k, \tag{17}$$

such that $\boldsymbol{P}(t) = \widetilde{\boldsymbol{P}}(t) + \widehat{\boldsymbol{P}}(t)$ and $\boldsymbol{Q}(t) = \widetilde{\boldsymbol{Q}}(t) + \widehat{\boldsymbol{Q}}(t)$ for all $t \in \mathbb{S}$. Let $\widetilde{\boldsymbol{V}}(t) := 2\boldsymbol{R}\widetilde{\boldsymbol{P}}(t) + 2\boldsymbol{X}\widetilde{\boldsymbol{Q}}(t) \in \mathbb{R}^k$, where $\widetilde{\boldsymbol{V}}(t)$ represents the voltage drop caused by non-EV loads connected to the distribution feeder at time $t\Delta$. By way of the linearity of Eq. (12), it can be obtained that

$$\boldsymbol{V}(t) := \boldsymbol{V}^0 - \widetilde{\boldsymbol{V}}(t) - \big(2\boldsymbol{R}\widehat{\boldsymbol{P}}(t) + 2\boldsymbol{X}\widehat{\boldsymbol{Q}}(t)\big). \tag{18}$$

Let $\mathcal{V}(t) := \boldsymbol{V}^0 - \widetilde{\boldsymbol{V}}(t) \in \mathbb{R}^k$ denote the *baseline voltages* at time $t\Delta$, where g^{th} element in vector $\mathcal{V}(t)$ represents the squared voltage magnitude of node $g \in \mathbb{V}$ when there are no EVs grid-connected to the distribution feeder at time $t\Delta$. As proposed in [8], it is considered that EVs charge (and discharge) real power (in kW) only. That is, $\widehat{q}^g(t) = 0$ for all $t \in \mathbb{S}$ and for all $g \in \mathbb{V}$, implying $\widehat{\boldsymbol{Q}}(t) = \mathbf{0}$. Substituting $\mathcal{V}(t)$ and $\widehat{\boldsymbol{Q}}(t)$ in Eq. (18) yields

$$\boldsymbol{V}(t) := \mathcal{V}(t) - 2\boldsymbol{R}\widehat{\boldsymbol{P}}(t). \tag{19}$$

Let $\boldsymbol{\mathcal{X}}(t) := \left[\, x_1(t), \dots, x_n(t), \dots, x_h(t) \,\right]^\top \in \mathbb{R}^h$, where the n^{th} element in $\boldsymbol{\mathcal{X}}(t)$ represents the charge (or discharge) rate of $\text{EV}_n (n \in \mathbb{H})$ at time $t\Delta$. Then, using the definitions in Eqs. (10) and (16), it can be derived that

$$\widehat{\boldsymbol{P}}(t) := \boldsymbol{\Upsilon}\boldsymbol{\mathcal{X}}(t), \tag{20}$$

for all $t \in \mathbb{S}$. Let $\boldsymbol{D} := -2\boldsymbol{R}\boldsymbol{\Upsilon}$ with $\boldsymbol{D} := \left[\, \boldsymbol{D}_1, \dots, \boldsymbol{D}_n, \dots, \boldsymbol{D}_h \,\right] \in \mathbb{R}^{k\times h}$ ($\boldsymbol{D}_n \in \mathbb{R}^k, n \in \mathbb{H}$), so that Eqs. (19) and (20) can be combined as

$$\boldsymbol{V}(t) := \mathcal{V}(t) + \boldsymbol{D}\boldsymbol{\mathcal{X}}(t). \tag{21}$$

To expand Eq. (21) in the temporal direction considering the planning time-horizon $[0, T]$, the vectors $\boldsymbol{V}$ and $\mathcal{V}$ are defined as $\boldsymbol{V} := \left[\, \boldsymbol{V}(1)^\top, \dots, \boldsymbol{V}(t)^\top, \dots, \boldsymbol{V}(\ell)^\top \,\right]^\top \in \mathbb{R}^{k\ell}$ and $\mathcal{V} := \left[\, \mathcal{V}(1)^\top, \dots, \mathcal{V}(t)^\top, \dots, \mathcal{V}(\ell)^\top \,\right]^\top \in \mathbb{R}^{k\ell}$. Then, the squared voltage magnitudes of all nodes $g \in \mathbb{V}$ across all time-intervals $t \in \mathbb{S}$, is succinctly defined by

$$\boldsymbol{V} := \mathcal{V} + \sum_{n=1}^{h} \overline{\boldsymbol{D}}_n \boldsymbol{x}_n \tag{22}$$

where $\overline{\mathcal{D}}_n := \mathcal{D}_n \oplus \cdots \oplus \mathcal{D}_n \oplus \mathcal{D}_n \in \mathbb{R}^{k\ell \times \ell}$ (ℓ times execution of $\oplus$ operation) for all $n \in \mathbb{H}$. Lastly, a network constraint is introduced to maintain all nodal voltages within the operational range $[\underline{\upsilon}, \overline{\upsilon}]$, where $\underline{\upsilon} \in \mathbb{R}$ and $\overline{\upsilon} \in \mathbb{R}$ are the lower and upper bounds on voltage magnitude, respectively. Using Eq. (22), the corresponding *voltage constraint* can be written as

$$\underline{\upsilon}^2 \mathbf{1} \leq \mathcal{V} + \sum_{n=1}^{h} \overline{\mathcal{D}}_n \boldsymbol{x}_n \leq \overline{\upsilon}^2 \mathbf{1}, \tag{23}$$

where $\mathbf{1} \in \mathbb{R}^{k\ell}$. Importantly, the voltage constraint (23) is coupled by the battery profiles $\boldsymbol{x}_n$ of all EVs that are connected from various locations of the distribution feeder.

With the above as background, this paper seeks to minimize the operational costs that are incurred by all EV customers $n \in \mathbb{H}$ over the planning time-horizon $[0, T]$, where the operational cost corresponding to customer $n \in \mathbb{H}$, denoted by $\Omega_n(\boldsymbol{x}_n)$, is defined in (8). Hence, the optimization problem is to minimize

$$\sum_{n \in \mathbb{H}} \Omega_n(\boldsymbol{x}_n) := \sum_{n=1}^{h} \Big(\sum_{t=1}^{\ell} \big(\Delta \eta(t) x_n(t) + \alpha_n x_n(t)^2 \big) \Big), \tag{24}$$

subject to voltage constraint (23) and individual EV constraints in QP-1. The following lemma expresses the respective constrained minimization problem as a centralized QP.

Lemma 2 (*QP-2*). *The minimization of operational costs of all EV customers in expression (24), subject to the voltage constraint (23) and each EV-specific battery constraints (9b)–(9c), can be succinctly written as the following centralized QP:*

$$\min_{\mathbf{X} \in \mathbb{R}^{\ell h}} \mathbf{X}^\top \mathbf{H} \mathbf{X} + \mathbf{C}^\top \mathbf{X} \tag{25a}$$

subject to

$$\mathcal{A}_1 \mathbf{X} \geq \mathcal{B}_1 \tag{25b}$$

$$\mathcal{A}_2 \mathbf{X} = \mathcal{B}_2 \tag{25c}$$

where

$$\begin{aligned}
\mathbf{X} &:= \left[\, \boldsymbol{x}_1^\top, \ldots, \boldsymbol{x}_n^\top, \ldots, \boldsymbol{x}_h^\top \,\right]^\top && \in \mathbb{R}^{\ell h}, \\
\mathbf{H} &:= \oplus_{n=1}^{h} \boldsymbol{H}_n && \in \mathbb{R}^{\ell h \times \ell h}, \\
\mathbf{C} &:= \left[\, \boldsymbol{c}^\top, \ldots, \boldsymbol{c}^\top, \ldots, \boldsymbol{c}^\top \,\right]^\top && \in \mathbb{R}^{\ell h}, \\
\mathcal{A}_1 &:= \left[\, \mathbb{A}^\top \quad \mathbb{D}^\top \quad -\mathbb{D}^\top \,\right]^\top && \in \mathbb{R}^{(4\ell h + 2k\ell) \times \ell h}, \\
\mathbb{A} &:= \oplus_{n=1}^{h} \boldsymbol{A}_n && \in \mathbb{R}^{4\ell h \times \ell h}, \\
\mathbb{D} &:= \left[\, \overline{\mathcal{D}}_1, \ldots, \overline{\mathcal{D}}_n, \ldots, \overline{\mathcal{D}}_h \,\right] && \in \mathbb{R}^{k\ell \times \ell h}, \\
\mathcal{B}_1 &:= \left[\, \mathbf{u}^\top \quad \underline{\boldsymbol{w}}^\top \quad \overline{\boldsymbol{w}}^\top \,\right] && \in \mathbb{R}^{(4\ell h + 2k\ell)}, \\
\mathbf{u} &:= \left[\, \boldsymbol{b}_1^\top, \ldots, \boldsymbol{b}_n^\top, \ldots, \boldsymbol{b}_h^\top \,\right]^\top && \in \mathbb{R}^{4\ell h}, \\
\underline{\boldsymbol{w}} &:= \underline{\upsilon}^2 \mathbf{1} - \mathcal{V} && \in \mathbb{R}^{k\ell}, \\
\overline{\boldsymbol{w}} &:= -\overline{\upsilon}^2 \mathbf{1} + \mathcal{V} && \in \mathbb{R}^{k\ell}, \\
\mathcal{A}_2 &:= \oplus_{n=1}^{h} \bar{\boldsymbol{A}}_n && \in \mathbb{R}^{4\ell h \times \ell h}, \\
\mathcal{B}_2 &:= \left[\, \bar{\boldsymbol{b}}_1^\top, \ldots, \bar{\boldsymbol{b}}_n^\top, \ldots, \bar{\boldsymbol{b}}_h^\top \,\right]^\top && \in \mathbb{R}^{4\ell h}
\end{aligned}$$

and $\boldsymbol{x}_n$, $\boldsymbol{H}_n$, $\boldsymbol{A}_n$, $\bar{\boldsymbol{A}}_n$, $\boldsymbol{b}_n$, $\bar{\boldsymbol{b}}_n$ for all $n \in \mathbb{H}$ and $\boldsymbol{c}$ are defined in QP-1.

Proof. The result directly follows from Eqs. (23), (24) and Lemma 1. The objective function (25a) minimizes the total operational cost of EV customers defined in (24). Constraint (25b) combines voltage constraint (23) and the aggregated constraint (9b) for all EVs in $\mathbb{H}$. Constraint (25c) aggregates constraint (9c) for all EVs in $\mathbb{H}$. ∎

In the proposed implementation, a CO solves QP-2 and notifies the resultant EV battery profile $\boldsymbol{x}_n$ to each EV customer $n \in \mathbb{H}$. Throughout, the process of an EV customer $n \in \mathbb{H}_1$ implementing the CO-specified battery profile obtained from QP-2 is referred to as *Network-aware EV Charging-Discharging (N-EVCD)*, and the process of an EV customer $n \in \mathbb{H}_2$ implementing the CO-specified battery profile obtained from QP-2 is referred to as simply *Network-aware EV Charging (N-EVC)*.

For ease of reference, key notation introduced in the preceding text are summarized in Appendix.

Remark 1. While the non-linear power flow equations (e.g., DistFlow equations [37]) are more accurate, their inclusion in EV-based optimization problems with a fine time resolution and a large number of EVs makes the optimization problem presently intractable for near-real-time control applications. Thus, the LinDistFlow equations in [30] were proposed to support the formulation of mathematical optimization problems that can be solved in polynomial time to facilitate faster computations. Specifically, the LinDistFlow equations are derived from the DistFlow equations by assuming that the line losses are negligible compared to line flows. According to [30] and [39], such an approximation tends to introduce a small relative error, typically on the order of 1% [40]. A straightforward adjustment of the voltage constraint to accommodate for linearization errors caused by discarding line losses in the LinDistFlow equations is to maintain a safety buffer of 1% about the permissible voltage limits — i.e., setting the lower voltage bound to a slightly higher limit (e.g., $\underline{\upsilon} \approx 0.96$ p.u.) and the upper voltage bound to a slightly lower limit (e.g., $\overline{\upsilon} \approx 1.04$ p.u.) — with respect to a voltage delivery standard of $\pm 5\%$ about the nominal voltage.

3.4. Receding horizon optimization (RHO)-based network-aware EV battery scheduling

To accommodate EV charge requirements that are unknown to the CO ahead of EV grid-connection, and to support updates in prespecified EV departure times, a RHO-based implementation for N-EVC(D) is proposed as outlined in Algorithm 1.

Algorithm 1: Receding Horizon Optimization (RHO)-based N-EVC(D)

1 **Initialize** time-step $j = 0$ and $\ell = T/\Delta$.
2 **Repeat** at each time-step j,
3 Each newly joined $\mathrm{EV}_n (n \in \mathbb{H})$ that arrived over the time interval $(\max\{(j-1), 0\}\Delta,\ j\Delta)$ sends their charging specification $\Lambda_n := \{a_n, d_n, \sigma_n, \hat{u}_n, \ddot{u}_n, \underline{u}_n, \overline{u}_n, \overline{x}_n, \underline{x}_n, \overline{\mu}_n, \underline{\mu}_n\}$ to the CO.
4 Each grid-connected $\mathrm{EV}_n (n \in \mathbb{H})$ that intends to depart earlier or later than the scheduled time $[d_n \Delta | j]$ resends Λ_n to the CO, incorporating the updated index d_n. In case where an EV leaves unexpectedly, the target SoC will potentially not be adhered.
5 The CO solves QP-2 over the time window $[j\Delta, (j+\ell)\Delta]$ and yields a sequence of control actions $\boldsymbol{x}_n := \{x_n[1|j], \ldots, x_n[t|j], \ldots, x_n[\ell|j]\}$ for each grid-connected $\mathrm{EV}_n (n \in \mathbb{H})$.
6 The CO notifies to each grid-connected $\mathrm{EV}_n (n \in \mathbb{H})$ the charge or discharge rate to be applied, which is obtained for the first time-index of the control sequence $x_n(j) := x_n[1|j]$.
7 Each grid-connected $\mathrm{EV}_n (n \in \mathbb{H})$ charges or discharges at a rate of $x_n(j)$ over the time interval $\big(j\Delta, (j+1)\Delta\big)$.
8 The CO estimates the battery SoC for each $\mathrm{EV}_n (n \in \mathbb{H})$ as per the specific EV battery model.
9 The CO updates $\hat{u}_n := u_n[1|j]$ and $d_n = d_n - 1$ for each $\mathrm{EV}_n (n \in \mathbb{H})$, in preparation for the next time-step.
10 Shift the time horizon by updating $j = j + 1$ and repeat Steps 3 - 10.

Receding horizon optimization is a real-time optimization technique that involves repeatedly solving an optimization problem over a moving time horizon. At each current time $j\Delta$, a future time window with size, say, $[j\Delta, (j+\ell)\Delta]$, is considered, and an optimal control sequence

$\boldsymbol{x}_n := \{x_n[1|j], \ldots, x_n[t|j], \ldots, x_n[\ell|j]\}$ is determined relative to the current time-step j. Here, the notation $[t|j]$ denotes prediction time-step t relative to current time-step j, as in [41]. In order to handle unexpected changes in the system after time $(j+1)\Delta$, only $x_n[1|j]$ for each EV$_n (n \in \mathbb{H})$ is applied, and the time-window is moved forward to time $(j+1)\Delta$.

In contrast to the EV scheduling methods proposed in [7–10,14, 19,22], Algorithm 1 enables EVs to connect and disconnect from the grid without prior notice, leading to a more practical implementation. Algorithm 1 also supports updates in SoC estimates at each time-step in order to improve the performance of the algorithm in reaching a customer-specified target SoC ahead of the departure time. Extensions of Algorithm 1 to incorporate updates in target SoC and updates in real-time non-EV demand are straight forward.

4. Numerical simulations

In this section, the performance of the proposed EV charge–discharge scheduling method is evaluated on a modified IEEE 13 node test feeder, consistent with the approach taken in [8]. Specifically, a single-phase representation of the IEEE 13 node test feeder is adopted, in which the transformer between nodes 2 and 3, the switch between nodes 6 and 7 and all capacitor banks are discarded, as illustrated in Fig. 2.

The following numerical simulations consider EV charging and discharging of $h = 600$ customers distributed across a medium voltage distribution feeder. In particular, with reference to Fig. 2, each node, except nodes 0, 1 and 6, serves 60 customers such that $N^g = 60$ for $g \in \{2, \ldots, 5, 7, \ldots, 12\}$ and $N^g = 0$ for $g \in \{0, 1, 6\}$. At each node serving 60 EV customers, half of the customers are equipped with gridable EVs and the remainder are equipped with charge-only EVs. The customers are assigned different EV models as reported in [42], with battery capacities (c_n) lying in the range $[16, 90]$ kWh. Further, each customer is assumed to have a level-2 charger supporting a typical maximum charge rate of $\overline{x}_n = 6.6$ kW, as in [8]. For customers in $\mathbb{H}_1$, a maximum discharge rate of $\underline{x}_n = -6.6$ kW is additionally considered. The EV arrival and departure times (a_n and d_n) are reflective of survey data gathered by the Victorian Department of Transport in Australia [43], which contains individual vehicle travel records for a 24 h period. As in [8], the initial SOC of each EV ($\hat{u}_n$) is within [0.3, 0.6] times the battery capacity — such that there is a uniform distribution across all EV initial SOC settings. Following [24], the minimum SoC ($\underline{u}_n$) and maximum SoC ($\overline{u}_n$) for each EV are considered as fractions of 0.2 and 0.85 of the battery capacity, respectively. The charge efficiency ($\overline{\mu}_n$) and discharge efficiency ($\underline{\mu}_n$) for each EV are set to 0.9 and 1.1, respectively. Further, α_n is fixed as $\alpha_n = 5 \times 10^{-4}$ \$/kW^2 for each EV.

The non-EV power consumption ($\boldsymbol{z}_n$) for each of the $h = 600$ customers is obtained from a real dataset [44] publicly released by Ausgrid, an electricity distribution company in New South Wales, Australia [45]. The extracted data corresponds to the residential power consumption of a set of 300 residential customers on 5th July 2012, a day on which several peak demand conditions were observed. The dataset is then duplicated to populate non-EV power consumption for $h = 600$ customers across the day.

To maintain a high level of power quality throughout the medium voltage feeder, the ANSI C84.1 standard is followed with a maximum voltage threshold of 5% above the nominal voltage, and a minimum voltage threshold of 5% below the nominal voltage, i.e., $\underline{v} = 0.95$ p.u. and $\overline{v} = 1.05$ p.u.

As illustrated in Fig. 3, a ToU financial policy is considered as employed by the AGL Energy, an energy provider in Australia [46]. All simulations are conducted in Python 3.8.2 + CVXPY [47] on a MacBook Pro with Intel Core i5 and 8 GB memory.

In the numerical simulations that follow, two *simulation settings* are considered: *Setting 1* has a heterogeneous load arrangement wherein customers $n \in \mathbb{H}$ are assigned with heterogeneous non-EV load profiles and heterogeneous EV arrival-departure times — all consistent with the descriptions above. By contrast, *Setting 2* consists of a homogeneous load arrangement wherein all customers $n \in \mathbb{H}$ have the same non-EV demand profile $\boldsymbol{z}_n$ and the same EV charging specification given by $\Lambda_n := \{a_n : 10, d_n : 41, c_n : 75, \hat{u}_n : 40, \ddot{u}_n : 64, \underline{u}_n : 15, \overline{u}_n : 64, \overline{x}_n : 6.6, \underline{x}_n : -6.6, \overline{\mu}_n : 0.9, \underline{\mu}_n : 1.1\}$.

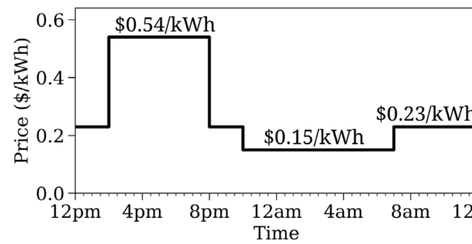

Fig. 3. Pricing profile $\boldsymbol{\eta}$ where the *off-peak* period is from 10 pm – 7 am, the *shoulder-peak period* is from 7 am – 2 pm and 8 pm – 10 pm, and the *peak* period is from 2 pm – 8 pm.

Table 1
Simulation scenarios.

	Scenario 1	Scenario 2	Scenario 3
Simulation setting	Setting 1	Setting 1	Setting 2
Implementation by EVs in $\mathbb{H}_1$ (gridable EVs)	P-EVCD	N-EVCD	N-EVCD
Implementation by EVs in $\mathbb{H}_2$ (charge-only EVs)	P-EVC	N-EVC	N-EVC

4.1. Assessing the benefit of N-EVC(D)

In this section, simulation settings 1 and 2 are incorporated into three *Simulation Scenarios*, as outlined in Table 1. Fig. 4 presents the power flow profiles and nodal voltage profiles corresponding to each of the three scenarios in Table 1.

For each scenario in Table 1, Fig. 4(a,c,e) presents the sum of non-EV load profiles $\boldsymbol{z}_n$ of all customers $n \in \mathbb{H}$ defined by $\sum_n \boldsymbol{z}_n$, the sum of EV battery profiles $\boldsymbol{x}_n$ of all customers $n \in \mathbb{H}$ defined by $\sum_n \boldsymbol{x}_n$, and the sum of grid power profiles $\boldsymbol{y}_n$ of all customers $n \in \mathbb{H}$ defined by $\sum_n \boldsymbol{y}_n$. Throughout, $\sum_n \boldsymbol{z}_n$ is referred to as the *aggregate non-EV load profile*, $\sum_n \boldsymbol{x}_n$ is referred to as the *aggregate battery profile*, and $\sum_n \boldsymbol{y}_n$ is referred to as the *aggregate grid power profile*. As illustrated in Fig. 4(a,c,e), the aggregate non-EV load profile ($\sum_n \boldsymbol{z}_n$) rises to its peak during the peak-pricing period and then gradually declines through the shoulder-pricing period to the off-peak-pricing period, consistent with the pricing profile $\boldsymbol{\eta}$ in Fig. 3.

For each scenario in Table 1, Fig. 4(b,d,f) presents the *baseline voltage profiles* denoted by $\mathcal{V}^{\frac{1}{2}} \in \mathbb{R}^{k\ell}$ and the *resultant nodal voltage profiles* denoted by $\boldsymbol{V}^{\frac{1}{2}} \in \mathbb{R}^{k\ell}$, where $\mathcal{V}$ and $\boldsymbol{V}$ were previously defined in Eq. (22). Recall, the baseline voltage profiles $\mathcal{V}^{\frac{1}{2}}$ are attributed to the non-EV load, whereas the resultant nodal voltage profiles $\boldsymbol{V}^{\frac{1}{2}}$ are attributed to the total load (EV and non-EV load). In a special case where none of the EVs are connected to the distribution network, the resultant nodal voltage profiles reduce to the baseline voltage profiles, i.e., $\boldsymbol{V}^{\frac{1}{2}} = \mathcal{V}^{\frac{1}{2}}$. Each of the nodal voltage profiles in Fig. 4(b,d,f) are grouped into four clusters, that by inspection, exhibited similar voltage variations. Cluster 1 consists of nodes 2, 3, 4, 5, Cluster 2 consists of nodes 7, 8, 12, Cluster 3 consists of nodes 9, 10, and Cluster 4 consists of node 11. Geographically, Cluster 1 contains nodes that are located closer to the feeder head, followed by nodes in clusters 2, 3 and 4, respectively. The envelopes enclosing the respective nodal voltage profiles corresponding to each cluster are presented in Fig. 4(b,d,f), with dashed lines representing the baseline voltage profiles $\mathcal{V}^{\frac{1}{2}}$ and solid lines representing the resultant voltage profiles $\boldsymbol{V}^{\frac{1}{2}}$.

Fig. 4(a–b) considers Scenario 1, where the process of EV charging and discharging is coordinated via P-EVC(D). Recall, P-EVC(D)

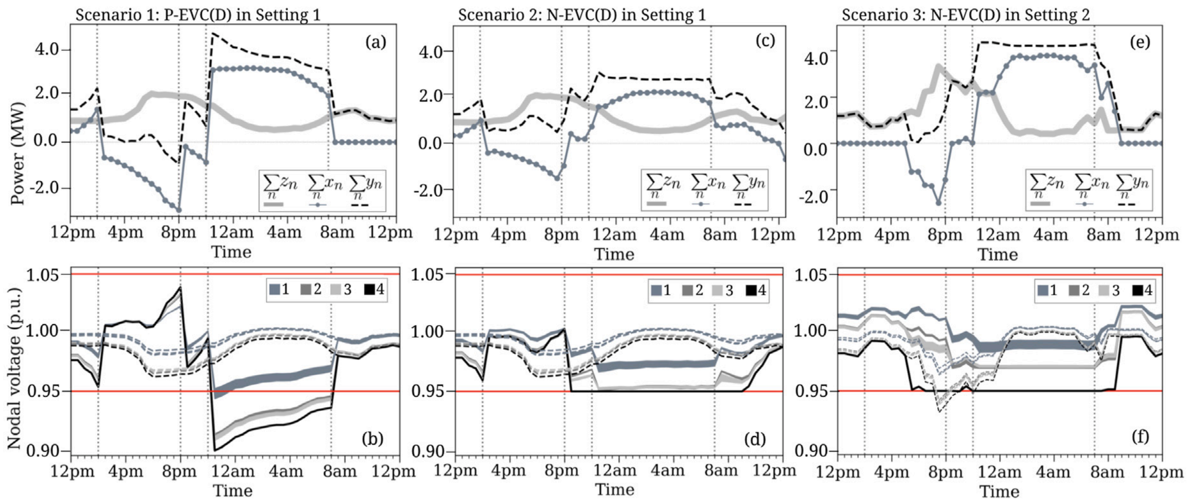

Fig. 4. (a,c,e): The aggregate non-EV load profile ($\sum_n z_n$), the aggregate battery profile ($\sum_n x_n$), the aggregate grid power profile ($\sum_n y_n$), and **(b,d,f)**: the nodal voltage profiles, corresponding to each scenario in Table 1. In Figs (b,d,f), the dashed curves represent the envelopes of baseline voltage profiles (considering only the non-EV load), $\mathcal{V}^{\frac{1}{2}}$, and the solid curves represent the envelopes of resultant nodal voltage profiles (considering both EV and non-EV load), $\boldsymbol{V}^{\frac{1}{2}}$. The envelopes in different colors correspond to different node clusters shown in the figure legend: Cluster 1 (nodes 2,3,4,5), Cluster 2 (nodes 7, 8, 12), Cluster 3 (nodes 9, 10) and Cluster 4 (node 11). The red lines mark the upper and lower voltage boundaries.

implements the solution to QP-1 that is defined in Lemma 1. It can be clearly observed that the aggregate grid power profile in Fig. 4(a) has two prominent peaks — at 2 pm and 10.30 pm — which are 2.54 times and 2.98 times greater than the corresponding aggregate non-EV load ($\sum_n z_n$) at those times, respectively. In Fig. 4(a), the aggregate grid power profile ($\sum_n y_n$) is negative at certain time points in the peak period and positive at all other times. At times when it is negative (i.e., when $\sum_n y_n(t) < 0$), the gridable EVs discharge to support the non-EV demand and deliver surplus energy back to the grid. To get prepared for discharge operations taking place in the peak pricing period, the gridable EVs (particularly with lower SoCs) fill their batteries as much as possible ahead of the peak-pricing period, which results in a short charging period from 12 – 2 pm in the shoulder-peak period. The aggregate battery profile ($\sum_n x_n$) continues to rise from 12 – 2 pm (leading to the load peak at 2 pm) as more and more gridable EVs become available for charging. During the peak pricing period, the gridable EVs contribute to peak-curtailment via V2G and thereby improve their operational savings. The highest load peak in the off-peak pricing period (at 10.30 pm) is formed when all gridable and charge-only EVs commence charging to satisfy their charge requirements. In Fig. 4(b), the envelopes of baseline voltage profiles, $\mathcal{V}^{\frac{1}{2}}$, for each of the four clusters, are within ±5% of the nominal voltage. However, the envelopes of resultant voltage profiles arising from P-EVC(D), $\boldsymbol{V}^{\frac{1}{2}}$, are below 5% of the nominal voltage in all clusters.

Fig. 4(c–d) considers Scenario 2, where the process of EV charging and discharging is coordinated via N-EVC(D), which is implemented along with RHO as outlined in Algorithm 1. Recall, N-EVC(D) implements the solution to QP-2 in Lemma 2. Since both scenarios 1 and 2 are based on simulation Setting 1, the aggregate non-EV load profiles ($\sum_n z_n$) in Fig. 4(a) and Fig. 4(c) are identical. However, the aggregate grid power profile ($\sum_n y_n$) in Fig. 4(c) is flatter (less prominent peaks and valleys) when compared to Fig. 4(a). More specifically, the aggregate grid power profile obtained from N-EVC(D) in Fig. 4(c) has a peak of 3.02 MW at 10.30 pm, which is 36% less than the highest load peak observed with P-EVC(D) in Fig. 4(a). Such a peak load reduction with N-EVC(D) is obtained because QP-2 includes a voltage constraint which restricts EVs to charge and discharge at lower magnitudes in order to avoid extensive voltage deviations. As shown in Fig. 4(d), N-EVC(D) maintains voltages across all nodes to stay within the upper and lower limit of ±5% of the nominal voltage. Although voltage rise above 5% of the nominal voltage is not observed in any of the four clusters with either P-EVC(D) in Fig. 4(b) or N-EVC(D) in Fig. 4(d), the voltage rise is considerably reduced with N-EVC(D) when compared to P-EVC(D).

It is worth noting that the computational time required to solve QP-1 for each EV_n in Scenario 1 is, on average, 53 milliseconds, with the CVXPY Python solver. The coupled voltage constraint (23) adds an additional level of complexity, which requires, on average, 36 seconds to solve QP-2 on each time-step of the receding time horizon in Scenario 2.[1]

Fig. 4(e–f) demonstrates the results for Scenario 3, which implements RHO-based N-EVC(D) considering a simulation setting where all customers have the same non-EV load profile $\boldsymbol{z}_n$ and the same EV charging specification Λ_n, as per Setting 2. In other words, it is considered that all customers in Scenario 3 have the same trend in non-EV power consumption, the same EV charge requirement and the same time duration available for charging the EVs. Despite such similarities, the envelopes of baseline voltage profiles resulting from the non-EV load, $\mathcal{V}^{\frac{1}{2}}$, and the envelopes of nodal voltage profiles resulting from the total load, $\boldsymbol{V}^{\frac{1}{2}}$, are different across various clusters of nodes, as seen in Fig. 4(f). In Fig. 4(e), the aggregate non-EV load profile ($\sum_n z_n$) peaks at 7.30 pm, with a more pronounced peak than the aggregate non-EV load peak observed in Fig. 4(a) or Fig. 4(c). Consequently, the envelopes of baseline voltage profiles, $\mathcal{V}^{\frac{1}{2}}$, for clusters 3 and 4 are below 0.95 p.u. from 7 – 9 pm, as shown in Fig. 4(f). By contrast, the envelopes of voltage profiles arising from N-EVC(D), $\boldsymbol{V}^{\frac{1}{2}}$, are within the acceptable ±5% threshold, for all clusters. Thus, N-EVC(D) corrects the observed baseline voltage violation (caused by the non-EV load), eventually improving the power quality across the test feeder.

In Fig. 4(b,d,f), the voltage profile of node 11 (Cluster 4) is more frequently the closest to the upper and lower voltage boundaries. Hence, voltage constraint at node 11 is more likely to be binding. Conceptually, node 11 is the furthest from the feeder head in terms of line impedance, and therefore the voltage at node 11 is impacted by the power consumption (and injection) of EV and non-EV loads connected to all nodes of the distribution feeder.

[1] The computational time required to solve QP-2 involving 6000 EVs is, on average, 48 seconds.

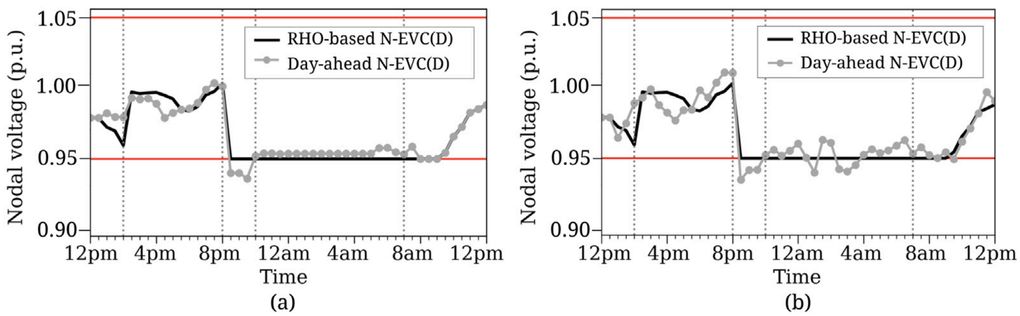

Fig. 5. The voltage profile of node 11 when N-EVC(D) is implemented with RHO (RHO-based N-EVC(D) as per Algorithm 1) and without RHO (day-ahead N-EVCD). Fig. 5(a) considers the case where day-ahead estimated EV arrival times are different from actual EV arrival times, and Fig. 5(b) additionally considers the case where day-ahead forecasted non-EV load is different from actual non-EV load.

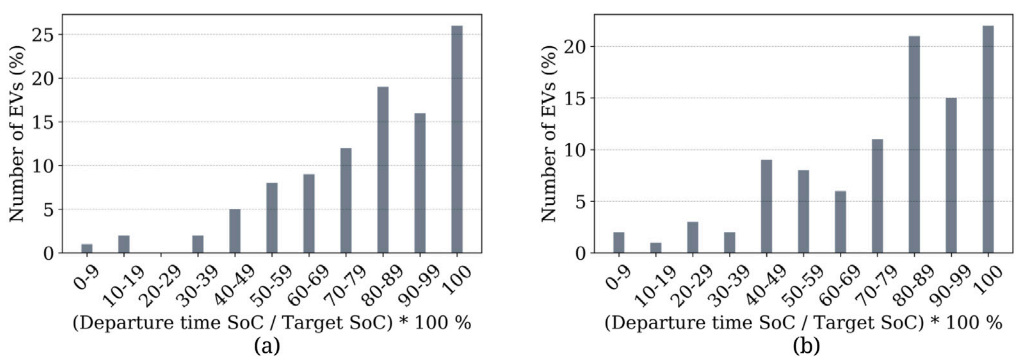

Fig. 6. The departure time SoC as a percentage of the target SoC when N-EVC(D) is implemented in the day-ahead (i.e., without RHO).

4.2. Assessing the benefit of RHO-based N-EVC(D)

In this section, the benefits of RHO-based N-EVC(D) are assessed by considering the impact of non-deterministic EV arrival times and uncertain non-EV load. For this simulation, actual arrival times of EVs a_n and actual non-EV load of customers $\boldsymbol{z}_n$ are considered as per Setting 1. The methodology employed in [41] is used to emulate the day-ahead arrival time for each EV$_n$, denoted by $\hat{a}_n$, and the day-ahead non-EV load profile for each customer $n \in \mathbb{H}$, denoted by $\hat{\boldsymbol{z}}_n$. In more detail, the day-ahead arrival time for each EV$_n$ is emulated by including uncertainty as $\hat{a}_n := a_n + \delta$, where δ is a random number generated from a normal distribution of mean zero with a standard deviation of 20% about actual arrival time a_n. Moreover, the day-ahead non-EV load forecast for each customer $n \in \mathbb{H}$ is emulated by including uncertainty as $\hat{z}_n(t) = z_n(t) + \epsilon(t)$ for all $t \in \mathbb{S}$, where $\epsilon(t)$ is a random number generated from a normal distribution of mean zero with a standard deviation of 20% of $z_n(t)$. Here, the standard deviation of 20% is consistent with the approach in [41].

Fig. 5 depicts the nodal voltage profile of node 11 (Cluster 4) when N-EVC(D) is implemented with RHO (*RHO-based N-EVC(D)*) and without RHO (*day-ahead N-EVC(D)*) for two important cases, where Fig. 5(a) includes the uncertainty of EV arrival times and Fig. 5(b) includes the uncertainty of non-EV load in addition to the uncertainty of EV arrival times. While the day-ahead N-EVC(D) method implements EV charge-discharge profiles that are determined a day-ahead using various types of estimated and forecasted data, the RHO-based N-EVC(D) method continuously updates EV charge-discharge profiles in near-real-time to address various forms of uncertainties. In Fig. 5(a), it is seen that the nodal voltage profile with day-ahead N-EVC(D) is different from the nodal voltage profile with RHO-based N-EVC(D) due to the slight differences between actual EV arrival times (a_n) and estimated EV arrival times ($\hat{a}_n$). Further, it is observed that implementing N-EVC(D) without RHO results in under-voltage conditions between 8.30 pm to 10 pm. From Fig. 5(b), it is inferred that when uncertainty of non-EV load is combined with uncertainty of EV arrival times, the day-ahead N-EVC(D) method aggravates violations of the voltage constraint. By contrast, implementing RHO-based N-EVC(D) improves supply voltages with no voltage excursions observed in either Fig. 5(a) or Fig. 5(b). It is worth mentioning that RHO-based N-EVC(D) accommodates incoming EVs without any prior notice and supports near real-time updates in non-EV demand forecasts — all of which enable greater preservation of the voltage constraint as observed in Fig. 5(a) and Fig. 5(b).

Fig. 6(a) and Fig. 6(b) report the departure time SoC of each EV when they follow battery profiles computed by the day-ahead N-EVC(D) method in Fig. 5(a) and Fig. 5(b), respectively. It is seen from Fig. 6(a) and Fig. 6(b) that only a portion of EVs (26% and 22%) reach their target SoC ($\ddot{u}_n$) completely. Moreover, the SoC on departure for 10% of EVs in Fig. 6(a) and 17% of EVs in Fig. 6(b) is less than half of their target SoC. Conversely, when RHO-based N-EVC(D) is implemented as in Fig. 5(a) and Fig. 5(b), all EVs attain their target SoC ahead of the departure time.

From the results presented in Figs. 5 and 6, it can be deduced that the N-EVC(D) method must be combined with RHO, in order to satisfy both the required distribution network voltage delivery requirements and the EV customer charge preferences.

4.3. Assessing the customer benefit

In this section, a set of customers, one from each node, is carefully selected to quantify operational costs for EV charging and discharging. For the purpose of comparison, Setting 2 is specifically chosen, such that the EV charging specification Λ_n and the non-EV load profile $\boldsymbol{z}_n$ remain the same for all customers. For each customer $n \in \mathbb{H}$ picked from each node $g \in \mathbb{V}$, Fig. 7 presents the operational cost ($\Omega_n(\boldsymbol{x}_n)$)

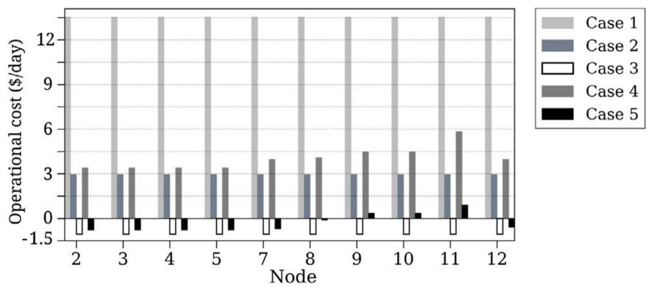

Fig. 7. Operational costs $\Omega_n(\boldsymbol{x}_n)$ attributed to a set of customers selected from each node in the distribution test feeder.

pertaining to 5 cases of EV charging, namely, **Case 1**: uncoordinated EV charging, **Case 2**: P-EVC, **Case 3**: P-EVCD, **Case 4**: N-EVC and **Case 5**: N-EVCD.

For Case 1 with uncoordinated EV charging, each $\mathrm{EV}_n(n \in \mathbb{H})$ commences charging at full power $\overline{x}_n$ immediately upon arrival and continues charging at the same rate of $\overline{x}_n$ until the battery is charged up to the target SoC $\ddot{u}_n$. According to Fig. 7, the largest operational cost for each customer corresponds to Case 1 (uncoordinated EV charging) — where no optimization-based method is applied for EV charging. By contrast, the lowest operational cost (or rather the greatest operational saving) for each customer corresponds to Case 3 (P-EVCD) where V2G is enabled, followed by Case 2 (P-EVC) where V2G is disabled.

In cases 1–3 where network voltage conditions are excluded, each customer receives an identical EV battery profile, and as such, the operational cost stays the same for each customer across the test feeder. In cases 4 and 5, the operational costs vary across customers as a result of the network voltage constraint. In particular, the operational costs in Case 4 (N-EVC) are greater than Case 2 (P-EVC), and the operational costs in Case 5 (N-EVCD) are greater than Case 3 (P-EVCD), implying that addressing the voltage constraint potentially leads to an increase in operational costs for the customers. Specifically, customers located at nodes with a larger line impedance (e.g., nodes in clusters 3 and 4) incur larger increases in operational costs. In both cases 4 and 5, the customer at node 11 incurs the largest operational cost. It can also be observed that in Case 5 (N-EVCD), customers closer to the feeder head accrue operational benefits ($\Omega_n(\boldsymbol{x}_n) < 0$), whereas customers located far from the feeder head accrue operational costs ($\Omega_n(\boldsymbol{x}_n) > 0$). Nevertheless, all customers partaking in either Case 4 or 5 (proposed N-EVC(D) method) receive an operational cost reduction of 92% – 111% (latter corresponds to a 11% gain) when compared to uncoordinated EV charging.

4.4. Discussion

In summary, key findings from the numerical simulations are listed as follows.

- P-EVC(D) yields lower operational costs (or greater operational savings) compared to uncoordinated EV charging and N-EVC(D); however, P-EVC(D) exacerbates voltage variability, which leads to voltage violations across a distribution feeder, particularly at nodes in the extremity of the feeder.
- The requirement to address voltage constraint in N-EVC(D) potentially leads to an increase in operational costs compared to P-EVC(D). However, N-EVC(D) yields significantly lower operational costs compared to uncoordinated EV charging and it also improves supply voltages without requiring protection schemes to correct for any potential voltage violation. Protection schemes that disconnect EV charging infrastructure to correct for sustained voltage excursions would adversely impact the EV customer both financially and in terms of meeting their exact charge requirements.
- To mitigate large voltage fluctuations, N-EVC(D) returns comparatively higher charge rates to EVs located closer to the feeder head and lower charge rates to EVs located closer to the feeder extremities.
- Even if all customers and their EVs have the same non-EV load profile and the same EV specification, the charge-discharge profiles obtained from N-EVC(D) are different across the customers, resulting in different operational costs.
- In the absence of advanced knowledge of exact EV arrival times and non-EV load profiles, RHO based N-EVC(D) as opposed to day-ahead N-EVC(D) allows for considerable improvements in voltage regulation in addition to achieving the customer-specified target SoC ahead of EV departure.

In future work, the numerical simulations will be extended to investigate voltage variability of unbalanced distribution grids when supplemented with rooftop PV power generation. Future work will also explore extensions of N-EVC(D) to incorporate dynamic distribution grid constraints such as thermal network constraints. Furthermore, it is envisioned that RHO based N-EVC(D), when combined with distributed algorithms (facilitating distributed computations by EVs), will potentially reduce the computational complexity associated with solving QP-2.

5. Conclusion

This paper presented an Electric Vehicle (EV) battery scheduling method called N-EVC(D) for coordinating EV charge (and discharge) rates to improve supply voltages along a distribution feeder. The optimization problem for N-EVC(D) was posed as a quadratic program, with an objective function to minimize operational costs associated with EV charging (and discharging) in accordance with a time-of-use net metering financial policy. A coupled voltage constraint was included in the quadratic program to alleviate non-compliant voltage excursions outside the operational limits of the distribution network. A receding horizon optimization-based N-EVC(D) algorithm was also proposed to accommodate various sources of uncertainties including unexpected EV arrival and departure times. Through numerical simulations, it was demonstrated that N-EVC(D) achieved an operational cost reduction of 92% – 111% compared to uncoordinated EV charging. N-EVC(D) also achieved a peak load reduction of 36% compared to a benchmark method that omitted voltage constraints when minimizing EV operational costs. Furthermore, the receding horizon optimization-based N-EVC(D) method improved supply voltages in cases of unexpected EV arrival times and non-EV load forecast errors. Importantly, the receding horizon optimization-based N-EVC(D) method outperformed the day-ahead N-EVC(D) method with all EVs attaining their target state of charge ahead of departure.

CRediT authorship contribution statement

Nanduni I. Nimalsiri: Conceptualization, Methodology, Software, Validation, Formal analysis, Investigation, Data curation, Writing - original draft, Writing - review & editing, Visualization, Project administration. **Elizabeth L. Ratnam:** Conceptualization, Methodology, Validation, Formal analysis, Investigation, Writing - review & editing, Visualization, Supervision, Project administration. **Chathurika P. Mediwaththe:** Conceptualization, Methodology, Validation, Formal analysis, Investigation, Writing - review & editing, Visualization, Supervision, Project administration. **David B. Smith:** Conceptualization, Methodology, Validation, Formal analysis, Investigation, Writing - review & editing, Visualization, Supervision, Project administration. **Saman K. Halgamuge:** Conceptualization, Validation, Formal analysis, Investigation, Writing - review & editing, Visualization, Supervision, Project administration.

Declaration of competing interest

The authors declare that they have no known competing financial interests or personal relationships that could have appeared to influence the work reported in this paper.

Acknowledgment

Nanduni I. Nimalsiri acknowledges the financial support of an Australian National University (ANU) Postgraduate Research Scholarship and a CSIRO Data61 PhD Scholarship.

Appendix

A summary of key notation used in the problem formulation:

t	Time index	n	Customer index
$\mathbb{S}$	Set of time indices	ℓ	Number of time indices in $\mathbb{S}$
$[0,T]$	Time horizon under consideration (h)	Δ	Length of a time interval (h)
$\mathbb{H}$	Set of customers	h	Number of customers in $\mathbb{H}$
$\mathbb{H}_1$	Set of customers with gridable EVs	$\mathbb{H}_2$	Set of customers with charge-only EVs
$\eta(t)$	Price of electricity over the period $\left((t-1)\Delta, t\Delta\right)$ ($/kWh)	$\boldsymbol{\eta}$	Pricing profile

A summary of key notation specific to EV$_n$ ($n \in \mathbb{H}$):

a_n	Arrival time index	d_n	Intended departure time index
$\hat{u}_n$	Initial SoC (kWh)	$\ddot{u}_n$	Target SoC (kWh)
$\overline{x}_n$	Maximum charge rate (kW)	$\underline{x}_n$	Maximum discharge rate (kW)
σ_n	Battery capacity (kWh)	α_n	Battery degradation constant ($/kW^2)
$u_n(t)$	SoC at time $t\Delta$ (kWh)	$\boldsymbol{u}_n$	SoC profile

A summary of key notation specific to customer $n \in \mathbb{H}$:

$x_n(t)$	(Dis)charge rate over the period $\left((t-1)\Delta, t\Delta\right)$ (kW)	$\boldsymbol{x}_n$	Battery profile
$z_n(t)$	Non-EV load over the period $\left((t-1)\Delta, t\Delta\right)$ (kW)	$\boldsymbol{z}_n$	Non-EV load profile
$y_n(t)$	Measured power through meter M over the period $\left((t-1)\Delta, t\Delta\right)$ (kW)		
$\Omega_n(\cdot)$	Operational cost function	$\boldsymbol{y}_n$	Grid power profile

A summary of key notation specific to the distribution network model:

g	Node index	N^g	Number of customers connected to node g
$v^g(t)$	Voltage at node g at time $t\Delta$ (p.u.)	v^0	Voltage at node 0 (p.u.)
$\underline{v}$	Minimum voltage magnitude (p.u.)	$\overline{v}$	Maximum voltage magnitude (p.u.)
$\mathcal{V}$	Set of nodes including node 0 (feeder head)		
$\mathbb{V}$	Set of nodes excluding node 0 (feeder head)		
(ij)	Distribution line connecting node i and node j		
$\mathcal{E}$	Set of distribution lines of the feeder		
$\mathcal{E}^g$	Set of distribution lines on the unique path from node 0 to node g		
$p^g(t), q^g(t)$	Real, reactive power consumed at node g over the period $\left((t-1)\Delta, t\Delta\right)$ (kW, kVAR)		
$\widetilde{p}^g(t), \widetilde{q}^g(t)$	Real, reactive power consumed by non-EV load at node g over the period $\left((t-1)\Delta, t\Delta\right)$		
$\widehat{p}^g(t), \widehat{q}^g(t)$	Real, reactive power consumed by EVs at node g over the period $\left((t-1)\Delta, t\Delta\right)$		

References

[1] Shareef H, Islam MM, Mohamed A. A review of the stage-of-the-art charging technologies, placement methodologies, and impacts of electric vehicles. Renew Sustain Energy Rev 2016;64:403–20.

[2] Dubey A, Santoso S. Electric vehicle charging on residential distribution systems: Impacts and mitigations. IEEE Access 2015;3:1871–93.

[3] Dong X, Mu Y, Xu X, Jia H, Wu J, Yu X, Qi Y. A charging pricing strategy of electric vehicle fast charging stations for the voltage control of electricity distribution networks. Appl Energy 2018;225:857–68.

[4] Nimalsiri NI, Mediwaththe CP, Ratnam EL, Shaw M, Smith DB, Halgamuge SK. A survey of algorithms for distributed charging control of EVs in smart grid. IEEE Trans Intell Transp Syst 2019;21:4497–515.

[5] De Hoog J, Alpcan T, Brazil M, Thomas D, Mareels I. Optimal charging of electric vehicles taking distribution network constraints into account. IEEE Trans Power Syst 2014;30:365–75.

[6] Richardson P, Flynn D, Keane A. Optimal charging of electric vehicles in low-voltage distribution systems. IEEE Trans Power Syst 2012;27:268–79.

[7] Zhan K, Hu Z, Song Y, Luo Z, Xu Z, Jia L. Coordinated electric vehicle charging strategy for optimal operation of distribution network. In *Proc. IEEE PES 3rd Innovative Smart Grid Technol.*, Europe, 2012, pp. 1–6.

[8] Liu M, Phanivong PK, Shi Y, Callaway DS. Decentralized charging control of EVs in residential distribution networks. IEEE Trans Control Syst Technol 2017;27:266–81.

[9] Huo X, Liu M. Decentralized electric vehicle charging control via a novel shrunken primal-multi-dual subgradient (SPMDS) algorithm. In *Proc. IEEE 59th Conf. Decis. Control*, 2020, pp. 1367–73.

[10] Cao C, Wu Z, Chen B. Electric vehicle–grid integration with voltage regulation in radial distribution networks. Energies 2020;13:1802.

[11] Nazarloo A, Feyzi MR, Sabahi M, Sharifian MBB. Improving voltage profile and optimal scheduling of V2G energy based on a new method. Adv Electr Comput Eng 2018;18:81–9.

[12] Richardson P, Flynn D, Keane A. Local versus centralized charging strategies for electric vehicles in low voltage distribution systems. IEEE Trans Smart Grid 2012;3:1020–8.

[13] Al-Awami AT, Sortomme E, Akhtar GMA, Faddel S. A voltage-based controller for an electric-vehicle charger. IEEE Trans Veh Technol 2015;65:4185–96.

[14] Clement-Nyns K, Haesen E, Driesen J. The impact of vehicle-to-grid on the distribution grid. Electr Power Syst Res 2011;81:185–92.

[15] Luo X, Chan KW. Real-time scheduling of electric vehicles charging in low-voltage residential distribution systems to minimise power losses and improve voltage profile. IET Gener Transm Distrib 2013;8:516–29.

[16] Lazarou S, Vita V, Christodoulou C, Ekonomou L. Calculating operational patterns for electric vehicle charging on a real distribution network based on renewables' production. Energies 2018;11:2400.

[17] Vita V, Lazarou S, Christodoulou CA, Seritan G. On the determination of meshed distribution networks operational points after reinforcement. Appl Sci 2019;9:3501.

[18] Sun W, Neumann F, Harrison GP. Robust scheduling of electric vehicle charging in LV distribution networks under uncertainty. IEEE Trans Ind Appl 2020;56:5785–95.

[19] Bharati G, Paudyal S. Coordinated control of distribution grid and electric vehicle loads. Electr Power Syst Res 2016;140:761–8.

[20] Shekari T, Golshannavaz S, Aminifar F. Techno-economic collaboration of PEV fleets in energy management of microgrids. IEEE Trans Power Syst 2016;32:3833–41.

[21] Crow ML, et al. Electric vehicle scheduling considering co-optimized customer and system objectives. IEEE Trans Sustain Energy 2017;9:410–9.

[22] Leou R-C. Optimal charging/discharging control for electric vehicles considering power system constraints and operation costs. IEEE Trans Power Syst 2015;31:1854–60.

[23] Suyono H, Rahman MT, Mokhlis H, Othman M, Illias HA, Mohamad H. Optimal scheduling of plug-in electric vehicle charging including time-of-use tariff to minimize cost and system stress. Energies 2019;12:1500.

[24] Xing H, Fu M, Lin Z, f Y. Decentralized optimal scheduling for charging and discharging of plug-in electric vehicles in smart grids. IEEE Trans Power Syst 2016;31:4118–27.

[25] Casini M, Vicino A, Zanvettor GG. A receding horizon approach to peak power minimization for EV charging stations in the presence of uncertainty. Int J Electr Power Energy Syst 2021;126:106567.

[26] Yi Z, Scoffield D, Smart J, Meintz A, Jun M, Mohanpurkar M, Medam A. A highly efficient control framework for centralized residential charging coordination of large electric vehicle populations. Int J Electr Power Energy Syst 2020;117:105661.

[27] Wang GC, Ratnam E, Haghi HV, Kleissl J. Corrective receding horizon EV charge scheduling using short-term solar forecasting. Renew Energy 2019;130:1146–58.

[28] Mediwaththe CP, Smith DB. Game-theoretic electric vehicle charging management resilient to non-ideal user behavior. IEEE Trans Intell Transp Syst 2018;19:3486–95.

[29] Ratnam EL, Weller SR, Kellett CM. Central versus localized optimization-based approaches to power management in distribution networks with residential battery storage. Int J Electr Power Energy Syst 2016;80:396–406.
[30] Baran ME, Wu FF. Network reconfiguration in distribution systems for loss reduction and load balancing. IEEE Power Eng Rev 1989;9:101–2.
[31] Nimalsiri N, Smith D, Ratnam E, Mediwaththe C, Halgamuge S. A decentralized electric vehicle charge scheduling scheme for tracking power profiles. In *Proc. IEEE PES Innovative Smart Grid Technol.*, 2020, pp. 1–5.
[32] Chang W-Y. The state of charge estimating methods for battery: A review. Int Sch Res Not 2013.
[33] Ratnam EL, Weller SR, Kellett CM. An optimization-based approach to scheduling residential battery storage with solar PV: Assessing customer benefit. Renew Energy 2015;75:123–34.
[34] Ratnam EL, Weller SR, Kellett CM. Scheduling residential battery storage with solar PV: Assessing the benefits of net metering. Appl Energy 2015;155:881–91.
[35] Rivera J, Wolfrum P, Hirche S, Goebel C, Jacobsen H-A. Alternating direction method of multipliers for decentralized electric vehicle charging control. In *Proc. IEEE 52nd Conf. Decis. Control*, 2013, pp. 6960–65.
[36] Hoke A, Brissette A, Smith K, Pratt A, Maksimovic D. Accounting for lithium-ion battery degradation in electric vehicle charging optimization. IEEE J Emerg Sel Top Power Electron 2014;2:691–700.
[37] Baran M, Wu FF. Optimal sizing of capacitors placed on a radial distribution system. IEEE Trans Power Deliv 1989;4:735–43.
[38] Mediwaththe CP, Blackhall L. Network-aware demand-side management framework with a community energy storage system considering voltage constraints. IEEE Trans Power Syst 2020.
[39] Farivar M, Chen L, Low S. Equilibrium and dynamics of local voltage control in distribution systems. In *Proc. IEEE 52nd Conf. Decis. Control*, 2013, pp. 4329–34.
[40] Lin W, Bitar E. Decentralized stochastic control of distributed energy resources. IEEE Trans Power Syst 2017;33:888–900.
[41] Ratnam EL, Weller SR. Receding horizon optimization-based approaches to managing supply voltages and power flows in a distribution grid with battery storage co-located with solar PV. Appl Energy 2018;210:1017–26.
[42] Battery University. Bu-1003: Electric vehicle (EV). 2021, https://batteryuniversity.com/learn/article/electric_vehicle_ev, (Accessed 25 Feb 2021).
[43] Victoria State Government - Department of Transport. VISTA Data and Publications; 2020, https://transport.vic.gov.au/about/data-and-research/vista/vista-data-and-publications (Accessed 1 March 2020).
[44] Ratnam EL, Weller SR, Kellett CM, Murray AT. Residential load and rooftop PV generation: an Australian distribution network dataset. Int J Sustain Energy 2017;36:787–806.
[45] Ausgrid. Solar home electricity data. 2020, https://www.ausgrid.com.au/Industry/Our-Research/Data-to-share/Solar-home-electricity-data (Accessed 1 March 2020).
[46] AGL. Standard retail contracts. 2020, https://www.agl.com.au/help/rates-contracts/standard-contracts, (Accessed 1 March 2020).
[47] Diamond S, Boyd S. CVXPY: A python-embedded modeling language for convex optimization. J Mach Learn Res 2016;17:1–5.

5.2 Summary and Contributions

This chapter presented a centrally coordinated algorithm that optimised charging and discharging of EVs (bidirectional flow of electricity to and from the EV batteries) to minimise the associated operational costs, while maintaining quasi-steady-state voltage magnitudes along a distribution feeder (assumed balanced) within the prescribed thresholds and satisfying each EV's charging requirement before their prespecified departure time.

First, the topology of a *residential power system* associated with a single EV customer was defined. Then, an optimisation problem in the form of a Quadratic Program (QP), named QP-1, was proposed for the charge and discharge scheduling of an EV in the previously defined residential power system. Three customer-related objectives were considered in the objective function of QP-1: the first was to reduce the daily payments for electricity received from the grid for EV charging; the second was to increase daily profits arising from the delivery of electricity to the grid via EV discharging; and the third was to reduce the battery degradation costs resulting from frequent EV charging and discharging. These three customer objectives were combined in the *operational cost*, which was minimised in QP-1. By accounting for the battery degradation within the operational cost minimisation, the battery lifetime was improved. A financial policy of net-metering accompanied with a ToU pricing regime was considered for the propose of electricity billing and compensation. The constraints of QP-1 included limitations of EV charging (and discharging) infrastructure and EV battery state-of-health thresholds and the requirement to satisfy the EV's charging requirement before the intended departure time. It should be noted that the charge and discharge efficiencies of the battery model employed in this work have to be the same, in order to obtain a QP-based solution. Otherwise, the optimisation problem results in a mixed discrete programming problem, as previously described in Chapter 4.

The implementation of the solution to QP-1, referred to as *Price-based EV Charging and Discharging* (P-EVCD), was considered as a benchmark in the analysis of the performance of the network-aware approach to EV charging and discharging.

To design the network-aware approach to EV charging and discharging, a radial distribution feeder model was assumed, which served multiple EV customers, each of whom was associated with a residential power system (as defined previously). Then, nodal voltage constraints were derived using the LinDistFlow model in [Baran and Wu, 1989a,b] to prevent under- and over-voltage conditions stemming from bidirectional power flows in the distribution grid. In the respective voltage constraints, the nodal voltages strongly coupled the individual EV charge and discharge rates in form of a linear inequality. A centralised optimisation problem was then formulated as a QP, named QP-2, to minimise the operational cost (as defined previously) that is accrued to each of the EV customers, while complying with each of their individual constraints (as detailed previously) and the formalised nodal voltage constraints. The implementation of the solution to QP-2 was referred to as *Network-aware EV Charging and Discharging* (N-EVCD). Finally, QP-2 was incorporated into a Receding-

Horizon Optimisation (RHO)-based algorithm, in order to support near-real-time N-EVCD operations. In the RHO-based N-EVCD algorithm, each EV executed a charge-discharge profile as specified by a centralised operator who solved QP-2 over a receding time horizon.

The performance of the proposed algorithm was evaluated by means of numerical simulations carried out on a modified IEEE 13 node test feeder. In simulations, the N-EVCD approach was compared with the P-EVCD approach (in the absence of voltage constraints) and it was inferred that: (1) both approaches managed to satisfy EV charging demands within the specified time duration, however the P-EVCD approach caused non-compliant voltage excursions whereas the N-EVCD approach preserved voltage regulations as required by the distribution grid operators; (2) N-EVCD, when combined with RHO, offered better results in terms of managing uncertainties related to EV arrival-departure times and non-EV power consumption; (3) N-EVCD yielded lower operational costs compared to uncoordinated EV charging, however, slightly higher operational costs compared to P-EVCD, meaning that voltage regulation comes at a slightly increased operational cost to EV customers; and (4) with N-EVCD, the operational cost for charging the same amount of power vary across EV customers depending on their location in the distribution feeder.

To summarise, the main contributions of this chapter were as follows.

1. By leveraging a linearized power flow model (for faster computation) referred to as the LinDistFlow model [Baran and Wu, 1989b], the power flows and nodal voltages in a single-phase or balanced distribution feeder were captured to derive the voltage profile (temporal variation of voltage magnitude) resulting from the aggregated EV and non-EV power consumption (or injection) at each node in the distribution feeder. Accordingly, nodal voltage constraints were introduced to maintain supply voltages along a distribution feeder to be within operational limits.

2. An optimisation problem was formulated in the form of a QP to minimise operational costs accrued to EV customers for charging and discharging their EV batteries, while complying with individual EV battery constraints and the proposed nodal voltage constraints, and satisfying all of the heterogeneous EV charge requirements within the specified time duration that the EVs remained grid-connected. In this way, the proposed QP balanced the EV customers' objective of minimizing their daily operational costs attributed to EV charging and discharging, with the electrical distributor's objective to effectively manage supply voltages along the distribution feeder.

3. A RHO-based centralised algorithm was proposed to support near-real-time N-EVCD operations while accommodating non-deterministic EV arrivals and departures.

4. Numerical simulations were conducted to demonstrate the effectiveness of the proposed algorithm.

Results obtained from numerical simulations demonstrated that N-EVC(D) achieved an operational cost reduction of 92% – 111% compared to uncoordinated EV charging. Moreover, N-EVC(D) achieved a peak load reduction of 36% compared to P-EVC(D), which omitted voltage constraints when minimizing EV operational costs. Importantly, the receding horizon optimization-based N-EVC(D) method improved supply voltages in cases of unexpected EV arrival times and non-EV load forecast errors.

In the next chapter, we extend this work to enable voltage regulation in unbalanced distribution networks via a distributed optimisation-based algorithm for EV charging and discharging.

Chapter 6

A distributed optimisation-based approach to manage supply voltages in unbalanced distribution grids with EVs

While most of the existing studies, including our work in Chapter 5, focus on network-aware EV charging coordination in the context of a single-phase or balanced distribution network for simplicity of exposition, most distribution systems are typically unbalanced. Single-phase representations of the power flow equations cannot capture the steady-state voltage variability across phases in an unbalanced distribution network, and as such, algorithms developed on the basis of single-phase equivalent (balanced) distribution network models cannot address voltage regulation requirements in unbalanced distribution networks. Therefore, in this work, we attempt to fill this void by developing an approach to EV charging and discharging coordination in unbalanced distribution networks, with voltage limitations specifically taken into account.

This chapter combines the problem formulations from previous Chapter 5 and extends the optimisation approach presented in Chapter 5 in two important ways.

- Regulation of voltages in an unbalanced distribution network is considered.
- A distributed-optimisation based approach to coordinate EV charging and discharging is considered.

Of course, the presence of strongly coupled voltage constraints makes distributed optimisation challenging. To tackle this challenge, we exploit a distributed optimisation algorithm called the ADMM proposed in [Boyd et al., 2011], which blends the decomposability of the dual ascent method with the superior convergence properties of the method of multipliers. The basic idea of the ADMM algorithm is to to decompose the original problem into distributively solvable subproblems, which are then coordinated by a high-level master problem by means of some kind of signalling. ADMM, in particular, solves optimisation problems with a separable objective function and coupled constraints, and as such, it naturally becomes a good candidate to solve our optimisation problem considered in this work. Importantly, the ADMM-based method is proven to ensure the convergence in a finite number of iterations.

On another perspective, most of the existing distributed EV charging approaches for voltage regulation, such as [Liu et al., 2017; Liu and Sahraei-Ardakani, 2019; Huo and Liu, 2020; Zhou et al., 2020b; Then et al., 2021; Wang et al., 2020; Omran and Filizadeh, 2017; Zhang and Leung, 2018; Zhang et al., 2016], have the common limitation that they are susceptible to single point of failures, as they require a central entity (a coordinator/aggregator) to perform part of the computations and to transmit communication signals to and from each of the EVs. In fact, these approaches require all the communication signals (messages) to pass through the central coordinator, which results in a high communication overhead. Furthermore, these approaches raise privacy concerns for EV users since EVs have to notify their locally computed charge profiles to the central entity at each iteration of the algorithm to update the required signals for the next iteration. Hence, we are motivated to design a distributed coordination approach that is free of centralised message passing and centralised computations.

Although the ADMM algorithm suits our problem formulation, it still requires central updates that need to be performed by a central coordinator. Therefore, we leverage a fully parallelised distributed optimisation algorithm called the Dual Consensus – ADMM (DC-ADMM) in [Chang et al., 2014], which is a variant of the ADMM algorithm that combines the duality theory and the consensus formulation. By employing DC-ADMM, we eliminate the requirement of a central coordinator and thereby improve robustness against single-link/node failures. As reported in [Tsai et al., 2015], the DC-ADMM approach enjoys a much faster convergence rate as opposed to the approaches that use the subgradient method for optimization, which also implies a great reduction of the communication overhead.

In this chapter, we propose an algorithm based on the DC-ADMM approach, that manages supply voltages in unbalanced distribution grids by coordinating EV charging and discharging operations via peer-to-peer EV communication. The contributions in this chapter are presented in our submitted manuscript.

6.1 Submitted Manuscript

In our paper presented below, a distributively coordinated, network-aware EV charging and discharging approach is proposed to managing supply voltages in unbalanced residential distribution networks under minimal operational costs accrued to EV customers. Outcomes from this paper address (i) research objective Q1 of the thesis (see Chapter 1 - Section 1.2) by showing how to involve EVs in voltage regulation considering both charging and discharging of EV batteries, (ii) research objective Q2 by taking into account both EV customer economics and electrical distributor concerns on voltage regulatory requirements when scheduling EV charging and discharging; and (iii) research objective Q3 by proposing a fully distributed approach for computing EV charge-discharge schedules.

N. I. Nimalsiri, E. L. Ratnam, C. P. Mediwaththe, D. B. Smith, S. K. Halgamuge, "Distributed Optimisation-based Electric Vehicle Charging and Discharging in Unbalanced Distribution Grids,"
https://doi.org/10.36227/techrxiv.16920889.v1

Distributed Optimization-based Electric Vehicle Charging and Discharging in Unbalanced Distribution Grids

Nanduni I. Nimalsiri, Elizabeth L. Ratnam, *Senior Member, IEEE,* David B. Smith, *Member, IEEE,* Chathurika P. Mediwaththe, *Member, IEEE,* and Saman K. Halgamuge *Fellow, IEEE*

***Abstract*—Distributed optimization-based approaches of Electric Vehicle (EV) charging coordination are becoming increasingly important to enable a massive-scale EV rollout without driving costly distribution network reinforcement. This paper proposes an algorithm called Dis-Net-EVCD for distributedly coordinated, network-aware EV charging and discharging in unbalanced distribution grids, incorporating both EV customer economics (least cost charging) and distribution network considerations. Importantly, Dis-Net-EVCD ensures that the EVs are charged ahead of their expected departure time, without creating any voltage excursions in the distribution grid. The Alternating Direction Method of Multipliers (ADMM) underpins the development of Dis-Net-EVCD, wherein each EV iteratively determines its charge-discharge schedule locally via peer-to-peer communication with its neighbors. Numerical simulations carried out on the IEEE 13 node test feeder with 600 residential EVs demonstrate that EV customers implementing Dis-Net-EVCD yield a total operational cost reduction of 78% compared to uncoordinated EV charging, while also conforming with the voltage regulatory requirements. Moreover, Dis-Net-EVCD is shown to be approximately 60 times computationally faster than its centralized counterpart.**

***Index Terms*—Distributed optimization, electric vehicles, unbalanced distribution grids, vehicle-to-grid, voltage regulation.**

I. Introduction

Energy systems across the globe are transitioning to accommodate a dramatic uptake of EVs, promoting an environmentally, economically and socially sustainable transportation system [1]. However, without due consideration, a massive EV proliferation poses challenges for electrical distributors, especially when EV charging coincides with underlying peak load periods, creating conditions which lead to system voltage instabilities. It is therefore imperative to coordinate EV charging (and discharging) in a way that the voltages in distribution circuits stay within prescribed steady-state operating limits [2].

Several researchers have explored coordinated approaches of EV charging and discharging for voltage regulation in distribution grids, which can be classified into centralized approaches [2–6] and distributed approaches [7–20]. Rather than collecting all information and performing a central computation, distributed approaches support distributed and parallel computations by multiple agents that require limited information exchange [21]. As such, distributed approaches are more computationally efficient and scalable, allowing for larger EV populations to be coordinated across the distribution grid, while also empowering EV customers in the decision-making process. Many of the existing distributed EV charging approaches (see for instance [7–17, 20]) require a communication network with a star topology, in which all information is transmitted to EVs via a central coordinator/s (or aggregator/s). Such communication infrastructures demand huge investments [22] and are also prone to single point of failures. Alternatively, several EV charging approaches are proposed based on game theory [23], randomized Alternating Direction Method of Multipliers (ADMM) [22] and consensus algorithms [24], which operate via only local communication of EVs with neighboring agents (without having a central coordinator/s); however, none of them consider the underlying power distribution networks and the associated constraints.

Network-aware EV charging approaches facilitating distributed coordination are proposed in [7–19]. In [9, 10, 15, 17, 18], ADMM-based distributed EV charging schemes are proposed to avoid system voltages dropping below the permissible limits. Other distributed EV charging schemes operating within compliant steady-state voltage constraints include formulations based on droop control [11], game theory [16], shrunken primal-dual subgradient [7, 8] and multi-agent system modelling [13]. While the aforementioned literature is limited to EV charge-only operations, the distributed approaches in [12, 14] incorporate Vehicle-to-Grid (V2G) operation to further support voltage regulation.

In practice, three-phase distribution grids are typically unbalanced in both load and impedance across phases, especially when designed with single phase and two phase laterals. With the exception of [10], the distributed EV charging schemes in [7–19] incorporate power flow equations for single-phase representations of three-phase distribution grids, which cannot capture the steady-state voltage variability across phases in an unbalanced distribution grid. In [10], an economical approach of EV charging is proposed to minimize power supply costs subject to network constraints. Similar to [10], we seek to develop a cost-effective approach for EV charging, with system voltages maintained as per the required standards. Beyond [10], we seek to include V2G operations and remove the requirement for a central coordinator — reducing the risk of communication-based single point of failures.

In this paper, we propose an algorithm for Distributed and Network-aware EV Charging and Discharging, referred to as Dis-Net-EVCD, that minimizes operational costs accrued to EV customers while maintaining voltages in an unbalanced distribution grid within prescribed quasi-steady-state limits. Specifically, we consider EV customer operational costs associated with: (1) purchasing (or otherwise being compen-

The authors are with the Australian National University, Australia (e-mail: nanduni.nimalsiri, elizabeth.ratnam, chathurika.mediwaththe, saman.halgamuge@anu.edu.au; david.smith@data61.csiro.au).

N. I. Nimalsiri and D. B. Smith are also with Data61, CSIRO, Australia.

S. K. Halgamuge is also with the University of Melbourne, Australia.

sated for delivering) electricity on a Time-of-Use (ToU) net-metering tariff; and (2) battery degradation due to frequent charging and discharging. Dis-Net-EVCD also accommodates individual EV preferences and battery constraints, including EV charge-discharge rate limits, EV battery state-of-health thresholds, and customer-specified charge requirements.

Central to Dis-Net-EVCD is an ADMM-based decomposition approach, in which the underlying centralized optimization problem is decomposed into a set of tractable subproblems that are solved by EVs in parallel by exchanging limited information with neighboring EVs in an arbitrary (connected) peer-to-peer communication network (the information exchange between EVs is limited to the Lagrangian dual variables associated with the network constraints). Importantly, Dis-Net-EVCD eliminates the central operator/s (as opposed to other ADMM-based network-aware EV charge strategies in [9, 10, 15, 17–19]) and also improves EV user privacy as there is no no need for the customers to transmit their private EV information to the communication network. Moreover, Dis-Net-EVCD operates in near-real-time and also accommodates non-deterministic EV arrivals and departures.

The contributions of this paper are summarized as follows:

1) By leveraging from ADMM, duality theory and consensus theory, we propose an algorithm called Dis-Net-EVCD, for network-aware EV charging and discharging, where EVs determine their charge-discharge strategies locally and simultaneously. Dis-Net-EVCD aims to solve two problems: the first is to benefit the customers by minimizing their operational costs attributed to EV charging; and the second is to benefit the electrical distributors by regulating voltage magnitudes in unbalanced distribution grids to stay within permissible limits. That is, Dis-Net-EVCD carefully balances reductions in EV operational costs against improvements in supply voltages across the distribution grid. Importantly, Dis-Net-EVCD is distributed and only requires neighbor-wise communications, eliminating the need for a central coordinator/s.
2) We prove that Dis-Net-EVCD asymptotically converges to the globally optimal solution of the underlying optimization problem, where EVs fulfill their heterogeneous charge requirements with minimal operational costs, and in compliance with network constraints and individual battery constraints.

The remainder of the paper is organized as follows. Section II introduces a residential EV energy system. Section III formulates a centralized optimization problem for network-aware EV charging and discharging, followed by the proposed distributed algorithm in Section IV. Section V presents our numerical simulations and Section VI concludes the paper.

Notation

$\mathbb{R}^\ell$ (and $\mathbb{C}^\ell$) denote ℓ-dimensional vectors of real numbers (and complex numbers, respectively) where, as usual, $\mathbb{R}^1 = \mathbb{R}$ (and $\mathbb{C}^1 = \mathbb{C}$). $\mathbb{R}^{m\times n}$ (and $\mathbb{C}^{m\times n}$) denote m-by-n dimensional matrices of real numbers (and complex numbers). $\mathbf{0}$ denotes the all-zeros column vector, $\mathbf{1}$ denotes the all-ones column vector, and $\mathbf{I}$ denotes the identity matrix, where the context will make clear the dimensions intended. Given a matrix $\boldsymbol{A} \in \mathbb{R}^{n\times m}$ (or $\mathbb{C}^{n\times m}$), $[\boldsymbol{A}]_{i,j} \in \mathbb{R}$ (or $\mathbb{C}$) denotes the entry in row i and column j, and $\boldsymbol{A}^\top \in \mathbb{R}^{m\times n}$ (or $\mathbb{C}^{m\times n}$) denotes its transpose. Given two matrices $\boldsymbol{A} \in \mathbb{R}^{m\times n}$ and $\boldsymbol{B} \in \mathbb{R}^{p\times q}$, $\boldsymbol{C} := \boldsymbol{A} \oplus \boldsymbol{B} = \mathrm{diag}(\boldsymbol{A}, \boldsymbol{B}) \in \mathbb{R}^{(m+p)\times(n+q)}$ denotes the matrix direct sum satisfying $[\boldsymbol{C}]_{i,j} = [\boldsymbol{A}]_{i,j}$ when $i \le m$ and $j \le n$, $[\boldsymbol{C}]_{i,j} = [\boldsymbol{B}]_{(i-m),(j-n)}$ when $i > m$ and $j > n$, and $[\boldsymbol{C}]_{i,j} = 0$ elsewhere.

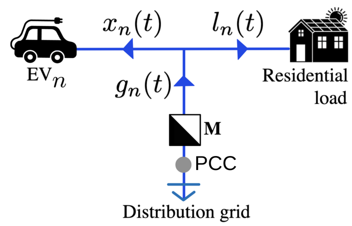

Fig. 1. Residential EV energy system (REES) illustrating the electrical path from customer $n \in \mathcal{N}$ to the wider distribution grid. Bi-directional smart meter $\mathbf{M}$ measures and records power flow $g_n(t)$ for the purpose of electricity billing and compensation. For each $n \in \mathcal{N}$, the power balance equation $g_n(t) = l_n(t) + x_n(t)$ holds for all $t \in \mathcal{S}$, where arrows associated with $x_n(t)$, $l_n(t)$ and $g_n(t)$ represent the assumed direction of positive power flow.

II. Preliminaries

A. Residential EV Energy System (REES)

Fig. 1 illustrates the topology of a *Residential EV Energy System* (REES) of a single customer, consisting of an EV and a residential load situated behind the Point of Common Coupling (PCC). The residential load represents the net load resulting from total non-EV power consumption and co-located rooftop solar generation of the residence (if there is any). The set of REESs are indexed by $\mathcal{N} := \{1, \ldots, n, \ldots, N\}$, such that the EV grid-connected from customer residence $n \in \mathcal{N}$ is represented by EV$_n$.

We consider a planning time-horizon $[0, T\Delta]$ consisting of T time-intervals of length Δ (in hours). The set of time indices is given by $\mathcal{S} := \{1, \ldots, t, \ldots, T\}$, where a time-interval is denoted by $\big((t-1)\Delta, t\Delta\big)$.

The power flows in Fig. 1 are as follows. The measured power (in kW) through meter $\mathbf{M}$ is denoted by $g_n(t) \ge 0$ (or $g_n(t) < 0$), which is the power delivered from (to) the grid to (from) customer $n \in \mathcal{N}$ over the time-interval $\big((t-1)\Delta, t\Delta\big)$. Accordingly, the *grid power profile* of customer $n \in \mathcal{N}$ over $[0, T\Delta]$ is defined as $\boldsymbol{g}_n := [g_n(1), \ldots, g_n(t), \ldots, g_n(T)]^\top \in \mathbb{R}^T$. Throughout, EV-indices are sub-scripted and time-indices are parenthesized.

The non-EV residential power consumption of customer $n \in \mathcal{N}$ in excess (or deficit) of the renewable power generation (if there is any) (in kW) over the time-interval $\big((t-1)\Delta, t\Delta\big)$ is represented by $l_n(t) \ge 0$ (or $l_n(t) < 0$) for all $t \in \mathcal{S}$. Accordingly, the day-ahead *non-EV power profile* of customer $n \in \mathcal{N}$ over $[0, T\Delta]$ is defined by $\boldsymbol{l}_n := [l_n(1), \ldots, l_n(t), \ldots, l_n(T)]^\top \in \mathbb{R}^T$. Likewise, the power (in kW) delivered to (from) EV$_n$ over the time-interval $\big((t-1)\Delta, t\Delta\big)$ is denoted by $x_n(t) \ge 0$ (or $x_n(t) < 0$) for all $t \in \mathcal{S}$. That is, $x_n(t) > 0$ when charging and $x_n(t) < 0$ when discharging. Accordingly, the *power profile* of EV$_n$ over $[0, T\Delta]$ is defined by $\boldsymbol{x}_n := [x_n(1), \ldots, x_n(t), \ldots, x_n(T)]^\top \in \mathbb{R}^T$.

Each EV$_n$ ($n \in \mathcal{N}$) is associated with a set of parameters that include the arrival time index $a_n \in \mathcal{S}$, intended departure time index $d_n \in \mathcal{S}$, battery capacity c_n (in kWh), initial State-of-Charge (SoC) $\hat{\sigma}_n$ (in kWh), target SoC at the departure σ_n^* (in kWh), limits for minimum SoC $\underline{\sigma}_n$ and maximum SoC $\overline{\sigma}_n$ (in kWh), energy conversion efficiency of (dis)charging μ_n, and limits for maximum charge rate $\overline{x}_n$ and maximum discharge rate $\underline{x}_n$ (in kW). Clearly, if EV_n is charge-only, then $\underline{x}_n = 0$. In this work, we consider a scenario where the EV owner, upon arrival at home, must specify an expected departure time d_n and a target SoC σ_n^* that is feasible to reach within the respective departure time, i.e., the condition $\sigma_n^* \leq \hat{\sigma}_n + (d_n - a_n)\overline{x}_n\overline{\mu}_n\Delta$ must hold [2, 25]. The collective charging specifications for EV_n are represented by $\Lambda_n := \{a_n, d_n, c_n, \hat{\sigma}_n, \sigma_n^*, \underline{\sigma}_n, \overline{\sigma}_n, \mu_n, \underline{x}_n, \overline{x}_n\}$. Following [23], the SoC of EV_n at time $t\Delta$ ($t \in \mathcal{S}$) is obtained by

$$\sigma_n(t) := \sigma_n(t-1) + \Delta\mu_n x_n(t), \tag{1}$$

where $\sigma_n(a_n) = \hat{\sigma}_n$. Accordingly, the *SoC profile* of EV_n is defined by $\boldsymbol{\sigma}_n := [\sigma_n(1), \ldots, \sigma_n(t), \ldots, \sigma_n(T)]^\top \in \mathbb{R}^T_{\geq 0}$.

B. EV battery constraints

Each EV_n ($n \in \mathcal{N}$) is operated subject to the following constraints. To prevent battery over-charging (and discharging), the SoC is constrained such that $\underline{\sigma}_n \leq \sigma_n(t) \leq \overline{\sigma}_n$ for all $t \in \mathcal{S}$, which implies that the SoC profile, $\boldsymbol{\sigma}_n$, must satisfy

$$\underline{\sigma}_n \mathbf{1} \leq \boldsymbol{\sigma}_n \leq \overline{\sigma}_n \mathbf{1}. \tag{2}$$

To simplify the notation, we define $\underline{c}_n := \frac{(\underline{\sigma}_n - \hat{\sigma}_n)}{\Delta}$ and $\overline{c}_n := \frac{(\overline{\sigma}_n - \hat{\sigma}_n)}{\Delta}$ and combine (1) and (2) as

$$\underline{c}_n \mathbf{1} \leq \mathbf{T}_n \boldsymbol{x}_n \leq \overline{c}_n \mathbf{1}, \tag{3}$$

where $\mathbf{T}_n = [t_{ij}] \in \mathbb{R}^{T \times T}$ denotes a matrix satisfying $t_{ij} = \mu_n$ for $i \geq j$ and $t_{ij} = 0$ elsewhere.

Due to the limited charging (and discharging) power of the battery, the constraint $\underline{x}_n \leq x_n(t) \leq \overline{x}_n$ is introduced for all $t \in \mathcal{S}$, which implies that the power profile, $\boldsymbol{x}_n$, must satisfy

$$\underline{x}_n \mathbf{1} \leq \boldsymbol{x}_n \leq \overline{x}_n \mathbf{1}. \tag{4}$$

To incorporate the EV charging demand e_n, where $e_n := \sigma_n^* - \hat{\sigma}_n$ (in kWh), the constraint $\sigma_n(T) = \sigma_n^*$ is enforced, which when combined with (1) yields

$$\mathbf{1}^\top \boldsymbol{x}_n = e_n / \Delta. \tag{5}$$

To limit the duration of EV charging (and discharging) to the period the EV is grid-connected ($[a_n, d_n]$), a diagonal matrix $\boldsymbol{\mathcal{L}}_n \in \mathbb{R}^{T \times T}$ is defined, in which $[\boldsymbol{\mathcal{L}}_n]_{i,i} = 1$ ($1 \leq i \leq T$) if the EV is available across the time-interval $\big((i-1)\Delta, i\Delta\big)$ and $[\boldsymbol{\mathcal{L}}_n]_{i,i} = 0$ otherwise. Formally, if $i = j$ and $a_n < i \leq d_n$, then $[\boldsymbol{\mathcal{L}}_n]_{i,i} = 1$, otherwise $[\boldsymbol{\mathcal{L}}_n]_{i,i} = 0$. Clearly, if $i \neq j$ then $[\boldsymbol{\mathcal{L}}_n]_{i,i} = 0$. Accordingly, the power profile $\boldsymbol{x}_n$ is further constrained by

$$(\mathbf{I} - \boldsymbol{\mathcal{L}}_n)\ \boldsymbol{x}_n = \mathbf{0}. \tag{6}$$

By combining the set of EV battery constraints (3)-(6), the feasibility set of power profiles for EV_n can be succinctly written as

$$\Psi_n := \{\boldsymbol{x}_n : \boldsymbol{A}_n \boldsymbol{x}_n \geq \boldsymbol{b}_n,\ \bar{\boldsymbol{A}}_n \boldsymbol{x}_n = \bar{\boldsymbol{b}}_n\}, \tag{7}$$

where $\boldsymbol{A}_n := \begin{bmatrix}\mathbf{I} & -\mathbf{I} & \mathbf{T}_n^\top & -\mathbf{T}_n^\top\end{bmatrix}^\top \in \mathbb{R}^{4T \times T}$, $\bar{\boldsymbol{A}}_n := \begin{bmatrix}\mathbf{1} & (\mathbf{I} - \boldsymbol{\mathcal{L}}_n)\end{bmatrix}^\top \in \mathbb{R}^{(T+1) \times T}$, $\boldsymbol{b}_n := \begin{bmatrix}\underline{x}_n \mathbf{1}^\top & -\overline{x}_n \mathbf{1}^\top & \underline{c}_n \mathbf{1}^\top & -\overline{c}_n \mathbf{1}^\top\end{bmatrix}^\top \in \mathbb{R}^{4T}$, and $\bar{\boldsymbol{b}}_n := \begin{bmatrix}\frac{e_n}{\Delta} & \mathbf{0}^\top\end{bmatrix}^\top \in \mathbb{R}^{T+1}$ with $\mathbf{I} \in \mathbb{R}^{T \times T}$, $\mathbf{T}_n \in \mathbb{R}^{T \times T}$, $\mathbf{1} \in \mathbb{R}^T$ and $\mathbf{0} \in \mathbb{R}^T$. In (7), the inequality constraint combines (3)-(4) and the equality constraint combines (5)-(6).

C. EV operational costs

A financial policy of *net metering*, as in [26], is considered, where each customer is compensated for delivering power to the grid at the same rate as they are billed for consuming power from the grid. Daily variations in electricity price are represented by the *price profile* $\boldsymbol{\eta} := [\eta(1), \ldots, \eta(t), \ldots, \eta(T)]^\top \in \mathbb{R}^T$, where $\eta(t)$ is the price of electricity (in \$/kWh) over the time period $\big((t-1)\Delta, t\Delta\big)$. The *operational cost* (in \$/day) accrued to customer $n \in \mathcal{N}$ is then defined by

$$\Omega_n(\boldsymbol{x}_n) := \textstyle\sum_{t=1}^T \{\Delta\eta(t)x_n(t) + \alpha_n x_n(t)^2\}, \tag{8}$$

where α_n is a (small) regularization parameter that yields a smoother power profile $\boldsymbol{x}_n$ by avoiding unnecessary charge-discharge cycles. In this way, the second term in (8) (first introduced in [27]) acts as a proxy for the battery degradation cost, which can be alternatively represented by other cost functions as presented in [28]. The first term in (8) represents the time-varying cost (or profit) attributed to EV charging and discharging. Specifically, a positive value of $\Omega_n(\boldsymbol{x}_n)$ represents a financial cost, whereas a negative value of $\Omega_n(\boldsymbol{x}_n)$ represents a financial benefit.

III. Problem Formulation

This section formulates an optimization problem for EV charging and discharging in an unbalanced three phase distribution grid, which serves N customers ($\in \mathcal{N}$), each of whom is represented by a REES depicted in Fig. 1.

A. Unbalanced distribution grid model

We consider a three phase, unbalanced, radial distribution feeder with two phase and single phase laterals, represented by a graph $\mathcal{G} = \{\mathcal{V}, \mathcal{E}\}$. The set of vertices $\mathcal{V} := \{0, \ldots, i, \ldots, k\}$ represents nodes along the feeder and the edge-set $\mathcal{E} \subseteq \mathcal{V} \times \mathcal{V}$ represents line segments along the feeder, with $|\mathcal{E}| = k$. Node 0 is the root node (feeder head) that represents an infinite bus, which decouples interactions along the feeder from the wider power grid. The edge $(ij) \in \mathcal{E}$ exists if there is a line segment between nodes i and j ($i, j \in \mathcal{V}$), with node i being closest to the feeder head. Graph $\mathcal{G}$ is assumed to be simple with no repeated edges or self loops for any $i \in \mathcal{V}$, i.e., $(ii) \notin \mathcal{E}$. For each vertex $i \in \mathbb{V}$, where $\mathbb{V} := \mathcal{V} \setminus \{0\} = \{1, \ldots, i, \ldots, k\}$, the set of edges on the unique path from node 0 to node i is denoted by $\mathcal{E}^i \subseteq \mathcal{E}$.

Each vertex $i \in \mathcal{V}$ (and each edge $(ij) \in \mathcal{E}$) is either a single phase, two phase, or three phase node (or line, respectively). In what follows, phases are denoted by ϕ and ψ, where $\phi, \psi \in \{a, b, c\}$. The set of phases at node $i \in \mathcal{V}$ is denoted by Φ^i, e.g., $\Phi^i = \{a, b, c\}$ for a 3-phase node i. Typically, node 0 is a 3-phase node, i.e., $\Phi^0 = \{a, b, c\}$. The set of phases along edge $(ij) \in \mathcal{E}$ is denoted by Φ^{ij}, e.g., $\Phi^{ij} = \{a, b, c\}$ for a 3-phase line segment. If edge (ij) exists, then the set of phases along edge (ij) is a subset of the phases present at both node i and node j, i.e., $\Phi^{ij} \subseteq (\Phi^i \cap \Phi^j)$.

Let $\{(i{:}\phi)\}_{\phi \in \Phi^i}$ represent the tuple of phases at node $i \in \mathbb{V}$, e.g., if node i is 3-phase, then $\{(i{:}\phi)\}_{\phi \in \Phi^i} = \{(i{:}a), (i{:}b), (i{:}c)\}$. Let $\mathcal{K} = \cup_{i \in \mathbb{V}} \{(i{:}\phi)\}_{\phi \in \Phi^i}$, where $|\mathcal{K}| = K$ represents the sum of the total number of phases across all nodes in $\mathbb{V}$. Each element $(i{:}\phi) \in \mathcal{K}$ represents a *supply point* that serves $N^{(i:\phi)} \geq 0$ number of customers, such that $\sum_{i\in\mathbb{V}} \sum_{\phi\in\Phi^i} N^{(i:\phi)} = N$. We label the customers in $\mathcal{N}$ by initializing the customer index as $n = 1$ and then incrementing n through all customers at a supply point, and across all supply points in $\mathcal{K}$ in ascending order, respectively.

We identify the location of each customer with reference to a supply point, $(i{:}\phi) \in \mathcal{K}$. Let $\boldsymbol{\Upsilon}$ denote a binary matrix with rows indexed by elements of $\mathcal{K}$ and columns indexed by elements of $\mathcal{N}$, such that $[\boldsymbol{\Upsilon}]_{(i:\phi),n} = 1$ if customer $n \in \mathcal{N}$ is connected to supply point $(i{:}\phi) \in \mathcal{K}$ and $[\boldsymbol{\Upsilon}]_{(i:\phi),n} = 0$ otherwise. More formally,

$$\boldsymbol{\Upsilon} \;\coloneqq\; \oplus_{i\in\mathcal{V}}\big(\oplus_{\phi\in\Phi^i}\boldsymbol{\Upsilon}^{(i:\phi)}\big) \in \mathbb{R}^{K\times N}_{\geq 0}, \tag{9}$$

where $\boldsymbol{\Upsilon}^{(i:\phi)} = \mathbf{1}^\top \in \mathbb{R}^{1\times N^{(i:\phi)}}_{\geq 0}$ for each $(i{:}\phi) \in \mathcal{K}$.

Let $\mathrm{r}^{ij,\phi\psi}$ and $\mathrm{x}^{ij,\phi\psi}$ denote the (self or mutual) resistance and reactance of line segment $(ij) \in \mathcal{E}$, respectively, where ϕ and ψ represent each of the phases along the line segment. Then $z^{ij,\phi\psi} \coloneqq \mathrm{r}^{ij,\phi\psi} + \mathrm{i}\mathrm{x}^{ij,\phi\psi}$, so that each line segment has a complex impedance $\boldsymbol{z}^{ij}$, where for a three-phase line segment

$$\boldsymbol{z}^{ij} = \begin{bmatrix} z^{ij,aa} & z^{ij,ab} & z^{ij,ac} \\ z^{ij,ba} & z^{ij,bb} & z^{ij,bc} \\ z^{ij,ca} & z^{ij,cb} & z^{ij,cc} \end{bmatrix} \in \mathbb{C}^{3\times 3}. \tag{10}$$

Let $Z^{ij,\phi\psi} \coloneqq \sum_{(\hat{i}\hat{j})\in(\mathcal{E}^i\cap\mathcal{E}^j)} z^{\hat{i}\hat{j},\phi\psi} \in \mathbb{C}$ denote the sum of (self or mutual) impedances along the unique path that is common to the paths from node 0 to node i, and from node 0 to node j, such that both paths incorporate phases ϕ and ψ. For instance, in Fig. 2, $Z^{79,ab} = z^{01,ab} + z^{16,ab}$.

Let $\omega = e^{-\frac{2\pi\mathrm{i}}{3}}$ and let $[[\phi]]$ denote phase ϕ as a numeral, where we assign $[[a]] = 0$, $[[b]] = 1$ and $[[c]] = 2$. Let $\boldsymbol{R} \in \mathbb{R}^{K\times K}_{\geq 0}$ and $\boldsymbol{X} \in \mathbb{R}^{K\times K}_{\geq 0}$ be two square matrices with rows and columns indexed by elements of $\mathcal{K}$, such that $[\boldsymbol{R}]_{(i:\phi),(j:\psi)} \coloneqq 2\mathbb{R}\mathrm{e}\{(Z^{ij,\phi\psi})^* \cdot \omega^{[[\phi]]-[[\psi]]}\} \in \mathbb{R}$ and $[\boldsymbol{X}]_{(i:\phi),(j:\psi)} \coloneqq -2\mathbb{I}\mathrm{m}\{(Z^{ij,\phi\psi})^* \cdot \omega^{[[\phi]]-[[\psi]]}\} \in \mathbb{R}$ for $i,j \in \mathbb{V}$, $\phi \in \Phi^i$, $\psi \in \Phi^j$. Here, $\mathbb{R}\mathrm{e}\{\cdot\}$ and $\mathbb{I}\mathrm{m}\{\cdot\}$ denote the real and imaginary parts, respectively, and $(\cdot)^*$ denotes the complex conjugate.

Let $v^{(i:\phi)}(t)$ denote the squared voltage magnitude of phase $\phi \in \Phi^i$ at node $i \in \mathbb{V}$, at time $t\Delta$, and let $\boldsymbol{v}^i(t) \coloneqq [\{v^{(i:\phi)}(t)\}_{\phi\in\Phi^i}]^\top \in \mathbb{R}^{|\Phi^i|}$ for all $i \in \mathbb{V}$, $t \in \mathcal{S}$. Then, by concatenating voltages across all supply points in $\mathcal{K}$ at time $t\Delta$, we define $\boldsymbol{V}(t) \coloneqq [\boldsymbol{v}^1(t)^\top, \ldots, \boldsymbol{v}^i(t)^\top, \ldots, \boldsymbol{v}^k(t)^\top]^\top \in \mathbb{R}^K$. Let v^0 denote the squared voltage magnitude of each phase at root node 0, which we set to the squared nominal voltage. Then we define $\boldsymbol{V}^0 \coloneqq v^0\mathbf{1} \in \mathbb{R}^K$.

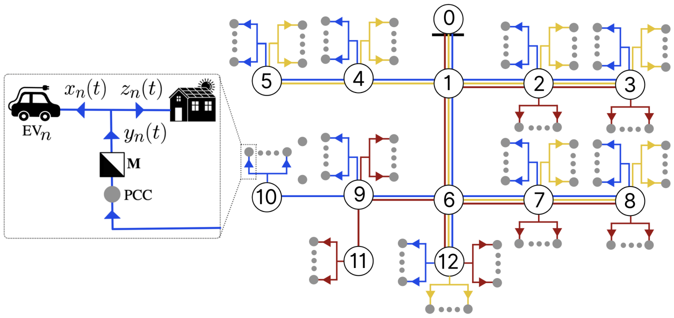

Fig. 2. The IEEE 13 node test feeder [29], a representative unbalanced distribution circuit where $k = 12$ and $K = 29$. Following the setup in [7], $N^{(i:\phi)} = 0$ for nodes $i \in \{1, 6\}$ and $N^{(i:\phi)} \geq 0$ for nodes $i \in \{2, \ldots, 5, 7, \ldots, 12\}$. Left: an expanded view of a REES connected to single-phase node 10.

Let $p^{(i:\phi)}(t) \geq 0$ (or $p^{(i:\phi)}(t) < 0$) and $q^{(i:\phi)}(t) \geq 0$ (or $q^{(i:\phi)}(t) < 0$) denote the net real power (in kW) and net reactive power (in kVAR) consumption (or injection), respectively, on phase $\phi \in \Phi^i$ at node $i \in \mathbb{V}$ over the period $\big((t-1)\Delta, t\Delta\big)$. Specifically, $p^{(i:\phi)}(t)$ and $q^{(i:\phi)}(t)$ are the net real and reactive powers arising from $N^{(i:\phi)}$ number of customers attached to supply point $(i{:}\phi)$. Let $\boldsymbol{p}^i(t) \coloneqq [\{p^{i:\phi}\}_{\phi\in\Phi^i}(t)]^\top \in \mathbb{R}^{|\Phi^i|}$ and $\boldsymbol{q}^i(t) \coloneqq [\{q^{i:\phi}\}_{\phi\in\Phi^i}(t)]^\top \in \mathbb{R}^{|\Phi^i|}$ for $i \in \mathbb{V}$, $t \in \mathcal{S}$. Then the net real power and reactive power consumed (and injected) across all supply points in $\mathcal{K}$ over the period $\big((t-1)\Delta, t\Delta\big)$ are defined by $\boldsymbol{P}(t) \coloneqq [\boldsymbol{p}^1(t)^\top, \ldots, \boldsymbol{p}^i(t)^\top, \ldots, \boldsymbol{p}^k(t)^\top]^\top \in \mathbb{R}^K$ and $\boldsymbol{Q}(t) \coloneqq [\boldsymbol{q}^1(t)^\top, \ldots, \boldsymbol{q}^i(t)^\top, \ldots, \boldsymbol{q}^k(t)^\top]^\top \in \mathbb{R}^K$.

Recall, the supply point $(i{:}\phi) \in \mathcal{K}$ serves $N^{(i:\phi)}$ number of customers, meaning that the EV and non-EV loads in all of their REESs contribute to the net real and net reactive power flows, $p^{(i:\phi)}(t)$ and $q^{(i:\phi)}(t)$, respectively. To represent the non-EV power flows at a single supply point $(i{:}\phi) \in \mathcal{K}$, we denote by $\widetilde{p}^{(i:\phi)}(t) \geq 0$ (or $\widetilde{p}^{(i:\phi)}(t) < 0$) and $\widetilde{q}^{(i:\phi)}(t) \geq 0$ (or $\widetilde{q}^{(i:\phi)}(t) < 0$) the net real power (in kW) and net reactive power (in kVAR) consumed (or injected) by all non-EV loads connected to phase $\phi \in \Phi^i$ at node $i \in \mathbb{V}$ over the period $\big((t-1)\Delta, t\Delta\big)$. Likewise, to represent EV power flows at a single supply point $(i{:}\phi) \in \mathcal{K}$, we denote by $\widehat{p}^{(i:\phi)}(t) \geq 0$ (or $\widehat{p}^{(i:\phi)}(t) < 0$) and $\widehat{q}^{(i:\phi)}(t) \geq 0$ (or $\widehat{q}^{(i:\phi)}(t) < 0$) the net real power (in kW) and net reactive power (in kVAR) consumed (or injected) by all EVs connected to phase $\phi \in \Phi^i$ at node $i \in \mathbb{V}$ over the period $\big((t-1)\Delta, t\Delta\big)$.

Let $\widetilde{p}^i(t) \coloneqq [\widetilde{p}^{(i:\phi)}(t)\}_{\phi\in\Phi^i}]^\top \in \mathbb{R}^{|\Phi^i|}$, $\widehat{p}^i(t) \coloneqq [\{\widehat{p}^{(i:\phi)}(t)\}_{\phi\in\Phi^i}]^\top \in \mathbb{R}^{|\Phi^i|}$, $\widetilde{q}^i(t) \coloneqq [\widetilde{q}^{(i:\phi)}(t)\}_{\phi\in\Phi^i}]^\top \in \mathbb{R}^{|\Phi^i|}$, and $\widehat{q}^i(t) \coloneqq [\{\widehat{q}^{(i:\phi)}(t)\}_{\phi\in\Phi^i}]^\top \in \mathbb{R}^{|\Phi^i|}$ for all $i \in \mathbb{V}$, $t \in \mathcal{S}$. Then, by concatenating power flows across all supply points over the period $\big((t-1)\Delta$, we define $\widetilde{\boldsymbol{P}}(t) \coloneqq [\widetilde{p}^1(t)^\top, \ldots, \widetilde{p}^i(t)^\top, \ldots, \widetilde{p}^k(t)^\top]^\top \in \mathbb{R}^K$, $\widetilde{\boldsymbol{Q}}(t) \coloneqq [\widetilde{q}^1(t)^\top, \ldots, \widetilde{q}^i(t)^\top, \ldots, \widetilde{q}^k(t)^\top]^\top \in \mathbb{R}^K$, $\widehat{\boldsymbol{P}}(t) \coloneqq [\widehat{p}^1(t)^\top, \ldots, \widehat{p}^i(t)^\top, \ldots, \widehat{p}^k(t)^\top]^\top \in \mathbb{R}^K$ and $\widehat{\boldsymbol{Q}}(t) \coloneqq [\widehat{q}^1(t)^\top, \ldots, \widehat{q}^i(t)^\top, \ldots, \widehat{q}^k(t)^\top]^\top \in \mathbb{R}^K$ for all $t \in \mathcal{S}$.

To model the physics of unbalanced, radial distribution grids, we leverage the power flow equations proposed in [30, 31], which is an extension of the LinDistFlow (linearized DistFlow) equations designed for single-phase grids to the unbalanced setting. Specifically, the lineraized power flow equations in [30, 31] are derived by dropping the terms related to losses, such that $p^{(i:\phi)}(t) = \widetilde{p}^{(i:\phi)}(t) + \widehat{p}^{(i:\phi)}(t)$ and $q^{(i:\phi)}(t) = \widetilde{q}^{(i:\phi)}(t) + \widehat{q}^{(i:\phi)}(t)$ for all $i \in \mathbb{V}$, $\phi \in \Phi^i$, $t \in \mathcal{S}$, implying $\boldsymbol{P}(t) = \widetilde{\boldsymbol{P}}(t) + \widehat{\boldsymbol{P}}(t)$, $\boldsymbol{Q}(t) = \widetilde{\boldsymbol{Q}}(t) + \widehat{\boldsymbol{Q}}(t)$ for all $t \in \mathcal{S}$. Then the unbalanced version of the LinDistFlow equation becomes,

$$\boldsymbol{V}(t) = \boldsymbol{V}^0 - \boldsymbol{R}\boldsymbol{P}(t) - \boldsymbol{X}\boldsymbol{Q}(t). \tag{11}$$

Let $\widetilde{\boldsymbol{V}}(t) \coloneqq \boldsymbol{V}^0 - \boldsymbol{R}\widetilde{\boldsymbol{P}}(t) - \boldsymbol{X}\widetilde{\boldsymbol{Q}}(t) \in \mathbb{R}^K$ represent the squared *baseline voltages* arising from the aggregate non-EV load, which we refer to as the *baseline load* over the period $\big((t-1)\Delta, t\Delta\big)$. To simplify our formulations, we assume EVs only consume or supply real power[i], as done in [2, 7]. That is, $\widehat{q}^{(i:\phi)}(t)=0$ for all $t\in\mathcal{S}$, $i\in\mathbb{V}$ and $\phi\in\Phi^i$, implying $\widehat{\boldsymbol{Q}}(t)=\mathbf{0}$. Consequently, Eq. (11) becomes,

$$\boldsymbol{V}(t)=\widetilde{\boldsymbol{V}}(t)-\boldsymbol{R}\widehat{\boldsymbol{P}}(t). \tag{12}$$

For the special case where all EVs are disconnected, $\widehat{\boldsymbol{P}}(t)=\mathbf{0}$, so that the grid voltages reduce to the baseline voltages, i.e., $\boldsymbol{V}(t)^{\frac{1}{2}}=\widetilde{\boldsymbol{V}}(t)^{\frac{1}{2}}$. We now reformulate (12) in terms of the power transfer from each EV_n ($n\in\mathcal{N}$). To do that, we define by $\boldsymbol{\mathcal{X}}(t):=[x_1(t),\dots,x_n(t),\dots,x_N(t)]^\top\in\mathbb{R}^N$ the set of charge and discharge rates of all EVs over the period $\big((t-1)\Delta,t\Delta\big)$, where the n^{th} element represents the charge (or discharge) rate of $\text{EV}_n(n\in\mathcal{N})$. Then, by combining Eq. (9) with $\boldsymbol{\mathcal{X}}(t)$, $\widehat{\boldsymbol{P}}(t)$ can be alternatively written as

$$\widehat{\boldsymbol{P}}(t)=\boldsymbol{\Upsilon}\boldsymbol{\mathcal{X}}(t) \tag{13}$$

for all $t\in\mathcal{S}$. Let $\boldsymbol{D}:=-\boldsymbol{R}\boldsymbol{\Upsilon}\in\mathbb{R}^{K\times N}$, where $\boldsymbol{D}=[\boldsymbol{D}_1,\dots,\boldsymbol{D}_n,\dots,\boldsymbol{D}_N]$ and $\boldsymbol{D}_n\in\mathbb{R}^K$ for $n\in\mathcal{N}$. Combining Eqs. (12)-(13) gives $\boldsymbol{V}(t)=\widetilde{\boldsymbol{V}}(t)+\boldsymbol{D}\boldsymbol{\mathcal{X}}(t)$. Then by expanding $\boldsymbol{V}(t)$ in the temporal direction over a time-horizon $[0,T\Delta]$, we obtain $\boldsymbol{V}:=[\boldsymbol{V}(1)^\top,\dots,\boldsymbol{V}(t)^\top,\dots,\boldsymbol{V}(T)^\top]^\top\in\mathbb{R}^{KT}$. Let $\widetilde{\boldsymbol{V}}:=[\widetilde{\boldsymbol{V}}(1)^\top,\dots,\widetilde{\boldsymbol{V}}(t)^\top,\dots,\widetilde{\boldsymbol{V}}(t)^\top]^\top\in\mathbb{R}^{KT}$, and let $\overline{\boldsymbol{D}}_n:=\oplus_1^T\boldsymbol{D}_n\in\mathbb{R}^{KT\times T}$ for $n\in\mathcal{N}$. Then,

$$\boldsymbol{V}=\widetilde{\boldsymbol{V}}+\textstyle\sum_{n=1}^N\overline{\boldsymbol{D}}_n\boldsymbol{x}_n. \tag{14}$$

B. Network-aware EV battery scheduling

We now formulate a centralized EV charge-discharge optimization problem, in which we constrain the voltage magnitude on each phase $\phi\in\Phi^i$ at each node $i\in\mathbb{V}$, to stay within an operational range $[\underline{v}^{(i:\phi)}\ ,\overline{v}^{(i:\phi)}\ ]$, where $\underline{v}^{(i:\phi)}\in\mathbb{R}$ and $\overline{v}^{(i:\phi)}\in\mathbb{R}$ denote the respective lower and upper bounds for the voltage magnitude. By defining $\underline{\boldsymbol{v}}:=[[\{\underline{v}^{1:\phi}\}_{\phi\in\Phi^1}],\dots,[\{\underline{v}^{i:\phi}\}_{\phi\in\Phi^i}],\dots,[\{\underline{v}^{k:\phi}\}_{\phi\in\Phi^k}]]^\top\in\mathbb{R}^K$ and $\overline{\boldsymbol{v}}:=[[\{\overline{v}^{1:\phi}\}_{\phi\in\Phi^1}],\dots,[\{\overline{v}^{i:\phi}\}_{\phi\in\Phi^i}],\dots,[\{\overline{v}^{k:\phi}\}_{\phi\in\Phi^k}]]^\top\in\mathbb{R}^K$, we constrain the voltages given by Eq. (14) as follows

$$\underline{\boldsymbol{V}}\quad\le\quad\boldsymbol{V}=\widetilde{\boldsymbol{V}}+\textstyle\sum_{n=1}^N\overline{\boldsymbol{D}}_n\boldsymbol{x}_n\quad\le\quad\overline{\boldsymbol{V}}, \tag{15}$$

where $\underline{\boldsymbol{V}}:=[\underline{\boldsymbol{v}}^\top,\dots,\underline{\boldsymbol{v}}^\top,\dots,\underline{\boldsymbol{v}}^\top]^\top\in\mathbb{R}^{KT}$ and $\overline{\boldsymbol{V}}:=[\overline{\boldsymbol{v}}^\top,\dots,\overline{\boldsymbol{v}}^\top,\dots,\overline{\boldsymbol{v}}^\top]^\top\in\mathbb{R}^{KT}$. To make the presentation clearer, we define $\boldsymbol{\Gamma}_n:=[\overline{\boldsymbol{D}}_n^\top\ -\overline{\boldsymbol{D}}_n^\top]^\top\in\mathbb{R}^{2KT\times T}$ and $\boldsymbol{w}:=[(\overline{\boldsymbol{V}}-\widetilde{\boldsymbol{V}})^\top\ (-\underline{\boldsymbol{V}}+\widetilde{\boldsymbol{V}})^\top]^\top\in\mathbb{R}^{2KT}$, such that the *voltage constraint* can alternatively be expressed as

$$\textstyle\sum_{n=1}^N\boldsymbol{\Gamma}_n\boldsymbol{x}_n\le\boldsymbol{w}. \tag{16}$$

For each customer $n\in\mathcal{N}$, the operational cost accrued by EV_n over the planning time-horizon $[0,T\Delta]$ is given by $\Omega_n(\boldsymbol{x}_n)$ (8), and in this paper, we seek to minimize the total operational cost accrued by all customers, $\sum_{n\in\mathcal{N}}\Omega_n(\boldsymbol{x}_n)$, subject to the feasibility sets Ψ_n (7) and the voltage constraint (16). Accordingly, the centralized optimization problem ($\mathcal{P}1$) is succinctly written as,

$$\min_{\boldsymbol{x}_1,\dots,\boldsymbol{x}_N\in\mathbb{R}^T}\quad\textstyle\sum_{n=1}^N\Omega_n(\boldsymbol{x}_n) \tag{$\mathcal{P}1.1$}$$

$$\text{subject to}\quad\boldsymbol{x}_n\in\Psi_n\quad;\ \forall n\in\mathcal{N}, \tag{$\mathcal{P}1.2$}$$

$$\textstyle\sum_{n=1}^N\boldsymbol{\Gamma}_n\boldsymbol{x}_n\le\boldsymbol{w}, \tag{$\mathcal{P}1.3$}$$

where ($\mathcal{P}1.2$) is separable and ($\mathcal{P}1.3$) is coupled across EVs.

[i]Inclusion of reactive powers for EVs and non-EV loads, $\widehat{q}^{(i:\phi)}(t)$ and $\widetilde{q}^{(i:\phi)}(t)$, doubles the number of decision variables in the optimization problem, however, Algorithm 1 remains still applicable with a slight variation in the definition of $\boldsymbol{u}_n$, where $\boldsymbol{u}_n$ becomes $\boldsymbol{u}_n:=[\boldsymbol{x}_n^\top\quad\boldsymbol{q}_n^\top\quad\boldsymbol{s}_n^\top]^\top$.

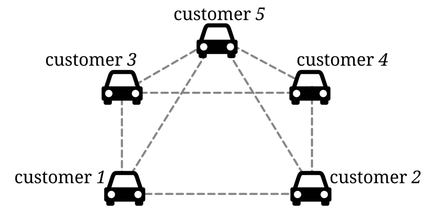

Fig. 3. An example of a peer-to-peer communication network represented by a graph $\mathcal{G}=\{\mathcal{N},\mathcal{E}\}$, where $\mathcal{N}=\{1,2,3,4,5\}$ and $\mathcal{E}=\{(12),(13),(15),(24),(25),(34),(35),(45)\}$. Moreover, $\mathcal{N}_1=\{2,3,5\}$, $\mathcal{N}_2=\{1,4,5\}$, $\mathcal{N}_3=\{1,4,5\}$, $\mathcal{N}_4=\{2,3,5\}$ and $\mathcal{N}_5=\{1,2,3,4\}$.

IV. A Distributed Approach for Network-aware EV Battery Scheduling

Drawing on the ADMM theory [32] and the consensus theory [33], we now develop a fully parallelized, distributed optimization-based algorithm to solve the optimization problem ($\mathcal{P}1$), defined in Section III. Specifically, the proposed algorithm assumes a peer-to-peer EV communication network with no central entity, wherein EVs determine their power profiles locally by exchanging coordination signals amongst themselves.

A. EV communication network

Consider a peer-to-peer communication network represented by an undirected graph $\mathcal{G}:=\{\mathcal{N},\mathcal{E}\}$, where the vertex-set $\mathcal{N}=\{1,\dots,n,\dots,N\}$ is the set of EV customers (as defined in Section II) and the edge-set $\mathcal{E}\subseteq\mathcal{N}\times\mathcal{N}$ is the set of communication links between EV customers (an example is presented in Fig. 3). The presence of edge $(nm)\in\mathcal{E}$ enables customer n to exchange information with customer m. Accordingly, $\mathcal{N}_n:=\{m\in\mathcal{N}\mid(nm)\in\mathcal{E}\}$ is defined as the set of neighboring customers from which customer n can receive information.

B. Proposed algorithm formulation

The optimization problem ($\mathcal{P}1$) in its present form cannot be solved directly using ADMM. Therefore, we first transform the inequality constraint ($\mathcal{P}1.3$) into an equality by introducing a vector of slack variables $\boldsymbol{s}_n\in\mathbb{R}^{2KT}$ for each customer $n\in\mathcal{N}$, which satisfy

$$\textstyle\sum_{n=1}^N\big(\boldsymbol{\Gamma}_n\boldsymbol{x}_n+\boldsymbol{s}_n\big)=\boldsymbol{w}. \tag{17}$$

Let $\boldsymbol{u}_n:=[\boldsymbol{x}_n^\top\quad\boldsymbol{s}_n^\top]^\top\in\mathbb{R}^{T+2KT}$ and $\mathcal{S}_n:=\{\boldsymbol{s}_n{:}\boldsymbol{s}_n\ge\mathbf{0}\}$. Then we define an indicator function $\mathcal{I}_n(\boldsymbol{u}_n)$ for each customer $n\in\mathcal{N}$ as

$$\mathcal{I}_n(\boldsymbol{u}_n):=\begin{cases}0 & \text{if}\quad\boldsymbol{u}_n\in\Xi_n,\\ \infty & \text{if}\quad\boldsymbol{u}_n\notin\Xi_n,\end{cases} \tag{18}$$

where $\Xi_n:=\Psi_n\times\mathcal{S}_n$ (Ψ_n is defined in (7)).

Lemma 1. *Let the local cost function for a single EV customer $n\in\mathcal{N}$ be denoted by $f_n(\boldsymbol{u}_n):=\Omega_n(\boldsymbol{u}_n)+\mathcal{I}_n(\boldsymbol{u}_n)$. Let $\boldsymbol{\xi}_n:=\begin{bmatrix}\boldsymbol{\Gamma}_n & \mathbf{I}\end{bmatrix}^\top\in\mathbb{R}^{2KT\times(T+2KT)}$ where $\mathbf{I}\in\mathbb{R}^{2KT\times 2KT}$. Then the optimization problem ($\mathcal{P}1$) is equivalent to the optimization problem ($\mathcal{P}2$), which is defined by*

$$\min_{\boldsymbol{u}_1,\dots,\boldsymbol{u}_N\in\mathbb{R}^{T+2KT}}\quad\textstyle\sum_{n=1}^N f_n(\boldsymbol{u}_n) \tag{$\mathcal{P}2.1$}$$

$$\text{subject to}\quad\textstyle\sum_{n=1}^N\boldsymbol{\xi}_n\boldsymbol{u}_n=\boldsymbol{w}. \tag{$\mathcal{P}2.2$}$$

The result follows directly by substituting voltage constraint (17) *and indicator function* (18) *into* ($\mathcal{P}1$). ■

Since strong duality holds for optimization problem ($\mathcal{P}2$) [34], we formulate its dual optimization problem ($\mathcal{P}3$) as

$$\min_{\boldsymbol{\lambda}\in\mathbb{R}^{2KT}} \sum_{n=1}^{N} \left(\boldsymbol{\Theta}_n(\boldsymbol{\lambda}) + \tfrac{1}{N}\boldsymbol{\lambda}^\top \boldsymbol{w}\right) \qquad (\mathcal{P}3.1)$$

$$\text{where } \boldsymbol{\Theta}_n(\boldsymbol{\lambda}) = \max_{\boldsymbol{u}_n\in\mathbb{R}^{T+2KT}} \left(-f_n(\boldsymbol{u}_n) - \boldsymbol{\lambda}^\top \boldsymbol{\xi}_n \boldsymbol{u}_n\right) \quad (\mathcal{P}3.2)$$

for all $n \in \mathcal{N}$. Here, $\boldsymbol{\lambda} \in \mathbb{R}^{2KT}$ is the Lagrange dual variable vector corresponding to constraint ($\mathcal{P}2.2$). Since $\boldsymbol{\lambda}$ is a global vector that requires to be computed by a central entity, the optimization problem ($\mathcal{P}3$) is not separable across customers. Interestingly, by leveraging the Dual Consensus - ADMM (DC-ADMM [35]) approach, a distributed counterpart for ($\mathcal{P}3$) can be obtained. We start by making the following assumption on graph $\mathcal{G}$.

Assumption 1. *Graph $\mathcal{G} := \{\mathcal{N}, \mathcal{E}\}$ is connected, that is, for every pair of vertices in $\mathcal{N}$, there exists a path of edges in $\mathcal{E}$ that connects them.*

Next, each customer $n \in \mathcal{N}$ is allocated with a local copy (estimate) of $\boldsymbol{\lambda}$, denoted by $\boldsymbol{\lambda}_n \in \mathbb{R}^{2KT}$. In this way, it is possible to remove the requirement for a central entity and incorporate $\boldsymbol{\lambda}_n$ as a *coordination signal* amongst EV customers connected via a peer-to-peer communication network. Then, under Assumption 1, ($\mathcal{P}3$) can be equivalently written as ($\mathcal{P}4$):

$$\min_{\substack{\boldsymbol{\lambda}_1,\ldots,\boldsymbol{\lambda}_N\in\mathbb{R}^{2KT}\\ \{\boldsymbol{\beta}_{nm}\}\in\mathbb{R}^{2KT}}} \sum_{n=1}^{N} \left(\boldsymbol{\Theta}_n(\boldsymbol{\lambda}_n) + \tfrac{1}{N}\boldsymbol{\lambda}_n^\top \boldsymbol{w}\right) \qquad (\mathcal{P}4.1)$$

$$\text{subject to} \quad \boldsymbol{\lambda}_n = \boldsymbol{\beta}_{nm} \quad ; \forall m \in \mathcal{N}_n,\ n \in \mathcal{N}, \quad (\mathcal{P}4.2)$$

$$\boldsymbol{\lambda}_m = \boldsymbol{\beta}_{nm} \quad ; \forall m \in \mathcal{N}_n,\ n \in \mathcal{N}, \quad (\mathcal{P}4.3)$$

where $\{\boldsymbol{\beta}_{nm}\}_{n\in\mathcal{N}, m\in\mathcal{N}_n} \in \mathbb{R}^{2KT}$ is the sequence of consensus auxiliary variables. According to ($\mathcal{P}4$), each customer $n \in \mathcal{N}$ can minimize its local objective function in ($\mathcal{P}4.1$) subject to their local consensus constraints in ($\mathcal{P}4.2$)-($\mathcal{P}4.3$).

Let $\{\boldsymbol{\mu}_{nm}\} \in \mathbb{R}^{2KT}$ and $\{\boldsymbol{\gamma}_{nm}\} \in \mathbb{R}^{2KT}$ denote the Lagrange dual variable vectors corresponding to constraints ($\mathcal{P}4.2$) and ($\mathcal{P}4.3$), respectively. Then, the iterative ADMM algorithm provides the following updates at each iteration $\tau(>0)$. Throughout, the iteration number is superscripted within square brackets.

$$\boldsymbol{\mu}_{nm}^{[\tau]} = \boldsymbol{\mu}_{nm}^{[\tau-1]} + \tfrac{\rho}{2}(\boldsymbol{\lambda}_n^{[\tau-1]} - \boldsymbol{\lambda}_m^{[\tau-1]}) \quad ; \forall m \in \mathcal{N}_n, \quad (19a)$$

$$\boldsymbol{\gamma}_{nm}^{[\tau]} = \boldsymbol{\gamma}_{nm}^{[\tau-1]} + \tfrac{\rho}{2}(\boldsymbol{\lambda}_m^{[\tau-1]} - \boldsymbol{\lambda}_n^{[\tau-1]}) \quad ; \forall m \in \mathcal{N}_n, \quad (19b)$$

where $\rho > 0$ is a penalty parameter. The initial values of $\boldsymbol{\mu}_{nm}$ and $\boldsymbol{\gamma}_{nm}$ are set as $\boldsymbol{\mu}_{nm}^{[0]} = \boldsymbol{0}$ and $\boldsymbol{\gamma}_{nm}^{[0]} = \boldsymbol{0}$ for all $n \in \mathcal{N}$, $m \in \mathcal{N}_n$. Let $\boldsymbol{\nu}_n^{[\tau]} := \sum_{m\in\mathcal{N}_n}(\boldsymbol{\mu}_{nm}^{[\tau]} + \boldsymbol{\gamma}_{mn}^{[\tau]}) \in \mathbb{R}^{2KT}$, which when combined with (19a) and (19b) yields

$$\boldsymbol{\nu}_n^{[\tau]} = \boldsymbol{\nu}_n^{[\tau-1]} + \rho \sum_{m\in\mathcal{N}_n}(\boldsymbol{\lambda}_n^{[\tau-1]} - \boldsymbol{\lambda}_m^{[\tau-1]}). \quad (20)$$

Next, $\boldsymbol{\lambda}_n^{[\tau]}$ is updated by solving the following *subproblem* for each customer $n \in \mathcal{N}$,

$$\boldsymbol{\lambda}_n^{[\tau]} = \arg\min_{\boldsymbol{\lambda}_n} \Big\{ \Theta_n(\boldsymbol{\lambda}_n) + \tfrac{1}{N}\boldsymbol{\lambda}_n^\top \boldsymbol{w} + \boldsymbol{\lambda}_n^\top \boldsymbol{\nu}_n^{[\tau]} + \rho \sum_{m\in\mathcal{N}_n} \left\| \boldsymbol{\lambda}_n - \tfrac{\boldsymbol{\lambda}_n^{[\tau-1]} + \boldsymbol{\lambda}_m^{[\tau-1]}}{2} \right\|_2^2 \Big\}. \quad (21)$$

Substituting $\Theta_n(\boldsymbol{\lambda}_n)$ from ($\mathcal{P}4$) into (21) shows that the above *subproblem* (21) is a min-max optimization problem, which is given by

$$\boldsymbol{\lambda}_n^{[\tau]} = \arg\min_{\boldsymbol{\lambda}_n}\max_{\boldsymbol{u}_n} \Big\{ -f_n(\boldsymbol{u}_n) - \boldsymbol{\lambda}_n^\top \boldsymbol{\xi}_n \boldsymbol{u}_n + \tfrac{1}{N}\boldsymbol{\lambda}_n^\top \boldsymbol{w} + \boldsymbol{\lambda}_n^\top \boldsymbol{\nu}_n^{[\tau]} + \rho \sum_{m\in\mathcal{N}_n} \left\| \boldsymbol{\lambda}_n - \tfrac{\boldsymbol{\lambda}_n^{[\tau-1]} + \boldsymbol{\lambda}_m^{[\tau-1]}}{2} \right\|_2^2 \Big\}. \quad (22)$$

Following [35], the objective function in (22) is convex in $\boldsymbol{\lambda}_n$ for any $\boldsymbol{u}_n$, and is concave in $\boldsymbol{u}_n$ for any $\boldsymbol{\lambda}_n$, hence the min-max theorem ([36], Proposition 2.6.2) can be applied to compute $\boldsymbol{\lambda}_n^{[\tau]}$. That is, the subproblem (22) for each customer $n \in \mathcal{N}$ can be solved by considering its max-min counterpart

$$\boldsymbol{\lambda}_n^{[\tau]} = \arg\max_{\boldsymbol{u}_n}\min_{\boldsymbol{\lambda}_n} \Big\{ -f_n(\boldsymbol{u}_n) - \boldsymbol{\lambda}_n^\top \boldsymbol{\xi}_n \boldsymbol{u}_n + \tfrac{1}{N}\boldsymbol{\lambda}_n^\top \boldsymbol{w} + \boldsymbol{\lambda}_n^\top \boldsymbol{\nu}_n^{[\tau]} + \rho \sum_{m\in\mathcal{N}_n} \left\| \boldsymbol{\lambda}_n - \tfrac{\boldsymbol{\lambda}_n^{[\tau-1]} + \boldsymbol{\lambda}_m^{[\tau-1]}}{2} \right\|_2^2 \Big\}, \quad (23)$$

where the outer maximizer $\boldsymbol{u}_n$ and the inner minimizer $\boldsymbol{\lambda}_n$ are determined by

$$\boldsymbol{u}_n^{[\tau]} = \arg\min_{\boldsymbol{u}_n\in\Xi_n} \Big\{ f_n(\boldsymbol{u}_n) + \tfrac{\rho}{4|\mathcal{N}_n|} \Big\| \tfrac{1}{\rho}\Big(\boldsymbol{\xi}_n \boldsymbol{u}_n - \tfrac{1}{N}\boldsymbol{w}\Big) - \tfrac{1}{\rho}\boldsymbol{\nu}_n^{[\tau]} + \sum_{m\in\mathcal{N}_n}\Big(\boldsymbol{\lambda}_n^{[\tau-1]} + \boldsymbol{\lambda}_m^{[\tau-1]}\Big) \Big\|_2^2 \Big\}, \quad (24)$$

$$\boldsymbol{\lambda}_n^{[\tau]} = \tfrac{1}{2|\mathcal{N}_n|} \Big\{ \sum_{m\in\mathcal{N}_n}\Big(\boldsymbol{\lambda}_n^{[\tau-1]} + \boldsymbol{\lambda}_m^{[\tau-1]}\Big) - \tfrac{1}{\rho}\boldsymbol{\nu}_n^{[\tau]} + \tfrac{1}{\rho}\Big(\boldsymbol{\xi}_n \boldsymbol{u}_n^{[\tau]} - \tfrac{1}{N}\boldsymbol{w}\Big) \Big\}. \quad (25)$$

Consequently, the solution to subproblem (22) is obtained for each customer $n \in \mathcal{N}$ by first solving the subproblem (24) with respect to the primal variable $\boldsymbol{u}_n$, followed by evaluating $\boldsymbol{\lambda}_n$ using Eq. (25). Importantly, while DC-ADMM handles the dual problem in ($\mathcal{P}3$), it directly yields the primal optimal solution to ($\mathcal{P}2$), as stated in the following theorem.

Theorem 1. *Suppose Assumption 1 holds. Then*

(1) the sequence of dual variables, $\{\boldsymbol{\lambda}_n^{[\tau]}\}_{n\in\mathcal{N}}$, as defined in (25)*, converges to $\boldsymbol{\lambda}$, and*

(2) the sequence of primal variables, $\{\boldsymbol{u}_n^{[\tau]}\}_{n\in\mathcal{N}}$, as defined in (24)*, converges to $\{\boldsymbol{u}_n\}_{n\in\mathcal{N}}$.*

The proof is in the Appendix. ■

With the above as background, Algorithm 1 presents our approach to distributed EV charging and discharging, referred to as Dis-Net-EVCD. In Algorithm 1, each of the computational steps is executed by each customer $n \in \mathcal{N}$ in parallel without requiring the intervention of a central coordinator. More importantly, Dis-Net-EVCD respects EV user privacy as EVs coordinate amongst themselves by exchanging locally computed $\boldsymbol{\lambda}_n$ vectors, which do not carry EV-specific operational information nor EV-specific battery parameters.

In addition, Algorithm 1 is implemented with *Receding Horizon Optimization (RHO)*, whereby lines 2-21 are repeatedly executed on time intervals of Δ. For each repetition of lines 2-21, a time index denoted by $\ell \geq 0$ is incremented and the optimization is performed considering a time window $[\ell\Delta, (\ell+T)\Delta]$. In this way, Algorithm 1 accommodates non-deterministic (or near-real-time updates to) EV arrival-departure times and EV charging demands.

In more detail, Algorithm 1 consists of an ADMM based *iterative routine* from lines 7-13 and a *receding-horizon routine*, as in [2], from lines 16-20. The iterative routine from lines 7-13 is executed until an agreed $\boldsymbol{\lambda}_n$ is reached across all customers in $\mathcal{N}$. We note that the computational steps within the iterative routine (i.e., lines 10-12) require as inputs, quantities that are either locally known by customer n (e.g., Λ_n, $f_n(\boldsymbol{u}_n)$,

Algorithm 1: Dis-Net-EVCD

1 Initialize time index $\ell = 0$.
2 **repeat**
3 **foreach** *grid-connected customer* $n \in \mathcal{N}$ **do**
4 Initialize $\boldsymbol{\lambda}_n^{[0]} = \mathbf{0} \in \mathbb{R}^{2KT}$, $\boldsymbol{\nu}_n^{[0]} = \mathbf{0} \in \mathbb{R}^{2KT}$.
5 Initialize iteration index $\tau = 0$.
6 **repeat**
7 Let $\tau = \tau + 1$.
8 **foreach** *grid-connected customer* $n \in \mathcal{N}$ **do**
9 Receive $\boldsymbol{\lambda}_m^{[\tau-1]}$ from each neighbor $m \in \mathcal{N}_n$.
10 With $\{\boldsymbol{\lambda}_m^{[\tau-1]}\}_{m \in \mathcal{N}_n}$, update $\boldsymbol{\nu}_n^{[\tau]}$ as per Eq. (20).
11 With $\boldsymbol{\nu}_n^{[\tau]}$ and $\{\boldsymbol{\lambda}_m^{[\tau-1]}\}_{m \in \mathcal{N}_n}$, solve subproblem (24) and obtain $\boldsymbol{u}_n^{[\tau]}$.
12 With $\{\boldsymbol{\lambda}_m^{[\tau-1]}\}_{m \in \mathcal{N}_n}$, $\boldsymbol{\nu}_n^{[\tau]}$ and $\boldsymbol{u}_n^{[\tau]}$ from lines 9-11, update $\boldsymbol{\lambda}_n^{[\tau]}$ as per Eq. (25).
13 Broadcast $\boldsymbol{\lambda}_n^{[\tau]}$ to all neighbors in $\mathcal{N}_n$.
14 **until** a stopping criterion, as in [37], is satisfied;
15 **foreach** *grid-connected customer* $n \in \mathcal{N}$ **do**
16 Let $\boldsymbol{u}_n = \boldsymbol{u}_n^{[\tau]}$ from line 11.
17 Let $\{x_n[1|\ell], \ldots, x_n[T|\ell]\} = \{u_n(1), \ldots, u_n(T)\}$, where the notation $[t|\ell]$ represents prediction time index t relative to current time index ℓ for all $t \in \mathcal{S}$, as in [2].
18 Charge (or discharge) the EV battery by $x_n[1|\ell]$ over the time-interval $\big(\ell\Delta, (\ell+1)\Delta\big)$.
19 **if** $x_n[1|\ell] \geq 0$ **then** $\mu_n[1|\ell] = \overline{\mu}_n$, **else** $\mu_n[1|\ell] = \underline{\mu}_n$.
20 Update Λ_n, such that $\hat{\sigma}_n = \hat{\sigma}_n + \Delta x_n[1|\ell]\mu_n[1|\ell]$ and $a_n = \ell + 1$, in preparation for the next time interval.
21 Advance the time index $\ell = \ell + 1$.

$\boldsymbol{\xi}_n$) or are collected from its neighbors (e.g., $\{\boldsymbol{\lambda}_m^{[\tau-1]}\}_{m \in \mathcal{N}_n}$), supporting a fully distributed implementation.

During each iteration of the iterative routine from lines 7-13, each customer $n \in \mathcal{N}$ first receives the local estimates $\{\boldsymbol{\lambda}_m^{[\tau-1]}\}_{m \in \mathcal{N}_n}$ from its neighbors $m \in \mathcal{N}_n$, and executes the recursive tasks in lines 10-12, which entail local updates of $\boldsymbol{\nu}_n^{[\tau]}, \boldsymbol{u}_n^{[\tau]}$ and $\boldsymbol{\lambda}_n^{[\tau]}$. In line 10, the sequence of $\{\boldsymbol{\lambda}_m^{[\tau-1]}\}_{m \in \mathcal{N}_n}$ vectors received from the neighbors of customer n are incorporated into Eq. (20) and the dual vector $\boldsymbol{\nu}_n^{[\tau]}$ is updated. Subsequently, in line 11, $\boldsymbol{\nu}_n^{[\tau]}$ jointly with $\{\boldsymbol{\lambda}_m^{[\tau-1]}\}_{m \in \mathcal{N}_n}$ enables the customer to calculate $\boldsymbol{u}_n^{[\tau]}$ by solving the quadratic subproblem (24). Then, in line 12, $\boldsymbol{\lambda}_n^{[\tau]}$ is updated as per Eq. (25) to proceed to the next iteration. Likewise, the iterative routine continues until a predefined stopping criterion is reached. As proposed in [37], the iterative routine in this paper is set to stop when the iteration number τ exceeds τ^{max} (e.g., $\tau^{max} = 1000$) or $\epsilon = \max\big\{\big\|\boldsymbol{\nu}_n^{[\tau]} - \boldsymbol{\nu}_n^{[\tau-1]}\big\|_2^2, \big\|\boldsymbol{u}_n^{[\tau]} - \boldsymbol{u}_n^{[\tau-1]}\big\|_2^2, \big\|\boldsymbol{\lambda}_n^{[\tau]} - \boldsymbol{\lambda}_n^{[\tau-1]}\big\|_2^2\big\}$ is less than a prespecified tolerance $\bar{\epsilon}$ (i.e., $\epsilon < \bar{\epsilon}$). We emphasize that Algorithm 1 is computationally efficient and easy to implement, since line 11 solves a convex optimization problem — for which commercial or open-source software [38] is available — and the updates in lines 10 and 12 involve simple arithmetic computations.

V. Numerical simulations

We evaluate Dis-Net-EVCD on the IEEE 13 node test feeder, consistent with the simulation set-up described in [31]. More specifically, the IEEE 13 node test feeder is available from [29], and it represents an unbalanced distribution circuit with single phase and two phase laterals as depicted in Fig. 2.

We consider charging and discharging of $N = 600$ customers with charge-only EVs and gridable EVs (V2G-enabled EVs) dispersed across the IEEE 13 node feeder, such that $N^{i,\phi} = 0$ for $\phi \in \Phi^i$ where $i \in \{1, 6\}$, $N^{i,\phi} = 26$ for $\phi \in \Phi^i$ where $i \in \{2,3,4,5,7,8,9,12\}$, $N^{i,\phi} = 27$ for $\phi \in \Phi^i$ where $i \in \{10, 11\}$. Customers are assigned different EV models as described in [39], with battery capacities, c_n, ranging from $[16, 90]$ kWh. Following [7], each customer $n \in \mathcal{N}$ is equipped with a level-2 charger supporting a maximum charge rate of $\overline{x}_n = 6.6$ kW and a maximum discharge rate of $\underline{x}_n = -6.6$ kW. The remaining design parameters for each EV are as described in [2], where the initial SOC of each EV$_n$, $\hat{u}_n$, is within $[0.3, 0.5]$ times the battery capacity, such that there is a uniform distribution across all initial SOCs. For each EV$_n$, $\underline{\sigma}_n = 0.2 \times c_n$, $\overline{\sigma}_n = 0.85 \times c_n$, $\alpha_n = 5 \times 10^{-4}$ and $\mu_n = 0.9$.

Our simulations consider a 24-hour time-horizon with $\Delta = 0.5$ and $T = 48$. The EV arrival and departure times, a_n and d_n, are reflective of survey data [40] gathered by the Victorian Department of Transport in Australia, which contains individual vehicle travel records for a 24 hour period.

The non-EV power consumption, $\boldsymbol{l}_n$, for each customer is obtained from a real-world dataset [41] consisting of residential load collected from households within an Australian distribution grid, as publicly released by Ausgrid, an electricity distribution company in NSW, Australia. The extracted data corresponds to residential energy consumption and solar PV power generation from a set of 300 residential customers on the 5th July 2012, a day on which several peak load conditions were observed. The extracted Ausgrid data is duplicated to populate non-EV power consumption for $h = 600$ customers. We consider a ToU financial policy as reported by AGL Energy, an Australian energy provider.

Consistent with [7], a voltage threshold of $\pm 4.6\%$ about the nominal voltage 1 p.u. is considered. All simulations are conducted in Python 3.8.2 + CVXPY [38] on a MacBook Pro with an Intel Core i5 and 8 GB memory.

In Figs. 4(a-b), we present numerical simulations corresponding to a scenario referred to as *Price-based EV Charging and Discharging (P-EVCD)*, where each EV implements a power profile designed to minimizing operational costs in the absence of voltage constraints. That is, with P-EVCD, each EV$_n$ ($n \in \mathcal{N}$) minimizes the operational cost function $\Omega_n(\boldsymbol{x}_n)$ defined in (8), subject to a local constraint set Ψ_n as defined in (7). By contrast, Figs. 4(c-d) present numerical simulations corresponding to Dis-Net-EVCD, where EVs determine power profiles as per Algorithm 1, so as to minimize operational costs subject to the voltage constraints and local constraint sets Ψ_n of all EVs in $\mathcal{N}$.

In Fig. 4(a) and Fig. 4(c), we present the sum of non-EV power profiles of all customers ($\sum_{n \in \mathcal{N}} \boldsymbol{l}_n$), referred to as the *Aggregate Non-EV Load Profile* (ANLP), the sum of EV power profiles of all customers ($\sum_{n \in \mathcal{N}} \boldsymbol{x}_n$), referred to as the *Aggregate EV Load Profile* (AELP), and the sum of grid power profiles of all customers ($\sum_{n \in \mathcal{N}} \boldsymbol{g}_n$), referred to as the *Aggregate Load Profile* (ALP). As illustrated in Fig. 4(a) and Fig. 4(c), the ANLP peaks during the peak-pricing period and then gradually declines through the shoulder-pricing period to

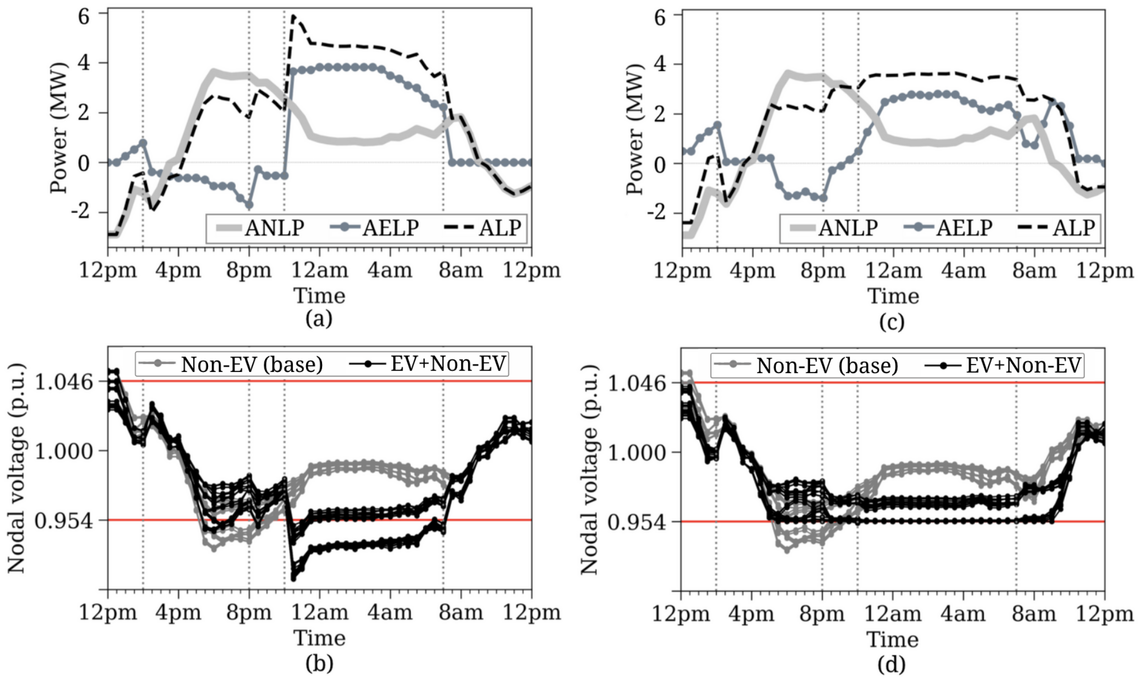

Fig. 4. (a-b) Aggregate load profiles and voltage profiles at each of the supply points $(i{:}\phi) \in \mathcal{K}$ when customers implement P-EVCD. (c-d) Corresponding aggregate load profiles and voltage profiles when customers implement Dis-Net-EVCD as per Algorithm 1. (a,c) Aggregate Non-EV Load Profile (ANLP), $\sum_n \boldsymbol{z}_n$, Aggregate EV Load Profile (AELP), $\sum_n \boldsymbol{x}_n$, and Aggregate Load Profile (ALP), $\sum_n \boldsymbol{y}_n$. (b,d) Grey dotted curves represent the baseline voltage profiles, $\widetilde{\boldsymbol{V}}^{\frac{1}{2}}$ (arising from non-EV load as in Eq. (14)). Black dotted curves represent the grid voltage profiles, $\boldsymbol{V}^{\frac{1}{2}}$ (arising from both EV and non-EV load as in Eq. (14)). Red lines are the upper and lower voltage boundaries.
Vertical dashed lines separate pricing periods in $\boldsymbol{\eta}$, where the off-peak period is from 10 pm – 7 am, the shoulder-peak period is from 7 am – 2 pm and 8 pm – 10 pm, and the peak period is from 2 pm – 8 pm (taken from [42]).

the off-peak-pricing period, consistent with the price profile $\boldsymbol{\eta}$.

In Fig. 4(b) and Fig. 4(d), we present the voltage profile corresponding to each supply point $(i{:}\phi) \in \mathcal{K}$, which is defined by $[\boldsymbol{v}^{(i:\phi)}]^{1/2} := [v^{(i:\phi)}(1)^{1/2}, \ldots, v^{(i:\phi)}(T)^{1/2}]^\top \in \mathbb{R}^T$. In particular, the grey dotted lines represent the *baseline voltage profiles* arising from the non-EV load, and black dotted lines represent the *grid voltage profiles* arising from the combined EV and non-EV load. An important observation from Fig. 4(b) and Fig. 4(d) is that some baseline voltage profiles drop to voltages below 0.954 p.u. (between 5 – 9.30 pm) and rises to voltages above 1.046 p.u. (between 12 – 12.30 pm), which are outside the aforementioned voltage operating limits.

Consider P-EVCD as in Figs. 4(a-b). In Fig. 4(a), we observe that the ALP falls to -2.85 MW and rises to 6 MW. The ALP valley corresponding to -2.85 MW occurs at 12 pm when the non-EV load is at its lowest — a consequence of surplus rooftop PV generation. The ALP peak corresponding to 6 MW occurs at 10.30 pm, when EVs collectively charge during the off-peak pricing period. In Fig. 4(a), we also observe that the AELP reflects a short charging period from 12 – 2 pm (coincident with shoulder-peak pricing period), arising from gridable EVs (in particular, gridable EVs with lower SoCs). Here, the gridable EV batteries charge ahead of the peak pricing period, in preparation for a discharging cycle during the peak pricing period. We further observe that the AELP continues to rise from 12 - 2 pm, as a consequence of more gridable EVs grid-connecting, and thus being available for charging. Then, during the peak period from 2 – 8 pm, we observe that the AELP reflects a discharging period, where gridable EVs are compensated to reduce their operational costs. From 2 - 8 pm, the AELP gradually descends as a consequence of more gridable EVs grid-connecting, and thus being available for discharging. Then, during the shoulder pricing period from 8 – 10 pm, we observe that the AELP reflects a decrease in EV discharge load, since most EVs have an insufficient SoC to continue discharging, and fewer EVs (who have arrived late) continue to discharge.

In Fig. 4(a), we observe that the AELP reflects a substantial charging load during the off-peak pricing period from 10 pm – 7 am, which fills the over-night valley of the ANLP. As a result, in Fig. 4(b), we observe that the grid voltage profiles arising from P-EVCD (black dotted curves) undergo voltage dips that exceed the lower voltage boundary — resulting in voltage violations across the IEEE 13 node distribution feeder. Specifically, the largest voltage violation in Fig. 4(b) occurs at 10.30 pm, coincident with the highest ALP peak in Fig. 4(a), which is caused by the enormous charging load during the off-peak pricing period.

Consider Dis-Net-EVCD as in Figs. 4(c-d). In Fig. 4(c), we observe that the ALP corresponding to Dis-Net-EVCD is flatter (with less prominent peaks and valleys) when compared to the ALP from P-EVCD in Fig. 4(a). Specifically, the ALP in Fig. 4(c) has a peak of 3.66 MW at 10.30 pm, which is 39% less than the respective ALP peak in Fig. 4(a). Such a peak load reduction is a result of the voltage constraint incorporated in Dis-Net-EVCD, which restricts EV charging and discharging to levels that maintain voltages within upper and lower limits. In Fig. 4(d), we observe that when EVs implement Dis-Net-EVCD, the grid voltage profiles (black dotted curves) across all supply points in the feeder remain within the upper and lower limit of $\pm 4.6\%$ about the nominal voltage. Importantly, Dis-Net-EVCD, as opposed to P-EVCD, corrects the voltage violations in baseline voltage profiles as observed from 12 – 12.30 pm and from 5 – 9.30 pm, and regulates the grid voltage profiles to be within the operating voltage envelope across the day. In addition, Dis-Net-EVCD completes all EV charging demands ahead of their departures.

The total operational cost, $\sum_{n=1}^{N} \Omega_n(\boldsymbol{x}_n)$, corresponding to P-EVCD in Figs. 4(a-b) is 391 AUD, and Dis-Net-EVCD in Figs. 4(c-d) is 483 AUD, meaning that voltage regulation with Dis-Net-EVCD results in an increased operational cost compared to P-EVCD. However, Dis-Net-EVCD significantly reduces operational costs (by 78%) when compared to uncoordinated EV charging (where EVs are assumed to be charging at their full power immediately upon arrival), in which case the operational cost is 2173 AUD.

The computational time required to produce the results depicted in Figs. 4(c-d) was approximately 5.4 s for each time index ℓ of the receding time horizon. The respective computational time excluded latencies associated with peer-to-peer communication. A centralized CVXPY Python solver, would otherwise take 5.5 minutes to produce the same results. That is, Dis-Net-EVCD is approximately 60 times more computationally efficient when compared to its centralized counterpart, where a central entity is assumed to be computing the power profiles for all EVs.

In Fig. 5, we compare the convergence of Dis-Net-EVCD with an alternative distributed and iterative algorithm called Distributed Lagrangian Primal-Dual Subgradient (DLPDS), proposed in [43]. In Fig. 5, the *error* is the normalized objective function gap between the centralized (global) algorithmic solver and the distributed algorithmic solver, corresponding to a respective iteration. Formally, error $= \frac{(obj - obj^*)}{obj^*}$, where obj^* denotes the objective function ($\mathcal{P}1.1$) result obtained with the centralized solver and obj denotes the objective function ($\mathcal{P}1.1$) result obtained with the distributed algorithm at a certain iteration. With Dis-Net-EVCD, we observe that the error reduces to 10^{-5} within only 45 iterations. In fact, the speed of convergence with Dis-Net-EVCD is much faster than DLPDS. Moreover, DLPDS also requires the communication network to be strongly connected and doubly stochastic [43], whereas Dis-Net-EVCD simply requires the communication network to be connected.

In Fig. 6, we quantify the error introduced through linearization of the unbalanced IEEE 13 node feeder, by comparing the grid voltage profiles computed with the non-linear DistFlow equations derived in [44], against the LinDistFlow equations derived in [30, 31]. Specifically, we apply the EV power profiles returned by Dis-Net-EVCD together with the residential load profiles, $\boldsymbol{l}_n$, to compute the grid voltage profiles for the linearized and non-linearized representations of IEEE 13 node feeder. In Fig. 6, we observe that the voltage gap between the linearized and non-linearized representations is as low as 0.004 p.u. Importantly, by including a lower voltage constraint of 0.954 p.u. within Dis-Net-EVCD, we observe that the voltage drop across the IEEE 13 node feeder is limited to 0.95 p.u. with a DistFlow representation of the power flow equations. A steady-state voltage of 0.95 p.u is within the voltage operating standard, as reported in [7, 45]. That is, by reducing the voltage operating envelope (i.e., by reserving a buffer voltage zone) within Dis-Net-EVCD, it is possible to correct for voltage deviations corresponding to line losses that are otherwise omitted in the LinDistFlow equations.

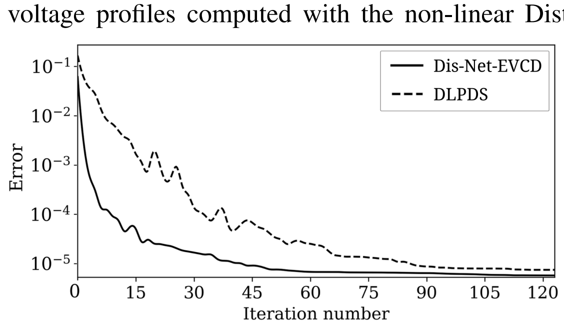

Fig. 5. Convergence of Dis-Net-EVCD against DLPDS [43]. The error versus iteration number.

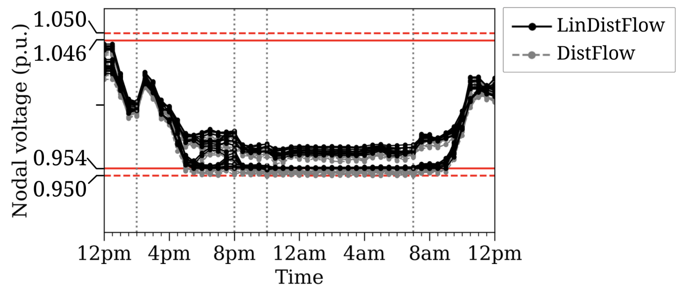

Fig. 6. Black and grey dotted lines are grid voltage profiles obtained using the LinDistFlow model [30, 31] and the DistFlow model [44], repectively.

In this work, we have employed residential EVs for voltage regulation, however, extensions of Dis-Net-EVCD to also incorporate other forms of residential battery storage systems and community energy storage systems, are possible. Our future work includes incorporating power flow limits and dynamic thermal grid constraints, incorporating EV-based inverter reactive power control, and incorporating uncertainties of non-EV demand and PV power generation.

VI. Conclusion

We have presented a distributed optimization-based, network-aware algorithm called Dis-Net-EVCD to coordinate EV charging and discharging in unbalanced distribution grids. Specifically, Dis-Net-EVCD reduces the operational costs incurred by EV customers, while regulating voltages across the distribution grid to be within the operational limits. We have proved that Dis-Net-EVCD converges to the global optimum of the underlying optimization. Through numerical simulations, it was demonstrated that Dis-Net-EVCD achieved a peak load reduction of 39% compared to a benchmark method of EV charging that minimized customer operational costs in the absence of voltage constraints. Importantly, Dis-Net-EVCD satisfied all EV charge requirements ahead of their intended departure times while alleviating potential under- and over-voltage conditions, and thereby improving power quality across the distribution grid.

Appendix

A. Proof of Theorem 1

Part (1). In ($\mathcal{P}2$), $f_n(\boldsymbol{u}_n)$: $\mathbb{R}^{T+2KT} \to \mathbb{R} \cup \infty$ ($n \in \mathcal{N}$) is a proper closed function that is composed of a smooth component $\Omega_n(\boldsymbol{u}_n)$: $\mathbb{R}^{T+2KT} \to \mathbb{R} \cup \infty$ and a non-smooth component $\mathcal{I}_n(\boldsymbol{u}_n)$: $\mathbb{R}^{T+2KT} \to \mathbb{R}\cup\infty$. The coupling equality constraint ($\mathcal{P}2.2$) is linear. Strong duality holds for ($\mathcal{P}2$) [34]. Then, from [35], it follows that when $\tau \to \infty$,

$$\boldsymbol{\lambda}_n \to \boldsymbol{\lambda},\ \boldsymbol{\lambda}_n - \boldsymbol{\lambda}_m \to \mathbf{0};\ \forall m \in \mathcal{N}_n, \tag{26}$$

for each customer $n \in \mathcal{N}$. This completes the first part of the proof.

Part (2). We show that any limit point of $\{\boldsymbol{u}_n^{[\tau]}\}_{n\in\mathcal{N}}$ is asymptotically optimal to ($\mathcal{P}2$). That is, we show that when $\tau \to \infty$,

$$\partial f_n(\boldsymbol{u}_n^{[\tau]}) + \boldsymbol{\xi}_n^\top \boldsymbol{\lambda} \to \mathbf{0};\ \forall n \in \mathcal{N}, \tag{27}$$

$$\textstyle\sum_{n=1}^N \boldsymbol{\xi}_n \boldsymbol{u}_n^{[\tau]} - \boldsymbol{w} \to \mathbf{0}. \tag{28}$$

To show (27), we consider the optimality condition of (24),

$$\mathbf{0} = \partial f_n(\boldsymbol{u}_n^{[\tau]}) + \tfrac{1}{2|\mathcal{N}_n|}\boldsymbol{\xi}_n^\top \Big\{ \tfrac{1}{\rho}\Big(\boldsymbol{\xi}_n \boldsymbol{u}_n^{[\tau]} - \tfrac{1}{N}\boldsymbol{w}\Big) - \tfrac{1}{\rho}\boldsymbol{\nu}_n^{[\tau]} + \textstyle\sum_{m\in\mathcal{N}_n} \Big(\boldsymbol{\lambda}_n^{[\tau-1]} + \boldsymbol{\lambda}_m^{[\tau-1]}\Big)\Big\}. \tag{29}$$

Substituting $\boldsymbol{\lambda}_n^{[\tau]}$ in Eq. (25) into Eq. (29) yields

$$\mathbf{0} = \partial f_n(\boldsymbol{u}_n^{[\tau]}) + \boldsymbol{\xi}_n^\top \boldsymbol{\lambda}_n^{[\tau]}. \tag{30}$$

Since (30) holds for all τ, and $\boldsymbol{\lambda}_n \to \boldsymbol{\lambda}$ by (26), the statement (27) is true.

To show (28), we rewrite Eq. (25) as

$$\mathbf{0} = -\Big(\boldsymbol{\xi}_n \boldsymbol{u}_n^{[\tau]} - \tfrac{1}{N}\boldsymbol{w}\Big) + 2\rho \textstyle\sum_{m\in\mathcal{N}_n} \Big(\boldsymbol{\lambda}_n^{[\tau]} - \frac{\boldsymbol{\lambda}_n^{[\tau]} + \boldsymbol{\lambda}_m^{[\tau]}}{2}\Big) + \boldsymbol{\nu}_n^{[\tau]} + \rho \textstyle\sum_{m\in\mathcal{N}_n} \Big(\boldsymbol{\lambda}_n^{[\tau]} + \boldsymbol{\lambda}_m^{[\tau]} - \boldsymbol{\lambda}_n^{[\tau-1]} - \boldsymbol{\lambda}_m^{[\tau-1]}\Big). \tag{31}$$

Combining with Eq. (20), Eq. (31) can be simplified as

$$\mathbf{0} = -\Big(\boldsymbol{\xi}_n \boldsymbol{u}_n^{[\tau]} - \tfrac{1}{N}\boldsymbol{w}\Big) + \boldsymbol{\nu}_n^{[\tau+1]} + \rho \textstyle\sum_{m\in\mathcal{N}_n} \Big(\boldsymbol{\lambda}_n^{[\tau]} + \boldsymbol{\lambda}_m^{[\tau]} - \boldsymbol{\lambda}_n^{[\tau-1]} - \boldsymbol{\lambda}_m^{[\tau-1]}\Big). \tag{32}$$

Further, $\sum_{n=1}^N \boldsymbol{\nu}_n^{[\tau]} = \sum_{n=1}^N \sum_{m\in\mathcal{N}_n} (\boldsymbol{\mu}_{nm}^{[\tau]} + \boldsymbol{\gamma}_{nm}^{[\tau]}) = \mathbf{0}$. Then, summing up Eq. (32) through all customers $n \in \mathcal{N}$ yields

$$\textstyle\sum_{n=1}^N \boldsymbol{\xi}_n \boldsymbol{u}_n^{[\tau]} - \boldsymbol{w} = \rho \sum_{n=1}^N \sum_{m\in\mathcal{N}_n} \Big(\boldsymbol{\lambda}_n^{[\tau]} + \boldsymbol{\lambda}_m^{[\tau]} - \boldsymbol{\lambda}_n^{[\tau-1]} - \boldsymbol{\lambda}_m^{[\tau-1]}\Big). \tag{33}$$

According to Part (1), when $\tau \to \infty$, $\boldsymbol{\lambda}_n^{[\tau]} - \boldsymbol{\lambda}_n^{[\tau-1]} \to \mathbf{0}$ for each $n \in \mathcal{N}$. Combining that result with (33) verifies that the statement (28) is also true. This completes the second part of the proof.

References

[1] IEA, "Global EV Outlook," 2021. [Online]. Available: https://www.iea.org/reports/global-ev-outlook-2021.

[2] N. I. Nimalsiri, E. L. Ratnam, C. P. Mediwaththe, D. B. Smith, and S. K. Halgamuge, "Coordinated charging and discharging control of electric vehicles to manage supply voltages in distribution networks: Assessing the customer benefit," *App. Energy*, vol. 291, p. 116857, 2021.

[3] S. Deilami, A. S. Masoum, P. S. Moses, and M. A. Masoum, "Real-time coordination of plug-in electric vehicle charging in smart grids to minimize power losses and improve voltage profile," *IEEE Trans. Smart Grid*, vol. 2, no. 3, pp. 456–467, 2011.

[4] J. De Hoog, T. Alpcan, M. Brazil, D. Thomas, and I. Mareels, "Optimal charging of electric vehicles taking distribution network constraints into account," *IEEE Trans. Power Syst.*, vol. 30, no. 1, pp. 365–375, May 2014.

[5] F. Marra, G. Y. Yang, C. Træholt, E. Larsen, J. Østergaard, B. Blažič, and W. Deprez, "EV charging facilities and their application in LV feeders with photovoltaics," *IEEE Trans. Smart Grid*, vol. 4, no. 3, pp. 1533–1540, 2013.

[6] X. Sun and J. Qiu, "Hierarchical voltage control strategy in distribution networks considering customized charging navigation of electric vehicles," *IEEE Trans. Smart Grid*, 2021.

[7] M. Liu, P. K. Phanivong, Y. Shi, and D. S. Callaway, "Decentralized charging control of EVs in residential distribution networks," *IEEE Trans. Control Syst. Technol.*, vol. 27, no. 1, pp. 266–281, Nov. 2017.

[8] X. Huo and M. Liu, "Decentralized electric vehicle charging control via a novel shrunken primal-multi-dual subgradient (SPMDS) algorithm," in *Proc. IEEE 59th Conf. Decis. Control*, Dec. 2020, pp. 1367–1373.

[9] X. Zhou, S. Zou, P. Wang, and Z. Ma, "Voltage regulation in constrained distribution networks by coordinating electric vehicle charging based on hierarchical ADMM," *IET Gener. Transm. Distrib.*, vol. 14, no. 17, pp. 3444–3457, 2020.

[10] L. Zhang, V. Kekatos, and G. B. Giannakis, "Scalable electric vehicle charging protocols," *IEEE Trans. Power Syst.*, vol. 32, no. 2, pp. 1451–1462, 2016.

[11] J. Then, A. P. Agalgaonkar, and K. M. Muttaqi, "Coordination of spatially distributed electric vehicle charging for voltage rise and voltage unbalance mitigation in networks with solar penetration," in *Proc. IEEE Texas Power & Energy Conf.*, 2021, pp. 1–6.

[12] S. Wang, L. Du, and Y. Li, "Decentralized volt/var control of EV charging station inverters for voltage regulation," in *Proc. IEEE Transportation Electrification Conf. & Expo.*, 2020, pp. 604–608.

[13] N. G. Omran and S. Filizadeh, "A semi-cooperative decentralized scheduling scheme for plug-in electric vehicle charging demand," *Int. J. Electr. Energy Syst.*, vol. 88, pp. 119–132, 2017.

[14] S. Zhang and K.-C. Leung, "Joint optimal power flow routing and decentralized scheduling with vehicle-to-grid regulation service," in *Proc. IEEE Int. Conf. Commun. Control Comput. Technol. Smart Grids*, 2018, pp. 1–6.

[15] T. Rahman, Y. Xu, and Z. Qu, "Continuous-domain real-time distributed admm algorithm for aggregator scheduling and voltage stability in distribution network," *IEEE Trans. Autom. Sci. Eng.*, 2021.

[16] O. Beaude, Y. He, and M. Hennebel, "Introducing decentralized ev charging coordination for the voltage regulation," in *Proc. IEEE PES Innovative Smart Grid Technol. Europe*, 2013, pp. 1–5.

[17] S. Fahmy, R. Gupta, and M. Paolone, "Grid-aware distributed control of electric vehicle charging stations in active distribution grids," *Electric Power Systems Research*, vol. 189, p. 106697, 2020.

[18] X. Zhou, P. Wang, and Z. Gao, "Admm-based decentralized charging control of plug-in electric vehicles with coupling constraints in distribution networks," in *2018 37th Chinese Control Conference (CCC)*. IEEE, 2018, pp. 2512–2517.

[19] X. Zhou, S. Zou, P. Wang, and Z. Ma, "Admm-based coordination of electric vehicles in constrained distribution networks considering fast charging and degradation," *IEEE Transactions on Intelligent Transportation Systems*, vol. 22, no. 1, pp. 565–578, 2020.

[20] X. Kou, F. Li, J. Dong, M. Starke, J. Munk, Y. Xue, M. Olama, and H. Zandi, "A scalable and distributed algorithm for managing residential demand response programs using alternating direction method of multipliers (admm)," *IEEE Transactions on Smart Grid*, vol. 11, no. 6, pp. 4871–4882, 2020.

[21] D. K. Molzahn, F. Dörfler, H. Sandberg, S. H. Low, S. Chakrabarti, R. Baldick, and J. Lavaei, "A survey of distributed optimization and control algorithms for electric power systems," *IEEE Trans. Smart Grid*, vol. 8, no. 6, pp. 2941–2962, 2017.

[22] S.-C. Tsai, Y.-H. Tseng, and T.-H. Chang, "Communication-efficient distributed demand response: A randomized admm approach," *IEEE Trans. Smart Grid*, vol. 8, no. 3, pp. 1085–1095, 2015.

[23] M. Latifi, A. Rastegarnia, A. Khalili, and S. Sanei, "Agent-based decentralized optimal charging strategy for plug-in electric vehicles," *IEEE Trans. Ind. Electron.*, vol. 66, no. 5, pp. 3668–3680, 2018.

[24] L. Wang and B. Chen, "Distributed control for large-scale plug-in electric vehicle charging with a consensus algorithm," *Int. J. Electr. Power & Energy Syst.*, vol. 109, pp. 369–383, 2019.

[25] N. I. Nimalsiri, E. L. Ratnam, D. B. Smith, C. P. Mediwaththe, and S. K. Halgamuge, "Coordinated charge and discharge scheduling of electric vehicles for load curve shaping," *IEEE Trans. Intell. Transp. Syst.*, 2021.

[26] E. L. Ratnam, S. R. Weller, and C. M. Kellett, "Central versus localized optimization-based approaches to power management in distribution networks with residential battery storage," *Int. J. Electr. Power & Energy Syst.*, vol. 80, pp. 396–406, Sep. 2016.

[27] J. Rivera, P. Wolfrum, S. Hirche, C. Goebel, and H.-A. Jacobsen, "Alternating direction method of multipliers for decentralized electric vehicle charging control," in *Proc. IEEE 52nd Conf. Decis. Control*, 2013, pp. 6960–6965.

[28] A. Hoke, A. Brissette, K. Smith, A. Pratt, and D. Maksimovic, "Accounting for lithium-ion battery degradation in electric vehicle charging optimization," *IEEE J. Emerging Sel. Top. Power Electron.*, vol. 2, no. 3, pp. 691–700, 2014.

[29] W. H. Kersting, “Radial distribution test feeders,” *IEEE Trans. Power Syst.*, vol. 6, no. 3, pp. 975–985, 1991.
[30] L. Gan and S. H. Low, “Convex relaxations and linear approximation for optimal power flow in multiphase radial networks,” in *Proc. IEEE Power Syst. Comput. Conf.*, 2014, pp. 1–9.
[31] D. B. Arnold, M. Sankur, R. Dobbe, K. Brady, D. S. Callaway, and A. Von Meier, “Optimal dispatch of reactive power for voltage regulation and balancing in unbalanced distribution systems,” in *IEEE Power Energy Soc. Gen. Meet.*, 2016, pp. 1–5.
[32] S. Boyd, N. Parikh, and E. Chu, *Distributed optimization and statistical learning via the alternating direction method of multipliers*. Now Publishers Inc, 2011.
[33] G. Mateos, J. A. Bazerque, and G. B. Giannakis, “Distributed sparse linear regression,” *IEEE Trans. Signal Process.*, vol. 58, no. 10, pp. 5262–5276, 2010.
[34] D. P. Bertsekas and J. N. Tsitsiklis, *Parallel and distributed computation: numerical methods*. Prentice-Hall Inc., 1989, vol. 23.
[35] T.-H. Chang, M. Hong, and X. Wang, “Multi-agent distributed optimization via inexact consensus ADMM,” *IEEE Trans. Signal Process.*, vol. 63, no. 2, pp. 482–497, 2014.
[36] D. Bertsekas, A. Nedic, and A. Ozdaglar, *Convex analysis and optimization*. Athena Scientific, 2003, vol. 1.
[37] G. Chen and J. Li, “A fully distributed ADMM-based dispatch approach for virtual power plant problems,” *Appl. Math. Modell.*, vol. 58, pp. 300–312, 2018.
[38] S. Diamond and S. Boyd, “CVXPY: A Python-embedded modeling language for convex optimization,” *J. Mach. Learn. Res.*, vol. 17, no. 83, pp. 1–5, 2016.
[39] Battery University. Bu-1003: Electric vehicle (EV). [Online]. Available: https://batteryuniversity.com/article/bu-1003-electric-vehicle-ev
[40] Victorian Integrated Survey of Travel and Activity. [Online]. Available: https://transport.vic.gov.au/about/data-and-research/vista
[41] E. L. Ratnam, S. R. Weller, C. M. Kellett, and A. T. Murray, “Residential load and rooftop PV generation: an australian distribution network dataset,” *Int. J. Sustainable Energy*, vol. 36, no. 8, pp. 787–806, 2017.
[42] AGL. Standard retail contracts. [Online]. Available: https://www.agl.com.au/help/rates-contracts/standard-contracts
[43] M. Zhu and S. Martínez, “On distributed convex optimization under inequality and equality constraints,” *IEEE Trans. Autom. Control*, vol. 57, no. 1, pp. 151–164, 2011.
[44] M. Baran and F. F. Wu, “Optimal sizing of capacitors placed on a radial distribution system,” *IEEE Trans. Power Delivery*, vol. 4, no. 1, pp. 735–743, 1989.
[45] A. Standerd, “For electric power systems and equipment-voltage ratings (60 hz),” *ANSI C84*, pp. 1–2006, 2006.

6.2 Summary and Contributions

This chapter presented a distributed optimisation-based coordination algorithm that optimised charging and discharging of EVs (bidirectional flow of electricity to and from the EV batteries) to minimise the associated customer operational costs, while maintaining quasi-steady-state voltage magnitudes along an unbalanced distribution feeder within the prescribed thresholds and satisfying each EV's charging requirement before their departure.

The representation of the residential energy system associated with a single EV customer and the definition of the operational cost accrued to an EV customer were all consistent with Chapter 5, with the exception of some notational changes made to improve the clarity and presentation of this chapter.

For the problem of voltage regulation, a three-phase unbalanced, radial distribution network model was introduced, which consisted of single phase and two phase laterals. Each node and each line segment in the distribution feeder was considered to be either single phase, two phase, or three phase. The distribution feeder consisted of multiple customer connection points corresponding to each phase of each node, referred to as *supply points*, to which multiple customers connected via their residential energy systems.

The centralised optimisation problem for coordinating EV charging and discharging remained the same as in Chapter 5, with an exception in the voltage constraints that were modified to incorporate an unbalanced distribution grid. The newer voltage constraints introduced in this chapter were derived using the linear approximation of three phase power flow proposed in [Gan and Low, 2014; Arnold et al., 2016], and they ensured that the voltage magnitudes across all phases of all nodes (i.e., across all supply points) in the distribution feeder stayed within the operational limits. Same as with the optimisation problem proposed in our previous work in Chapter 5, the voltage constraints coupled the individual EV charge and discharge rates in form of a linear inequality.

To efficiently solve the proposed constraint-coupled centralised optimisation problem, a distributed algorithm called Dis-Net-EVCD (*Distributed and Network-aware EV Charging and Discharging*) was developed using the DC-ADMM algorithm. Central to the proposed Dis-Net-EVCD algorithm was a distributed communication framework that was built upon the assumption of a connected graph of agents, where each agent represented an EV in the distribution network. By means of peer-to-peer communication, the agents cooperated to minimise the sum of their local cost functions (operational cost functions) subject to both local constraints (consistent with the N-EVCD approach in Chapter 5) and the voltage constraints. The ability of Dis-Net-EVCD to perform computational tasks in parallel, dramatically reduced the computation time compared to solving the optimisation problem centrally. Different from the other ADMM-based EV charging algorithms, such as [Zhou et al., 2020b; Zhang et al., 2016], Dis-Net-EVCD required only neighbor-wise EV communication, implying a large reduction of communication overhead. More importantly, the information exchange between neighboring EVs was restricted to communicating a vector of Lagrange multipliers associated with the voltage constraints, which do not carry EV-specific operational information nor EV-specific battery parameters.

To summarise, the main contributions of this chapter were as follows.

1. By leveraging the power flow equations in [Gan and Low, 2014; Arnold et al., 2016], a voltage profile representing the temporal variation of voltage magnitude corresponding to each supply point in an unbalanced distribution network, that resulted from the aggregated EV and non-EV power consumption (or injection) of end-customers, was formulated. Accordingly, voltage constraints were introduced to maintain voltages at all supply points to be within the operational limits.

2. A quadratic optimisation problem was formulated to minimise operational costs accrued to EV customers with respect to charging and discharging their EV batteries, while satisfying all of the heterogeneous EV charge requirements within the specified time duration and complying with individual EV battery constraints (local to each EV) and the proposed voltage constraints (couples EVs). Importantly, the proposed optimisation problem balanced the EV customers' objective of minimizing their daily operational costs attributed to EV charging and discharging, with the electrical distributor's objective to effectively manage supply voltages along the distribution feeder.

3. Using the DC-ADMM concept, a distributed optimisation-based algorithm called Dis-Net-EVCD was developed to obtain the solution to the underlying optimisation problem through local EV computations and limited information exchange with neighboring agents (EVs) via peer-to-peer communication. The merits of the proposed algorithm include: 1) it poses minimal computational requirements to EVs; 2) it guarantees convergence; 3) it improves EV customer privacy by not transmitting any EV-specific operational parameters, SoC details or charge-discharge profiles to the communication network; and 4) it eliminates the need for a centralised coordinator (or aggregator) to support EV coordination, making the algorithm scalable and tolerant to network faults.

4. A proof was included confirming the optimality of Dis-Net-EVCD in obtaining the globally optimal solution to the proposed optimisation problem.

5. To support near-real-time EV charging and discharging operations, Dis-Net-EVCD was integrated with a receding-horizon optimization based implementation, wherein EVs updated their charge-discharge control sequences over a receding time horizon.

6. To demonstrate the effectiveness of Dis-Net-EVCD, numerical simulations were carried out on the IEEE 13 node test feeder populated with a real-world dataset of residential load collected from households within an Australian distribution network and the simulation results were analysed.

Results obtained from numerical simulations demonstrated that Dis-Net-EVCD preserved grid voltage constraints and achieved a peak load reduction of 39% compared to P-EVCD (introduced in Chapter 5), where customer operational costs were minimized in the absence of voltage constraints. Moreover, EV customers implementing Dis-Net-EVCD yielded a total operational cost reduction of 78% compared to uncoordinated EV charging. All these benefits were obtained while also complying with each individual EV constraints and satisfying each EV's charge requirement ahead of their departure.

Numerical simulation results further demonstrated that Dis-Net-EVCD was approximately 60 times computationally faster than its centralized counterpart. It was also shown that the error between solutions obtained from the centralized approach and the distributed approach reduces to 10^{-5} within only 45 iterations. Dis-Net-EVCD was then benchmarked against a state-of-the-art distributed and iterative algorithm that employ the Lagrangian primal-dual subgradient method, which revealed that Dis-Net-EVCD achieved much faster convergence (approximately twice) compared to the benchmark algorithm.

Chapter 7

Conclusion and Future Work

7.1 Concluding Remarks

Given the dire need to address the increasingly urgent problem of global climate change, EVs are becoming an attractive solution due to their apparent socio-economic and environmental benefits. Pleasingly, a substantial level of EV-grid integration is anticipated in the near future, making EVs an indispensable component of the smart grid. Nonetheless, the electric load imposed by EV charging at a massive scale potentially leads to negative impacts on power grid stability, especially when EV coordination is unavailable. Hence, this thesis focused on exploring demand-side approaches via coordinated EV charging and discharging to mitigate such adverse impacts and sustain high EV penetration rates in existing distribution grids without creating the need for costly grid augmentation. Specifically, we studied coordinated EV charging and discharging approaches incorporating various requirements from the EV user's perspective and grid operator's perspective.

In Part 1 of the thesis, we provided background on EV charging use cases and reviewed the currently available EV grid impact studies, highlighting challenges associated with widespread EV adoption. The review of EV grid impact studies suggested that coordination of EV charging operations is an effective approach to addressing those challenges. Accordingly, we carried out an extensive literature review of existing algorithmic approaches for coordinated EV charging, with an emphasis on optimisation-based approaches. Based on our literature review, we identified several limitations in the existing EV charging approaches designed for grid congestion management and voltage regulation, which we considered for further study in Parts 2 and 3 of the thesis.

In the introductory Chapter 1- Section 1.2, we summarised three main questions to which we sought answers. Part 2 of this thesis answered Q1 and Q3 by developing demand-side approaches for grid congestion management via controlled EV charging and discharging, implemented together with distributed EV coordination to enhance scalability of implementation. Then, Part 3 of this thesis answered Q1, Q2, and Q3 by developing network-aware demand-side approaches for centralised and distributed EV coordination, which incorporated both EV customer economics and electrical distributor concerns on voltage stability.

In more detail, the second part of the thesis addressed the problem of managing grid congestion by means of load curve shaping via coordinated EV charging and discharging. To reduce the grid congestion, several optimisation-based load curve shaping tools were proposed, whereby the EV charge and discharge rates were coordinated in a distributed manner. Through numerical simulations, we showed that by executing the proposed approaches, EVs can assist power system operators looking to: (1) align the load (power consumption) profile following an arbitrary power profile; (2) flatten the load profile by shifting EV power demands to load curve valleys; and (3) reduce the peak demand approaching network capacity constraints by EV discharging during peak periods — while still satisfying all of their charging demands. In an application seeking to schedule EV charging to track the PV generation profile of a microgrid, the algorithm proposed in Chapter 3 managed to successfully align the final load profile (composed of aggregated EV and non-EV load) with the PV generation profile, while getting all EVs to their desired SoC before each of their expected departure times. Then, in another application seeking to schedule both EV charging and discharging to flatten the load curve of a low voltage transformer serving a residential community, the algorithm proposed in Chapter 4 achieved a load variance reduction by 47-65%, and also outperformed state-of-the-art algorithms in terms of the computational time and the extent to which the flatness was achieved.

The coordinated EV charging and discharging approaches studied in Chapters 3 and 4 relieved significant stress on the power grid. However, they did not guarantee a stable voltage profile across the distribution network, which was another important requirement from the electrical distributor's perspective. We found that grid voltages are mostly impacted by EV charging, and hence considered voltage-secure EV charging for further study in the third part of the thesis.

Moreover, existing studies in the literature were found to be based only on either financial performance objectives or operational performance objectives. Hence, we identified the importance of developing EV coordination approaches combining both financial performance objectives and operational performance objectives, which established the basis for our studies in Part 3 of the thesis.

In more detail, the third part of the thesis addressed the problem of managing bi-directional power flows arising from EV charging and discharging for improving the voltage stability in a distribution grid. Specifically, two coordinated EV charging and discharging approaches were proposed, the first of which managed supply voltages in a single-phase (or balanced) distribution grid and the other managed supply voltages in an unbalanced distribution grid. Additionally, the proposed approaches satisfied daily charging demands of EVs with minimal operational costs, in the context of time-based electricity tariffs and net metering policies. We also found that the inclusion of battery degradation cost as a part of the customer operational cost is important, since otherwise the EVs may end up with a large number of charge-discharge cycles leading to loss of lifetime of the battery.

With respect to regulation of system voltages, we identified two issues that potentially arise in distribution networks due to significant penetration of EVs partaking in G2V and V2G operation, namely: (i) peak loads that lead to significant voltage drops falling below set tolerances; and (ii) reverse power flows that lead to significant voltage rise exceeding set tolerances. We first considered addressing those issues considering a single-phase distribution network and proposed a RHO-based, network-aware EV charging and discharging algorithm, in which the optimisation was performed centrally. Next we extended that algorithm to manage supply voltages in an unbalanced distribution network via a distributed-optimisation based algorithm, driven by peer-to-peer EV communication. Through numerical simulations, we showed that by executing the proposed algorithms, EVs can assist power system operators to maintain a stable voltage profile along the distribution feeder while also getting EV charge requirements fulfilled with minimal operational costs and within a prespecified time duration.

Our numerical simulations confirmed that minimizing the operational costs accrued to individual EV customers without considering distribution network aspects, potentially leads to undesirable consequences for the grid, including regulatory voltage violations. It was then demonstrated that such undesirable consequences can be mitigated by coordinating EV charging and discharging operations to balance the EV customer benefit of reducing operational costs with the electrical distributor benefit of improving supply voltage profiles. Specifically, in an application seeking to schedule EV charging and discharging to manage supply voltages in a single-phase distribution network, the algorithm proposed in Chapter 5 managed to maintain all nodal voltages within the nominal range while yielding a 92% – 111% reduction in the customer operational costs, compared to uncoordinated EV charging. Then, in an application seeking to schedule EV charging and charging to manage supply voltages in an unbalanced distribution network, the algorithm proposed in Chapter 6 maintained voltages along the distribution feeder within the operational limits while yielding an operational cost reduction of 78% compared to uncoordinated EV charging. Further, in an assessment of the customer benefits from the proposed algorithms, we found that customers located at the far end of the feeder receive higher operational costs compared to those customers closer to the feeder head, as a result of the voltage constraints. With both algorithms presented in Chapter 5 and Chapter 6, significant reductions in peak load and/or reverse power flow were observed. Those reductions together with reductions in EV customer operational costs resulted in a win-win solution from the perspectives of both EV customers and electrical distributors.

7.2 Future Work

The EV charging and discharging coordination approaches presented in this thesis have the potential to be extended in several directions as described below.

1. **Battery SoC models and battery degradation models**.
   Recently, the capital costs associated with purchasing EV batteries have fallen rapidly, meaning that EVs may soon be as cheap to consumers as conventional vehicles. It is expected that this trend of decreasing battery costs will continue

into the next decade [Cavanagh et al., 2015] and that more advanced battery and charger technologies will come into use. Hence, future work could extend the battery SoC models (representing the change of SoC of the battery over time) employed in this thesis in a direction to incorporate more specific battery SoC models, as in [Chang, 2013].
Moreover, to capture the exact operational effects of EV charging and discharging on battery lifetime, it would be interesting to further consider including more accurate and descriptive battery degradation models in the operational optimisation, as opposed to the one that we employed in Part 3 of the thesis.

2. **Pricing schemes.**
   In this thesis, we considered minimising the electricity costs attributed to EV charging and discharging, in the context of net metering with time-of-use electricity prices. Extensions to include other types of financial policies in place of net-metering and other types of pricing schemes, such as real-time pricing schemes, are certainly possible.

3. **Distribution network constraints**.
   In Part 3 of this thesis, we considered EV charging and discharging subject to distribution voltage constraints. Future work to incorporate other network constraints, such as power flow limits approaching network capacity and thermal limits across distribution lines and transformers, is possible. It is also worthy to explore extensions of the algorithms proposed in this thesis to mitigate the phase imbalance in distribution grids. For example, a constraint might be introduced to restrict the complex phase voltages to be within a small circle centred on the nominal voltage.

4. **Fairness in charging**.
   In Part 3 of this thesis, our numerical simulation results demonstrated that EV customers participating in the voltage regulation service received varying operational costs depending on their location in the distribution feeder. For example, EV customers who connected from the weakest nodes of the distribution feeder (mostly located towards the ends of the feeder) experienced large voltage deviations, which restricted them from charging or discharging at higher rates, and thereby incurred comparatively higher operational costs compared to EV customers who connected from more stable nodes (mostly closer to the feeder head). As such, a question that naturally rises is the notion of fairness across EV customers, which needs to be addressed to realise the full potential of EV-assisted DSM. One possible solution is to include a different pricing scheme (e.g., a distribution location marginal pricing scheme such as in [Sabillon et al., 2019; Li et al., 2013; Huang et al., 2014]) or design an appropriate pricing scheme that captures spatial information of customers to charge and

compensate them at variable rates.

5. **EV charging considering uncertainties.**
   In this thesis, we incorporated uncertainties of EV arrival and departure times when scheduling EVs for charging, however, the problem of EV charge scheduling is associated with more uncertain scenarios, as we described in Chapter 2. Hence, optimisation of EV charging considering different forms of uncertainties is an interesting research direction. For example, in our formulations, we assumed that the forecasts of non-EV power consumption of customers are available and precise. However, those forecasts are often subject to errors, and therefore improvements of our algorithms to accommodate those forecast errors will make them more suitable for practical implementation.
   Moreover, in this thesis, we considered receding-horizon optimisation-based techniques to support near-real-time coordination of EVs with random arrivals and departures, which required the computation of EV charge-discharge profiles repeatedly at every time step. As the length of a single time-step in the underlying optimisation problem gets smaller and smaller, such approaches will become computationally expensive. Therefore, it is worth exploring better ways to reduce the computational overhead in the respective implementations.

6. **Consideration of various topologies of residential energy systems**.
   In Part 3 of this thesis, we assumed a topology of a residential energy system corresponding to each customer that consists of a single EV. Extensions to other types of topologies where a customer owns multiple EVs, for example, are left for future research.
   Recently, there continues to be significant deployment in residential-scale battery storage co-located with grid-integrated residential-scale (rooftop) solar PV, giving rise to topologies of residential energy systems where both EVs and battery storage systems co-exist. Therefore, it is of interest to extend the EV coordination approaches presented in this thesis to consider residential energy systems with such topologies.
   It is also of interest to extend the algorithms proposed in this thesis that focused on residential EV charging to other venues, such as EV charging in urban areas and parking lots, which are based on different topologies of energy systems.

7. **Implementation with other voltage regulation schemes**.
   Another interesting future work is to integrate N-EVCD and Dis-Net-EVCD with other voltage regulation schemes that may be in operation, e.g., ones utilizing the reactive power capability of solar PV inverters. It is worth exploring how the proposed algorithms interact with such schemes that are already in operation.

8. **Consideration of non-participating EV users in demand-side management**.
   Individual EV users are quite varied and some might not like to take the risk of relying on demand-side approaches for charging their EVs. Hence, considering a more practical system that comprises of two sets of EV users, participating and non-participating EV users, will make the implementations more real.

9. **Provision of ancillary services**.
   It is also an interesting research direction to combine the approaches proposed in this thesis with functions such as frequency control, which specifically provides ancillary services to the grid.

10. **Communication interruptions.**
    In Chapters 3-5 of this thesis, we assumed that two-way communication infrastructure between the centralised coordinator and each EV customer is available and lossless. Likewise, in Chapter 6 of this thesis, we assumed that peer-to-peer communication infrastructure between EVs is available and lossless. Potential extensions to our algorithms might consider more realistic scenarios where these communications are less reliable and subject to network delays, failures, or bandwidth constraints.

11. **Extensive numerical simulations.**
    In Part 3 of this thesis, we considered the IEEE 13 node test feeder for simulation. Further numerical simulations in larger distribution feeders, such as IEEE 123 node test feeder, will reveal better insights of the performance of proposed algorithms in this thesis.

Bibliography

Ahmed, M. A. and Kim, Y.-C., 2017. Performance analysis of communication networks for EV charging stations in residential grid. In *Proceedings of the 6th ACM Symposium on Development and Analysis of Intelligent Vehicular Networks and Applications*, 63–70. (cited on page 4)

Ahn, C.; Li, C.-T.; and Peng, H., 2011. Optimal decentralized charging control algorithm for electrified vehicles connected to smart grid. *Journal of Power Sources*, 196, 23 (2011), 10369–10379. (cited on page 45)

Al-Awami, A. T. and Sortomme, E., 2011. Coordinating vehicle-to-grid services with energy trading. *IEEE Transactions on smart grid*, 3, 1 (2011), 453–462. (cited on pages 19 and 20)

Al-Awami, A. T.; Sortomme, E.; Akhtar, G. M. A.; and Faddel, S., 2015. A voltage-based controller for an electric-vehicle charger. *IEEE Transactions on Vehicular Technology*, 65, 6 (2015), 4185–4196. (cited on page 53)

Alirezaei, M.; Noori, M.; and Tatari, O., 2016. Getting to net zero energy building: Investigating the role of vehicle to home technology. *Energy and Buildings*, 130 (2016), 465–476. (cited on page 3)

Alonso, M.; Amaris, H.; Germain, J. G.; and Galan, J. M., 2014. Optimal charging scheduling of electric vehicles in smart grids by heuristic algorithms. *Energies*, 7, 4 (2014), 2449–2475. (cited on page 49)

Amjad, M.; Ahmad, A.; Rehmani, M. H.; and Umer, T., 2018. A review of EVs charging: From the perspective of energy optimization, optimization approaches, and charging techniques. *Transportation Research Part D: Transport and Environment*, 62 (2018), 386–417. (cited on page 4)

ARENA, 2021. Electric vehicles. https://arena.gov.au/renewable-energy/electric-vehicles. Accessed 14 Sep. 2021. (cited on page 14)

Arnold, D. B.; Sankur, M.; Dobbe, R.; Brady, K.; Callaway, D. S.; and Von Meier, A., 2016. Optimal dispatch of reactive power for voltage regulation and balancing in unbalanced distribution systems. In *Proceedings of the IEEE Power and Energy Society General Meeting*, 1–5. IEEE. (cited on pages 113 and 114)

Baran, M. and Wu, F. F., 1989a. Optimal sizing of capacitors placed on a radial distribution system. *IEEE Transactions on Power Delivery*, 4, 1 (1989), 735–743. (cited on page 97)

Baran, M. E. and Wu, F. F., 1989b. Network reconfiguration in distribution systems for loss reduction and load balancing. *IEEE Power Engineering Review*, 9, 4 (1989), 101–102. (cited on pages 97 and 98)

Barone, G.; Buonomano, A.; Calise, F.; Forzano, C.; and Palombo, A., 2019. Building to vehicle to building concept toward a novel zero energy paradigm: Modelling and case studies. *Renewable and Sustainable Energy Reviews*, 101 (2019), 625–648. (cited on page 3)

Benetti, G.; Delfanti, M.; Facchinetti, T.; Falabretti, D.; and Merlo, M., 2014. Real-time modeling and control of electric vehicles charging processes. *IEEE Transactions on Smart Grid*, 6, 3 (2014), 1375–1385. (cited on page 49)

Bessa, R. J. and Matos, M. A., 2012. Economic and technical management of an aggregation agent for electric vehicles: A literature survey. *European Transactions on Electrical Power*, 22, 3 (2012), 334–350. (cited on page 21)

Bharati, G. and Paudyal, S., 2016. Coordinated control of distribution grid and electric vehicle loads. *Electric Power Systems Research*, 140 (2016), 761–768. (cited on page 53)

Bhattarai, B. P.; Myers, K. S.; Bak-Jensen, B.; and Paudyal, S., 2017. Multi-time scale control of demand flexibility in smart distribution networks. *Energies*, 10, 1 (2017), 37. (cited on page 16)

Binetti, G.; Davoudi, A.; Naso, D.; Turchiano, B.; and Lewis, F. L., 2015. Scalable real-time electric vehicles charging with discrete charging rates. *IEEE Transactions on Smart Grid*, 6, 5 (2015), 2211–2220. (cited on page 45)

Bishop, J. D.; Axon, C. J.; Bonilla, D.; Tran, M.; Banister, D.; and McCulloch, M. D., 2013. Evaluating the impact of V2G services on the degradation of batteries in phev and ev. *Applied Energy*, 111 (2013), 206–218. (cited on page 18)

Borge-Diez, D.; Icaza, D.; Açikkalp, E.; and Amaris, H., 2021. Combined vehicle to building (V2B) and vehicle to home (V2H) strategy to increase electric vehicle market share. *Energy*, 237 (2021), 121608. (cited on page 3)

Boyd, S.; Parikh, N.; and Chu, E., 2011. *Distributed optimization and statistical learning via the alternating direction method of multipliers*. Now Publishers Inc. (cited on page 100)

Buonomano, A., 2020. Building to vehicle to building concept: A comprehensive parametric and sensitivity analysis for decision making aims. *Applied Energy*, 261 (2020), 114077. (cited on page 3)

Callaway, D. S. and Hiskens, I. A., 2010. Achieving controllability of electric loads. *Proceedings of the IEEE*, 99, 1 (2010), 184–199. (cited on pages 2, 19, and 41)

Cao, C.; Wu, Z.; and Chen, B., 2020. Electric vehicle–grid integration with voltage regulation in radial distribution networks. *Energies*, 13, 7 (2020), 1802. (cited on page 52)

Cao, Y.; Tang, S.; Li, C.; Zhang, P.; Tan, Y.; Zhang, Z.; and Li, J., 2011. An optimized EV charging model considering TOU price and SOC curve. *IEEE Transactions on Smart Grid*, 3, 1 (2011), 388–393. (cited on page 19)

Carley, S.; Krause, R. M.; Lane, B. W.; and Graham, J. D., 2013. Intent to purchase a plug-in electric vehicle: A survey of early impressions in large us cites. *Transportation Research Part D: Transport and Environment*, 18 (2013), 39–45. (cited on page 1)

Cavanagh, K.; Ward, J.; Behrens, S.; Bhatt, A.; Ratnam, E.; Oliver, E.; and Hayward, J., 2015. Electrical energy storage: technology overview and applications. *CSIRO, Australia*, (2015). https://www.aemc.gov.au/sites/default/files/content/7ff2f36d-f56d-4ee4-a27b-b53e01ee322c/CSIRO-Energy-Storage-Technology-Overview.pdf. (cited on page 119)

Celli, G.; Pilo, F.; Soma, G. G.; Cicoria, R.; Mauri, G.; Fasciolo, E.; and Fogliata, G., 2013. A comparison of distribution network planning solutions: Traditional reinforcement versus integration of distributed energy storage. In *Proceedings of the IEEE Grenoble Conference*, 1–6. IEEE. (cited on page 1)

Chang, T.-H.; Hong, M.; and Wang, X., 2014. Multi-agent distributed optimization via inexact consensus ADMM. *IEEE Transactions on Signal Processing*, 63, 2 (2014), 482–497. (cited on page 101)

Chang, W.-Y., 2013. The state of charge estimating methods for battery: A review. *International Scholarly Research Notices*, 2013 (2013). (cited on page 119)

Chen, N.; Quek, T. Q.; and Tan, C. W., 2012. Optimal charging of electric vehicles in smart grid: Characterization and valley-filling algorithms. In *Proceedings of the IEEE 3rd International Conference on Smart Grid Communications*, 13–18. IEEE. (cited on page 44)

Chen, N.; Tan, C. W.; and Quek, T. Q., 2014. Electric vehicle charging in smart grid: Optimality and valley-filling algorithms. *IEEE Journal of Selected Topics in Signal Processing*, 8, 6 (2014), 1073–1083. (cited on pages 41 and 49)

Clement, K.; Haesen, E.; and Driesen, J., 2009. Coordinated charging of multiple plug-in hybrid electric vehicles in residential distribution grids. In *Proceedings of the IEEE PES Power Systems Conference and Exposition*, 1–7. IEEE. (cited on page 50)

Clement-Nyns, K.; Haesen, E.; and Driesen, J., 2009. The impact of charging plug-in hybrid electric vehicles on a residential distribution grid. *IEEE Transactions on power systems*, 25, 1 (2009), 371–380. (cited on pages 20 and 50)

Clement-Nyns, K.; Haesen, E.; and Driesen, J., 2011. The impact of vehicle-to-grid on the distribution grid. *Electric Power Systems Research*, 81, 1 (2011), 185–192. (cited on pages 18 and 50)

Colmenar-Santos, A.; de Palacio-Rodriguez, C.; Rosales-Asensio, E.; and Borge-Diez, D., 2017. Estimating the benefits of vehicle-to-home in islands: The case of the Canary Islands. *Energy*, 134 (2017), 311–322. (cited on page 3)

Cvetkovic, I.; Thacker, T.; Dong, D.; Francis, G.; Podosinov, V.; Boroyevich, D.; Wang, F.; Burgos, R.; Skutt, G.; and Lesko, J., 2009. Future home uninterruptible renewable energy system with vehicle-to-grid technology. In *Proceedings of the IEEE Energy Conversion Congress and Exposition*, 2675–2681. IEEE. (cited on page 3)

De Hoog, J.; Alpcan, T.; Brazil, M.; Thomas, D. A.; and Mareels, I., 2014. Optimal charging of electric vehicles taking distribution network constraints into account. *IEEE Transactions on Power Systems*, 30, 1 (2014), 365–375. (cited on pages 50 and 51)

de Hoog, J.; Muenzel, V.; Jayasuriya, D. C.; Alpcan, T.; Brazil, M.; Thomas, D. A.; Mareels, I.; Dahlenburg, G.; and Jegatheesan, R., 2015. The importance of spatial distribution when analysing the impact of electric vehicles on voltage stability in distribution networks. *Energy Systems*, 6, 1 (2015), 63–84. (cited on page 49)

de Hoog, J.; Thomas, D. A.; Muenzel, V.; Jayasuriya, D. C.; Alpcan, T.; Brazil, M.; and Mareels, I., 2013. Electric vehicle charging and grid constraints: Comparing distributed and centralized approaches. In *Proceedings of the IEEE Power & Energy Society General Meeting*, 1–5. IEEE. (cited on page 83)

Deilami, S.; Masoum, A. S.; Moses, P. S.; and Masoum, M. A., 2011. Real-time coordination of plug-in electric vehicle charging in smart grids to minimize power losses and improve voltage profile. *IEEE Transactions on Smart Grid*, 2, 3 (2011), 456–467. (cited on pages 20 and 50)

Dharmakeerthi, C.; Mithulananthan, N.; and Saha, T. K., 2011. Overview of the impacts of plug-in electric vehicles on the power grid. In *Proceedings of the IEEE PES Innovative Smart Grid Technologies*, 1–8. IEEE. (cited on page 1)

Di Giorgio, A.; Liberati, F.; and Canale, S., 2014. Electric vehicles charging control in a smart grid: A model predictive control approach. *Control Engineering Practice*, 22 (2014), 147–162. (cited on page 48)

Dogger, J. D.; Roossien, B.; and Nieuwenhout, F. D., 2010. Characterization of li-ion batteries for intelligent management of distributed grid-connected storage. *IEEE Transactions on Energy Conversion*, 26, 1 (2010), 256–263. (cited on page 18)

Dong, X.; Mu, Y.; Xu, X.; Jia, H.; Wu, J.; Yu, X.; and Qi, Y., 2018. A charging pricing strategy of electric vehicle fast charging stations for the voltage control of electricity distribution networks. *Applied Energy*, 225 (2018), 857–868. (cited on page 53)

Earl, J. and Fell, M. J., 2019. Electric vehicle manufacturers' perceptions of the market potential for demand-side flexibility using electric vehicles in the United Kingdom. *Energy Policy*, 129 (2019), 646–652. (cited on pages 1 and 2)

El-Bayeh, C. Z.; Alzaareer, K.; Aldaoudeyeh, A.-M. I.; Brahmi, B.; and Zellagui, M., 2021. Charging and discharging strategies of electric vehicles: A survey. *World Electric Vehicle Journal*, 12, 1 (2021), 11. (cited on pages 5 and 19)

energysage, 2021. Electric vehicle manufacturers and companies. https://www.energysage.com/electric-vehicles/buyers-guide/top-ev-companies. (cited on page 1)

Erdogan, N.; Erden, F.; and Kisacikoglu, M., 2018. A fast and efficient coordinated vehicle-to-grid discharging control scheme for peak shaving in power distribution system. *Journal of Modern Power Systems and Clean Energy*, 6, 3 (2018), 555–566. (cited on page 46)

Erol-Kantarci, M. and Hussein, T. M., 2010. Prediction-based charging of PHEVs from the smart grid with dynamic pricing. In *IEEE Local Computer Network Conference*, 1032–1039. IEEE. (cited on pages 19 and 20)

Fachrizal, R.; Shepero, M.; van der Meer, D.; Munkhammar, J.; and Widén, J., 2020. Smart charging of electric vehicles considering photovoltaic power production and electricity consumption: a review. *ETransportation*, 4 (2020), 100056. (cited on page 2)

Fang, X.; Misra, S.; Xue, G.; and Yang, D., 2011. Smart grid—the new and improved power grid: A survey. *IEEE Communications Surveys & tutorials*, 14, 4 (2011), 944–980. (cited on page 2)

Farhangi, H., 2009. The path of the smart grid. *IEEE Power and Energy Magazine*, 8, 1 (2009), 18–28. (cited on page 2)

Fernandez, L. P.; San Román, T. G.; Cossent, R.; Domingo, C. M.; and Frias, P., 2010. Assessment of the impact of plug-in electric vehicles on distribution networks. *IEEE Transactions on Power Systems*, 26, 1 (2010), 206–213. (cited on page 41)

Finn, P.; Fitzpatrick, C.; and Connolly, D., 2012. Demand side management of electric car charging: Benefits for consumer and grid. *Energy*, 42, 1 (2012), 358–363. (cited on page 2)

Foley, A.; Tyther, B.; Calnan, P.; and Gallachóir, B. Ó., 2013. Impacts of electric vehicle charging under electricity market operations. *Applied Energy*, 101 (2013), 93–102. (cited on page 16)

Franco, J. F.; Rider, M. J.; and Romero, R., 2015. A mixed-integer linear programming model for the electric vehicle charging coordination problem in unbalanced electrical distribution systems. *IEEE Transactions on Smart Grid*, 6, 5 (2015), 2200–2210. (cited on pages 50 and 51)

Gago, R. G.; Pinto, S. F.; and Silva, J. F., 2016. G2V and V2G electric vehicle charger for smart grids. In *Proceedings of the IEEE International Smart Cities Conference*, 1–6. IEEE. (cited on page 3)

Gallager, R. G., 1968. Information theory and reliable communication. 588 (1968). (cited on pages 47 and 56)

Galus, M. D.; Vayá, M. G.; Krause, T.; and Andersson, G., 2013. The role of electric vehicles in smart grids. *Wiley Interdisciplinary Reviews: Energy and Environment*, 2, 4 (2013), 384–400. (cited on page 4)

Gan, L. and Low, S. H., 2014. Convex relaxations and linear approximation for optimal power flow in multiphase radial networks. In *Proceedings of the Power Systems Computation Conference*, 1–9. IEEE. (cited on pages 51, 113, and 114)

Gan, L.; Topcu, U.; and Low, S. H., 2012a. Optimal decentralized protocol for electric vehicle charging. *IEEE Transactions on Power Systems*, 28, 2 (2012), 940–951. (cited on pages 42, 43, 45, and 48)

Gan, L.; Topcu, U.; and Low, S. H., 2012b. Stochastic distributed protocol for electric vehicle charging with discrete charging rate. In *Proceedings of the IEEE Power and Energy Society General Meeting*, 1–8. IEEE. (cited on page 43)

García-Villalobos, J.; Zamora, I.; San Martín, J. I.; Asensio, F. J.; and Aperribay, V., 2014. Plug-in electric vehicles in electric distribution networks: A review of smart charging approaches. *Renewable and Sustainable Energy Reviews*, 38 (2014), 717–731. (cited on pages 2 and 19)

Gelazanskas, L. and Gamage, K. A., 2014. Demand side management in smart grid: A review and proposals for future direction. *Sustainable Cities and Society*, 11 (2014), 22–30. (cited on page 2)

Ghavami, A.; Kar, K.; Bhattacharya, S.; and Gupta, A., 2013. Price-driven charging of plug-in electric vehicles: Nash equilibrium, social optimality and best-response convergence. In *Proceedings of the 47th Annual Conference on Information Sciences and Systems*, 1–6. IEEE. (cited on page 42)

Gkatzikis, L.; Koutsopoulos, I.; and Salonidis, T., 2013. The role of aggregators in smart grid demand response markets. *IEEE Journal on Selected Areas in Communications*, 31, 7 (2013), 1247–1257. (cited on page 21)

Gong, X.; Lin, T.; and Su, B., 2011. Survey on the impact of electric vehicles on power distribution grid. In *Proceedings of the IEEE Power Engineering and Automation Conference*, vol. 2, 553–557. IEEE. (cited on pages 1 and 16)

Graham, J. D. and Brungard, E., 2021. Consumer adoption of plug-in electric vehicles in selected countries. *Future Transportation*, 1, 2 (2021), 303–325. (cited on page 1)

Green II, R. C.; Wang, L.; and Alam, M., 2011. The impact of plug-in hybrid electric vehicles on distribution networks: A review and outlook. *Renewable and Sustainable Energy Reviews*, 15, 1 (2011), 544–553. (cited on page 16)

Gungor, V. C.; Sahin, D.; Kocak, T.; Ergut, S.; Buccella, C.; Cecati, C.; and Hancke, G. P., 2011. Smart grid technologies: Communication technologies and standards. *IEEE Transactions on Industrial Informatics*, 7, 4 (2011), 529–539. (cited on pages 3 and 18)

Haddadian, G.; Khodayar, M.; and Shahidehpour, M., 2015. Accelerating the global adoption of electric vehicles: barriers and drivers. *The Electricity Journal*, 28, 10 (2015), 53–68. (cited on page 1)

Haines, G.; McGordon, A.; Jennings, P.; and Butcher, N., 2009. The simulation of vehicle-to-home systems–using electric vehicle battery storage to smooth domestic electricity demand. *EVER Monaco*, (2009). (cited on page 3)

Han, S.; Han, S.; and Sezaki, K., 2010. Development of an optimal vehicle-to-grid aggregator for frequency regulation. *IEEE Transactions on smart grid*, 1, 1 (2010), 65–72. (cited on pages 17 and 20)

Hannan, M. A.; Hoque, M. M.; Hussain, A.; Yusof, Y.; and Ker, P. J., 2018. State-of-the-art and energy management system of lithium-ion batteries in electric vehicle applications: Issues and recommendations. *IEEE Access*, 6 (2018), 19362–19378. (cited on page 15)

He, P.; Li, M.; Zhao, L.; Venkatesh, B.; and Li, H., 2016. Water-filling exact solutions for load balancing of smart power grid systems. *IEEE Transactions on Smart Grid*, 9, 2 (2016), 1397–1407. (cited on page 57)

He, P.; Zhao, L.; Zhou, S.; and Niu, Z., 2013. Water-filling: A geometric approach and its application to solve generalized radio resource allocation problems. *IEEE Transactions on Wireless Communications*, 12, 7 (2013), 3637–3647. (cited on page 56)

He, T.; Lu, D. D.-C.; Wu, M.; Yang, Q.; Li, T.; and Liu, Q., 2021. Four-quadrant operations of bidirectional chargers for electric vehicles in smart car parks: G2V, V2G, and V4G. *Energies*, 14, 1 (2021), 181. (cited on page 3)

He, Y.; Venkatesh, B.; and Guan, L., 2012. Optimal scheduling for charging and discharging of electric vehicles. *IEEE Transactions on Smart Grid*, 3, 3 (2012), 1095–1105. (cited on pages 17 and 19)

Heredia, W. B.; Chaudhari, K.; Meintz, A.; Jun, M.; and Pless, S., 2020. Evaluation of smart charging for electric vehicle-to-building integration: A case study. *Applied Energy*, 266 (2020), 114803. (cited on page 3)

Hildermeier, J.; Kolokathis, C.; Rosenow, J.; Hogan, M.; Wiese, C.; and Jahn, A., 2019. Smart ev charging: A global review of promising practices. *World Electric Vehicle Journal*, 10, 4 (2019), 80. (cited on page 2)

Hiskens, I. and Callaway, D., 2009. Achieving controllability of plug-in electric vehicles. In *Proceedings of the IEEE Vehicle Power and Propulsion Conference*, 1215–1220. IEEE. (cited on pages 2 and 41)

Hosseini, S. S.; Badri, A.; and Parvania, M., 2012. The plug-in electric vehicles for power system applications: The vehicle to grid (V2G) concept. In *Proceedings of the IEEE International Energy Conference and Exhibition*, 1101–1106. IEEE. (cited on page 3)

Hu, J.; Morais, H.; Sousa, T.; and Lind, M., 2016a. Electric vehicle fleet management in smart grids: A review of services, optimization and control aspects. *Renewable and Sustainable Energy Reviews*, 56 (2016), 1207–1226. (cited on page 4)

Hu, Z.; Zhan, K.; Zhang, H.; and Song, Y., 2016b. Pricing mechanisms design for guiding electric vehicle charging to fill load valley. *Applied Energy*, 178 (2016), 155–163. (cited on page 41)

Huang, M.; Caines, P. E.; and Malhamé, R. P., 2007. Large-population cost-coupled LQG problems with nonuniform agents: individual-mass behavior and decentralized ε-Nash equilibria. *IEEE Transactions on Automatic Control*, 52, 9 (2007), 1560–1571. (cited on page 42)

Huang, S.; Wu, Q.; Oren, S. S.; Li, R.; and Liu, Z., 2014. Distribution locational marginal pricing through quadratic programming for congestion management in distribution networks. *IEEE Transactions on Power Systems*, 30, 4 (2014), 2170–2178. (cited on page 119)

Huo, X. and Liu, M., 2020. Decentralized electric vehicle charging control via a novel shrunken primal-multi-dual subgradient (SPMDS) algorithm. In *Proceedings of the 59th IEEE Conference on Decision and Control*, 1367–1373. IEEE. (cited on pages 52 and 101)

Hutterer, S.; Affenzeller, M.; and Auinger, F., 2012. Evolutionary optimization of multi-agent control strategies for electric vehicle charging. In *Proceedings of the 14th Annual Conference Companion on Genetic and Evolutionary Computation*, 3–10. (cited on page 19)

IEA, 2021. *Global EV Outlook*. International Energy Agency. https://www.iea.org/reports/global-ev-outlook-2021. (cited on page 1)

Igbinovia, F. O.; Fandi, G.; Mahmoud, R.; and Tlustý, J., 2016. A review of electric vehicles emissions and its smart charging techniques influence on power distribution grid. *Journal of Engineering Science & Technology Review*, 9, 3 (2016). (cited on page 2)

Ioakimidis, C. S.; Thomas, D.; Rycerski, P.; and Genikomsakis, K. N., 2018. Peak shaving and valley filling of power consumption profile in non-residential buildings using an electric vehicle parking lot. *Energy*, 148 (2018), 148–158. (cited on pages 46 and 47)

Ipakchi, A. and Albuyeh, F., 2009. Grid of the future. *IEEE Power and Energy Magazine*, 7, 2 (2009), 52–62. (cited on page 16)

Islam, M. R.; Lu, H.; Hossain, J.; and Li, L., 2020a. Multiobjective optimization technique for mitigating unbalance and improving voltage considering higher penetration of electric vehicles and distributed generation. *IEEE Systems Journal*, 14, 3 (2020), 3676–3686. (cited on page 51)

Islam, M. R.; Lu, H.; Hossain, M.; and Li, L., 2019a. Mitigating unbalance using distributed network reconfiguration techniques in distributed power generation grids with services for electric vehicles: A review. *Journal of Cleaner Production*, 239 (2019), 117932. (cited on page 19)

Islam, M. R.; Lu, H.; Hossain, M. J.; and Li, L., 2019b. Multi-objective dynamic phase re-configuration technique to mitigate the unbalance due to penetration of electric vehicles. In *Proceedings of the 9th International Conference on Power & Energy Systems*, 1–5. IEEE. (cited on page 51)

Islam, M. R.; Lu, H.; Hossain, M. J.; and Li, L., 2020b. Optimal coordination of electric vehicles and distributed generators for voltage unbalance and neutral current compensation. *IEEE Transactions on Industry Applications*, 57, 1 (2020), 1069–1080. (cited on page 51)

Jenkins, N.; Liyanage, K.; Wu, J.; and Yokoyama, A., 2012. *Smart Grid*. Wiley. (cited on page 2)

Jian, L.; Xue, H.; Xu, G.; Zhu, X.; Zhao, D.; and Shao, Z., 2012. Regulated charging of plug-in hybrid electric vehicles for minimizing load variance in household smart microgrid. *IEEE Transactions on Industrial Electronics*, 60, 8 (2012), 3218–3226. (cited on pages 46 and 47)

Jian, L.; Zheng, Y.; and Shao, Z., 2017. High efficient valley-filling strategy for centralized coordinated charging of large-scale electric vehicles. *Applied Energy*, 186 (2017), 46–55. (cited on pages 20 and 41)

Jin, C.; Tang, J.; and Ghosh, P., 2013. Optimizing electric vehicle charging with energy storage in the electricity market. *IEEE Transactions on Smart Grid*, 4, 1 (2013), 311–320. (cited on pages 17, 19, and 20)

Kapustin, N. O. and Grushevenko, D. A., 2020. Long-term electric vehicles outlook and their potential impact on electric grid. *Energy Policy*, 137 (2020), 111103. (cited on page 1)

Karfopoulos, E. L. and Hatziargyriou, N. D., 2012. A multi-agent system for controlled charging of a large population of electric vehicles. *IEEE Transactions on Power Systems*, 28, 2 (2012), 1196–1204. (cited on pages 42 and 47)

Karfopoulos, E. L. and Hatziargyriou, N. D., 2015. Distributed coordination of electric vehicles providing V2G services. *IEEE Transactions on Power Systems*, 31, 1 (2015), 329–338. (cited on page 47)

Kasprzyk, L.; Pietracho, R.; and Bednarek, K., 2018. Analysis of the impact of electric vehicles on the power grid. In *Proceedings of the E3S Web of Conferences*, vol. 44, 00065. EDP Sciences. (cited on page 1)

Kaur, K.; Dua, A.; Jindal, A.; Kumar, N.; Singh, M.; and Vinel, A., 2015. A novel resource reservation scheme for mobile PHEVs in V2G environment using game theoretical approach. *IEEE Transactions on Vehicular Technology*, 64, 12 (2015), 5653–5666. (cited on page 47)

Kempton, W. and Tomić, J., 2005a. Vehicle-to-grid power fundamentals: Calculating capacity and net revenue. *Journal of power sources*, 144, 1 (2005), 268–279. (cited on page 17)

Kempton, W. and Tomić, J., 2005b. Vehicle-to-grid power implementation: From stabilizing the grid to supporting large-scale renewable energy. *Journal of power sources*, 144, 1 (2005), 280–294. (cited on page 17)

Kersting, W. H., 2006. *Distribution system modeling and analysis*. CRC press. (cited on page 50)

Khaligh, A. and Dusmez, S., 2012. Comprehensive topological analysis of conductive and inductive charging solutions for plug-in electric vehicles. *IEEE Transactions on Vehicular Technology*, 61, 8 (2012), 3475–3489. (cited on page 15)

Khan, S. U.; Mehmood, K. K.; Haider, Z. M.; Bukhari, S. B. A.; Lee, S.-J.; Rafique, M. K.; and Kim, C.-H., 2018. Energy management scheme for an ev smart charger V2G/G2V application with an ev power allocation technique and voltage regulation. *Applied Sciences*, 8, 4 (2018), 648. (cited on page 16)

Khodayar, M. E.; Wu, L.; and Shahidehpour, M., 2012. Hourly coordination of electric vehicle operation and volatile wind power generation in scuc. *IEEE Transactions on Smart Grid*, 3, 3 (2012), 1271–1279. (cited on pages 19 and 20)

Kim, H.-J.; Lee, J.; and Park, G.-L., 2012. Constraint-based charging scheduler design for electric vehicles. In *Asian Conference on Intelligent Information and Database Systems*, 266–275. Springer. (cited on page 20)

Kisacikoglu, M. C.; Bedir, A.; Ozpineci, B.; and Tolbert, L. M., 2012. PHEV-EV charger technology assessment with an emphasis on V2G operation. *Oak Ridge Nat. Lab., Oak Ridge, TN, USA, Tech. Rep. ORNL/TM-2010/221*, (2012). (cited on page 3)

Kisacikoglu, M. C.; Erden, F.; and Erdogan, N., 2018. Distributed control of PEV charging based on energy demand forecast. *IEEE Transactions on Industrial Informatics*, 14, 1 (Jan. 2018), 332–341. (cited on page 48)

Kong, P.-Y. and Karagiannidis, G. K., 2016. Charging schemes for plug-in hybrid electric vehicles in smart grid: A survey. *IEEE Access*, 4 (2016), 6846–6875. (cited on pages 2, 4, 16, 17, and 19)

Kundu, S. and Hiskens, I. A., 2012. Hysteresis-based charging control of plug-in electric vehicles. In *Proceedings of the IEEE 51st IEEE Conference on Decision and Control*, 5598–5604. IEEE. (cited on page 44)

Kundur, P.; Paserba, J.; Ajjarapu, V.; Andersson, G.; Bose, A.; Canizares, C.; Hatziargyriou, N.; Hill, D.; Stankovic, A.; Taylor, C.; et al., 2004. Definition and classification of power system stability IEEE/CIGRE joint task force on stability terms and definitions. *IEEE Transactions on Power Systems*, 19, 3 (2004), 1387–1401. (cited on page 49)

Kwon, M. and Choi, S., 2016. An electrolytic capacitorless bidirectional EV charger for v2g and v2h applications. *IEEE Transactions on Power Electronics*, 32, 9 (2016), 6792–6799. (cited on page 3)

Kwon, M.; Jung, S.; and Choi, S., 2015. A high efficiency bi-directional EV charger with seamless mode transfer for V2G and V2H application. In *Proceedings of the IEEE Energy Conversion Congress & Exposition*, 5394–5399. IEEE. (cited on page 3)

Lazzeroni, P.; Olivero, S.; Repetto, M.; Stirano, F.; and Vallet, M., 2019. Optimal battery management for vehicle-to-home and vehicle-to-grid operations in a residential case study. *Energy*, 175 (2019), 704–721. (cited on page 3)

Le Floch, C.; Belletti, F.; and Moura, S., 2016. Optimal charging of electric vehicles for load shaping: A dual-splitting framework with explicit convergence bounds. *IEEE Transactions on Transportation Electrification*, 2, 2 (2016), 190–199. (cited on page 47)

Le Floch, C.; Belletti, F.; Saxena, S.; Bayen, A. M.; and Moura, S., 2015. Distributed optimal charging of electric vehicles for demand response and load shaping. In *2015 54th IEEE Conference on Decision and Control (CDC)*, 6570–6576. IEEE. (cited on page 47)

Lee, J.; Kim, H.-J.; Park, G.-L.; and Jeon, H., 2012. Genetic algorithm-based charging task scheduler for electric vehicles in smart transportation. In *Asian Conference on Intelligent Information and Database Systems*, 208–217. Springer. (cited on page 20)

Li, C.; Luo, F.; Chen, Y.; Xu, Z.; An, Y.; and Li, X., 2017. Smart home energy management with vehicle-to-home technology. In *Proceedings of the 13th IEEE international conference on control & automation*, 136–142. IEEE. (cited on page 3)

Li, Q.; Cui, T.; Negi, R.; Franchetti, F.; and Ilic, M. D., 2011. On-line decentralized charging of plug-in electric vehicles in power systems. *arXiv preprint arXiv:1106.5063*, (2011). (cited on pages 19 and 42)

Li, R.; Wu, Q.; and Oren, S. S., 2013. Distribution locational marginal pricing for optimal electric vehicle charging management. *IEEE Transactions on Power Systems*, 29, 1 (2013), 203–211. (cited on page 119)

Li, W.; Lin, Z.; Zhou, H.; and Yan, G., 2019. Multi-objective optimization for cyber-physical-social systems: A case study of electric vehicles charging and discharging. *IEEE Access*, 7 (2019), 76754–76767. (cited on pages 47 and 57)

Liu, C.; Chau, K.; Wu, D.; and Gao, S., 2013. Opportunities and challenges of vehicle-to-home, vehicle-to-vehicle, and vehicle-to-grid technologies. *Proceedings of the IEEE*, 101, 11 (2013), 2409–2427. (cited on page 3)

Liu, M.; Phanivong, P. K.; and Callaway, D. S., 2018. Customer-and network-aware decentralized EV charging control. In *Proceedings of the Power Systems Computation Conference*, 1–7. IEEE. (cited on page 52)

Liu, M.; Phanivong, P. K.; Shi, Y.; and Callaway, D. S., 2017. Decentralized charging control of electric vehicles in residential distribution networks. *IEEE Transactions on Control Systems Technology*, 27, 1 (2017), 266–281. (cited on pages 44, 45, 51, 52, and 101)

Liu, M. and Sahraei-Ardakani, M., 2019. Chance-constrained shrunken-primal-dual subgradient (CC-SPDS) approach for decentralized electric vehicle charging control. In *Proceedings of the IEEE PES Innovative Smart Grid Technologies Asia*, 1520–1525. (cited on pages 52 and 101)

López, M. A.; De La Torre, S.; Martín, S.; and Aguado, J. A., 2015. Demand-side management in smart grid operation considering electric vehicles load shifting and vehicle-to-grid support. *International Journal of Electrical Power and Energy Systems*, 64 (2015), 689–698. (cited on page 2)

Lukic, S. and Pantic, Z., 2013. Cutting the cord: Static and dynamic inductive wireless charging of electric vehicles. *IEEE Electrification Magazine*, 1, 1 (2013), 57–64. (cited on page 15)

Luo, F.; Ranzi, G.; Kong, W.; Dong, Z. Y.; and Wang, F., 2018. Coordinated residential energy resource scheduling with vehicle-to-home and high photovoltaic penetrations. *IET Renewable Power Generation*, 12, 6 (2018), 625–632. (cited on page 3)

Luo, X. and Chan, K. W., 2014. Real-time scheduling of electric vehicles charging in low-voltage residential distribution systems to minimise power losses and improve voltage profile. *IET Generation, Transmission & Distribution*, 8, 3 (2014), 516–529. (cited on pages 51 and 83)

Luo, Z.; Hu, Z.; Song, Y.; Xu, Z.; Liu, H.; Jia, L.; and Lu, H., 2012. Economic analyses of plug-in electric vehicle battery providing ancillary services. In *Proceedings of the IEEE International Electric Vehicle Conference*, 1–5. IEEE. (cited on pages 2 and 17)

Luo, Z.; Hu, Z.; Song, Y.; Xu, Z.; and Lu, H., 2013a. Optimal coordination of plug-in electric vehicles in power grids with cost-benefit analysis—part I: Enabling techniques. *IEEE Transactions on Power Systems*, 28, 4 (2013), 3546–3555. (cited on page 47)

Luo, Z.; Hu, Z.; Song, Y.; Xu, Z.; and Lu, H., 2013b. Optimal coordination of plug-in electric vehicles in power grids with cost-benefit analysis—part II: A case study in china. *IEEE Transactions on Power Systems*, 28, 4 (2013), 3556–3565. (cited on page 47)

Ma, R.; Chen, H.-H.; Huang, Y.-R.; and Meng, W., 2013. Smart grid communication: Its challenges and opportunities. *IEEE Transactions on Smart Grid*, 4, 1 (2013), 36–46. (cited on page 3)

Ma, W.-J.; Gupta, V.; and Topcu, U., 2014. On distributed charging control of electric vehicles with power network capacity constraints. In *Proceedings of the American Control Conference*, 4306–4311. IEEE. (cited on page 43)

Ma, Z.; Callaway, D.; and Hiskens, I., 2012. Optimal charging control for plug-in electric vehicles. In *Control and Optimization Methods for Electric Smart Grids*, 259–273. Springer. (cited on page 41)

Ma, Z.; Callaway, D. S.; and Hiskens, I. A., 2011a. Decentralized charging control of large populations of plug-in electric vehicles. *IEEE Transactions on Control Systems Technology*, 21, 1 (2011), 67–78. (cited on pages 42, 43, and 45)

Ma, Z.; Hiskens, I.; and Callaway, D., 2011b. A decentralized MPC strategy for charging large populations of plug-in electric vehicles. *IFAC Proceedings Volumes*, 44, 1 (2011), 10493–10498. (cited on page 42)

Ma, Z.; Zou, S.; Liu, X.; and Hiskens, I., 2015. Efficient coordination of electric vehicle charging using a progressive second price auction. In *Proceedings of the American Control Conference*, 2999–3006. IEEE. (cited on page 43)

Ma, Z.; Zou, S.; Ran, L.; Shi, X.; and Hiskens, I. A., 2016. Efficient decentralized coordination of large-scale plug-in electric vehicle charging. *Automatica*, 69 (2016), 35–47. (cited on page 43)

Malhotra, A.; Binetti, G.; Davoudi, A.; and Schizas, I. D., 2017. Distributed power profile tracking for heterogeneous charging of electric vehicles. *IEEE Transactions on Smart Grid*, 8, 5 (Sep. 2017), 2090–2099. (cited on page 48)

Markel, T.; Kuss, M.; and Denholm, P., 2009. Communication and control of electric drive vehicles supporting renewables. In *Proceedings of the IEEE Vehicle Power & Propulsion Conference*, 27–34. IEEE. (cited on page 18)

Mediwaththe, M. G. C. P., 2017. *Game-theoretic Methods for Small-scale Demand-side Management in Smart Grid*. Ph.D. thesis, The University of New South Wales Australia. (cited on page 65)

Meikandasivam, S. et al., 2018. Optimal distribution of plug-in-electric vehicle's storage capacity using water filling algorithm for load flattening and vehicle prioritization using ANFIS. *Electric Power Systems Research*, 165 (2018), 120–133. (cited on pages 48 and 57)

Mesarić, P. and Krajcar, S., 2015. Home demand side management integrated with electric vehicles and renewable energy sources. *Energy and Buildings*, 108 (2015), 1–9. (cited on page 2)

Mets, K.; D'hulst, R.; and Develder, C., 2012. Comparison of intelligent charging algorithms for electric vehicles to reduce peak load and demand variability in a distribution grid. *Journal of Communications and Networks*, 14, 6 (2012), 672–681. (cited on page 16)

Mohammadi, J.; Vayá, M. G.; Kar, S.; and Hug, G., 2016. A fully distributed approach for plug-in electric vehicle charging. In *Proceedings of the Power Systems Computation Conference*, 1–7. IEEE. (cited on page 46)

Momoh, J. A., 2012. *Smart grid: fundamentals of design and analysis*, vol. 63. John Wiley & Sons. (cited on page 2)

Monteiro, V.; Gonçalves, H.; and Afonso, J. L., 2011. Impact of electric vehicles on power quality in a smart grid context. In *Proceedings of the 11th International Conference on Electrical Power Quality and Utilisation*, 1–6. IEEE. (cited on page 1)

Mou, Y.; Xing, H.; Lin, Z.; and Fu, M., 2014. Decentralized optimal demand-side management for PHEV charging in a smart grid. *IEEE Transactions on Smart Grid*, 6, 2 (2014), 726–736. (cited on pages 47 and 56)

Mu, Y.; Wu, J.; Jenkins, N.; Jia, H.; and Wang, C., 2014. A spatial–temporal model for grid impact analysis of plug-in electric vehicles. *Applied Energy*, 114 (2014), 456–465. (cited on page 41)

Mukherjee, J. C. and Gupta, A., 2014. A review of charge scheduling of electric vehicles in smart grid. *IEEE Systems Journal*, 9, 4 (2014), 1541–1553. (cited on page 19)

Mullan, J.; Harries, D.; Bräunl, T.; and Whitely, S., 2012. The technical, economic and commercial viability of the vehicle-to-grid concept. *Energy Policy*, 48 (2012), 394–406. (cited on page 17)

Mwasilu, F.; Justo, J. J.; Kim, E.-K.; Do, T. D.; and Jung, J.-W., 2014. Electric vehicles and smart grid interaction: A review on vehicle to grid and renewable energy sources integration. *Renewable and Sustainable Energy Reviews*, 34 (2014), 501–516. (cited on page 18)

Nguyen, H. K. and Song, J. B., 2012. Optimal charging and discharging for multiple phevs with demand side management in vehicle-to-building. *Journal of Communications and networks*, 14, 6 (2012), 662–671. (cited on page 3)

Nimalsiri, N.; Smith, D.; Ratnam, E.; Mediwaththe, C.; and Halgamuge, S., 2020. A decentralized electric vehicle charge scheduling scheme for tracking power profiles. In *Proceedings of the IEEE Power & Energy Society Innovative Smart Grid Technologies Conference*, 1–5. IEEE. (cited on pages 7 and 9)

Nimalsiri, N. I.; Mediwaththe, C. P.; Ratnam, E. L.; Shaw, M.; Smith, D. B.; and Halgamuge, S. K., 2019. A survey of algorithms for distributed charging control of electric vehicles in smart grid. *IEEE Transactions on Intelligent Transportation Systems*, 21, 11 (2019), 4497–4515. (cited on pages 2, 4, 7, 8, 20, and 41)

Nimalsiri, N. I.; Ratnam, E. L.; Mediwaththe, C. P.; Smith, D. B.; and Halgamuge, S. K., 2021a. Coordinated charging and discharging control of electric vehicles to manage supply voltages in distribution networks: Assessing the customer benefit. *Applied Energy*, 291 (2021), 116857. (cited on pages 7 and 10)

Nimalsiri, N. I.; Ratnam, E. L.; Smith, D. B.; Mediwaththe, C. P.; and Halgamuge, S. K., 2021b. Coordinated charge and discharge scheduling of electric vehicles for load curve shaping. *IEEE Transactions on Intelligent Transportation Systems*, (2021). (cited on pages 7 and 9)

Nimalsiri, N. I.; Ratnam, E. L.; Smith, D. B.; Mediwaththe, C. P.; and Halgamuge, S. K., 2021c. Distributed optimization-based electric vehicle charging and discharging in unbalanced distribution grids. *TechRxiv. Preprint*, (2021). (cited on pages 8 and 11)

Omran, N. G. and Filizadeh, S., 2017. A semi-cooperative decentralized scheduling scheme for plug-in electric vehicle charging demand. *International Journal of Electrical Power and Energy Systems*, 88 (2017), 119–132. (cited on page 101)

Ortega-Vazquez, M. A., 2014. Optimal scheduling of electric vehicle charging and vehicle-to-grid services at household level including battery degradation and price uncertainty. *IET Generation, Transmission & Distribution*, 8, 6 (2014), 1007–1016. (cited on pages 46 and 47)

Ota, Y.; Taniguchi, H.; Nakajima, T.; Liyanage, K. M.; Baba, J.; and Yokoyama, A., 2011. Autonomous distributed V2G (vehicle-to-grid) satisfying scheduled charging. *IEEE Transactions on Smart Grid*, 3, 1 (2011), 559–564. (cited on page 17)

Pajic, J.; Rivera, J.; Zhang, K.; and Jacobsen, H.-A., 2018. Eva: Fair and auditable electric vehicle charging service using blockchain. In *Proceedings of the 12th ACM International Conference on Distributed and Event-based Systems*, 262–265. (cited on page 44)

Palomar, D. P. and Fonollosa, J. R., 2005. Practical algorithms for a family of water filling solutions. *IEEE Transactions on Signal Processing*, 53, 2 (2005), 686–695. (cited on page 56)

Pang, C.; Kezunovic, M.; and Ehsani, M., 2012. Demand side management by using electric vehicles as distributed energy resources. In *Proceedings of the IEEE International Electric Vehicle Conference*, 1–7. IEEE. (cited on pages 2 and 3)

Pillai, J. R. and Bak-Jensen, B., 2010. Impacts of electric vehicle loads on power distribution systems. In *Proceedings of the IEEE Vehicle Power & Propulsion Conference*, 1–6. IEEE. (cited on page 16)

Pinto, J.; Monteiro, V.; Gonçalves, H.; Exposto, B.; Pedrosa, D.; Couto, C.; and Afonso, J. L., 2013. Bidirectional battery charger with grid-to-vehicle, vehicle-to-grid and vehicle-to-home technologies. In *Proceedings of the 39th Annual Conference of the IEEE Industrial Electronics Society*, 5934–5939. IEEE. (cited on page 3)

Putrus, G.; Suwanapingkarl, P.; Johnston, D.; Bentley, E.; and Narayana, M., 2009. Impact of electric vehicles on power distribution networks. In *Proceedings of the IEEE Vehicle Power & Propulsion Conference*, 827–831. IEEE. (cited on pages 1 and 16)

Rahbari-Asr, N. and Chow, M.-Y., 2014. Cooperative distributed demand management for community charging of PHEV/PEVs based on KKT conditions and consensus networks. *IEEE Transactions on Industrial Informatics*, 10, 3 (2014), 1907–1916. (cited on page 45)

Rahman, I.; Vasant, P. M.; Singh, B. S. M.; Abdullah-Al-Wadud, M.; and Adnan, N., 2016. Review of recent trends in optimization techniques for plug-in hybrid, and electric vehicle charging infrastructures. *Renewable and Sustainable Energy Reviews*, 58 (2016), 1039–1047. (cited on pages 4 and 19)

Rajakaruna, S.; Shahnia, F.; and Ghosh, A., 2015. *Plug In Electric Vehicles in Smart Grids: Integration Techniques*. Springer. (cited on page 2)

Rajendhar, P. and Jeyaraj, B. E., 2020. A water filling energy distributive algorithm based HEMS in coordination with PEV. *Sustainable Energy, Grids and Networks*, 22 (2020), 100360. (cited on pages 48 and 57)

Restrepo, M.; Morris, J.; Kazerani, M.; and Canizares, C. A., 2016. Modeling and testing of a bidirectional smart charger for distribution system EV integration. *IEEE Transactions on Smart Grid*, 9, 1 (2016), 152–162. (cited on page 3)

Richardson, D. B., 2013. Electric vehicles and the electric grid: A review of modeling approaches, impacts, and renewable energy integration. *Renewable and Sustainable Energy Reviews*, 19 (2013), 247–254. (cited on page 16)

Richardson, P.; Flynn, D.; and Keane, A., 2011. Optimal charging of electric vehicles in low-voltage distribution systems. *IEEE Transactions on Power Systems*, 27, 1 (2011), 268–279. (cited on pages 50 and 83)

Richardson, P.; Flynn, D.; and Keane, A., 2012. Local versus centralized charging strategies for electric vehicles in low voltage distribution systems. *IEEE Transactions on Smart Grid*, 3, 2 (2012), 1020–1028. (cited on pages 20 and 53)

Rivera, J.; Wolfrum, P.; Hirche, S.; Goebel, C.; and Jacobsen, H.-A., 2013. Alternating direction method of multipliers for decentralized electric vehicle charging control. In *Proceedings of the 52nd IEEE Conference on Decision and Control*, 6960–6965. IEEE. (cited on page 44)

Rizvi, S. A. A.; Xin, A.; Masood, A.; Iqbal, S.; Jan, M. U.; and Rehman, H., 2018. Electric vehicles and their impacts on integration into power grid: A review. In *Proceedings of the 2nd IEEE Conference on Energy Internet and Energy System Integration*, 1–6. IEEE. (cited on pages 1 and 16)

Saad, W.; Han, Z.; Poor, H. V.; and Basar, T., 2012. Game-theoretic methods for the smart grid: An overview of microgrid systems, demand-side management, and smart grid communications. *IEEE Signal Processing Magazine*, 29, 5 (2012), 86–105. (cited on page 65)

Saber, A. Y. and Venayagamoorthy, G. K., 2010. Intelligent unit commitment with vehicle-to-grid — A cost-emission optimization. *Journal of Power Sources*, 195, 3 (2010), 898–911. (cited on page 17)

Saber, A. Y. and Venayagamoorthy, G. K., 2011. Resource scheduling under uncertainty in a smart grid with renewables and plug-in vehicles. *IEEE systems journal*, 6, 1 (2011), 103–109. (cited on pages 17, 19, and 20)

Sabillon, C.; Mohamed, A. A.; Venkatesh, B.; and Golriz, A., 2019. Locational marginal pricing for distribution networks: Review and applications. In *Proceedings of the IEEE Electrical Power and Energy Conference*, 1–5. IEEE. (cited on page 119)

Sahinler, G. B. and Poyrazoglu, G., 2020. V2G applicable electric vehicle chargers, power converters and their controllers: A review. In *Proceedings of the 2nd Global Power, Energy and Communication Conference*, 59–64. IEEE. (cited on page 3)

Salah, F.; Ilg, J. P.; Flath, C. M.; Basse, H.; and Van Dinther, C., 2015. Impact of electric vehicles on distribution substations: A Swiss case study. *Applied Energy*, 137 (2015), 88–96. (cited on page 41)

Sanguesa, J. A.; Torres-Sanz, V.; Garrido, P.; Martinez, F. J.; and Marquez-Barja, J. M., 2021. A review on electric vehicles: Technologies and challenges. *Smart Cities*, 4, 1 (2021), 372–404. (cited on page 1)

Schneider, K.; Gerkensmeyer, C.; Kintner-Meyer, M.; and Fletcher, R., 2008. Impact assessment of plug-in hybrid vehicles on pacific northwest distribution systems. In *Proceedings of the IEEE Power and Energy Society General Meeting - Conversion and Delivery of Electrical Energy in the 21st Century*, 1–6. IEEE. (cited on page 16)

SCHULLER, A. AND STUART, C., 2018. From cradle to grave: e-mobility and the energy transition. (2018). (cited on page 1)

SEMSAR, S.; SOONG, T.; AND LEHN, P. W., 2020. On-board single-phase integrated electric vehicle charger with V2G functionality. *IEEE Transactions on Power Electronics*, 35, 11 (2020), 12072–12084. (cited on page 3)

SETH, A. K. AND SINGH, M., 2020. Resonant controller of single-stage off-board EV charger in G2V and V2G modes. *IET Power Electronics*, 13, 5 (2020), 1086–1092. (cited on page 3)

SHAFIEE, S.; FOTUHI-FIRUZABAD, M.; AND RASTEGAR, M., 2013. Investigating the impacts of plug-in hybrid electric vehicles on power distribution systems. *IEEE Transactions on Smart Grid*, 4, 3 (2013), 1351–1360. (cited on pages 1 and 16)

SHAUKAT, N.; KHAN, B.; ALI, S.; MEHMOOD, C.; KHAN, J.; FARID, U.; MAJID, M.; ANWAR, S.; JAWAD, M.; AND ULLAH, Z., 2018. A survey on electric vehicle transportation within smart grid system. *Renewable and Sustainable Energy Reviews*, 81 (2018), 1329–1349. (cited on pages 1 and 16)

SHEKARI, T.; GOLSHANNAVAZ, S.; AND AMINIFAR, F., 2016. Techno-economic collaboration of PEV fleets in energy management of microgrids. *IEEE Transactions on Power Systems*, 32, 5 (2016), 3833–3841. (cited on page 54)

SHEN, Z.-J. M.; FENG, B.; MAO, C.; AND RAN, L., 2019. Optimization models for electric vehicle service operations: A literature review. *Transportation Research Part B: Methodological*, 128 (2019), 462–477. (cited on page 4)

SHUAI, W.; MAILLÉ, P.; AND PELOV, A., 2016. Charging electric vehicles in the smart city: A survey of economy-driven approaches. *IEEE Transactions on Intelligent Transportation Systems*, 17, 8 (2016), 2089–2106. (cited on pages 2 and 19)

SINGH, J. AND TIWARI, R., 2020. Cost benefit analysis for V2G implementation of electric vehicles in distribution system. *IEEE Transactions on Industry Applications*, 56, 5 (2020), 5963–5973. (cited on page 3)

SINGH, M.; KUMAR, P.; AND KAR, I., 2013. A multi charging station for electric vehicles and its utilization for load management and the grid support. *IEEE Transactions on Smart Grid*, 4, 2 (2013), 1026–1037. (cited on page 49)

SOJOUDI, S. AND LOW, S. H., 2011. Optimal charging of plug-in hybrid electric vehicles in smart grids. In *Proceedings of the IEEE Power and Energy Society General Meeting*, 1–6. IEEE. (cited on page 50)

SOLANKE, T. U.; RAMACHANDARAMURTHY, V. K.; YONG, J. Y.; PASUPULETI, J.; KASINATHAN, P.; AND RAJAGOPALAN, A., 2020. A review of strategic charging–discharging control of grid-connected electric vehicles. *Journal of Energy Storage*, 28 (2020), 101193. (cited on page 18)

Sortomme, E. and El-Sharkawi, M. A., 2010. Optimal charging strategies for unidirectional vehicle-to-grid. *IEEE Transactions on Smart Grid*, 2, 1 (2010), 131–138. (cited on pages 17 and 20)

Sortomme, E. and El-Sharkawi, M. A., 2011a. Optimal combined bidding of vehicle-to-grid ancillary services. *IEEE Transactions on Smart Grid*, 3, 1 (2011), 70–79. (cited on page 20)

Sortomme, E. and El-Sharkawi, M. A., 2011b. Optimal scheduling of vehicle-to-grid energy and ancillary services. *IEEE Transactions on Smart Grid*, 3, 1 (2011), 351–359. (cited on pages 17 and 20)

Sortomme, E.; Hindi, M. M.; MacPherson, S. J.; and Venkata, S., 2010. Coordinated charging of plug-in hybrid electric vehicles to minimize distribution system losses. *IEEE Transactions on Smart Grid*, 2, 1 (2010), 198–205. (cited on pages 19, 20, and 50)

Sovacool, B. K. and Hirsh, R. F., 2009. Beyond batteries: An examination of the benefits and barriers to plug-in hybrid electric vehicles (PHEVs) and a vehicle-to-grid (V2G) transition. *Energy Policy*, 37, 3 (2009), 1095–1103. (cited on page 18)

statista, 2021. Global plug-in electric vehicle market share in the first half of 2021, by main producer. https://www.statista.com/statistics/541390/global-sales-of-plug-in-electric-vehicle-manufacturers. Accessed 14 Sep. 2021. (cited on page 15)

Stüdli, S.; Crisostomi, E.; Middleton, R.; Braslavsky, J.; and Shorten, R., 2015. Distributed load management using additive increase multiplicative decrease based techniques. In *Plug In Electric Vehicles in Smart Grids*, 173–202. Springer. (cited on pages 17 and 46)

Stüdli, S.; Crisostomi, E.; Middleton, R.; and Shorten, R., 2012a. AIMD-like algorithms for charging electric and plug-in hybrid vehicles. In *Proceedings of the IEEE International Electric Vehicle Conference*, 1–8. IEEE. (cited on page 46)

Stüdli, S.; Crisostomi, E.; Middleton, R.; and Shorten, R., 2012b. A flexible distributed framework for realising electric and plug-in hybrid vehicle charging policies. *International Journal of Control*, 85, 8 (2012), 1130–1145. (cited on page 46)

Stüdli, S.; Crisostomi, E.; Middleton, R.; and Shorten, R., 2014. Optimal real-time distributed V2G and G2V management of electric vehicles. *International Journal of Control*, 87, 6 (2014), 1153–1162. (cited on page 46)

Stüdli, S.; Middleton, R. H.; and Braslavsky, J. H., 2013. A fixed-structure automaton for load management of electric vehicles. In *Proceedings of the European Control Conference*, 3566–3571. IEEE. (cited on pages 46 and 56)

Su, W. and Chow, M.-Y., 2011. Performance evaluation of an EDA-based large-scale plug-in hybrid electric vehicle charging algorithm. *IEEE Transactions on Smart Grid*, 3, 1 (2011), 308–315. (cited on pages 19 and 20)

Su, W.; Eichi, H.; Zeng, W.; and Chow, M.-Y., 2011. A survey on the electrification of transportation in a smart grid environment. *IEEE Transactions on Industrial Informatics*, 8, 1 (2011), 1–10. (cited on pages 1 and 16)

Sun, W.; Neumann, F.; and Harrison, G. P., 2020. Robust scheduling of electric vehicle charging in LV distribution networks under uncertainty. *IEEE Transactions on Industry Applications*, 56, 5 (2020), 5785–5795. (cited on page 53)

Sundstrom, O. and Binding, C., 2011. Flexible charging optimization for electric vehicles considering distribution grid constraints. *IEEE Transactions on Smart grid*, 3, 1 (2011), 26–37. (cited on page 20)

Tan, K. M.; Ramachandaramurthy, V. K.; and Yong, J. Y., 2014. Bidirectional battery charger for electric vehicle. In *Proceedings of the IEEE Innovative Smart Grid Technologies - Asia*, 406–411. IEEE. (cited on page 3)

Then, J.; Agalgaonkar, A. P.; and Muttaqi, K. M., 2021. Coordination of spatially distributed electric vehicle charging for voltage rise and voltage unbalance mitigation in networks with solar penetration. In *Proceedings of the IEEE Texas Power and Energy Conference*, 1–6. IEEE. (cited on pages 52 and 101)

Tsai, S.-C.; Tseng, Y.-H.; and Chang, T.-H., 2015. Communication-efficient distributed demand response: A randomized admm approach. *IEEE Transactions on Smart Grid*, 8, 3 (2015), 1085–1095. (cited on page 101)

Tse, C. G.; Maples, B. A.; and Kreith, F., 2016. The use of plug-in hybrid electric vehicles for peak shaving. *Journal of Energy Resources Technology*, 138, 1 (2016). (cited on page 46)

Tushar, M. H. K.; Zeineddine, A. W.; and Assi, C., 2017. Demand-side management by regulating charging and discharging of the EV, ESS, and utilizing renewable energy. *IEEE Transactions on Industrial Informatics*, 14, 1 (2017), 117–126. (cited on page 3)

Tuttle, D. P. and Baldick, R., 2012. The evolution of plug-in electric vehicle-grid interactions. *IEEE Transactions on Smart Grid*, 3, 1 (2012), 500–505. (cited on page 16)

Vandael, S.; Boucké, N.; Holvoet, T.; and Deconinck, G., 2010. Decentralized demand side management of plug-in hybrid vehicles in a smart grid. In *Proceedings of the 1st International Workshop on Agent Technologies for Energy Systems*, 67–74. (cited on pages 19 and 42)

Wallbox, 2021. Why bidirectional charging is the next big thing for EV owners. https://blog.wallbox.com/en-au/why-bidirectional-charging-is-the-next-big-thing-for-ev-owners. Accessed 14 Sep. 2021. (cited on pages 2 and 3)

Wang, G. C.; Ratnam, E.; Haghi, H. V.; and Kleissl, J., 2019. Corrective receding horizon ev charge scheduling using short-term solar forecasting. *Renewable Energy*, 130 (2019), 1146–1158. (cited on page 41)

Wang, Q.; Liu, X.; Du, J.; and Kong, F., 2016. Smart charging for electric vehicles: A survey from the algorithmic perspective. *IEEE Communications Surveys & Tutorials*, 18, 2 (2016), 1500–1517. (cited on pages 2 and 19)

Wang, S.; Du, L.; and Li, Y., 2020. Decentralized volt/var control of EV charging station inverters for voltage regulation. In *Proceedings of the IEEE Transportation Electrification Conference & Exposition*, 604–608. (cited on page 101)

Wang, W.; Xu, Y.; and Khanna, M., 2011. A survey on the communication architectures in smart grid. *Computer networks*, 55, 15 (2011), 3604–3629. (cited on page 3)

Wang, Z. and Wang, S., 2013. Grid power peak shaving and valley filling using vehicle-to-grid systems. *IEEE Transactions on Power Delivery*, 28, 3 (2013), 1822–1829. (cited on page 46)

Wen, C.-K.; Chen, J.-C.; Teng, J.-H.; and Ting, P., 2012. Decentralized plug-in electric vehicle charging selection algorithm in power systems. *IEEE Transactions on Smart Grid*, 3, 4 (2012), 1779–1789. (cited on page 19)

Wu, C.; Mohsenian-Rad, H.; and Huang, J., 2011a. Vehicle-to-aggregator interaction game. *IEEE Transactions on Smart Grid*, 3, 1 (2011), 434–442. (cited on page 17)

Wu, H. H.; Gilchrist, A.; Sealy, K.; Israelsen, P.; and Muhs, J., 2011b. A review on inductive charging for electric vehicles. In *Proceedings of the IEEE International Electric Machines & Drives conference*, 143–147. IEEE. (cited on page 15)

Wu, Q.; Nielsen, A. H.; Østergaard, J.; Cha, S.-T.; Marra, F.; and Andersen, P. B., 2010. Modeling of electric vehicles (evs) for ev grid integration study. In *European Conference SmartGrids & E-Mobility*. (cited on page 15)

Xia, L.; Mareels, I.; Alpcan, T.; Brazil, M.; de Hoog, J.; and Thomas, D. A., 2014. A distributed electric vehicle charging management algorithm using only local measurements. In *IEEE PES Innovative Smart Grid Technologies*, 1–5. IEEE. (cited on page 53)

Xiang, Y.; Hu, S.; Liu, Y.; Zhang, X.; and Liu, J., 2019. Electric vehicles in smart grid: a survey on charging load modelling. *IET Smart Grid*, 2, 1 (2019), 25–33. (cited on page 19)

Xiao, H.; Huimei, Y.; Chen, W.; and Hongjun, L., 2014. A survey of influence of electrics vehicle charging on power grid. In *Proceedings of the 9th IEEE Conference on Industrial Electronics and Applications*, 121–126. IEEE. (cited on page 1)

Xing, H.; Fu, M.; Lin, Z.; and Mou, Y., 2015. Decentralized optimal scheduling for charging and discharging of plug-in electric vehicles in smart grids. *IEEE Transactions on Power Systems*, 31, 5 (2015), 4118–4127. (cited on pages 15, 47, and 57)

Xing, H.; Lin, Z.; and Fu, M., 2017. A new decentralized algorithm for optimal load shifting via electric vehicles. In *Proceedings of the IEEE 36th China Control Conference*, 10708–10713. (cited on page 47)

Xu, Y. and Pan, F., 2012. Scheduling for charging plug-in hybrid electric vehicles. In *Proceedings of the IEEE 51st Conference on Decision and Control*, 2495–2501. IEEE. (cited on page 20)

Yi, Z.; Scoffield, D.; Smart, J.; Meintz, A.; Jun, M.; Mohanpurkar, M.; and Medam, A., 2020. A highly efficient control framework for centralized residential charging coordination of large electric vehicle populations. *International Journal of Electrical Power and Energy Systems*, 117 (2020), 105661. (cited on pages 20 and 41)

Yilmaz, M. and Krein, P., 2012a. Review of charging power levels and infrastructure for plug-in electric and hybrid vehicles and commentary on unidirectional charging. In *IEEE International Electrical Vehicle Conference*. (cited on page 3)

Yilmaz, M. and Krein, P. T., 2012b. Review of battery charger topologies, charging power levels, and infrastructure for plug-in electric and hybrid vehicles. *IEEE transactions on Power Electronics*, 28, 5 (2012), 2151–2169. (cited on page 16)

Yilmaz, M. and Krein, P. T., 2012c. Review of battery charger topologies, charging power levels, and infrastructure for plug-in electric and hybrid vehicles. *IEEE transactions on Power Electronics*, 28, 5 (2012), 2151–2169. (cited on page 16)

Yilmaz, M. and Krein, P. T., 2012d. Review of benefits and challenges of vehicle-to-grid technology. In *2012 IEEE Energy Conversion Congress and Exposition (ECCE)*, 3082–3089. IEEE. (cited on page 18)

Yilmaz, M. and Krein, P. T., 2012e. Review of integrated charging methods for plug-in electric and hybrid vehicles. In *Proceedings of the IEEE International Conference on Vehicular Electronics and Safety*, 346–351. IEEE. (cited on page 16)

Yilmaz, M. and Krein, P. T., 2012f. Review of the impact of vehicle-to-grid technologies on distribution systems and utility interfaces. *IEEE Transactions on Power Electronics*, 28, 12 (2012), 5673–5689. (cited on pages 17 and 18)

Yilmaz, M. and Krein, P. T., 2012g. Review of the impact of vehicle-to-grid technologies on distribution systems and utility interfaces. *IEEE Transactions on Power Electronics*, 28, 12 (2012), 5673–5689. (cited on page 18)

Zhan, K.; Hu, Z.; Song, Y.; Lu, N.; Xu, Z.; and Jia, L., 2015. A probability transition matrix based decentralized electric vehicle charging method for load valley filling. *Electric Power Systems Research*, 125 (2015), 1–7. (cited on page 43)

Zhan, K.; Hu, Z.; Song, Y.; Luo, Z.; Xu, Z.; and Jia, L., 2012. Coordinated electric vehicle charging strategy for optimal operation of distribution network. In *Proceedings of the 3rd IEEE PES Innovative Smart Grid Technologies Europe*, 1–6. IEEE. (cited on pages 49 and 50)

Zhan, K.; Xu, A.; Guo, X.; Wei, W.; and Jian, G., 2016. A hierarchical control method of massive plug-in electric vehicles for load valley filling. In *CIRED Workshop*, 1–4. IET. (cited on page 44)

Zhang, K.; Xu, L.; Ouyang, M.; Wang, H.; Lu, L.; Li, J.; and Li, Z., 2014a. Optimal decentralized valley-filling charging strategy for electric vehicles. *Energy Conversion and Management*, 78 (2014), 537–550. (cited on page 45)

Zhang, L.; Jabbari, F.; Brown, T.; and Samuelsen, S., 2014b. Coordinating plug-in electric vehicle charging with electric grid: Valley filling and target load following. *Journal of Power Sources*, 267 (2014), 584–597. (cited on pages 45 and 48)

Zhang, L.; Kekatos, V.; and Giannakis, G. B., 2016. Scalable electric vehicle charging protocols. *IEEE Transactions on Power Systems*, 32, 2 (2016), 1451–1462. (cited on pages 44, 51, 52, 101, and 113)

Zhang, S. and Leung, K.-C., 2018. Joint optimal power flow routing and decentralized scheduling with vehicle-to-grid regulation service. In *Proceedings of the IEEE International Conference on Communications, Control, and Computing Technologies for Smart Grids*, 1–6. (cited on pages 52 and 101)

Zhou, K.; Cheng, L.; Wen, L.; Lu, X.; and Ding, T., 2020a. A coordinated charging scheduling method for electric vehicles considering different charging demands. *Energy*, (2020), 118882. (cited on pages 46 and 47)

Zhou, X.; Zou, S.; Wang, P.; and Ma, Z., 2020b. Voltage regulation in constrained distribution networks by coordinating electric vehicle charging based on hierarchical ADMM. *IET Generation, Transmission & Distribution*, 14, 17 (2020), 3444–3457. (cited on pages 52, 101, and 113)

Zou, S.; Hiskens, I.; Ma, Z.; and Liu, X., 2017. Consensus-based coordination of electric vehicle charging. *IFAC-PapersOnLine*, 50, 1 (2017), 8881–8887. (cited on page 43)

Zou, S.; Ma, Z.; Liu, X.; and Hiskens, I., 2016. An efficient game for coordinating electric vehicle charging. *IEEE Transactions on Automatic Control*, 62, 5 (2016), 2374–2389. (cited on page 43)